Signatures of cellular immunity after vaccination and challenge that associate with clinical outcome of *Salmonella* Typhi infection

Deborah Cross (1122809)

Reading for Doctor of Philosophy in Paediatrics

The Queen's College

University of Oxford

Submitted Trinity Term 2021

Acknowledgement

To my supervisors, Professor Andrew Pollard, Dr Jennifer Hill and Dr Marije Verheul. If you ever doubted me, you never showed it and for that I am eternally grateful. Your patience, advice and continuous support have been invaluable. My progression as a scientist has been all the better for your mentorship.

To the wider enteric team. An especially big thank you to Ruth and Mari aka Team Gene for the 2am pizza chats and DNA extracting. Big thanks to Lisa Stockdale for the endless enthusiasm and advice, Celina Jin and Kate Emery for the invaluable clinical input, Daniel O'Connor and Irina Chelysheva for the bioinformatic discussions. Thank you to Lizzy Jones, Sonu Shrestha and Christoph Blohmke. I have learnt so much from each and every one of you.

To the OVG lab and clinical staff. Claudio Di Maso, Carla Ferreira Da Silva and Philomena Mwenu for arranging blood donations, Maria Moore for the challenge model knowledge and RedCap extracts, Merryn Voysey aka. fellow "friend of pre-clin" for the R and stats advice, Chris, Liz and Sagida for managing the lab and steering the ship during a global pandemic.

To the staff at the Stanford Human Immune Monitoring Center. A special thanks to Gerlinde Obsermoser for the coordination of the CyTOF study, Mike Leipold for his unmatched expertise and Holden Maeckar for hosting our stay in Stanford.

To the people who stopped me turning into an absolute crazy person. Luke, Laura, Aline and Amy, thank you for Fridays at the Rusty, the pandemic walks and generally being an amazing bunch of people. Thank you to everyone who gamely listened to my every thesis frustration and meltdown. You poor poor people, you're all gems, thank you for not screening my calls – Becky, Emily, Matt, Kseniya, the school gang, the undergrad gang. I love you all.

Many thanks to the Department of Paediatrics for providing funding for my studies, and to the Medical Sciences Division for the COVID-19 extension fund. This financial assistance was vital and without it I would not have been able to complete my studies so I am truly grateful.

To my family. Mum, Dad, Stu, Nan – thank you for the support, for letting me take over the kitchen during thesis writing and for the endless supply of food (shoutout to the burgers). I'm 99% certain that you still have no idea what on earth I've been *doing* for 3.5 years so I wrote a book to show you. I'll get a job now, pinky promise.

Absolutely no thanks whatsoever to COVID-19. You've been the absolute worst.

Declaration of Contributions

All mass cytometry data cleaning, normalisation, visualisation, statistical analyses and machine learning presented in this thesis were performed by the author. All research questions were conceived by the author with support and guidance from Professor Andrew Pollard, Dr Jennifer Hill and Dr Marije Verheul. Data from Chapter 3 have been previously published at Frontiers in Immunology.

All mass cytometry data were acquired by staff at the Stanford Human Immune Monitoring Center (HIMC) overseen by Dr Mike Leipold and Professor Holden Maecker. Project coordination was facilitated by Dr Gerlinde Obermoser.

PBMC, serum, plasma and stool samples analysed in this study were collected and processed by clinical research staff at the Oxford Vaccine Group as part of a Phase IIb vaccine efficacy trial run between 2015 and 2017. Trial management team was headed by Dr. Celina Jin with oversight from Professor Andrew Pollard.

Vi-antibody titres and Fc-mediated functional measurements presented in Chapter 3 and Chapter 4 were performed by Dr Celina Jin and Dr Jennifer Hill at the Ragon Institute with oversight from Professor Galit Alter.

Vi-specific *ex vivo* ELISpots presented in Chapter 3 were performed by Elizabeth Jones and Dr Celina Jin.

Quantification of sCD40L, CX_3CL1 and CXCL1 in serum presented in Chapter 4 was performed by Elizabeth Jones.

NK flow cytometry panel and cytotoxicity assay optimisations presented in Chapter 5 were performed by the author with oversight from Dr Jennifer Hill and Dr Marije Verheul.

Quantification of TNFα and IFNγ in plasma presented in Chapter 6 was performed by Morwenna Tamblyn under the supervision of the author and Dr Marije Verheul.

List of publications

1. Cross D, Drury R, Hill J, Pollard AJ. Epigenetics in Sepsis: Understanding Its Role in Endothelial Dysfunction, Immunosuppression, and Potential Therapeutics. Front Immunol. 2019 Jun 18;10:1363. doi: 10.3389/fimmu.2019.01363. PMID: 31275313; PMCID: PMC6591469.

2. Cross DL, Verheul MK, Leipold MD, Obermoser G, Jin C, Jones E, Starr JS, Mohorianu I, Blohmke CJ, Maecker HT, Napolitani G, Hill J, Pollard AJ. Vi-Vaccinations Induce Heterogeneous Plasma Cell Responses That Associate With Protection From Typhoid Fever. Front Immunol. 2020 Dec 3;11:574057. doi: 10.3389/fimmu.2020.574057. PMID: 33424833; PMCID: PMC7793947.

Abstract

Background

Salmonella Typhi (*S.* Typhi), the aetiological cause of typhoid fever, is responsible for up to 20.6 million infections every year, the majority of which occur in children under 15 years of age. A Vi-tetanus toxoid conjugate vaccine (Vi-TT) has proven to be highly protective against the development of typhoid fever and vaccine implementation is expected to have a significant effect on rates of disease in endemic settings.

Research question 1

Cellular immunity is likely to play a substantial role in protection from typhoid fever. However, early progression of disease remains poorly understood in humans as these immunological responses can rarely be examined prior to symptom onset. Understanding of host responses is further impeded by lack of appropriate animal models of *S.* Typhi infection. Human challenge studies offer an opportunity to circumvent these issues and offer valuable insights.

Research question 2

Clinical presentation of typhoid fever is highly heterogeneous with severe complications often requiring hospitalisation. Identification of individuals at risk of worsened outcome is critical for proper treatment and improved prognosis. C-reactive protein (CRP) and white blood cell count (WBC) are commonly used as prognostic indicators of patient condition, however, measures such as CRP are not always available in resource limited settings. In addition, few previous studies have sought to assess whether these indicators are optimally suited to this purpose in the context of typhoid fever. Whether better correlates of disease severity can be identified to serve this purpose is an unanswered question.

To address these identified gaps in knowledge, a longitudinal study of cellular immunity was conducted following *S.* Typhi infection in a human challenge model. This work aimed to assess:

1. The progression of immune responses in peripheral blood after infection and the effect of Vi-vaccination.
2. The utility of blood count ratios as biomarkers of disease severity.
3. The impact of vaccination on severity biomarkers and symptom presentation.

Methods

Peripheral blood samples (PBMCs) and full blood count were collected from individuals enrolled in a Phase IIb clinical trial and human challenge study evaluating the efficacy of two typhoid fever vaccines, Vi-PS and Vi-TT. Enrolled individuals were UK residents with no previous history of typhoid fever. Participants were randomised to receive either a single dose of Vi-TT (Bharat Biotech), Vi-PS (Sanofi Pasteur) or a control vaccine, MenACWY (GlaxoSmithKline). Approximately 1 month after vaccination, participants were challenged with 1-5 x 10^4 CFU of *S.* Typhi. PBMCs and full blood count were collected at baseline, following vaccination and for several days after infection until either diagnosis or for up to two weeks after challenge. Following diagnosis or completion of the 2-week observation period, participants were treated with antibiotics.

PBMCs where phenotyped by mass cytometry measuring 37 markers in total (n = 57 participants, protected: n = 28, diagnosed: n = 29). Cellular subsets were identified by clustering analysis and differential abundance of populations after infection were assessed by negative binomial mixture models. Signatures of cellular immunity were identified by partial least squares-discriminant analysis (PLS-DA) and their association with infection outcome was evaluated.

During challenge, participants completed an online diary self-assessing development of symptoms and relative severity. Participants were asked to report on the following with a grade between 0 (symptom not present) to 3 (severe): headache, feeling generally unwell, abdominal pain, constipation, cough, diarrhoea, joint pain, loss of appetite, muscle pain and nausea. Subpopulations of participants with differing symptom profiles at diagnosis were identified by latent profile analysis (LPA).

Results

Early infection: Within 24 hours of infection, PBMC composition was significantly perturbed by *S.* Typhi infection in all participants regardless of whether they were protected or developed acute disease (defined as either positive blood culture or persistent fever). PLS-DA identified 3 profiles of cellular immunity at the 24-hour timepoint (referred to henceforward as A, B and C) that were differentially associated with the development of typhoid fever. Profile A had the highest proportion of protected participants (80%, n = 15). These individuals exhibited a significant expansion of $CD16^{+}$ monocytes after challenge in comparison to other profiles, as well as having higher frequencies of naïve B-cells at baseline. Conversely, participants in profile C had the lowest proportion of protected participants (8.3%, n = 12) and were found to have high baseline frequencies of terminally differentiated (TEMRA) T-cells and significant recirculation of $CD62L^{+}$ memory IgA^{+} and IgG^{+} B-cells after infection. Remaining individuals developed an intermediatory profile (Profile B, n = 25), characterized by absence of both changes in monocytes and memory B-cells. Participants in all profiles showed significant expansion in $CD62L^{+}$ $CD56^{dim}$ NK cells. Vaccination status was modestly associated with profile of cellular immunity although the proportion of vaccinees in each profile was not significantly different.

Acute disease: Two symptom profiles, profile A (n = 34) and profile B (n = 12), were identifiable in individuals that developed acute symptoms after challenge. Participants in profile B reported significantly greater numbers of symptoms ($p = 1.02 \times 10^{-6}$) and higher prevalence of fever ($p = 8.97 \times 10^{-4}$). On evaluation of full blood count data, neutrophil-to-lymphocyte

ratio (NLR) and eosinophil-to-lymphocyte ratio (ELR) were both significantly perturbed in all individuals with typhoid fever ($p = 3.42 \times 10^{-11}$ and $p = 1.93 \times 10^{-11}$ respectively), however perturbation of NLR and ELR was statistically greater in participants in profile B. This suggests these biomarkers could successfully identify more severe clinical presentation of disease. Additionally, NLR and ELR were found to be more sensitive identifiers of profile B participants than either CRP or WBC. Vi-TT vaccination, but not Vi-PS, significantly lowered NLR and number of self-reported symptoms. In vaccinees, NLR was significantly negatively correlated with Vi-IgG titres but not Vi-IgA or Vi-IgM suggesting Vi-IgG titres may play a significant role in reducing disease severity.

Conclusions

In conclusion, signatures of immunity are identifiable in peripheral blood as early as 24 hours after oral challenge. These profiles have significant associations with outcome of infection but are only modestly associated with vaccination status.

This analysis suggests Vi-vaccination has a modulatory effect on symptom presentation in the event of acute disease. Vi-TT, but not Vi-PS vaccinees, developed significantly fewer symptoms than unvaccinated participants. NLR and ELR were significant, independent correlates of disease severity that may have prognostic potential in the management of typhoid fever.

Table of Contents

ACKNOWLEDGEMENT **I**

ABSTRACT **V**

LIST OF FIGURES **VIII**

1 INTRODUCTION **14**

1.1 ENTERIC FEVER **14**

1.1.1 GLOBAL BURDEN OF INFECTION 14

1.2 CHALLENGES IN ENTERIC FEVER RESEARCH **4**

1.2.1 TLR11 KNOCKOUT MICE 16

1.2.2 HUMANISED MICE 16

1.2.3 ORGANOIDS AND TISSUE CULTURE 17

1.2.4 HUMAN CHALLENGE MODELS 18

1.3 PATHOGENESIS OF TYPHOID FEVER **20**

1.3.1 EVOLUTION OF PATHOGEN 20

1.3.2 INVASION OF INTESTINAL EPITHELIA 20

1.3.3 DISSEMINATION 21

1.3.4 REPLICATION AT DISSEMINATED SITES 22

1.3.5 ROLE OF VI-ANTIGEN 22

1.3.6 PROTECTIVE HOST RESPONSES TO SALMONELLA INFECTION: INNATE IMMUNITY 24

1.3.7 PROTECTIVE HOST RESPONSES TO SALMONELLA INFECTION: ADAPTIVE RESPONSES 30

1.4 TYPHOID FEVER ELIMINATION: EFFECTIVE STRATEGIES FOR DISEASE CONTROL **35**

1.4.1 EVIDENCE FROM HISTORICAL ACCOUNTS OF TYPHOID ELIMINATION IN INDUSTRIALISED COUNTRIES 35

1.4.2 THE CURRENT STATE OF WATER AND SANITATION IN TYPHOID ENDEMIC COUNTRIES 36

1.4.3 Challenges to WASH reform: feasibility and alternative measures 36
1.4.4 The role for vaccination in the elimination of typhoid fever 44
1.4.5 Efficacy of Vi-vaccines 44
1.4.6 Usage of Vi-vaccines in immunisation programs 45
1.4.7 Expected impact of Vi-TT vaccines on transmission 48
1.4.8 Expected impact of Vi-TT vaccines on illness associated with typhoid 48
1.4.9 Expected impact of Vi-TT vaccines on antimicrobial resistance 49
1.4.10 Impact of COVID-19 on vaccine uptake 50
1.5 Mode of action of Vi-vaccines 51
1.5.1 Polysaccharide and polysaccharide conjugate vaccines 51
1.5.2 Cellular subsets involved in the development of antibodies 51
1.5.3 Antibody correlates of protection against typhoid fever 54
1.6 Thesis aims 57

2 GENERAL METHODS 59

2.1 Mass cytometry panel 59
2.2 Flow cytometry panel 63
2.3 Description of study samples 65
2.4 Processing of peripheral blood mononuclear cells (PBMCs) 66
2.5 Phenotyping by mass cytometry 68
2.6 Pre-processing of mass cytometry data 69
2.6.1 Debarcoding and bead normalisation 69
2.6.2 Batch correction 69
2.7 Data analysis 70
2.7.1 Clustering 71
2.7.2 Data visualisation 74
2.7.3 Statistical analysis 74

2.8 DETECTION OF VI-SPECIFIC ANTIBODY-SECRETING CELLS (ASCS) POST-VACCINATION 75

2.8.1 EX-VIVO ASSAY 75

2.8.2 MEMORY ASSAY 75

2.9 PHENOTYPING OF NK POPULATIONS BY FLOW CYTOMETRY 76

2.10 FUNCTIONAL CHARACTERISATION OF NK CELLS AFTER CHALLENGE 76

2.11 QUANTIFICATION OF SERUM CYTOKINES BY ENZYME LINKED IMMUNOSORBENT ASSAY (ELISA) 77

3 EVALUATION OF CELLULAR RESPONSES TO CONJUGATED AND UNCONJUGATED VI-VACCINES AND THEIR ASSOCIATION WITH PROTECTIVE HUMORAL IMMUNITY 79

3.1 INTRODUCTION 79

3.2 CHAPTER AIMS 80

3.3 METHODS 81

3.3.1 SOURCE OF SAMPLES 81

3.3.2 QUANTIFICATION OF VI-SPECIFIC ANTIBODY SECRETING CELLS (ASCS) 83

3.3.3 QUANTIFICATION OF VI-SPECIFIC ANTIBODY TITRES 83

3.3.4 MEASUREMENT OF VI-SPECIFIC ANTIBODY FUNCTIONS 83

3.3.5 STATISTICAL ANALYSIS 84

3.4 RESULTS 86

3.4.1 PLASMA CELLS EXPRESSING MUCOSAL MIGRATORY MARKERS DOMINATE THE RESPONSE TO VI-TT AND VI-PS 86

3.4.2 $CXCR3^+$ AND $CXCR3^-$ TFH RESPONSES ARE INDUCED BY VI-TT VACCINATION 93

3.4.3 $CD56^+$ COMPARTMENT, INCLUDING NK CELLS AND DCS, IS SIGNIFICANTLY PERTURBED BY VI-VACCINATION 93

3.4.4 CELLULAR RESPONSES STRONGLY CORRELATE WITH HUMORAL IMMUNITY IN VI-TT VACCINEES 103

3.4.5 FORMATION OF VI-SPECIFIC MEMORY B-CELLS WAS ASSOCIATED WITH CD4 T-CELL AND NK RESPONSES AFTER VI-TT VACCINATION 105

3.5 DISCUSSION 109

4 PBMC SIGNATURE OF EARLY INFECTION ASSOCIATES WITH RISK OF DEVELOPING ACUTE TYPHOID FEVER 116

4.1 INTRODUCTION 116

4.2 CHAPTER AIMS 117

4.3 METHODS 118

4.3.1 SOURCE OF SAMPLES 118

4.3.2 CYTOKINE QUANTIFICATION 118

4.3.3 ANTIBODY TITRE QUANTIFICATION AND FUNCTIONAL ANALYSIS 118

4.3.4 DIFFERENTIAL ABUNDANCE ANALYSIS 118

4.3.5 PARTIAL LEAST SQUARES DISCRIMINANT ANALYSIS (PLS-DA) 119

4.3.6 BASELINE MACHINE LEARNING METHODS 119

4.4 RESULTS 120

4.4.1 ACTIVATION OF INNATE AND ADAPTIVE SUBSETS IN PBMCS CAN BE DETECTED WITHIN 24 HOURS OF ORAL S. TYPHI INFECTION 120

4.4.2 OUTCOME OF INFECTION IS ASSOCIATED WITH THE 24-HOUR RESPONSE 126

4.4.3 VACCINATION STATUS AND ANTIBODY PROFILE IS MODESTLY ASSOCIATED WITH DEVELOPMENT OF CELLULAR IMMUNITY AFTER INFECTION 131

4.4.4 BASELINE FEATURES OF PARTICIPANT PBMC PROFILE PREDICT IMMUNE PROFILE AND OUTCOME GROUP 135

4.4.5 DETAILED CHARACTERISATION OF NK RESPONSES TO S. TYPHI INFECTION 142

4.5 DISCUSSION 149

5 ESTABLISHING CORRELATES OF DISEASE SEVERITY IN ACUTE TYPHOID FEVER AND THEIR ASSOCIATION WITH VI-VACCINATION STATUS 157

5.1 INTRODUCTION 157

5.2 CHAPTER AIMS 158

5.3 METHODS 159

5.3.1 SOURCE OF SAMPLES 159

5.3.2 SYMPTOM SCORING AND LATENT PROFILE ANALYSIS 159

5.4 RESULTS 161

5.4.1 BLOOD COUNT RATIOS ARE SIGNIFICANTLY PERTURBED BY DEVELOPMENT OF ACUTE TYPHOID FEVER 161

5.4.2 NEUTROPHIL: LYMPHOCYTE RATIO (NLR) AND EOSINOPHIL: LYMPHOCYTE RATIO (ELR) ARE INDEPENDENT, IMMUNOLOGICAL BIOMARKERS OF SYMPTOM SEVERITY IN HUMAN CHALLENGE MODEL PARTICIPANTS WITH ACUTE TYPHOID FEVER 164

5.4.3 NLR AND ELR ARE MODULATED BY VACCINATION STATUS AND ARE ASSOCIATED WITH PRE-CHALLENGE LEVELS OF VI-IGG1 TITRES 169

5.5 DISCUSSION 173

6 ACUTE PHASE PBMC RESPONSES CLASSIFY HEALTHY FROM DIAGNOSED PARTICIPANTS WITH TYPHOID FEVER. 179

6.1 INTRODUCTION 179

6.2 CHAPTER AIMS 180

6.3 METHODS 181

6.3.1 SOURCE OF SAMPLES 181

6.3.2 MASS CYTOMETRY 181

6.3.3 CYTOKINE MEASUREMENTS 181

6.3.4 DIFFERENTIAL ABUNDANCE ANALYSIS 181

6.3.5 MACHINE LEARNING 181

6.4 RESULTS 183

6.4.1 GLOBAL PBMC COMPOSITION IS PERTURBED BY THE DEVELOPMENT OF CLINICAL DISEASE 183

6.4.2 DESCRIPTIVE ANALYSIS OF PBMC RESPONSES AT ACUTE INFECTION 187

6.4.3 PBMC RESPONSES CLASSIFY HEALTHY AND DIAGNOSED SAMPLES 193

6.4.4 ASSOCIATION OF ALTERED POPULATIONS WITH CLINICAL PHENOTYPES 197

6.5 DISCUSSION 203

7 FINAL DISCUSSION 211

7.1 SUMMARY OF KEY FINDINGS 211

7.1.1 PRIMARY CELLULAR IMMUNE RESPONSES TO VI-VACCINES CORRELATE WITH DEVELOPMENT OF SEROLOGICAL FUNCTIONS AND MEMORY B-CELL GENERATION. 211

7.1.2 DISTINCT IMMUNOLOGICAL PROFILES ARE DETECTABLE WITHIN 24 HOURS OF INFECTION AND HAVE DIFFERENTIAL ASSOCIATIONS WITH OUTCOME OF CHALLENGE. 212

7.1.3 VI-VACCINATION AMELIORATES PRESENTATION OF TYPHOID FEVER 213

7.1.4 T-CELL SIGNATURE CLASSIFIES HEALTHY AND DIAGNOSED PARTICIPANTS WHILST AN INNATE IMMUNE SIGNATURE AT DIAGNOSIS IS PREDICTIVE OF BACTERIAL CLEARANCE 214

7.2 LIMITATIONS OF THE STUDY 215

7.2.1 OXFORD CHALLENGE MODEL COHORTS - RELEVANCE TO ENDEMIC SETTINGS 215

7.2.2 REPRESENTATIVE CHALLENGE DOSE AND STRAIN 216

7.2.3 DIAGNOSTIC CRITERIA AND RAPID INITIATION OF TREATMENT FOLLOWING DIAGNOSIS 217

7.2.4 CONTRIBUTIONS OF TISSUE IMMUNITY 217

7.3 FUTURE DIRECTIONS 219

7.3.1 INVESTIGATION OF THE MECHANISTIC ROLE OF NK CELLS IN MEMORY B-CELL FORMATION AFTER GLYCOCONJUGATE VACCINATION 219

7.3.2 MECHANISTIC ROLE FOR IDENTIFIED SUBSETS IN PROTECTION FROM ACUTE TYPHOID FEVER 219

7.3.3 CONTRIBUTION OF MUCOSAL IMMUNITY TO PROTECTION 220

7.3.4 EVALUATION OF BASELINE PBMC DIFFERENCES 221

7.3.5 COMPARISON OF BLOOD SIGNATURES WITH OTHER DISEASES 221

7.3.6 DEVELOPMENT OF A COMPOSITE PROGNOSTIC MARKER FOR TYPHOID FEVER MANAGEMENT 223

7.3.7 ROLE OF GRANULOCYTE COMPARTMENT IN INFECTION 223

7.4 CONTRIBUTION TO THE FIELD AND FINAL CONCLUSIONS 225

8 BIBLIOGRAPHY 227

List of Figures

Figure 2.1. Schematic diagram showing the timepoints at which samples were collected following vaccination and challenge for mass cytometry analysis.....67

Figure 2.2. Schematic of sample batching and inclusion of healthy donor control.....69

Figure 2.3. Examples of clustering evaluation metric plots. 73

Figure 2.4. Schematic of NK cytotoxicity assay assessing functions of cryopreserved NK cells after challenge.....77

Figure 3.1 Evaluation of plasma cell phenotype post-vaccination. 88

Figure 3.2. Plasma cell composition in peripheral blood pre- and post-vaccination.....89

Figure 3.3. UMAP visualisation of plasma cell compartment.....90

Figure 3.4. Changes in plasma cell frequency after Vi-vaccination. 91

Figure 3.5. Ex vivo Vi-IgG ASC response after vaccination. 92

Figure 3.6. Evaluation of Tfh phenotype post-vaccination. 95

Figure 3.7. UMAP visualisation of $CD4^+$ $CXCR5^+$ T-cell response to vaccination. 96

Figure 3.8. Changes in T-cell frequency after Vi-vaccination. 97

Figure 3.9. Evaluation of $CD56^+$ clusters phenotype post-vaccination. 98

Figure 3.10. PCA plots of differentially expressed $CD56^+$clusters after Vi-vaccination. 99

Figure 3.11. Changes in $CD56^+$ cluster frequency after Vi-vaccination. 100

Figure 3.12. Log2FC in $CD56^+$ cluster frequencies from baseline.....101

Figure 3.13. Activation status of $CD56^+$ DCs.....102

Figure 3.14. Associations between antibody functions and cellular immunity. 104

Figure 3.15. Evaluation of high and low memory responders to Vi-TT vaccination. 106

Figure 3.16. Differences in cellular profile to Vi-TT immunisation between high and low memory responders.....107

Figure 3.17. Relationship between NK cells and Tfh after Vi-TT vaccination.....108

Figure 4.1. Differential abundance of PBMC subsets at 24 hours after oral infection with S. Typhi infection.....122

Figure 4.2. NK compartment is significantly altered by infection with S. Typhi. 123
Figure 4.3. Change in frequency of pDCs after challenge.....124
Figure 4.4. Changes in Th17 cells after challenge.....125
Figure 4.5. PLS-DA analysis reveals clusters of participants with differential likelihoods of diagnosis. 128
Figure 4.6. Evaluation of cellular immunity associated with protective profile.....129
Figure 4.7. Evaluation of cellular immunity associated with a susceptible profile. 130
Figure 4.8. Effect of vaccination on development of cellular immunity. 133
Figure 4.9. Differences in Vi-antibody function between immune profiles. 134
Figure 4.10. PBMC composition stability over one month. 138
Figure 4.11. Prediction of outcome using baseline PBMC composition. 139
Figure 4.12. Evaluation of association between B-cell and CD4-T-cell composition at baseline and immune profile after challenge. 140
Figure 4.13. Correlation between baseline frequency of B-cell subsets and participant age. Colour indicates immune profile. 141
Figure 4.14. Effect of cryopreservation on NK cell cytotoxicity. 144
Figure 4.15. Effect of incubation time and overnight rest on NK cell cytotoxicity. 145
Figure 4.16. Evaluation of NK phenotype after overnight rest. 146
Figure 4.17. NK phenotyping antibody titrations. 147
Figure 4.18. Example of NK phenotyping from one donor. (A) 148
Figure 5.1. Blood count perturbation at development of acute disease. 162
Figure 5.2. Evaluation of potential confounding factors in blood count ratio analysis. 163
Figure 5.3. Symptom profile analysis during acute typhoid fever.....166
Figure 5.4. Associations between ELR, NLR and definitions of disease severity. 167
Figure 5.5. ELR is strongly associated with self-reported symptom severity. 168
Figure 5.6. Prevalence of symptoms in Vi-vaccinated and unvaccinated participants with acute typhoid fever. 170
Figure 5.7. NLR is significantly lowered by Vi-TT vaccination. 171

Figure 5.8. NLR at diagnosis is correlated with Vi-antibody titres. 172

Figure 6.1. Global perturbation of PBMCs at acute infection. 184

Figure 6.2. Heatmap of differentially expressed subsets at diagnosis. 185

Figure 6.3. Fold change in PBMC subsets at diagnosis. 186

Figure 6.4. Perturbation of the monocyte compartment at diagnosis. 189

Figure 6.5. Non-specific staining of monocytes at diagnosis. 190

Figure 6.6. Perturbation of the B-cell compartment at diagnosis. 191

Figure 6.7. Perturbation of NK compartment at diagnosis. 192

Figure 6.8. Development of a classifier model on diagnosed and healthy samples. 194

Figure 6.9. T-cell signature at diagnosis. 195

Figure 6.10. Phenotype of γδ T-cells at diagnosis. 196

Figure 6.11. Evaluation of cellular responses at diagnosis and clinical presentation. 202

List of Tables

Table 1.1. Summary of licenced typhoid fever vaccines. 38

Table 1.2. Typhoid fever vaccines in development and experimental vaccines 42

Table 1.3. Global Vi-vaccine usage in both routine immunisation schedules and as a travellers vaccine. 46

Table 2.1. Details of antibodies used for mass cytometry phenotyping 59

Table 2.2. Details of antibodies used for innate immunity phenotyping panels 63

Table 2.3. Characteristics of participants included in mass cytometry cohort and the VAST study overall 66

Table 2.4. Summary of subsampling outputs. 70

Table 2.5. Summary of clustering settings applied. 71

Table 3.1. Overlap of samples across mass cytometry, ELISpot and serology data sets. 81

Table 4.1. Baseline inflammatory status prior to challenge. 137

Table 6.1. Univariate statistical testing for associations between leukocyte response and clinical presentation of typhoid fever. 198

Abbreviations

Abbreviation	Definition
S. Typhi	*Salmonella enterica* serovar Typhi
WASH	Water, sanitation and hygiene
HIMC	Human Immune Monitoring Center, Stanford University
HCM	Human challenge model
VAST	Vaccines against *Salmonella* Typhi
Vi-TT	Vi-tetanus toxoid conjugate vaccine
Vi-PS	Vi-unconjugated polysaccharide vaccine
MenACWY	Meningococcal vaccine against serotypes A, C, W and Y; control vaccine
Ctrl	MenACWY vaccinated individuals
D-28	28 days prior to challenge; day of vaccination
D-21	21 days prior to challenge; 7 days post-vaccination
D0	Day of challenge; 28 days after vaccination
D1	1 day after challenge
D2	2 days after challenge
D4	4 days after challenge
D7	7 days after challenge
TD	Typhoid fever diagnosed
nTD	No diagnosis of typhoid fever; protected
PBMC	Peripheral blood mononuclear cell
CFU	Colony forming units
ASC	Antibody secreting cell
NK cell	Natural Killer cell
ICS	Intracellular staining

RT	Room temperature
NBMM	Negative binomial mixture model
ELISA	Enzyme linked immunosorbent assay
XDR	Extensively drug resistant
WHO	World Health Organisation
GC	Germinal centre
Treg	CD4 regulatory T-cell
PC	Plasma cell
TI	T-cell independent
NTS	Non-typhoidal *Salmonella* disease

1 Introduction

1.1 Enteric fever

1.1.1 Global burden of infection

Enteric fever refers to a group of systemic, febrile illnesses caused by disseminated *Salmonella* infections. Aetiological causes include *Salmonella* Typhi (*S.* Typhi) and *Salmonella* Paratyphi A, B or C (*S.* Paratyphi) with S.Typhi being the most prevalent. In 2021, enteric fever remains endemic in numerous countries around the world particularly in regions of South East Asia and Africa[1]. In 2017, global incidence was estimated at 3.4 and 10.9 million cases of paratyphoid and typhoid fever respectively[2]. The greatest mortality and disease-associated disability is borne by young children, with peak estimated incidence occurring in children between 5 and 9 years of age. The social and economic impact of enteric fever is considerable; reported financial loss and burden on family members for affected households is substantial and made worse in hospitalised cases of disease[3].

Arriving at an accurate estimation of enteric fever burden is complicated although numerous estimates of incidence have been published[4–8]. It is assumed that hospitalised cases of enteric fever represent a fraction of the true burden as many in community settings have the means to self-treat with over-the-counter antibiotics[9]. An additional problem in accurately estimating burden is the poor performance of the most commonly used diagnostics. Blood culture continues to be the mainstay of *S.* Typhi and *S.* Paratyphi identification. Whilst the advent of automated blood culture systems (e.g. BACTEC) has significantly improved sensitivity, still only an estimated 61% of cases are detected[10]. Culture of bone marrow aspirates is significantly more sensitive (~91%) and considered the reference standard, however the necessary lumbar puncture involved limits its use and increases testing refusals[11]. Difficulties with accurately accounting for these factors, combined with a historically limited number of multi-centre surveillance studies, mean that estimates of enteric fever burden are likely to be an underestimate of cases.

Despite these limitations, huge progress has been made in our understanding of enteric fever epidemiology via improved surveillance studies and sophisticated modelling estimates (an excellent review of this progression is provided here[12]). Whilst overall case numbers over the last 20 years are declining, worrying increases in antimicrobial resistance have been observed. At present, considerable resources are being invested in enteric fever elimination measures ranging from sanitary reform to diagnostics and vaccination. Effective elimination will require a combination of all these measures.

1.2 Challenges for enteric fever research

Study of *S.* Typhi and *S.* Paratyphi pathogenesis and protective host responses has proven challenging. Typhoidal *Salmonella* serovars have a highly restrictive host tropism and, as such, cannot productively infect mice. Chimpanzees represent the only higher primate permissive to S. Typhi infection[13], however their endangered status ultimately precludes their use in research. Therefore, extrapolations from studies of murine *Salmonella* Typhimurium infection have been extensively used in lieu of an appropriate experimental model. The murine *S.* Typhimurium infection model has been heavily used due to an approximately similar presentation to typhoid fever in humans. Commonalities include development of fever, primary invasion at Peyer's patches, evidence of a predominantly mononuclear leukocyte infiltrate in the intestine, development of intestinal lesions and bacterial replication in the liver and spleen. The genetic background in mice confers differing susceptibility to infection, with C57BL/6 and BALB/c mice developing a lethal infection within a few weeks of challenge. High susceptibility in C57BL/6 and BALB/c strains is due to a mutation found within the cation transporter gene *Slc11a1* (Nramp1), leading to expression of a defective iron transporter in macrophage phagosomes[14]. The mutation prevents removal of critical ions from pathogen-containing phagosomes, allowing pathogen replication to progress unhindered[15]. Other mouse strains such as Sv129S6 and CBA have no mutation in this transporter and therefore develop a milder infection.

Ease of use and low cost have led to the predominance of the S. Typhimurium model in enteric fever research. However, clear differences in S. Typhimurium-host interactions exist between mouse and man. *S.* Typhimurium infection is a prevalent cause of gastroenteritis in humans, an attribute which is not observed during murine infection[16]. Furthermore, *S.* Typhimurium does not cause systemic bacteraemia or typhoid fever in immunocompetent humans. Therefore, the degree with which findings from the *S.* Typhimurium model can be directly applied to human disease is not entirely certain.

Over the past 12 years, efforts to improve upon or establish complementary *in vivo* and *in vitro* systems for the study of *Salmonella* pathogenesis have been made, some of which have conferred new insight and advanced our understanding of typhoid fever in humans. A brief overview of some of these developments and their caveats is provided prior to discussing pathogenesis in detail and host mechanisms of protection.

1.2.1 TLR11 knockout mice

An alternative model to *S.* Typhimurium infection was proposed in 2012 when mice deficient in TLR11 were shown to be susceptible to *S.* Typhi infection[17]. Mutation of TLR11, a murine TLR receptor absent in humans, was shown to be critical for resistance to *S.* Typhi infection at the epithelial barrier. These mice were substantially more immunocompetent that other efforts to create a *S.* Typhi-susceptible mouse model (i.e. a single-rather than multiple gene knockout, minimising potential for off-target effects), making it a promising system for evaluation of vaccine candidates. However, subsequent publications cast considerable doubt on the usefulness of this model, demonstrating that murine susceptibility to *S.* Typhi infection was highly variable[17,18]. In addition, these later studies present opposing findings regarding the recognition of flagellin by TLR11. Whilst disappointing, other efforts have shown promise for greater impact.

1.2.2 Humanised mice

More recently, humanised mice have been used as tools to clarify the importance of various *S.* Typhi virulence factors in establishing infection[19]. Several papers have reported the

use of humanised mice in studies of haematopoiesis, cancer and immune functions against human-restricted pathogens. Deletion of genes including a DNA-dependent protein kinase catalytic subunit and IL-2 receptor gamma led to severe combined immunodeficiency - SCID - in humans and mice. This phenotype is characterised by complete deficiency of mature T-cells, B-cells NK cells and complement, whilst dendritic cells and macrophages are present but defective. Engraftment of human haematopoietic stem cells in mice with SCID allows for development of human immune cells and in turn makes mice permissive to infection with human restricted pathogens such as *S.* Typhi[20,21]. Whilst this represents an attractive investigative tool in animal research, whether the complexity of human immune responses are truly recapitulated is still under debate (extensively reviewed here[22]). Of particular importance to research of enteric pathogens, reconstitution of gut associated lymphoid tissue and the microbiota in humanised mice has proven problematic[23]. Given the importance of the microbiota in immune regulation, it is of critical importance that this aspect is carefully considered.

1.2.3 Organoids and tissue culture

The first self-renewing intestinal organoid cultures were developed in 2009[24] and the merits of these systems in *Salmonella* research have been extensively reviewed here[25]. $Lgr5^+$ stem cells isolated from either small or large intestinal biopsies are differentiated into three-dimensional cultures of epithelial cells arranged in the crypt-villus formation. Cultures can also be generated from induced pluripotent stem cells, relegating the need for biopsies. All epithelial cells are represented in these cultures including M-cells, the specialised cell type overlying Peyer's patches and gut-associated lymphoid tissue, highly permissive to *S.* Typhi infection[26]. These 3D cultures recapitulate the physical organisation of the intestinal epithelium, providing a more representative *ex vivo* model than epithelial cell lines for researchers to explore enteric infection. These models are particularly useful for studying initial host-pathogen interactions[27] early after infection and bacterial virulence factors during invasion. Difficulties with accessing the intestinal tract in humans make these models an attractive alternative.

The major limitation of this system is the lack of organised lymphoid tissue (lymph nodes, Peyer's patches) associated with the epithelial layer. Intraepithelial lymphocytes such as T-cells are also absent. Therefore, study of leukocyte responses to infection cannot assessed in these models. In addition, organoid cultures fail to completely capture the *in vivo* effects of the mucus lining on host-pathogen interactions despite having functional goblet cells in their epithelium[28].

1.2.4 Human challenge models

An ideal option is the study of *S.* Typhi in human hosts. In 2009, the Oxford Vaccine Group developed a human challenge model of *S.* Typhi infection whereby healthy volunteers are infected with an antibiotic-susceptible strain of *S.* Typhi and closely monitored until development of disease – diagnosed either by the presence of a persistent fever or a positive blood culture, or in the absence of disease 14 days. The Oxford model shares common features with a series of enteric fever human challenge models used in the 1960s and 1970s at the University of Maryland[29]. These provided valuable insights into the importance of various *S.* Typhi virulence factors[30], intestinal histopathology[31] and association between infectious dose and disease[32]. Over the past 12 years, the Oxford model has been extensively used to study the early stages of pathogenesis and evaluate vaccine efficacy[33–41].

This model gives a unique opportunity to study protective mechanisms against *S.* Typhi in its natural host. Importantly, pathogenesis prior to the development of symptoms can be evaluated, something that is not possible in cohort studies in endemic settings. Furthermore, associations between early immunological responses and protection from symptomatic disease can be assessed. This in turns offers an opportunity to better understand infection and inform design of therapeutics such as vaccines.

There are two main limitations to the Oxford typhoid challenge model. Rapid administration of antibiotics upon diagnosis of infection differs from a typical infection in the field. The impact of this on development of adaptive memory responses is unclear and may impede their study in challenge models. Participants in challenge studies (adults, predominantly

ethnically white, raised in an industrialised country) are not representative of individuals most exposed to typhoid fever. Whilst there are clear ethical and practical reasons for these differences, the impact of these differences on host responses is unknown.

In-depth knowledge of pathogen-host interactions is essential for broadening our understanding of disease progression and protective mechanisms. In sum, a range of model systems have gained prominence within enteric fever research over the past decade which serve to complement our knowledge of *Salmonella* pathogenesis.

1.3 Pathogenesis of typhoid fever

1.3.1 Evolution of pathogen

The aetiological cause of typhoid fever is *Salmonella* Typhi. Infection is typified by bacterial dissemination from the gastrointestinal tract and replication within extraintestinal niches. This phenotype departs significantly from the presentation of non-typhoidal *Salmonella* infections in which patients present with self-limiting gastritis. In addition, typhoidal *Salmonella* serovars are significantly more restricted in terms of host tropism, only causing infections in humans[42]. Host restriction is largely attributed to loss of function mutations and formation of pseudogenes in the *S.* Typhi genome (approximately 4.1% of the genome)[43] which comprise a significantly higher proportion in comparison with *S.* Typhimurium (1%)[44]. *S.* Typhi expresses a number of virulence factors that confer significant advantages in invasion and survival within human hosts.

1.3.2 Invasion of intestinal epithelia

S. Typhi infects human hosts via contaminated food and drinking water. Whilst the majority of bacteria are eliminated in the stomach after consumption, the surviving bacilli progress to the gastrointestinal tract and cause disease. Bacterial motility and chemotaxis are mediated by flagella; insertion mutations rendering *S.* Typhi strains immotile were associated with significantly lower invasiveness[45]. Bacterial adhesion to the epithelial cell surface is also a critical step in pathogenesis. Fimbriae form filamentous protrusions that enable bacterial attachment to the epithelial cell surface; deletions in fimbrial gene clusters were shown to significantly lower *Salmonella* adherence and infection of epithelial cell lines *in vitro*[46].

Salmonella infection targets a number of cell types in the intestinal epithelium during invasion. In the murine typhoid model, experiments conducted in the early 1990s found that microfold cells (M-cells) within the follicle-associated epithelium were highly permissive points of invasion in the intestinal epithelial layer[47]. Progressive destruction of M-cells during infection lead to infection of adjacent enterocytes. However, more recent electron microscopy

studies using organoids have suggested that direct infection of enterocytes is also possible indicating that traversal of the intestinal epithelium can occur via multiple routes[48].

A key factor required for invasiveness is the type III secretion system (T3SS)-1 which is essential for virulence in the *S.* Typhimurium model. Encoded by Salmonella Pathogenicity Island-1 (SPI-1), this needle-like complex is required for translocation of bacterial effector proteins into the cytosol or cell membrane of target host cells. Here, effector proteins modulate actin polymerisation of the cytoskeleton. This has the effect creating protrusions or "ruffling" of the cell membrane[49,50]. In particular, actin-binding protein, SipA is integral to this process and increases bacterial uptake. Flagella may also play a role in this process; strains with genetic variation in flagella showed significant heterogeneity in ability to induce membrane ruffling and invasion in epithelial cells[51]. Optimal invasive conditions and virulence factor expression requires high osmolarity of the local environment[52].

1.3.3 Dissemination

Invasive bacteria are typically internalised by tissue-resident macrophages and dendritic cells in the subepithelial dome of Peyer's patches, either by phagocytosis or T3SS-mediated entry. Subsequent establishment of a systemic infection can be mediated by progression to the lymphatic system including mesenteric lymph nodes (MLNs). Dissemination of bacteria to the MLNs can occur either extracellularly or within $CCR7^+$ dendritic cells[53]. Alternatively, and through poorly understood mechanisms, bacteria gain entry to the blood where they spread to extraintestinal sites including bone marrow, liver, spleen and gall bladder. Populations involved in this process are ill-defined although it is believed that monocytes or $CD18^+$ phagocytes are likely actors[54].

The development of fever and other symptoms during disseminated *Salmonella* infections is primarily thought to be due to sensing of LPS followed by release of endogenous pyrogens[55]. Cytokines – IL-1, TNFα and IL-6 – are all characteristic of typhoid fever and are readily detectable in febrile patients[56]. High levels of endogenous pyrogens have been linked to worsened prognosis[57].

1.3.4 Replication at disseminated sites

Salmonella continues to replicate within phagocytic cells at disseminated sites. Early electron microscopy studies of infected HeLa cells demonstrated internalised *Salmonella* were contained with vacuoles in the cytosol[58]. The integrity of the vacuole is maintained by the T3SS-2 effector protein, SifA, encoded by SPI-2. Deletion of *sifA* inhibited bacterial sequestration[59]. SifA is also critical for inhibiting lysosome function and ensuring bacterial survival[60].

Approximately 5% of *S.* Typhi infections develop into a state of chronic carriage, largely through colonisation of the gallbladder and formation of biofilms[61]. Individuals with gallstones are at particularly high risk. Biofilm formation complicates treatment options as bacteria are resistant to antibiotic clearance[62]. Other virulence factors such as the typhoid toxin may also play a role in development of chronic persistence of *Salmonella*[63] whilst having minimal impact on the progression of early typhoid fever in humans or humanised mice[19,64].

One of the key determinants of pathogen survival is acquisition of nutrients, of which iron is especially important. Iron is key for *Salmonella* growth and proliferation[65]. Regulators of iron homeostasis, such as the ferric uptake regulator (Fur) superfamily, are highly conserved between *S.* Typhimurium and typhoidal *Salmonella* serovars, underlining their importance in pathogen virulence and survival[66]. *S.* Typhi in particular appears to be especially affect by iron restriction. Fur deletion in *S.* Typhi was found to lead to significantly poorer uptake and replication within macrophages *in vitro*[65]. The iron-chelating molecule, salmochelin siderophore was critical for pathogen fitness and dissemination in a genome-wide analysis of *S.* Typhi virulence factors in humanised mice[19].

1.3.5 Role of Vi-antigen

One of the most abundantly expressed virulence factors expressed by *S.* Typhi is the capsular polysaccharide or Vi antigen. Vi has a dynamic expression profile that is variable

depending on osmolarity of the local environment. As mentioned previously, high osmolarity (as is the case in the intestinal lumen) is required for optimal adherence and invasion of the intestinal epithelium[52,67]. Vi expression is low in high osmolar conditions and is dramatically increased by transition to a low osmolar environment (such as the intestinal epithelium)[68] therefore suggesting that Vi expression is mostly beneficial after invasion.

Expression of the Vi capsule minimises innate immune detection by masking other antigens such as LPS and flagella following invasion[69]. Masking of LPS has been shown to facilitate *S.* Typhi replication and survival within macrophages and suppress TNFα production[70,71]. In addition, serum-mediated killing via complement deposition is lower against *S.* Typhi in comparison with other *Salmonella* serovars such as *S.* Typhimurium. Phagocytosis of *S.* Typhi is significantly reduced indicating greater resistance to clearance mechanisms than Vi^- strains of *Salmonella*[72,73].

Despite these advantages, Vi expression is not an absolute requirement for bacterial dissemination. Although lower in prevalence, Vi^- strains have been detected in peripheral blood of typhoid fever patients[74–77]. Engineered Vi^- strains were found to have greater sensitivity to serum-mediated killing although were still capable of causing symptomatic infection and bacteraemia in infected volunteers[78]. In addition, other typhoidal *Salmonella* serovars such as S. Paratyphi A, do not express Vi but cause systemic disease. A recent study found that long-chain LPS on the surface of *S.* Paratyphi A conferred serum resistance similarly to Vi suggesting a possible convergent evolutionary mechanism of immune evasion[79].

1.3.6 Protective host responses to Salmonella infection: innate immunity

1.3.6.1 NK cells

Early bacterial containment is likely to rely on a number of simultaneous responses although the murine *S*. Typhimurium model has consistently highlighted the importance of IFNγ. Initial exponential growth of *Salmonella* in spleen or liver begins to plateau one week post-infection in CBA mice whereas IFNγ$^{-/-}$ mice fail to control growth of the bacterial population and die after 7-8 days[80]. The depletion of CD4 and CD8 T-cells does not influence bacterial control within the first 2 weeks of infection in WT mice[81], suggesting a T-cell independent source of IFNγ at early stages of disease is involved in containment. The NK cell response to virally-infected and malignant cells is well-reported, and there is growing appreciation for a role for NKs in intracellular bacterial infections. NK cells can be broadly divided on the basis of CD56 expression into two functionally distinctive subsets. CD56^{bright} NK cells are major cytokine producers and make up approximately 5-15% of the peripheral blood NK compartment. The remaining CD56^{dim} NK cells are a CD16-expressing subset capable of both natural and antibody-dependent cytotoxicity by release of perforin and granzymes[82].

NK cells have demonstrable *in vitro* anti-bacterial activity against a number of bacterial species including *S*. Typhi[83]. Several studies have identified LPS as one of the critical antigens required for NK activation[84,85] as O-antigen deficient bacterial strains fail to elicit significant IFNγ and TNFα production in infected mice. NK recognition of *S*. Typhi-infected cells also relies on activity of protein tyrosine kinases and protein kinase-C as blockade of enzymatic activity impairs identification of infected cells[86]. NK activity against *Salmonella* is highly dependent on monocyte-derived signals[84]; upregulation of early activation marker CD69 (critical for cytolytic activity) was impaired in infection of monocyte-depleted PBMC cultures. Both pro-inflammatory cytokine release and degranulation in response to infected monocytic cell lines have been reported[87].

Evidence for a protective role of NK cells against *S.* Typhimiurium *in vivo* has also been confirmed. The lethality of IFNγ deficiency was recapitulated in mice whose NK compartment had been depleted ($Thy1^+$ $CD4^-$ $CD8^-$), suggesting NK cells are crucial sources of early IFNγ with a major role in survival[88,89]. Another study found that murine *S.* Typhimurium infection induced an upregulation of NK chemoattractant production by the intestinal mucosa in an IL-18 dependent manner, a process that drove substantial chemotaxis of NK cells to the lamina propria[90]. Given the differences in host interactions between *Salmonella* serovars as described above, it is unclear whether a similar chemokine response to *S.* Typhi infection would be observed in humans. Release of IL-18 from the lamina propria has not been reported in organoid studies of *S.* Typhi infection although a comprehensive overview of NK-activating cytokines and chemoattractants was not the focus of this study[48]. IL-12 and IL-18 are essential for *in vitro* IFNγ production by NK cells in response to *Salmonella*-infected macrophages[89]. A highly comprehensive study of NK recognition of S. Typhimurium infected macrophages suggests NK effector functions can productively contribute to clearance of infection[89].
A couple of factors limit our understanding of NK involvement in *Salmonella* infection. Study of NK *in vitro* responses were largely performed using *S.* Typhimurium or Vi-negative strains of Ty2 therefore, it is unclear how expression of Vi alters NK recognition of infected cells and their subsequent activity. In addition, the drivers of NK chemotaxis or the site within the body where they exert their effector function has not been studied.

1.3.6.2 Monocytes

The role of monocytes in *Salmonella* infection is complex. They have been reported both as effectors involved in clearance of infection and as vectors for bacterial dissemination from the gut.

Inflammatory monocytes rapidly accumulate in the MLNs following oral infection with *S.* Typhimurium[91]. The mechanism of recruitment has not been elucidated, however, entry to the lymph node was shown to be independent of MadCAM-1 (ligand for CD62L, α4β7 and

VLA-4)[91]. Monocytes in this study produced the majority of iNOS and TNFα when compared to infiltrating neutrophils days after infection. In addition, they were also significant producers of IL-1β and suggesting a key role in bacterial containment. Studies in mice have largely focused on pro-inflammatory monocyte responses to *Salmonella* infection. Roles for other subsets such as intermediate and non-classical monocytes are not clearly established. $CD16^+$ monocytes including intermediate monocytes have been shown to expand significantly during infectious disease and are the major responders to bacterial and intracellular infections in humans, including HIV, TB and bacterial sepsis[92]. Intermediate monocytes can be rapidly mobilised to the lymph nodes following inflammatory stimulus[93] indicating a role in systemic immunity. In this study, expression of pro-inflammatory genes such as *IL-1b, IL-6, TNFa* and *TGFb* by infiltrating monocytes was significantly enriched. Whether these subsets play a role in clearance of *Salmonella* is unclear from literature.

In addition to effector functions, monocytic cells have been found to propagate *S.* Typhimurium dissemination in mice. $CD11c^+CX_3CR1^+$ dendritic cells are thought to be the primary cell type responsible for bacterial transport to the MLNs[94] although there is now considerable evidence for extracellular movement of bacteria. Dissemination to extraintestinal sites can be mediated by $CD18^+$ blood phagocytes[54,95]. More specific subset identification has not been performed although it is generally though that these represent monocytes[96] given that monocytes can traffic in and out of tissues to sample antigens without differentiating[97].

Monocyte responses during typhoid fever have been investigated. Monocytosis is characteristic of acute disease although our understanding of what happens prior to development of symptoms and any role in early containment has not been evaluated. Monocyte capacity to recognise S. Typhi was within 24 hours of infection in the Oxford typhoid human challenge model, although upregulation of activation markers, CD40 and CD38, did not occur until development of acute disease[36]. Investigating the involvement of monocytes in driving systemic bacteraemia in humans is complicated by relatively low frequency of bacilli detectable in peripheral blood. Whilst primary bacteraemia is detectable within 24 of infection by PCR[98],

blood culture methods are not sensitive enough to identify disseminating bacteria until at least 36-hours post-infection.

1.3.6.3 Neutrophils

Biopsy examinations have shown neutrophils are largely absent from the intestinal leukocyte infiltrate of acute typhoid fever patients which corroborates with the relatively mild gastrointestinal symptoms. Some influx at acute disease has been suggested by studies of hospitalised patients. Levels of calprotectin, a clinical biomarker of neutrophil-mediated inflammation, are elevated in stool and plasma of those with PCR-confirmed typhoid including fever[99].

The role of neutrophils in early typhoid fever in humans is less well characterised. Neutrophils have well-documented roles in preventing systemic bacteraemia of non-typhoidal *Salmonella* disease (NTS). NTS bacteraemia is rare in immunocompetent individuals, however, neutropenia is a significant risk factor for invasive NTS disease[100]. The rapid systemic dissemination of *S*. Typhi in contrast to a typical NTS infection is thought to be due to subversion of the neutrophil response. In intestinal organoids, *S*. Typhi elicits a significantly attenuated cytokine profile compared with *S*. Typhimurium[48]. Transcriptional profiling of infected organoids found the neutrophil chemoattractant CXCL1 was poorly upregulated after *S*. Typhi infection[101]. In addition, IL-8 (neutrophil chemoattractant) and TNFa (synergistic enhancer of neutrophil recruitment) expression were similar for *S*. Typhi-infected and uninfected organoids while strongly induced after *S*. Typhimurium infection[48]. This study also found *S*. Typhi infection caused significant polarisation with the few detectable cytokine responses showing an apical rather than basolateral release pattern. While *in vitro* data suggests that *S.* Typhimruium responses are stronger, signals for neutrophil chemotaxis are detectable in human *S.* Typhi infection; in the challenge model CXCL1 rises in serum within 12 hours of infection[102].

Dampening of neutrophil chemotaxis in typhoid relative to NTS is largely attributed to the Vi polysaccharide capsule, encoded by *viaB* locus. The capsule impairs innate immune recognition via a number of mechanisms. *Salmonella* antigens such as LPS and flagellin are

masked by Vi, preventing TLR-mediated activation[103]. Another mechanism is impairment of complement deposition and activation of the alternative pathway. This potently impedes neutrophil opsonophagocytosis, as well as the release of neutrophil chemokines.

1.3.7 Protective host responses to Salmonella infection: adaptive responses

Adaptive immunity is essential for long-term protection against infection. There has been great interest in the development of *Salmonella*-specific adaptive immunity given the implications for effective vaccine design. Concepts taken from research into adaptive immunity in the *S.* Typhimurium model conducted in 1980s and 1990s has formed the foundation of many vaccine design efforts that have been investigated over the last 20 years.

1.3.7.1 T-cells: CD4 Th1 and CD8 responses

CD4 Th1 responses have been repeatedly shown to be critical for the clearance of *Salmonella* infection in mice[104–106]. Th1 responses are activated *in vivo* by antigen presentation of bacterial epitopes on MHC class II molecules, and genetic variants in *HLA-DRB1* are strongly associated with enteric fever susceptibility in humans[107]. Dendritic cell accumulation in the Peyer's patches is essential for triggering $CD4^+$ T-cell responses as early as 6 hours after infection in mice[108]. In mice, activated $CD8a^+$ DCs prime naïve CD4 responses via MHC-TCR ligation, leading to secretion of IL-12. Production of IL-12 by antigen presenting cells is the essential step in driving T-cell-mediated IFNγ production. The importance of the Th1 pathway in protection of the host during *Salmonella* infection is evident in those with deficiencies in IL-12R expression who experience far greater disease severity and recurrent *Salmonella* and Mycobacterial infections[109]. During systemic salmonellosis, several Th1 related cytokines, including IFNγ, IL-12, IL-15 and IL-18, were shown to be increased in the serum of infected patients compared with healthy controls[110]. Gastrointestinal-restricted forms of *Salmonella* infection also caused an increase in IFNγ and IL-12 but had less effect on IL-15 and IL-18, suggesting these cytokines are triggered in response to the systemic phase of infection. IL-15, IL-12 and IL-18 are all upregulated within 12 hours of infection in human challenge model participants (Barton et al. unpublished observations) showing successful triggering of Th1 responses.

Despite many reports of strong T cell activation during infection *in vivo*, some studies have shown that *S.* Typhimurium can modulate MHC antigen presentation, inhibiting the development of T-cell responses against key *Salmonella* antigens[89,111,112]. Proposed mechanisms of inhibition include secretion of SPI-2 effector proteins that inhibit lysosomal maturation, and modulation of the number of MHC molecules reaching the cell surface. Another suggestion is that *Salmonella* replicates poorly once intracellular, lowering the quantity of antigen available to the cell for presentation[108]. Interestingly, the mechanism of bacterial internalisation and the infectious dose both appear to influence activation of T-cell responses. Phagocytosis of bacteria via Fc-mediated mechanisms increases antigen presentation and activation of CD4 responses in comparison with antibody-independent uptake[113] .This highlights a augmentative role for antibodies in boosting T-cell responses. Activation of T-cell responses depends on infectious dose of the inoculum with low doses failing to induce CD4 activation against flagellin[114].

The role of cytotoxic CD8 T-cells is less clear. Early studies of *Salmonella aroA* mutants suggested a modest, auxiliary role for $CD8^+$ T-cell responses in protection[106]. More recently, others have shown an unexpected role of MHC haplotype in triggering CTL IFNγ production[115]. Increased IFNγ production appeared to associate with improved outcome although the overall contribution of the CD8 response is still very small in comparison to that of CD4 T cells. Poor activation of CTL responses has been associated with poor priming largely due to localisation of *Salmonella* within the phagosome. *In vitro*-infected dendritic cells were unable to stimulate CD8 or CD4 T cell proliferation[116]. This report also suggested that cell-free bacteria had a contact-dependent inhibitory effect on T-cell activation. Other reports have shown that in comparison to another intracellular pathogen *Listeria monocytogenes*, the expansion and contraction of CTL responses to *Salmonella* is significantly delayed[117]. The authors note that even effector memory responses expand slowly, suggesting suboptimal priming. Inhibition of antigen presentation was suggested to not be an active process; *S.* Typhimurium was shown to proliferate poorly intracellularly which in turn may explain poor presentation[118]. Another mechanism suggested to contribute to delay in CD8 activation was

expression of exhaustion markers; one study found that *Salmonella*-infected DCs and B-cells express high levels of PD-1 ligands[119]. Blockade of these ligands restored CD8 proliferative capacity.

Data from human challenge studies have not provided support for delayed CTL activation as is seen in animal models. Fresnay *et al*. identified *Salmonella*-specific CTL responses in peripheral blood 2 days after diagnosis[34]. CTL responses including IL-17-producing subsets have also been identified after immunisation with Ty21a[120]. However, their association with protection from disease is unclear in seemingly conflicting reports[35,121], baseline *Salmonella*-specific CTL responses were associated with both worsened and improved clinical outcomes in different participant cohorts. More investigation into a role for CTL in response to *S.* Typhi exposure/infection is needed.

1.3.7.2 B-cells and antibodies

Whilst the importance of IFNγ and the Th1 response in elimination of intracellular infections is clearly established, a role for antibodies has been less straightforward to elucidate. Vaccination of genetically susceptible mice with an attenuated *S.* Typhimurium strain robustly induces *Salmonella*-specific antibodies. However, passive transfer of serum into naïve animals was not sufficient for protection. A combination of memory CD4 T-cells responses and serum were necessary for control of bacterial growth[122,123]. Both high and low affinity *Salmonella*-specific IgG2 antibodies were effectively shown to impede bacterial growth in macrophages of the spleen[124] although they were insufficient for clearance. Beyond antibody production, accessory functions of B-cells have also been described; depletion of B-cells led to suboptimal priming of the Th1 response in mice, suggesting B-cell antigen presentation is a key mechanism in the development of T-cell-mediated immunity[125–127].

Studies of humans have also shown that *Salmonella* infections productively induce a wide range of antibody responses. Serological surveys in endemic populations and data from human challenge models have provided extensive profiles of the antibodies elicited by

infection, with responses raised against flagellin, OmpA, HlyE, sipC, and LPS being common[128,129]. Responses to LPS during natural infection have been suggested to be critical for protection against reinfection. In a human challenge study in Maryland, individuals vaccinated with a Ty21a strain with high O-antigen expression had displayed greater resistance to disease than those receiving a low O-antigen expressing vaccine strain[130]. In contrast a more recent study failed to find an association between protection against rechallenge and LPS humoral immunity[131] therefore the relationship remains unclear.

Despite being a major virulence factor, antibody responses to the Vi capsular polysaccharide are rare after a single exposure; this is evident both in challenge model participants and studies of endemic populations where Vi antibody titres gradually increase with age, presumably with repeated exposures[132,133]. Weak induction of Vi antibody during infection may be the result of subversive mechanisms employed by *S.* Typhi to evade clearance, and a contributor to poor acquisition of natural immunity. Notably, chronic carriers have abnormally high levels of Vi-antibodies reaffirming that persistent exposure is necessary for the development of this response[134,135]. The importance of Vi-antibodies in protection against typhoid fever is undeniable given the huge success of Vi vaccines[40].

Antibody mediated clearance involves innate effector functions such as phagocytosis and antibody-dependent cellular cytotoxicity (ADCC) and requires cell types such as neutrophils, monocytes and NKs. A comprehensive study of vaccine-induced Vi-antibodies found robust induction of innate effector functions and associations with protection[136]. Whether naturally occurring Vi-antibodies induced after multiple exposures induce similar functional responses is unknown. In the context of *S.* Typhi infection, the extracellular position of bacteria at the mucosal surface and during transit to phagocytes below the epithelium places the bacteria available for the action of antibody-mediated killing processes. Mucosal antibody is known to be critical for containment of several pathogens and prevention/minimisation of systemic dissemination[137]. However, evaluation of mucosal antibody at the gastrointestinal surface is difficult and whether parenteral Vi vaccine-induced antibody has an effector role at the mucosal surface is unknown.

The relevance of protective mechanisms identified in model systems of enteric fever to the human pathology is a complex question to address. Furthermore, understanding of how these mechanisms can be modulated (or induced) by clinical intervention such as vaccination is of interest. Understanding of this second point confers a more detailed, mechanistic insight into the effect of therapeutics on immune responses to infection. This knowledge can in turn serve the development of better immunisations. The elimination of enteric fever in endemic settings will demand a multi-faceted approach, in which efficacious vaccines will play a key role.

1.4 Typhoid fever elimination: effective strategies for disease control

1.4.1 Evidence from historical accounts of typhoid elimination in industrialised countries

The elimination of typhoid presents a challenging task, requiring multiple strategies, both in the intermediate- and long- term. This section aims to establish the context for use of typhoid fever vaccines as part of wider efforts to break transmission and alleviate disease burden in endemic settings.

Secure provision of safe drinking water and adequate waste handling has demonstrably reduced the burden of enteric infection in industrialised countries, therefore similar efforts will be necessary in developing nations to end long-cycle transmission. The impact of water, sanitation and hygiene (or WASH) reforms have been assessed from historical accounts of elimination[138]. In Britain, the "great sanitary awakening" of the late 19th and early 20th centuries involved numerous of these interventions including the creation of closed sewerage systems for waste handling and the introduction of drinking water filtration and chlorination[139]. The effects of these measures, whilst largely examined through the lens of cholera, had substantial impact on all waterborne diseases including typhoid.

Obstacles to effective sanitary reforms in developing countries are both financial and logistical although the effect of these investments on disease rates is clear. Towards the end of the 19th century in Britain, marked expansion in financing of sanitation infrastructure (41% on average of the budget of local governing bodies) led to approximated a 30% decline in mortality, including near elimination of mortality attributable to waterborne diseases [140]. Re-emergence of cases in Britain following this sharp decline around the turn of the century have been largely attributed to lapses in water decontamination. Localised outbreaks of enteric fever since the introduction of sanitary reforms, most notably in Croydon, Maidenhead and Bolton highlights the critical role for water sterilisation in halting the spread of cases[141].Collectively, these observations exemplify the importance of sanitary intervention but also the considerable expense required to achieve them.

1.4.2 The current state of water and sanitation in typhoid endemic countries

Issues with regards to waste handling and water contamination, similar to those in Britain prior to major sanitary reforms, drive transmission in endemic settings today. Repeated exposure to untreated human waste is a major driver of typhoid transmission as can be seen from geographical clustering of cases; households in close proximity to open drains report the greatest incidences of typhoid[142,143]. A study examining the relationship between domestic sanitation and disease incidence reported that children in households with toilets discharging directly into open drains had almost four times greater incidence of enteric infection that children in other households[142]. Seasonal factors which affect transmission such as increased rainfall also seem to disproportionately affect those living in closest proximity to open drains[143].

Reducing faecal exposure by water purification is another strategy for curbing rates of enteric infection. Typically, households in regions endemic for typhoid fever do not rely on piped, chlorinated water as their primary supply and this is generally associated with increased socioeconomic status[144–146]. Piped water supplies are more common in urban areas than in rural areas. Major sources of drinking water include tube wells and boreholes, with largest prevalence of these methods in rural settings. Water purification in typhoid endemic settings is generally not centralised and is predominantly achieved by boiling. Surveys suggest these practices are at best inconsistently applied; in Demographic and Health Surveys conducted in Pakistan, India, Bangledesh and Nepal, the proportion of individuals who routinely treated their water prior to consumption was found to be extremely low[144–146]. Overall, rates of water treatment were lower in rural versus urban settings. The impact of consistent water treatment on rates of enteric infection is difficult to assess in isolation. However, as part of a wider strategy to reduce faecal exposure in at-risk populations, increasing adherence to water purification practices is likely to have a considerable impact of disease prevalence.

1.4.3 Challenges to WASH reform: feasibility and alternative measures

The improvements in sanitation required to make a tangible impact on disease are considerable. A number of practical and social factors can greatly limit progress in efforts to improve sanitation in typhoid endemic settings. Building of private household toilet facilities is hampered by constraints on space in urban housing, particularly informal housing such as slums. In addition, piping of chlorinated water into households demands a considerable overhaul in infrastructure that frequently comes at considerable cost. Without appropriate tools to reveal which (often hugely costly) sanitary measures will have the greatest benefits, policy makers are often left hesitating on which reforms to pursue.

Overcoming entrenched social attitudes towards sanitation is another hurdle. In India, open defecation is practiced with relative frequency compared to other neighbouring countries. Whilst results from the most recent DHS survey suggests a slow shift in attitudes away from this practice, it remains relatively widespread, particularly in rural settings. Attitudes towards the importance of water purification are also problematic and require time and effective, educational interventions to overcome. These challenges require considerable investment and time in order to achieve reduction of disease. Therefore, other more intermediate term solutions are required. One of the most efficient and effective of these is vaccination.

Table 1.1. Summary of licenced typhoid fever vaccines.

VACCINE	**FORMULATION**	**VACCINE TYPE**	**SCHEDULE**	**EFFICACY ESTIMATE**	**WHO PRE-QUALIFIED?**	**USAGE (ACCORDING TO WHO WEBSITE)**
TY21A (BERNA BIOTECH, LTD)	Capsule	Live attenuated	3-doses	67%[147] 62%[148] 42%[149]	No	Travellers
VI-PS (TYPHIM-VI, SANOFI PASTEUR)	Parenteral	Polysaccharide	1-dose	81%[150] 55%[151]	Yes	Travellers; at-risk groups; food handlers
VI-PS (TYPHERIX)				60%[152]		

VI-PS (VAX-TYVI, FINLAY INSTITUTE)				72%[153]		
VI-PS (ZERITYPH INJ, BORYUNG)						
VI-PS (TYPHO-VI, BIOMED)						
VI-PS (TYPHEVAC INJ, SHANGHAI						

INSTITUTE OF BIOLOGICAL PRODUCTS)						
VI-PS (TYPBAR, BHARAT BIOTECH)						
VI-REPA (LANZHOU INSTITUTE)	Parenteral	Glycoconjugate	1-dose	91%[154]	No	China only
VI-TT (TYPBAR-TCV, BHARAT BIOTECH)	Parenteral	Glycoconjugate	1-dose	55%[40] 89%[155]	Yes	Travellers Routine immunisation
VI-CRM197 (TYPHIBEV,	Parenteral	Glycoconjugate	1-dose	Licensed in non-inferiority study[156]	Yes	Travellers Routine immunisation

BIOLOGICAL E LIMITED)						

Table 1.2. Typhoid fever vaccines in development and experimental vaccines

VACCINE	FORMULATION	VACCINE TYPE	SCHEDULE	STAGE OF DEVELOPMENT	NUMBER OF PARTICIPANTS	SEROCONVERSION (%) IGG RESPONSE
M01ZH09	Oral	Live attenuated	1-dose	Phase II	187	62.2-86.1% (4 cohorts)[157]
VI-DT (SK CHEMICALS CO., LTD)	Parenteral	Glycoconjugate	2-dose	Phase I	144	81.2% (1st dose) 84.5% (2nd dose)[158]
TY800 (CELLDEX THERAPEUTICS)	Oral	Live attenuated	1-dose		11	NA[159]
CVD 906	Oral	Live attenuated	1-dose	Phase I	9	89%[160]
CVD 908	Oral	Live attenuated	1-dose	Phase I	36	
CVD 906-HTRA	Oral	Live attenuated	1-dose	Phase II	36	63-83%[161]
CVD 908-HTRA	Oral	Live attenuated	1-dose	Phase II	36	63-83%[162]

CVD 909	Oral	Live attenuated	1-dose	Phase I	32	63%[162]

1.4.4 The role for vaccination in the elimination of typhoid fever

Typhoid fever elimination efforts have been accelerated by the development and implementation of effective vaccines. In the case of *S.* Typhi, efficacious vaccines already exist and progress towards introduction over that past few years has gathered pace (see Table 1.1). Whilst much research has been conducted into other types of vaccine in the context of typhoid fever (Table 1.2), this discussion will specifically focus on Vi-vaccines. Vi-vaccines target the capsular antigen, Vi (virulence factor), expressed on the surface of *S.* Typhi. Expression of Vi is critical for bacterial invasion of the intestinal mucosa and evasion of the innate immune response. Two broad categories of Vi-vaccines have been developed; Vi-polysaccharide vaccines (Vi-PS), containing the purified Vi antigen, and Vi-conjugate vaccines (Vi-TCV), containing the purified Vi-antigen conjugated to a carrier protein. As of February 2021, two Vi-TCVs; Vi-TT (Bharat Biotech) and Vi-CRM197 (Biological E Limited); have received WHO pre-qualification for use in infants as young as 6 months of age[40,163].

1.4.5 Efficacy of Vi-vaccines

Both Vi-TT and Vi-PS have been proven to be highly effective in clinical trials (Table 1.1). In a human challenge model, Vi-TT had an estimated efficacy of 54·6% compared with unvaccinated controls[40]. A larger, randomised control trial (RCT) of 20,000 individuals in Nepal gave a higher estimate of 89%[155]. A further report from the Sindh province of Pakistan reported 89% efficacy in vaccinated children aged between 6 months and 10 years[164] in line with the Nepal trial. These data are encouraging and suggest high potential for impact on disease. Whilst Vi-PS also exhibits reasonable efficacy, the greater immunogenicity of Vi-TT (particularly in young children) and generation of immunological memory are factors that strongly favour glycoconjugates for implementation. The differing modes of action of these vaccines will be discussed in detail below.

Despite promising efficacy estimates, vaccine implementation still faces a number of challenges. These include precuring financial support, detailed study regarding the most

effective type of immunisation program and mitigating the effects of the COVID-19 pandemic. At time of writing, the impact of the pandemic on immunisation access is unquantified however, Vi-TT coverage, along with other childhood immunisations, is likely to be significantly affected.

1.4.6 Usage of Vi-vaccines in immunisation programs

Prior to the outbreak of COVID-19, implementation of Vi-TCVs in endemic settings was slowly becoming reality (Table 1.3). Several international organisations have pledged financial backing for Vi-TCV introduction. As of February 2021, Gavi, The Vaccine Alliance has dedicated financial support for Vi-TT introduction in three countries - Pakistan, Liberia and Zimbabwe[165]. Following outbreaks of extensively drug resistant (XDR) typhoid in Karachi and Hyderabad in 2016, Pakistan became the first country to introduce an emergency Vi-TT vaccination campaign targeting 200,000 children in the Singh province[166]. This was followed by a catch-up campaign in November 2019 of more than 10 million children.

Table 1.3. Global Vi-vaccine usage in both routine immunisation schedules and as a travellers vaccine. Information taken from the World Health Organisation website.

COUNTRY	VACCINE	SCHEDULE	COMMENTS	KNOWN COVID IMPACT
CHAD	Vi-TT	9 months		
LIBERIA	Vi-TT	9 months	Planned introduction for April 2020	Delayed introduction
MAURITIUS	Vi-TT	9 months	Travellers	
ZIMBABWE	Vi-TT	9 months	From June 2020 – and during outbreak response	Delayed introduction
CUBA	Vi-PS	10, 13, 16 years	At-risk groups	
USA	Vi-PS	2 years	At-risk groups	
BAHRAIN	Vi-PS	>= 2 years	Travellers; at-risk groups	
KUWAIT	Vi-PS		Food handlers	
UAE	Vi-TT		Travellers; at-risk groups	
BOSNIA AND HERZEGOVINA	Vi-PS		Travellers	
CYPRUS	Vi-TT		Travellers	
ISRAEL	Vi-TT		Travellers	
KAZAKHSTAN	Vi-PS		At-risk groups by occupation	
PORTUGAL	Vi-TT		Travellers	
ROMANIA	Vi-PS		Travellers	

SAN MARINO	Vi-TT		Travellers	
SERBIA	Vi-PS		Travellers	
SPAIN	Vi-TT		Travellers	
LAO PEOPLE'S DEMOCRATIC REPUBLIC	Vi-TT		not routine	
MALAYSIA	Vi-PS		Food handlers	
REPUBLIC OF KOREA	Vi-PS		At-risk groups	
SAMOA	Vi-TT		Planned introduction from April 2020	Delayed introduction
RUSSIAN FEDERATION		3 years, 18 years	Administered at 3 years of age and adults, with subsequent booster dose every 3 years	

1.4.7 Expected impact of Vi-TT vaccines on transmission

Prior to COVID-19, several publications estimated the impact of Vi-TCV implementation on transmission with optimism for substantial impact. The optimal vaccination strategy has been modelled in densely populated urban settings where the R_0 is high. Pitzer el al.[167] using a vaccine efficacy of 95% found that Vi-TCV intervention programs at school age were highly effective at reducing burden particularly when combined with a catch-up scheme for 6–15-year-olds. The same study also found vaccination during infancy (9 months) has a substantial impact on transmission.

This study further highlighted that the two major unknowns, the effect of vaccination on carriers and the contribution of carriers to transmission, are likely to significantly influence the results resulting in a major area of uncertainty to be addressed. The contribution of the human reservoir to transmission in endemic settings is hard to quantify. It is thought that carriers have a considerable impact in low-incidence settings and drive short-cycle transmission/explosive outbreaks. Impact in settings where the environmental reservoir is considerable is unclear although it is suggested to be low. Field data are necessary to evaluate this further.

This study also found that more aggressive vaccination programs were not sufficient to eliminate typhoid completely[167]. A more recent analysis using Vi-TT efficacy data generated from Jin *et al.*[40] found that the most cost-effective strategy for Vi-TT implementation involved routine immunisation of infants at 9 months followed by a catch up program for 6-15 year olds. This was the case for the majority of countries included in the analysis and benefits could be derived from a threshold of $200 USD per disability adjusted life year (DALY) averted[168]. Combined, these studies indicate a substantial benefit of Vi-TCV introduction.

1.4.8 Expected impact of Vi-TT vaccines on illness associated with typhoid

Beyond transmission, vaccination strategies may also contribute to reductions in symptomatic disease. The ramifications for this, in terms of reduced burden on healthcare

settings, are significant when the contribution of *S.* Typhi to febrile disease in these regions is considered. In a systematic review of infectious aetiologies of fever in Southeast Asia over the last 20 years, typhoid (4% of cases) was found to be the second most common cause in both inpatient and outpatient departments[169]. *S.* Typhi has been consistently observed as major causes of bacterial febrile illness in Asia for several decades[170]. S. Typhi has also been found as a major contributor to febrile illness and bloodstream infections across Africa[171].

Data for understanding the effect of vaccination on acute disease are scarce although human challenge models provide some insights. Jin *et al.* found that typhoid symptom scores were considerably lower in adults vaccinated with Vi-TT compared with Vi-PS and control arm participants[40]. Critically, a significant impact on fever was observed; 16% of those receiving Vi-TT developed fever compared with 31% of Vi-PS and 55% of control arm participants. Peak C-reactive protein (CRP) was lower in the Vi-TT arm of the trial compared with the Vi-PS and control arms, and fewer overall symptoms were reported. The impact of Vi-TT vaccination on more severe complications of typhoid, such as internal bleeding and perforations, are unknown. Whilst difficult to quantify, reducing the number presentations to hospital may ease some of the healthcare costs and burden in these regions.

1.4.9 Expected impact of Vi-TT vaccines on antimicrobial resistance

Vaccination is a key public health tool being used to tackle the growing spread of antimicrobial resistance (AMR). Typhoidal *Salmonella* is under active surveillance for AMR by the WHO[172]. As has been mentioned already, increased circulation of AMR strains of *S.* Typhi in recent years was a major impetus for the introduction of Vi-TT vaccines in settings such as Pakistan[166]. With antibiotic usage rendered ineffective against these strains, an emphasis on prevention via vaccination rather than treatment is required to decelerate concerning trends in AMR prevalence. To date, Vi-TT usage has not been implemented widely enough to measure the impact of vaccination on AMR. However, evidence for vaccines reducing AMR in other diseases has been reported; introduction of pneumococcal vaccines has had demonstrable impacts on AMR[173,174].

Excess morbidity and mortality due to antimicrobial treatment failure is likely to be underreported. Some studies have found limited evidence that the number of case fatalities in multi-drug resistant (MDR) infections is greater than in cases caused by strains sensitive to antibiotics. However, several reports have found the odds of severe complications such as shock, toxicity, GI bleeding and perforation, as well as considerably greater healthcare costs and length of stay in hospital, were significantly higher in patients with MDR infections[175]. Therefore, these data underscore both the human and economic costs of rising numbers of AMR cases and the need for intervention. Reductions in transmission of typhoidal *Salmonella* and/or symptomatic disease is likely to positively contribute to overall reductions in antibiotic usage.

1.4.10 Impact of COVID-19 on vaccine uptake

Prior to the COVID-19 pandemic, demand for Vi-TCVs was expected to increase rapidly over the next few years (estimated to peak between 2023 and 2026) primarily from African nations followed by Asia[176]. The impact of the COVID-19 pandemic and associated public health measures such as stay-at-home orders on routine immunisations is unquantified at time of writing, however several global health organisations have released warnings. Gavi, the WHO and UNICEF have stated that an estimated 80 million children under one year of age are at increased risk from vaccine-preventable diseases due to the pandemic[177]. The resultant increase in morbidity and mortality is expected to have disproportionate effects on low and middle-income countries. In Africa, a benefit-risk analysis found that the benefit of maintaining routine vaccinations outweighed the risks from SARS-CoV-2 in terms of excess deaths[178] supporting calls for routine immunisations to be continued as much as possible. The effect of this on global disease prevalence is likely to be considerable. The effect of COVID-19 on progress towards typhoid fever elimination is unclear but is likely to be substantial.

1.5 Mode of action of Vi-vaccines

1.5.1 Polysaccharide and polysaccharide conjugate vaccines

Vi-TT is a polysaccharide conjugate vaccine, noted for its improved immunogenicity above plain polysaccharide immunisations[40]. Immunogenicity of conjugate vaccines is enhanced through conjugation of the polysaccharide antigen to a carrier protein, usually a toxoid[179]. At an immunological level, conjugation effectively "converts" a T-cell independent (TI) antigen into a T-cell dependent (TD) antigen, the impact of which is discussed below. Conjugate vaccines were developed in the late 1980's and have been successfully used against several childhood infections including *Haemophilus influenzae* type b (Hib), and Streptococcal and Pneumococcal infections[180]. The impact of immunisations on disease burden in the under-5s over the last 30 years is substantial; mortality in this age group, adjusted for improvements in sanitation and nutrition, has fallen by more than 57%[181]. Whilst this is clearly not all attributable to conjugate vaccines, it underscores the potential impact that vaccines could have on remaining childhood bacterial diseases such as typhoid fever.

1.5.2 Cellular subsets involved in the development of antibodies

A multitude of cellular subsets are induced by vaccination and can be readily detected in peripheral blood. The association between productive cellular responses and immunogenic vaccination has been evaluated by both reductive and systems immunology approaches. Key features of cellular immunity against vaccination are discussed below and discussed in the context of glycoconjugates.

1.5.2.1 Plasma cells (PCs)

The goal of most licensed subunit vaccines is to induce antibody production that is maintained over the lifetime of the individual. The quantity, quality and longevity of vaccine-induced antibodies is determined by a number of factors including the nature of the vaccine antigen(s). As a TI antigen, unconjugated Vi-polysaccharide induces B-cell activation and

terminal differentiation into plasma cells without germinal centre formation, known as the extrafollicular pathway[179]. TI antigens are typically non-protein antigens and can be further categorised into two groups: TI-1 antigens, which activate polyclonal B-cells through co-engagement of TLRs e.g. LPS or bacterial polysaccharides and TI-2 antigens, which activate monoclonal B-cells through cross-linking of the BCR and cannot elicit responses via other receptors such as TLRs. Vi-polysaccharide is an example of a TI-2 antigen.

The rapidity of the B-cell response against TI-2 antigens is critical for containment of encapsulated bacteria[182]. Within the B-cell compartment, two major subsets are stimulated in response to TI-2 antigens; IgM^+ IgD^+ $CD27^+$ "memory" B-cells and B1 cells[183,184]. IgM^+ IgD^+ $CD27^+$ "memory" B-cells are readily identified in peripheral blood and often referred to as circulating marginal zone (MZ) B-cells. Whilst exhibiting high expression of the memory marker, CD27 and having evidence of somatic mutations in their BCR sequences[185], these cells are not thought to be a true memory population derived from germinal centre reactions[186]. Despite their ambiguous ontogeny, these cells have a comparable transcriptional profile to splenic MZ B-cells, distinguishing them from naïve and isotype-switched memory B-cells in blood[187]. MZ B-cells isolated from blood and spleen seven days after vaccination were also shown to express identical BCRs suggesting MZ B-cell recirculation. The importance of these cells in the prevention of invasive bacterial infection is evident in young children and asplenic adults whose MZ B-cell population is significantly reduced[188]. In addition, B1 cells can also participate in the response to TI-2 antigens against encapsulated bacteria. PCs derived from this response also produce low affinity IgM antibody responses.

Whilst immunogenic, TI antigens do not stimulate adaptive memory responses and therefore plain polysaccharide vaccines require regular booster doses in order to maintain protective serological levels of antibodies. T-cell dependent (TD) antigens generally produce higher affinity antibodies and memory B-cells which are critical for long term protection against disease. B-cells activated by TD antigens migrate within the lymph node to the border between the B-cell zone and the T-cell zone where they present antigen to T follicular helper (Tfh) cells[189]. T-cell help initiates the proliferation and differentiation of B-cells into extrafollicular

PCs and germinal centre PCs. Responses peak 7-10 days post-immunisation before cells undergoing apoptosis[190]. In the context of infection, the early extrafollicular response is critical for containment of infection. The extrafollicular response is localised within the medullary cords of the lymph node[191]. The germinal centre reaction preferentially favours activated B-cells expressing BCRs with lower antigen affinity; B-cells expressing higher affinity BCRs were shown to be enriched within the extrafollicular pathway[192]. This can be indirectly assessed by the amount of antigen that activated B-cells present to Tfh cells at the B-cell: T-cell border. Higher antigen density is a key feature for predicting the degree of T-cell help received by B-cells[192]. The germinal centre pathway is the predominant mechanism for memory B-cell formation. However, memory responses against TI antigens have been found[193]. Long-lived plasma cells against a model TI-2 antigen, NP-Ficoll, and pneumococcal capsular polysaccharide P3, have been found in mice and are critical for production of IgA after vaccination[194].

1.5.2.2 CD4 T-follicular helper cells (Tfh)

Tfh are essential for the development of high-affinity antibodies following immunisation. Tfh provide help to B-cells that enter the germinal centre (GC) pathway. The degree of Tfh help appears to be dependent on a number of factors including density of antigen presented on the B-cell surface, the number of competing B-cells within the same lymph node and antigen affinity therefore B-cells recognising rare epitopes with low affinity will be disadvantaged in this process[195]. This in turn is associated with receiving lower levels of Tfh help. The "help" that Tfh give is largely a milieu of cytokine signals, the most significant being IL-21, IL-4, CD40L and CXCL13[195,196]. Given that Tfh are a tissue resident subset, study of Tfh in humans after vaccination has been generally restricted to the study of Tfh-like cells that appear in circulation approximately seven days post-immunisation, and has largely been done in the context of flu vaccines[197]. The overriding phenotype of these Tfh is CXCR3 expression, and these cells are poor B-cell helpers *in vitro*. The antibody quality of flu vaccines is generally

low, therefore it has been suggested that CXCR3^{+} Tfh may be a biomarker of poor B-cell help[198].

1.5.2.3 Natural Killer (NK) cells

NK cells can shape the development of adaptive responses. Most importantly in the context of vaccination, perforin-dependent NK responses have been associated with suppression of somatic hypermutation in the germinal centre[199,200]. Whether NK cells can be induced by polysaccharides and conjugate vaccines is unclear. Several studies have identified increased numbers of CD56^{bright} NK cells after vaccination with viral vectored vaccines. In particular, NK expansion has been found following the Ad26-Ebola vaccine that was developed and deployed during the 2015 Ebola outbreak in Africa[201]. There is also evidence of NK effector function being induced after trivalent influenza vaccines, yellow fever vaccines or generally live attenuated/whole inactivated vaccines[200]. Possible adaptive NK responses may be induced by vaccination and confer enhanced cytotoxicity during acute responses to infection. Whether these vaccines induce potent enough IL-12, IL-15 or IL-18 responses to epigenetically enhance responsiveness of NKs for subsequent challenge is unclear.

1.5.3 Antibody correlates of protection against typhoid fever

The mechanisms by which antibodies or B-cells mediate protection from *Salmonella* species is not clear. However, improving our understanding of antibody-mediated functions, inducible by vaccination, that can protect from disease is critical for design of more efficacious immunisations. In addition, understanding of antibody responses that correlate with a protective outcome are essential for vaccine licensure and accelerated product development. In the context of Vi-vaccines, a correlate of protection has not been established although Vi-IgG has long been the readout for immunogenicity trials. Several groups have sought to determine an absolute protective threshold of Vi-IgG antibodies from efficacy studies. Protective thresholds between 0.6-1.2 ug/mL[202] and 1.4 and 2 ug/mL[203] have been proposed. Seroefficacy studies in endemic settings have also found that vaccine-induced Vi-IgG antibodies associate with reduced

disease[204]. However, in a human challenge model of infection, Vi-IgG titres were comparable between those that did and did not develop disease[40]. Therefore, the search for an effective correlate is ongoing.

Beyond absolute titres, investigation of antibody quality can give mechanistic insights into vaccine efficacy. A recent study profiled Vi-antibody-mediated cellular responses and their association with outcome of infection. Neutrophil phagocytosis was significantly associated with protection from disease[136]. In comparison with non-typhoidal *Salmonellae*, avoiding neutrophil infiltration is a key mechanism in by which *S*. Typhi evades immune destruction on infection. This mechanism may be evaded by vaccination have a significant effect on outcome of disease. The isotype responsible for mediating enhanced neutrophil phagocytosis was not established in this study although Vi-IgA quantity and quality were also associated with protection[136].

Other functional characteristics of Vi-antibodies have been reported, although not formally associated with protection in humans. Bactericidal activity of Vi-antibodies in sera of volunteers immunised with Vi-PS reduced bacterial growth by 50%[205], therefore vaccination successfully induces antibodies capable of complement-mediated killing. This measure correlates with protection in the case of other bacterial vaccines such as meningococcal vaccines[206]. Whether there are differences in bactericidal activity between antibodies induced by Vi-TT and Vi-PS vaccines has not been reported. Bactericidal titres against other *S*. Typhi antigens were associated with delayed onset of disease, reduced bacterial burden and reduced disease severity in a human challenge model of disease[207]. This implies antibody-mediated complement bacterial killing may be a key mechanism in natural and vaccine-mediated protection.

Other mechanisms by which antibodies drive protection include opsonisation of bacteria which in turn enhances recognition of bacilli by innate immune cells such as macrophage and dendritic cells[208,209]. Increased uptake of opsonised bacteria by dendritic cells was found to increase antigen presentation and enhance development of Th1 responses[113]. One study has suggested that antigen-specific B-cells may also perform antibody-independent

functions that are critical for protective immunity, such as antigen presentation to or cytokine stimulation of CD4 T-cells, facilitating the development of Th1 responses[127].

Whilst researchers have captured a detailed understanding of the antibody features that correlate with protection from typhoid fever, less is known about the cellular responses to vaccination that support their development. Innate and adaptive responses to Vi-TT and Vi-PS immunisations which associate with antibody quality and the development of memory B-cell responses have not been elucidated in detail. In addition, whether disease progression is strongly altered in the presence of systemic antibodies is also not clear from previous work. However, bettering our understanding of protective host responses and the effect of vaccination on their development have clear translational interest.

1.6 Thesis aims

Results chapter 1: Evaluation of cellular responses to conjugated and unconjugated Vi-vaccines and their association with protective humoral immunity

Aim 1: to report in detail the phenotype of innate and adaptive responses to Vi-PS and Vi-TT 7 days after vaccination and compare these responses between immunisations.

Aim 2: to associate the primary cellular response to vaccination with antibody quality and formation of memory B-cells.

Results chapter 2: PBMC signature of early infection associates with risk of developing acute typhoid fever

Aim 1: to report the phenotype of cellular responses detectable in peripheral blood to *S.* Typhi infection within the first few days of infection

Aim 2: to identify a cellular signature within the first few days of infection that distinguishes individuals the develop symptomatic disease from individuals that remain well after infection with *S.* Typhi.

Aim 3: to investigate whether the magnitude or phenotype of cellular responses to infection differs between vaccinated and unvaccinated individuals.

Results chapter 3: Establishing correlates of disease severity in acute typhoid fever and their association with Vi-vaccination status

Aim 1: to investigation prognostic potential of blood count ratios at typhoid fever diagnosis as biomarkers of severity of infection (as defined by self-reported symptoms).

Aim 2: to establish any relationship between severity biomarkers and vaccination status.

Aim 3: to investigate aspects of the serological response that are associated with severity biomarkers and amelioration of symptoms.

Results chapter 4: Acute phase PBMC responses classify healthy from diagnosed participants with typhoid fever.

Aim 1: to report the differences in cellular immunity between *S.* Typhi-infected individuals that remain well after challenge and infected individuals that develop acute disease.

Aim 2: to associate immunological measures such as cellular responses and cytokines with clinical measures of disease severity.

Aim 3: to determine whether vaccination ameliorates the presentation of symptomatic disease in comparison to unvaccinated individuals.

2 General methods

2.1 Mass cytometry panel

Table 2.1. Details of antibodies used for mass cytometry phenotyping

Cocktail	Metal	Metal source	Antibody	Antibody Clone	Antibody supplier
Barcoding	89Y	Fluidigm	CD45	HI100	Fluidigm
Barcoding	102Pd	Trace Sciences	CD45	HI100	Biolegend
Barcoding	105Pd	Trace Sciences	CD45	HI100	Biolegend
Barcoding	108Pd	Trace Sciences	CD45	HI100	Biolegend
Barcoding	110Pd	Trace Sciences	CD45	HI100	Biolegend
Primary	113In	Trace Sciences	CD57	HCD57	Biolegend
Primary	115In	Sigma-Aldrich	HLA-DR	G46.6	BD
Primary	141Pr	Fluidigm	CCR6	G034E3	Fluidigm
Primary	142Nd	Fluidigm	CD19	HIB19	Fluidigm
Primary	144Nd	Fluidigm	IgG	G18-145	BD
Primary	145Nd	Fluidigm	CD4	RPA-T4	Fluidigm

Primary	146Nd	Fluidigm	IgD	IA6-2	Fluidigm
Primary	147Sm	Fluidigm	CD20	2H7	Fluidigm
Primary	148Nd	Fluidigm	IgA	G18-1	BD
Primary	149Sm	Fluidigm	CD56	NCAM16.2	Fluidigm
Primary	150Nd	Fluidigm	CD86	IT2.2	Fluidigm
Primary	151Eu	Fluidigm	ICOS	C398.4A	Fluidigm
Primary	152Sm	Fluidigm	TCRgd	11F2	Fluidigm
Primary	153Eu	Fluidigm	CD45RA	HI100	Fluidigm
Primary	154Sm	Fluidigm	CD123	9F5	BD
Primary	155Gd	Fluidigm	CD27	L128	Fluidigm
Primary	156Gd	Fluidigm	CXCR3	G025H7	Fluidigm
Primary	NA	NA	NKG2A-PE	Z199	Beckman-Coulter
Secondary	158Gd	Fluidigm	anti-PE	PE001	Biolegend
Primary	159Tb	Fluidigm	CD11c	Bu15	Fluidigm
Primary	160Gd	Fluidigm	CD14	M5E2	Fluidigm
Primary	161Dy	Fluidigm	CD26	BA5b	Fluidigm
Primary	162Dy	Fluidigm	CD8a	RPA-T8	Fluidigm

Primary	163Dy	Fluidigm	CD33	WM53	Fluidigm
Primary	164Dy	Fluidigm	CD161	HP-3G10	Fluidigm
Primary	165Ho	Fluidigm	CD127	A019D5	Fluidigm
Primary	NA	NA	CCR10-APC	1B5	BD
Secondary	166Er	Fluidigm	anti-APC	APC003	Biolegend
Primary	167Er	Fluidigm	CCR7	G043H7	Fluidigm
Primary	168Er	Fluidigm	CCR9	L053E8	Fluidigm
Primary	169Tm	Fluidigm	CD25	2A3	Fluidigm
Primary	170Er	Fluidigm	CD3	UCHT1	Fluidigm
Primary	171Yb	Fluidigm	CXCR5	RF8B2	Fluidigm
Primary	172Yb	Fluidigm	CD38	HIT2	Fluidigm
Primary	173Yb	Fluidigm	a4b7	Act1	NIH AIDS Reagent Program
Primary	174Yb	Fluidigm	PD-1	EH12.2H7	Fluidigm
Primary	175Lu	Sigma-Aldrich	CD62L	DREG200	HIMC
Primary	176Yb	Fluidigm	CLA	HECA-452	Fluidigm
Primary	209Bi	Fluidigm	CD16	3G8	Fluidigm
Live-dead	Pt195	Fluidigm		cisplatin (nat. abund.)	Fluidigm

Intercalator	Ir191	Fluidigm		Intercalator	Fluidigm
Intercalator	Ir193	Fluidigm		Intercalator	Fluidigm

2.2 Flow cytometry panel

Table 2.2. *Details of antibodies used for innate immunity phenotyping panels*

Cocktail	Fluorochome	Antibody Target	Antibody supplier
NK cell phenotyping	PE-Cy5	CD3	BD
NK cell phenotyping	PE-Cy5	CD19	BD
NK cell phenotyping	PE-Cy5	CD33	BD
NK cell phenotyping	PE-Cy5	CD123	BD
NK cell phenotyping	PE-Cy7	CD56	BD
NK cell phenotyping	AlexaFluor700	CD16	BD
NK cell phenotyping	BV480	CD11b	BD
NK cell phenotyping	BV421	NKp30	BD
NK cell phenotyping	BV650	NKG2C	BD
NK cell phenotyping	BV711	CD69	BD
NK cell phenotyping	BV786	CD62L	BD
NK cell phenotyping	FITC	CD57	BD
NK cell phenotyping	BB700	NKG2A	BD

NK cell phenotyping	PE	NKp44	BD
NK cell phenotyping	PE-Cf594	NKG2D	BD
NK cell phenotyping	APC	NKp46	BD
NK cell cytotoxicity	AlexaFluor488	IFNg	BD
NK cell cytotoxicity	BV421	CD107a	BD
NK cell cytotoxicity	APC	MIP1b	BD
NK cell cytotoxicity	PE	IL-10	Biolegend

2.3 Description of study samples

All samples described in this study were taken from a clinical trial run at the Oxford Vaccine Group between 2015 and 2017[40]. Vaccines Against *Salmonella* Typhi (VAST) was a Phase IIb clinical trial and human challenge study. The aim of this trial was to assess the efficacy of a Vi-conjugate vaccine (**Vi-TT:** Typbar-TCV, Bharat Biotech, Hyderabad, India) with an unconjugated Vi-vaccine (**Vi-PS:** TYPHIM Vi, Sanofi Pasteur, Lyon, France). Detailed enrolment criteria are provided in Jin *et al*. Briefly, enrolment criteria were designed to exclude individuals previously exposed to typhoid or its antigens; requiring no previous diagnosis of typhoid fever, no long-term residency in a typhoid-endemic setting and no prior history of typhoid vaccination. Once enrolled, individuals were randomised 1:1:1 to receive either a Vi-TT or Vi-PS vaccine, or an unrelated control vaccine (**Control:** MENVEO, GlaxoSmithKline, Sovicille, Italy). The administered control vaccine confers no immunity against *S*. Typhi and therefore this cohort remains typhoid-naïve on the day of challenge. Vaccine efficacy was assessed one month after vaccination via a controlled exposure to *S*. Typhi. Individuals were challenged with 1-5 $x10^4$ colony forming units (CFU) of bacteria. Prior to ingestion of bacteria, participants drank a bicarbonate solution to neutralise stomach acid. This process increases the number of viable bacteria reaching the ileal mucosa and able to cause a productive infection. In previous studies, this process has given an attack rate of 70% in unvaccinated individuals[210]. Peripheral blood from study participants was sampled longitudinally throughout the vaccination and challenge period.

A subset of individuals was selected for detailed analysis of their cellular response to vaccination and infection (see Table 2.3 for details of participant characteristics). The number of individuals selected from each vaccine arm and outcome group was kept as equal as possible. The proportions of diagnosed: protected individuals in this cohort does not reflect the proportions of those seen in the wider clinical trial.

Selection was based on sample availability; individuals with the most complete time series were preferentially chosen for this analysis. Table 2.3 shows that characteristics of this cohort were similar to that of the overall VAST trial.

Table 2.3. Characteristics of participants included in mass cytometry cohort and the VAST study overall.

	Ethnicity (% Caucasian)	**Age (years)**	**Sex (% female)**	**Weight (kg)**
CyTOF	55/57 (96%)	30.2	24/57 (42%)	77.8
VAST	103/112(91%)	32.1	42/112(38%)	76.0

2.4 Processing of peripheral blood mononuclear cells (PBMCs)

Individuals were sampled both after vaccination (baseline (D0), 7 days after vaccination (D7) and 28 days after vaccination (D28)) and after challenge. The interval between vaccination and challenge was 28 days (+/- 4 days). Five time points after challenge were taken at baseline, one-, two- and four-days post-infection. The final time point was either seven days after challenge in individuals that were protected from disease or day of diagnosis in individuals that developed disease (see **Figure 2.1** for overview of sampling). Only individuals in the Vi-TT and Vi-PS groups had time points from the vaccination stages included. D28 after vaccination is equal to the D0 time point in the challenge period (day of challenge). Blood samples were collected in heparinised tubes and processed to isolate PBMCs within 6 hours of collection. Briefly, PBMCs were isolated from whole blood by Ficol-Hypaque density gradient centrifugation (10 minutes, 300g). Samples were cryopreserved in liquid nitrogen until use.

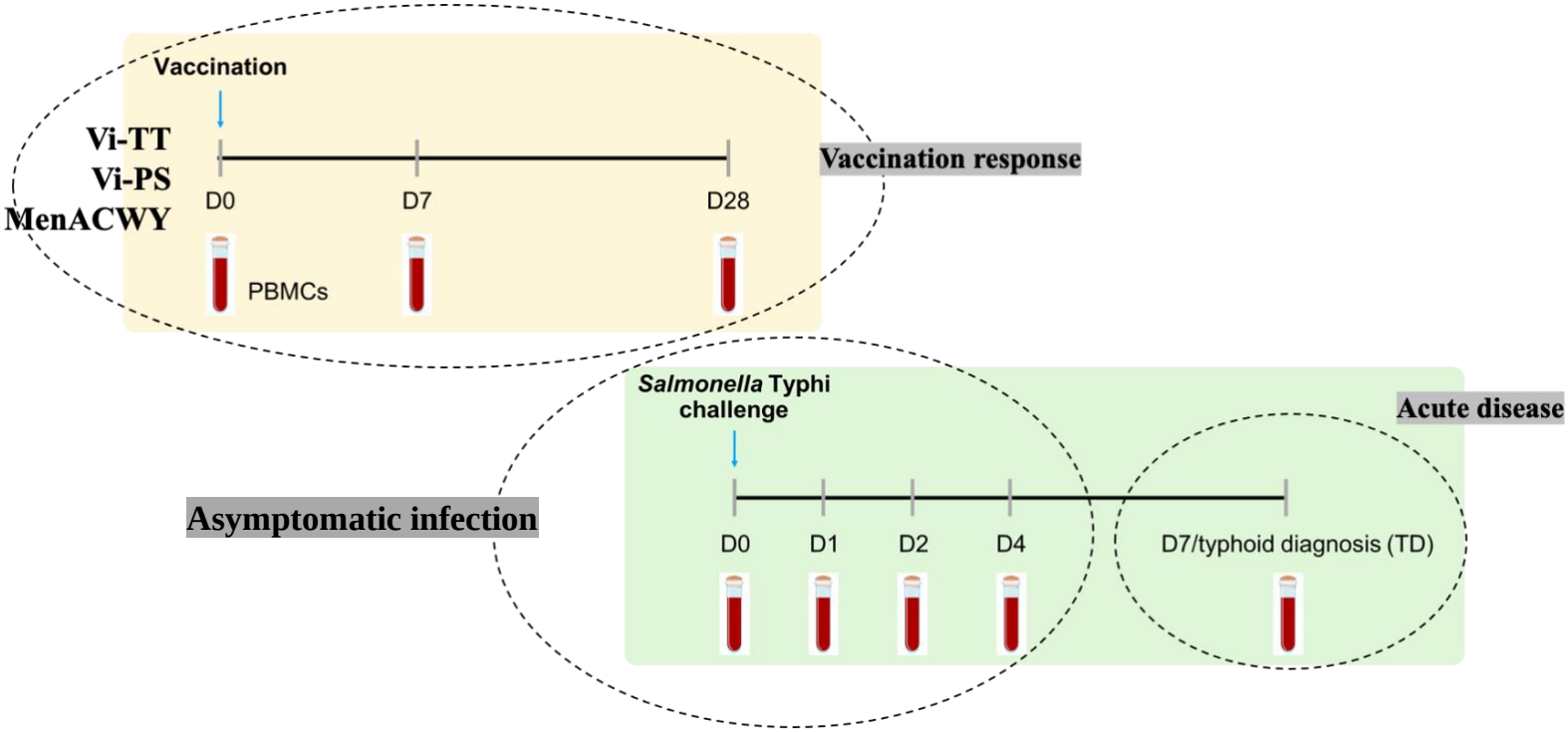


Figure 2.1. Schematic diagram showing the timepoints at which samples were collected following vaccination and challenge for mass cytometry analysis.

2.5 Phenotyping by mass cytometry

An antibody panel targeting 37 surface-expressed markers was used for phenotyping and allowed identification of all major PBMC subsets (see Table 2.1 above for details of the panel) including homing potential and activation states. Staining and data acquisition was performed at the Human Immune Monitoring Center (HIMC, Stanford University, Palo Alto, USA). A detailed staining protocol is provided in the **Error! Reference source not found.** section in the Supplementary Information).

Samples were acquired across 21 batches. PBMCs were thawed at 37°C then washed twice in RPMI with benzonase. Cell viability post-thaw was assessed by Vi-Cell (Beckman Coulter) prior to multiplexing. Each sample was uniquely barcoded with a combination of two palladium isotope-tagged CD45 antibodies prior to multiplexing; the combination of isotopes was used to delineate individual samples post-acquisition (Figure 2.2). All samples from a single study participant were added to a single tube together with a healthy donor reference sample (referred to herein as the "HIMC control") to assess batch effects. Individual samples were stained with designated barcoding cocktail at RT for 30 minutes then washed three times in CyFACS buffer. Pooled samples were stained in 50 washed three times with CyFACS buffer before incubating in 50 µL of secondary antibody cocktail at room temperature for 30 minutes. Cells were washed three times with CyFACS then stained at room temperature for a maximum of 5 minutes with cisplatin (Fluidigm, San Francisco, USA) to confirm viability and fixed in 3mL of 2% paraformaldehyde. The following day, nucleated cells were stained with an iridium intercalator (Fluidigm, San Francisco, USA) for 20 minutes at room temperature following cell permeabilisation. Finally, cells were washed three times in CyFACS and resuspended in MilliQ water with EQ normalisation beads to ~0.7 M cells/mL for acquisition on a mass cytometer. Data were acquired on Helios instruments (Fluidigm, San Francisco, USA) with an acquisition target of 250,000 events. The number of live intact singlets recovered per sample ranged from 20,000 – 150,000 events.

2.6 Pre-processing of mass cytometry data

2.6.1 Debarcoding and bead normalisation

Helios machine performance tends to diminish during acquisition; therefore, EQ normalisation beads are included to account for this source of technical variance. The Premessa R package (https://github.com/ParkerICI/premessa) was used to perform bead normalisation and debarcoding. Success of sample deconvolution was assessed in FlowJo v10.

2.6.2 Batch correction

Following debarcoding and bead normalisation, marker expression values were linearly scaled according to HIMC control sample to regress out batch-associated variance. The control sample acquired in the first batch (labelled throughout as batch 1) has been used as the study reference for all subsequently acquired batches. For each channel, the median (50th), 80th and 95th percentile signal were determined for the study reference and the HIMC control of a given batch, and a scaling factor was calculated. The method achieving the greatest reduction in variance (as measured by the median absolute deviation) in each channel was applied to the data. Full details of the method have been published[211].

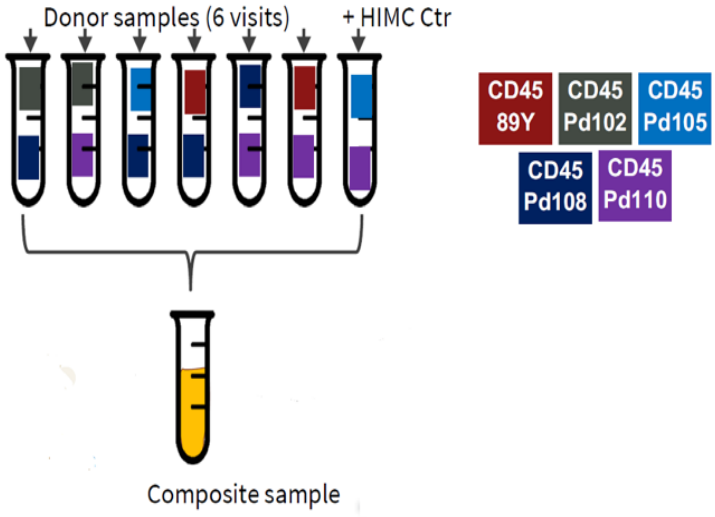


Figure 2.2. Schematic of sample batching and inclusion of healthy donor control.

2.7 Data analysis

Marker expression values were arcsinh-transformed (cofactor = 5) prior to clustering. Cell subsets (NK cells, monocytes, DCs, CD4 T-cells, CD8 T-cells, B-cells) were gated and subsampled to a user-specified cell count to ensure even input from all samples. In general, a subsampling value was chosen that was similar to the expected frequency of a given subset in PBMCs. Where there were insufficient cell numbers to obtain the user-specified subsample, subsampling with replacement was performed. To ensure representative subsamples, for each marker, median marker expression was required to fall between 90 and 110% of the original median and an interquartile range correction of 0.999. Some files were excluded from some analyses due to unsuccessful subsampling (summarised in the table below). Samples that failed to subsample (subsamples did not meet criteria above) generally had very low cell counts. See Table 2.4 for details of the numbers of successfully subsampled files and subsampling depth.

Table 2.4. Summary of subsampling outputs.

Subset	Number of gated files	Number of subsampled files	Number of cells subsampled/file
NK cells	340	324	10,000
Monocytes	340	334	15,000
DCs	340	215	2,000
CD4 T-cells	340	337	40,000
CD8 T-cells	340	339	20,000
B-cells	340	339	15,000

2.7.1 Clustering

Clustering analysis (using Kohonnen self-organising maps) was performed using the R package *FlowSOM*. Data were z-score standardised and logicle-transformed before clustering using Euclidean distance as the chosen distance metric. Subsampled files were clustered 1000 times with random seeds to determine robustness of populations identified. The most frequently identified number of k (clusters) was taken forward for further analyses (see Figure 2.3 for an example). Marker selection for clustering was based on literature searches and PCA-based non-redundancy scores (i.e. markers that explained a significant proportion of variance in data, see Figure 2.3 for an example). Chosen clustering settings are summarised in Table 2.5 to enable reproduction of presented results.

Table 2.5. Summary of clustering settings applied.

Subset	**Clustering markers**	**Chosen settings**
NK cells ($CD56^+$ events)	CD56, CD16, CD26, CD8a, CD161, CD45RA, CD27, CXCR3, NKG2A, CD127, CD57, HLA-DR, CD62L, CD11c, CD38, a4b7, PD-1	Seed = 882 *k* = 17
Monocytes ($CD33^+$ events)	CD33, CD14, CD16, CD11c, CD38, CD86, HLA-DR, CD62L, CCR7, CXCR3, a4b7	Seed = 123 *k* = 13
DCs (Lin^- $HLA\text{-}DR^+$ events)	CD11c, CD123, HLA-DR, CD38, CD86, CXCR3, CD26, CD16, CD45RA, CCR7, a4b7, CD62L	Seed = 136 *k* = 8
CD4 T-cells ($CD3^+$ $CD4^+$ events)	CD3, CD4, CD8, CD45RA, CCR7, TCRgd, CD25, CD127, PD-1, ICOS, CD38, CXCR3, CXCR5, CCR6, CCR10, CCR9, a4b7, HLA-DR, CD86, CD26	Seed = 71 *k* = 13

CD8 T-cells ($CD3^+$ $CD8^+$ events)	CD3, CD4, CD8a, CD45RA, CCR7, TCRgd, CD25, CD127, PD-1, ICOS, CD38, CXCR3, CXCR5, CCR6, CCR10, CCR9, a4b7, CD62L, CLA, HLA-DR, CD86, CD26, CD56, CD161	Seed = 88 *k* = 10
B cells ($CD19^+$events)	CD19, CD20, CD27, CD38, CD45RA, CCR7, CXCR3, HLA-DR, CXCR5, CCR6, CD62L, IgA, IgG, IgD, a4b7, CD86, CD25, PD-1	Seed = 140 *k* = 16

Cluster compactness and separation was assessed using Silhouette coefficients (see Figure 2.3 for an example). Confirmation of some clustering results was performed by manual gating in FlowJo v10.

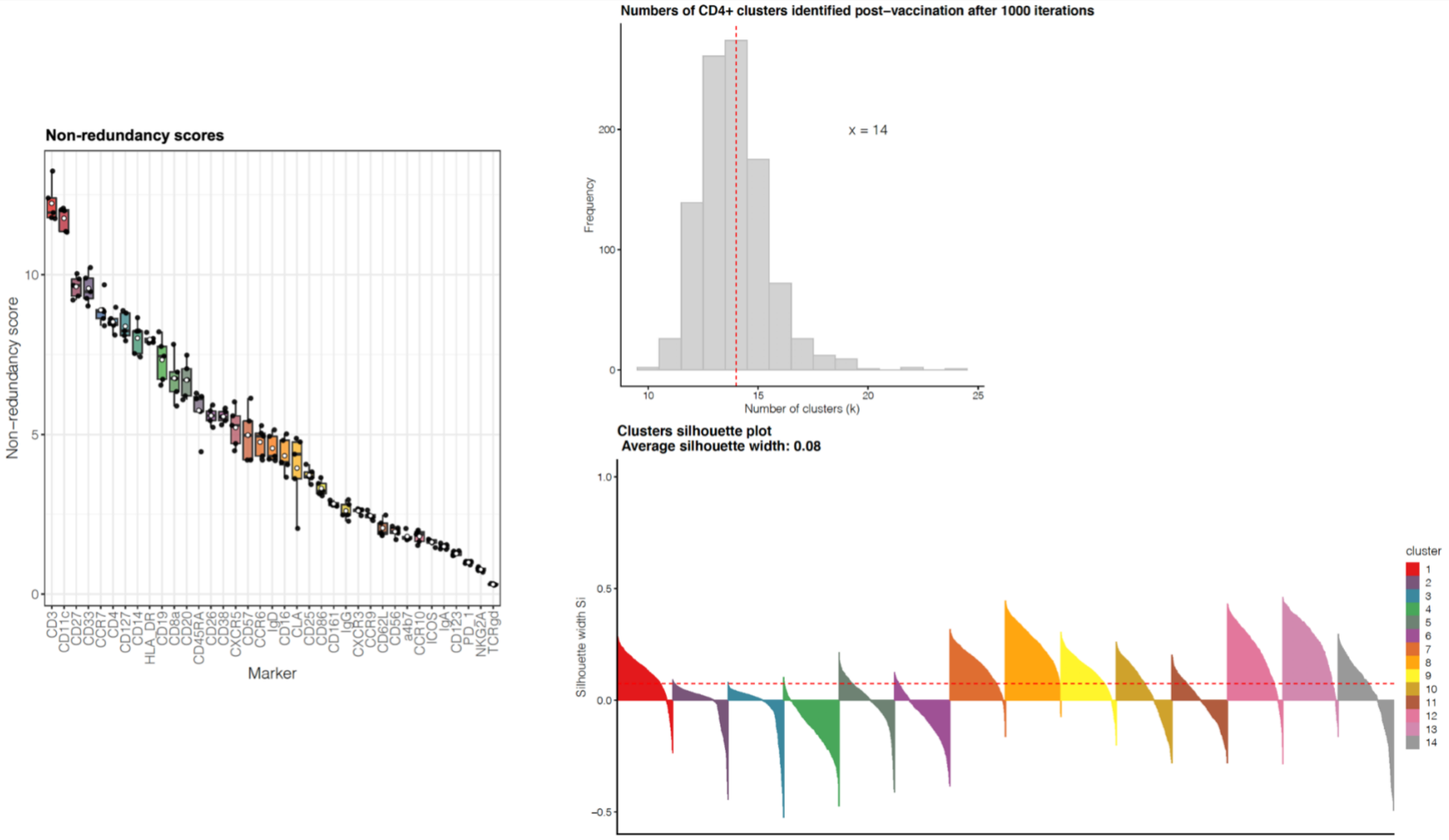


Figure 2.3. Examples of clustering evaluation metric plots. (A) Non-redundancy scores used to identify markers explaining highest proportion of variance in data. (B) Histogram showing number of clusters identified after 1000 repeats using a range of random seeds. (C) Evaluation of cluster compactness was performed using Silhouette widths. Subsample of 1000 events per cluster is visualised

2.7.2 Data visualisation

Arcsinh-transformed, median marker expression for each cluster was visualised using heatmaps. Marker enrichment scores for a given cluster (in comparison to the entire subset) was calculated using the *MEM* package[212]. PCA analysis (*stats* package) was visualised by timepoint, vaccine and outcome. Non-redundancy scores were calculated for each marker using principal component loadings according to the formula outlined in Levine *et al*[213]. Data were visualised by UMAP (*uwot* package); chosen settings were selected to give the best separation of rare subsets (see Table 2.5 for settings). Count generation, marker expression transformation and plotting were all performed using various *tidyverse* packages.

2.7.3 Statistical analysis

More detailed statistical methods are provided in the relevant chapters. Cluster counts, as a proportion of cells of the same lineage e.g. B-cells, were modelled using negative binomial mixture models (NBMMs) to identify populations differentially expressed during the course of vaccination and infection. Frequencies were modelled as the dependent variable with timepoint and other predictors included to evaluate differential expression. Participant ID was included as a random effect to model within-participant variability and model the over-dispersion of cluster proportions.

Univariate comparisons between study groups (e.g. outcome of infection, vaccine arm) were made for each subset identified via clustering using Wilcox sum-rank tests, with a Bonferroni correction applied to all p-values (FDR of 0.05 used to define significance). Dimensionality reduction techniques such as UMAP and PCA were included to Machine learning methods using count data are presented in the relevant chapters.

2.8 Detection of Vi-specific antibody-secreting cells (ASCs) post-vaccination

Vi-IgG-specific ASCs and memory B-cells were enumerated by ELISpot (MabTech, Nacka Strand, Sweden) pre-vaccination and at days 7, 10 and 28 post-vaccination.

2.8.1 Ex-vivo assay

Briefly, 96-well multiscreen filter plates were blocked with Vi-polysaccharide (Vi-polysaccharide, 12/244, NIBSC, Potters Bar, UK) at a concentration of 10ug/ml. Wells blocked with total Ig (anti-IgG, anti-IgA and anti-IgM) or sterile PBS served as positive and negative controls respectively. Plates were incubated overnight at 4°C. Plates were washed with sterile PBS five times (200 µL/well) and conditioned with complete media (RPMI supplemented with 10% heat inactivated foetal bovine serum, 1% L-glutamine, 1% penicillin/streptomycin, 1% MEM Non-essential amino acids, 1% sodium pyruvate, 0.1% b-mercaptoethanol) for at least 30 minutes prior to use. PBMC samples were thawed and washed twice in warmed RPMI with 2 µL benzonase added for the first wash (centrifugation at 300g for 10 minutes). Cells were counted twice on the Muse Cell Analyser (Merck Millipore, Darmstadt, Germany). All wells were loaded with $2x10^5$ PBMCs (3 Vi-coated wells, 3 negative controls and 3 positive controls per sample) and incubated at 37°C with 5% CO_2 and 95% humidity overnight. Plates were developed the next day with alkaline phosphatase-conjugated secondary antibodies and substrate development kits (Bio-Rad Laboratories Ltd, Watford, UK). Spots were measured using AID ELR03 ELISpot reader (Autoimmun Diagnostika, Strasburg, Germany). Samples for which no response was observed in the positive control wells were excluded from analysis. Data are presented as the number of ASCs per million, calculated by subtracting the mean signal in the PBS wells from the mean of the antigen-containing wells.

2.8.2 Memory assay

PBMC samples were thawed and washed as described above then plated on a 96-well U-bottom plate at $2x10^5$ cells per well. Cells were stimulated using mixture of R848 and IL-2 (MabTech, Nacka Strand, Sweden) for 3 days at 37°C with 5%CO_2 and 95% humidity. Following stimulation the assay is performed as described above.

2.9 Phenotyping of NK populations by flow cytometry

An NK phenotyping panel was developed to investigate responses observed after challenge in more detail. Table **2.2** gives details of the markers included. PBMCs were thawed at 37°C and washed twice in RPMI with benzonase. Sample viability and cell count were assessed by Muse cell analyzer (Merck Millipore, Darmstadt, Germany); cell count was adjusted to $2x10^7$ cells/mL. Fifty microlitres of sample was added to wells of a V-bottom plate (3 wells per sample). 50 µL of NK antibody staining cocktail was added to each well. Samples were incubated in the dark at room temperature for 30 minutes. Samples were washed twice in autoMACS running buffer (Miltenyi Biotec, Bergisch Gladbach, Germany) before fixing with 2% paraformaldehyde (BD Biosciences, USA). Data were acquired on the BD Fortessa.

2.10 Functional characterisation of NK cells after challenge

Functionality of NK populations were assessed in a flow-cytometry based cytotoxicity assay (see Figure 2.4 for schematic overview). PBMCs were thawed as described previously and total NK cells were isolated by autoMACS separation. NK cells (40,000 cells per sample) were stimulated for four hours (37°C, 5% CO_2) together with a target cell line (K562) at a target: effector ratio of 1:1, IL-2 (final concentration: 100 U/ml) and IL-15 (final concentration: 10 ng/ml). NK cells only and NK cells with PMA/ionomycin stimulation were included as negative and positive controls respectively. Anti-CD107a antibody was added to stimulation mix prior to incubation. NK cytokine/chemokine production and degranulation were assessed by flow cytometry. Following incubation, NK cells were incubated with 50 µL of surface marker cocktail (containing antibodies against CD56, CD16 and CD62L) for 30 minutes at RT. Cells were washed twice in autoMACS running buffer (Miltenyi Biotec, Bergisch Gladbach, Germany). Cells were permeabilised for 20 minutes at 4°C in BD Fix/Perm buffer (BD Biosciences, New Jersey, USA) followed by incubation in 50 µL of intracellular staining cocktail (containing antibodies against IFNγ and MIP1β (CCL4)) for 20 minutes. Cells were

washed twice in autoMACS running buffer before fixation in 2% paraformaldehyde. A healthy donor control was included in each plate to assess batch effects.

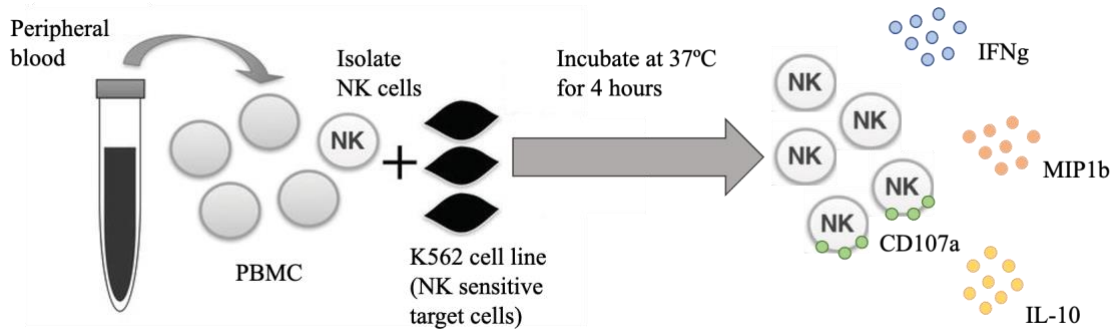


Figure 2.4. Schematic of NK cytotoxicity assay assessing functions of cryopreserved NK cells after challenge

2.11 Quantification of serum cytokines by enzyme linked immunosorbent assay (ELISA)

Quantification of IFNγ, TNFα, sCD40L, CX_3CL1 and CXCL1 was performed by ELISA (R&D Systems, Minneapolis, USA). A representative protocol for each ELISA is presented here.

For each assay, a 96-well plate was coated with capture antibody and incubated overnight at room temperature. Wells were washed 3 times with 0.05% Tween 20 in PBS. Wells were blocked with 300µL 1% BSA in PBS at room temperature for one hour. Wells were then washed 3 times as described above and 100µl of standard or sample was added to each well. Standards were 2-fold serial dilutions of recombinant target antigen (either IFNγ, TNFα, sCD40L, CX_3CL1 or CXCL1) in 1% BSA in PBS. Participant serum samples were diluted to an appropriate concentration depending on the assay. Plates were incubated for 2 hours at room temperature then washed as above.

Biotinylated detection antibody was diluted to protocol-specified concentration and 100µL added to each well. Plates were incubated for 2 hours at room temperature then washed as above. Streptavidin-HRP was diluted either 200-fold and 100 µL applied per well before incubating in the dark for 20 minutes. Wells were washed as above before adding 100µL of

substrate solution. Wells were incubated at room temperature in the dark for 10 minutes. 50µL of stop solution (2 N H_2SO_4) was added to each well and optical density at 450nm read using a microplate reader (Agilent, Santa Clara, USA). Analyte concentrations were interpolated from the standard curve generated using a 4-parameter logistic function fitted by Gen5 software (Agilent, Santa Clara, USA) and accounting for dilution factor.

3 Evaluation of cellular responses to conjugated and unconjugated Vi-vaccines and their association with protective humoral immunity

Sections of Chapter 3 have been published in Cross *et al*. Vi-Vaccinations Induce Heterogeneous Plasma Cell Responses That Associate With Protection From Typhoid Fever, *Frontiers in Immunology* 2020; **11**:574057.

3.1 Introduction

As subunit vaccines, both Vi-TT and Vi-PS mediate protection against disease by induction of antibodies. Fc-mediated functional properties of Vi-antibodies were recently shown to have differential associations with protection. Antibody-dependent neutrophil phagocytosis was found to be higher in individuals that remained well after infection, suggesting an important role of neutrophils in clearance of *S*. Typhi infection[136]. The antibody response and development of antibody functional properties involve numerous cellular subsets. Increases in antibody avidity and affinity require T-cell help, and vaccination with T-cell-dependent antigens such as Vi-TT has been consistently found to induce a transient rise in circulating T-follicular helper cells (cTfh) seven days after immunisation[195]. Functionally distinct cTfh subsets have been defined on the basis of CCR6 and CXCR3 marker expression and their capacity to assist B-cell antibody production *in vitro*. $CXCR3^+$ Tfh have been shown previously to be poor B-cell helpers[197] although they are frequently found to correlate with antibody titres in influenza vaccination studies[214]. There is limited consensus in literature regarding an association between cTfh subsets and induction of Fc-mediated functional responses. The phenotype of cTfh produced in response to Vi-TT immunisation has not been previously investigated.

Beyond T-cells, the importance of innate immunity, particularly NK cells in shaping the development of the adaptive response to vaccination is being increasingly appreciated. NK functions such as IFNg release have been both positively and negatively correlated with the development of antibody in different contexts. Other innate cell subsets such as DCs have a

clear role in the antibody response though antigen presentation to B-cells in the B-cell follicle of the lymph node, however the importance of migratory DCs in peripheral blood in this process is unclear. The magnitude and phenotype of innate responses to Vi-TT and Vi-PS vaccinations has not been evaluated previously.

Long-term vaccine-mediated protection requires more than just the initial antibody response. Protection from repeated infections requires persistence of antibody titres and generation of antigen-specific memory B-cells. The importance of the germinal centre in memory B-cell generation is well established. However, study of GC reactions in humans is difficult and requires highly specialist procedures. Whether peripheral blood responses to immunisation can act as early biomarkers of successful memory B-cell formation is unclear.

Human challenge studies provide an excellent model system to evaluate cellular immunity after vaccination. Deep phenotyping of vaccinees allows an opportunity for discovery of associations between the primary cellular responses to subunit vaccines such as Vi-PS and Vi-TT and development of desirable immunological outcomes.

3.2 Chapter aims

Aim 1: to report in detail the phenotype of innate and adaptive responses to Vi-PS and Vi-TT seven days after vaccination and compare responses to the two vaccines.

Aim 2: to associate the primary cellular response to vaccination with antibody quality and formation of memory B-cells.

3.3 Methods

3.3.1 Source of samples

Samples profiled by mass cytometry and Vi-specific ELISpot are detailed in Description of study samples. Overlap between datasets is presented in Table 3.1.

Table 3.1. Overlap of samples across mass cytometry, ELISpot and serology data sets.

Lab ID	CyTOF	Vi ASC	Vi Memory	Vi Serology
8016				
8019				
8030				
8034				
8041				
8084				
8095				
8117				
8134				
8140				
8144				
8146				
8149				
8152				
8197				
8218				
8231				
8246				
8257				
8296				
8310				
8314				
8320				
8324				
8347				
8348				
8358				
8362				
8364				
8392				
8400				
8409				
8422				

8423				
8431				
8467				
8477				
8520				
8527				
8552				
8558				
8594				
8602				
8623				
8624				
8642				
8661				
8690				
8691				
8704				
8733				
8743				
8763				
8780				
8783				
8788				
8789				
8823				
8826				
8840				
8842				
8843				
8848				
8866				
8873				
8874				
8877				
8895				
8907				
8930				
8974				
8994				

3.3.2 Quantification of Vi-specific antibody secreting cells (ASCs)

Number of Vi-specific ASCs were enumerated at baseline, 7 and 10 days after vaccination. Details of methods used are presented in the Detection of Vi-specific antibody-secreting cells (ASCs) post-vaccination section of the General Methods.

3.3.3 Quantification of Vi-specific antibody titres

Abundance of Vi-specific antibody subclasses was measured by bead-based multiplex assay in serum. Measurements were performed at Duke University by Lindsey Dahora and have been previously published[215]. Briefly, Purified Vi-polysaccharide was biotinylated and coupled with neutravadin-coated Luminex microspheres. Antigen-coated beads were then incubated with serum for 1 hour before a second incubation in PBS for 15 minutes. Bound Vi-specific-antibodies were detected using capture antibodies against IgG1, IgG2, IgG3, IgG4, IgA1 and IgA2. The capture antibody cocktail was incubated with beads for 30 minutes at room temperature protected from light. Unbound capture antibodies were removed by washing before data acquisition was performed using the Bio-Plex 200 platform. Fluorescence intensity was calculated accounting for serum dilution and subtraction of blank beads incubated without serum. Data are presented as $\log_2$ fold change. The lower limit of detection was set at an MFI of 100.

3.3.4 Measurement of Vi-specific antibody functions

Vi-specific antibody functions were measured at the Ragon Institute by Dr Jennifer Hill, Dr Celina Jin and Dr Bronwyn Gunn and have been previously published[136]).

3.3.4.1 Antibody dependent complement deposition (ADCD)

Vaccinee serum was incubated at 56°C for 1 hour to inactivate endogenous complement. Samples were then incubated with Vi-coupled beads 1 hour at room temperature. Guinea pig serum was added as a source of complement and incubated with the beads at 37°C

for 20 minutes. Beads were then washed twice in PBS and C3b deposition was assessed by staining with anti-C3b FITC antibody for 15 minutes at room temperature in the dark. Unbound antibody was removed by washing twice in PBS. Samples were acquired by BD Fortessa. Deposition was evaluated by MFI.

3.3.4.2 Antibody dependent cellular phagocytosis (ADCP)

Vi-coupled fluorescent beads were incubated with participant serum as described above before adding 2.5 x 10^4 THP-1 cells in a 96-well plate. Samples were incubated overnight at 37°C. The proportion of cells which had undertaken phagocytosis of beads and was evaluated by flow cytometry. A phagocytic score was determined by multiplying the proportion of cells which were positive for bead uptake by the MFI of the fluorescent population.

3.3.4.3 Antibody dependent NK activation (ADNK)

96-well plates were coated with streptavidin overnight before incubating with biotinylated Vi for 3 hours at 37°C. Plates were washed with PBS and vaccinee serum was added to wells for 2 hours at 37°C. Plates were washed with PBS following incubation and 5 x 10^4 NK cells, isolated from buffy coats, were added to each well. Plates were incubated for 5 hours at 37°C. CD107a was added to each well prior to incubation. Surface staining for CD56 and CD16 were performed for 30 minutes at room temperature in the dark, followed by intracellular staining for IFNγ and MIP1β for 20 minutes. Samples were analysed by flow cytometry.

3.3.5 Statistical analysis

Identification of cell populations was conducted by clustering analysis as described in the Data analysis section. Biological identification of clusters was performed manually by inspection of marker expression heatmaps and quantitatively using marker enrichment modelling (MEM). Clustering quality and separation was assessed using silhouette widths and visualisation in low dimensions using UMAP. Differential abundance of cellular subsets between baseline, 7 days and 28 days post-vaccination was performed as described in the

General Methods section. Timepoint was included as a predictor accounting for intra-individual collinearity by including participant ID as a random effect.

Variables associated with vaccine arm and memory responder status were evaluated by PCA analysis. All variables were z-score normalised prior to input. Complete observations only were included in the analysis. In cases of high data sparsity, Bayesian models were utilised to impute missing values.

Associations between the cellular response to vaccination and antibody profiles were investigated by Spearman correlation analysis. All statistical testing was corrected for multiple testing (unless stated otherwise). Dependence between categorical variables was assessed using Fisher's exact test. Differences in responses between vaccine arms, priming groups and memory responders were compared using Wilcox rank sum test. Participants without paired time points (pre- and post-vaccination) were excluded from some analyses.

3.4 Results

3.4.1 Plasma cells expressing mucosal migratory markers dominate the response to Vi-TT and Vi-PS

The phenotype of plasma cells responding to vaccination was assessed. Plasma cells were defined in this analysis as $CD19^{+}$ $CD20^{-}$ $CD27^{+}$ $CD38^{++}$ (manual gating scheme in Figure 3.1A). A wider analysis of the total B-cell compartment did not yield additional significant findings. Clustering analysis revealed four plasma cell populations in peripheral blood. UMAP analysis showed high separation between subsets suggesting distinctive phenotypic profiles (Figure 3.3A). Two of these populations expressed surface immunoglobulin IgA and comprised more than half of total plasma cells detected in blood, both at baseline and following immunisation (Figure 3.2). IgA-expressing populations were enriched for a number of mucosal migratory markers including CCR9, CCR10 and α4β7 (Figure 3.3B). The remaining two populations were of lower abundance and expressed surface IgG and IgD respectively (Figure 3.3B). Expression of α4β7 was evident on both of these subsets while expression of other mucosal markers was absent. Interestingly, lymph node markers such as CD62L (which has been frequently reported on plasma cells after systemic immunisation) was almost completely absent on all populations, as was CCR7 (Figure 3.3B). Other markers were detected in low abundance with some dim expression of CXCR3 found across several subsets. All plasma cell populations strongly expressed activation markers including HLA-DR and CD86 (Figure 3.1B). Prior to vaccination, plasma cells were rare in peripheral blood with the majority deriving from the IgA^{+} fractions (Figure 3.4A).

Plasma cells with two of the four identified phenotypes were significantly expanded in response to vaccination (Figure 3.4B). Fold rise from baseline was highly significant for both subsets in Vi-TT vaccinees whereas responses in Vi-PS were more subtle and failed to reach statistical significance after correction for multiple testing (Figure 3.4C). IgA^{+} plasma cells expressing CCR10 and α4β7, markers associated with migration to mucosal sites such as the intestinal tract, were strongly expanded in Vi-TT vaccinees ($p = 0.0025$, ***) and this response

was significantly greater in Vi-TT than Vi-PS (p = 0.00037, ****) (Figure 3.4C). Similarly, $\alpha4\beta7^+$ IgG^+ plasma cells also increased as a proportion of total B-cells (Vi-TT, p = 0.00036, ****) with a significantly greater fold rise in the Vi-TT arm (p = 0.00042, ****). Vaccine-induced plasma cell responses were strongly co-correlated with one another (R = 0.73, p < 0.0001). No expansion in frequency of IgA^+ plasma cells characterised by high expression of CCR9, a homing marker specific for migration to the small intestine, was observed after either vaccination. This suggests this low frequency population represents, constitutively circulating plasma cells that derive from mucosal reactions and play no part in the response to vaccination.

Antigen specificity of plasma cells in mass cytometry data was not assessed. However, frequencies of Vi-specific ASCs were enumerated separately by ELISpot (Figure 3.5A). Vi-specific IgG ASCs were detectable 7 days post-vaccination in both Vi-PS and Vi-TT vaccinees (Vi-PS: n = 35, Vi-TT: n = 39). Significantly higher frequencies of Vi-specific IgG ASCs were detected in Vi-TT vaccinees in comparison with Vi-PS; median 82.5 per 10^6 PBMCs (IQR: 10-141) versus 3 per 10^6 PBMCs (IQR 3-33.5) for Vi-TT and Vi-PS, respectively. Vi-IgA ASC responses were not assessed. A significant, moderate correlation between fold rise $\alpha4\beta7^+$ IgG^+ plasma cells and Vi-IgG ASCs was observed (R = 0.54, p < 0.001) (Figure 3.5B) suggesting a proportion of these cells were Vi-specific.

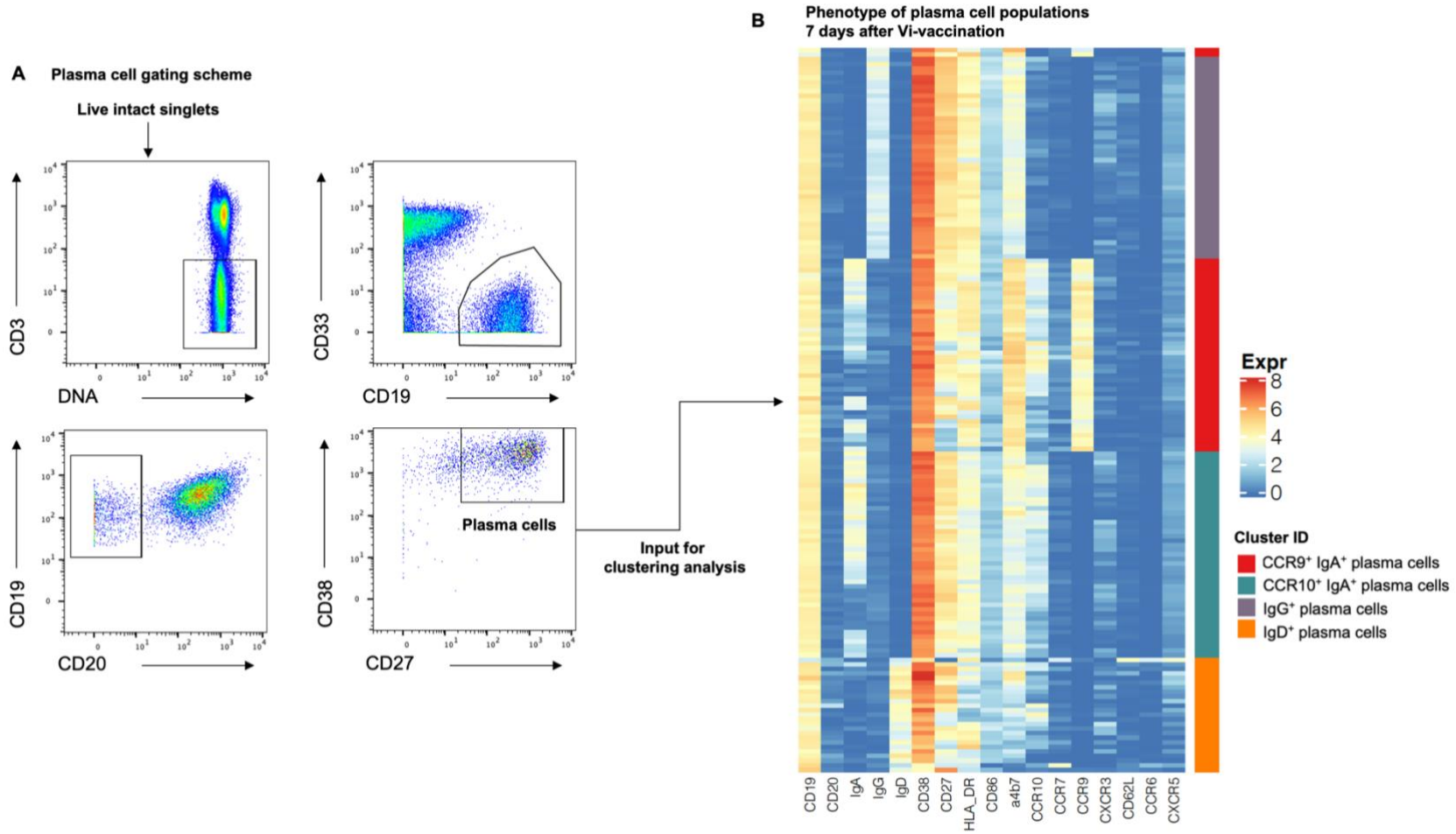


Figure 3.1 Evaluation of plasma cell phenotype post-vaccination. (A) Plasma cell gating scheme. (B) Heatmap of plasma cell subset median marker expression. Four plasma cell subsets were identified in peripheral blood of Vi-TT (n = 19) and Vi-PS (n = 20)-vaccinated volunteers 7 days after vaccination. Each row represents one individual. Marker expression was arcsinh-transformed prior to visualisation.

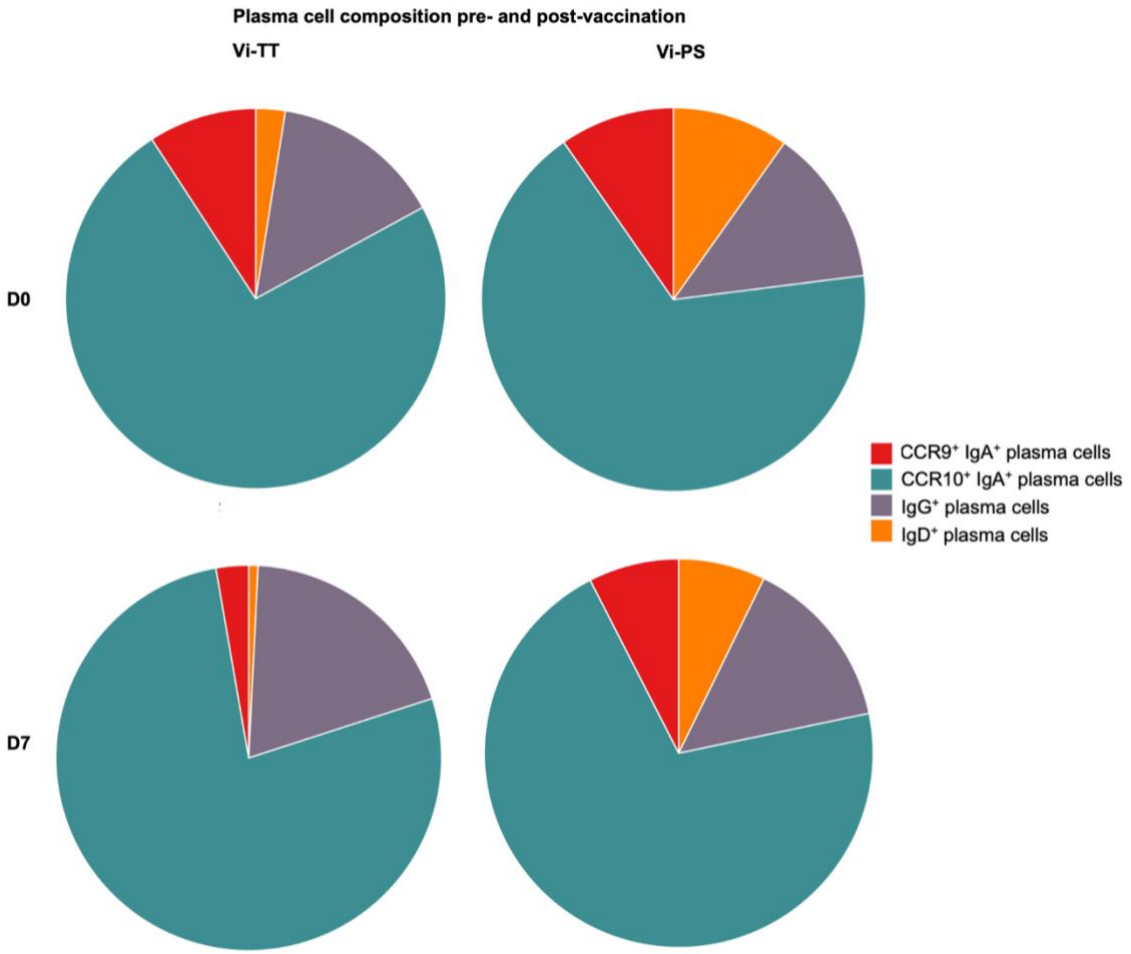


Figure 3.2. Plasma cell composition in peripheral blood pre- and post-vaccination. D0 = day of vaccination, D7 = seven days post-vaccination, Vi-TT = Vi-tetanus toxoid vaccine, Vi-PS = Vi-polysaccharide vaccine. Mean proportions across all participants at a given timepoint in each vaccine are plotted.

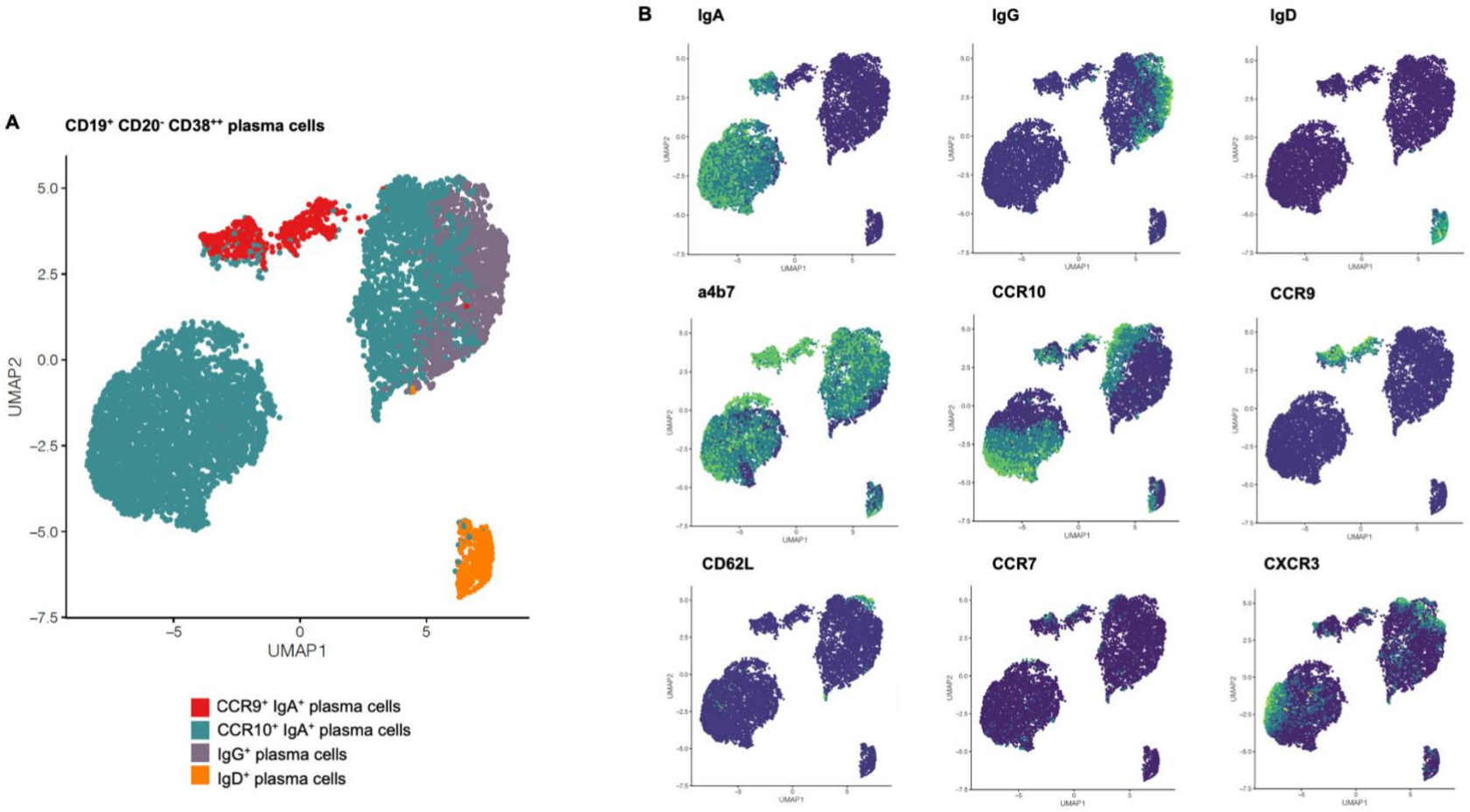


Figure 3.3. UMAP visualisation of plasma cell compartment. Nearest neighbours = 15, minimum distance – 0.2. (A) UMAP of plasma cell compartment (15,000 subsampled events visualised) coloured by cluster ID. Clustering performed by FlowSOM (self-organising maps). (B) UMAP of plasma cell compartment coloured by arcsinh-transformed marker expression (cofactor = 5). Lighter colour indicates stronger expression. Markers visualised here were used in clustering.

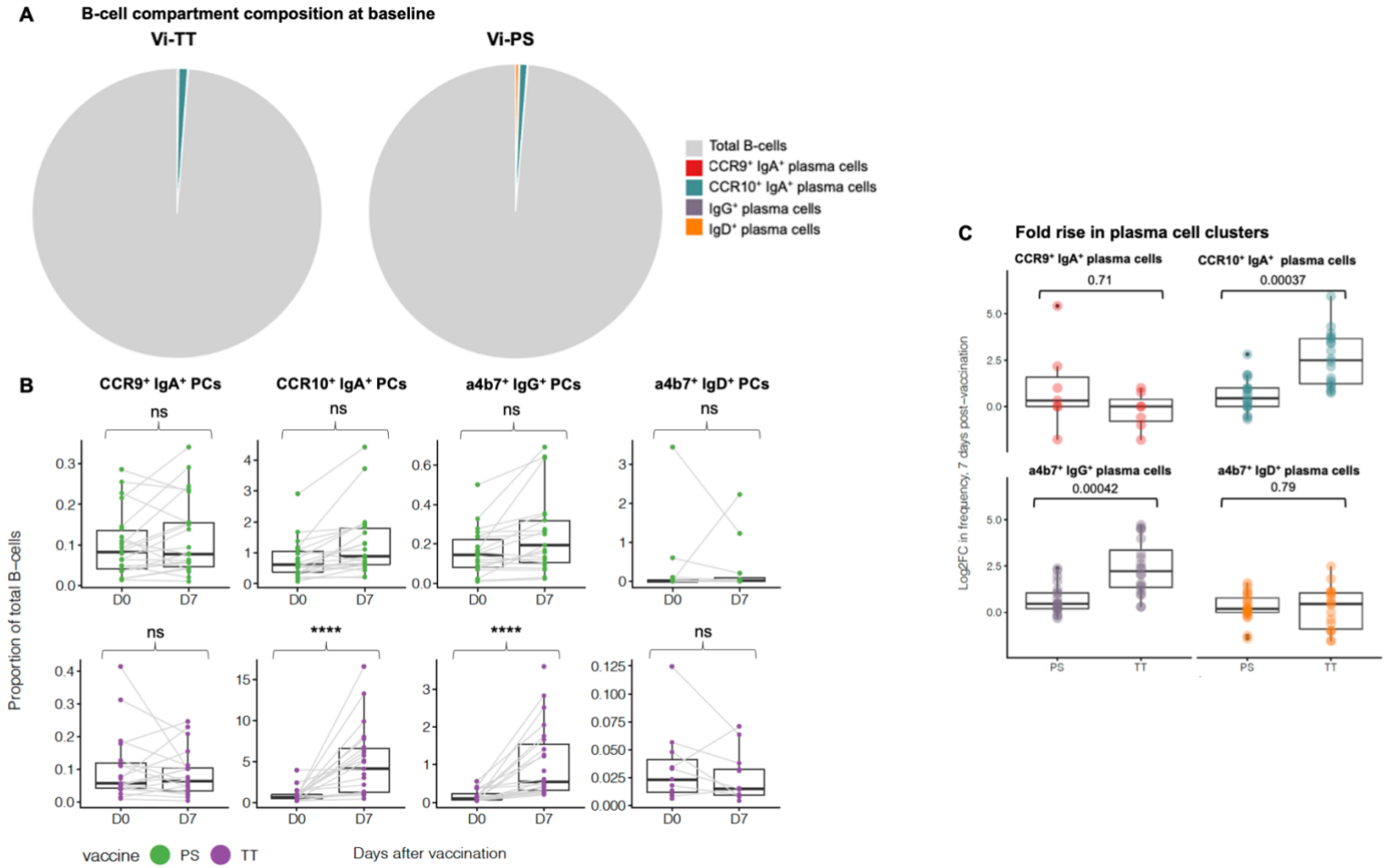


*Figure 3.4. Changes in plasma cell frequency after Vi-vaccination. Vi-TT = Vi-tetanus toxoid vaccine, Vi-PS = Vi-polysaccharide vaccine, PC = plasma cell, D0 = day of vaccination, D7 = seven days after vaccination (A) Plasma cell proportion of total B-cells at baseline (B) Change in subset frequency as a proportion of total B-cells after vaccination. Differential abundance between timepoints evaluated by negative binomial mixture models using participant ID as a covariate, adjusted for multiple testing. ns = $p > 0.05$, * = $p < 0.05$, ** = $p < 0.01$, *** = $p < 0.001$, **** = $p < 0.0001$. Number of participants per group: Vi-TT = 19, Vi-PS = 20. (C) Log2FC in plasma cell clusters 7 days after vaccination. Vaccine arms compared by Wilcox rank sum test.*

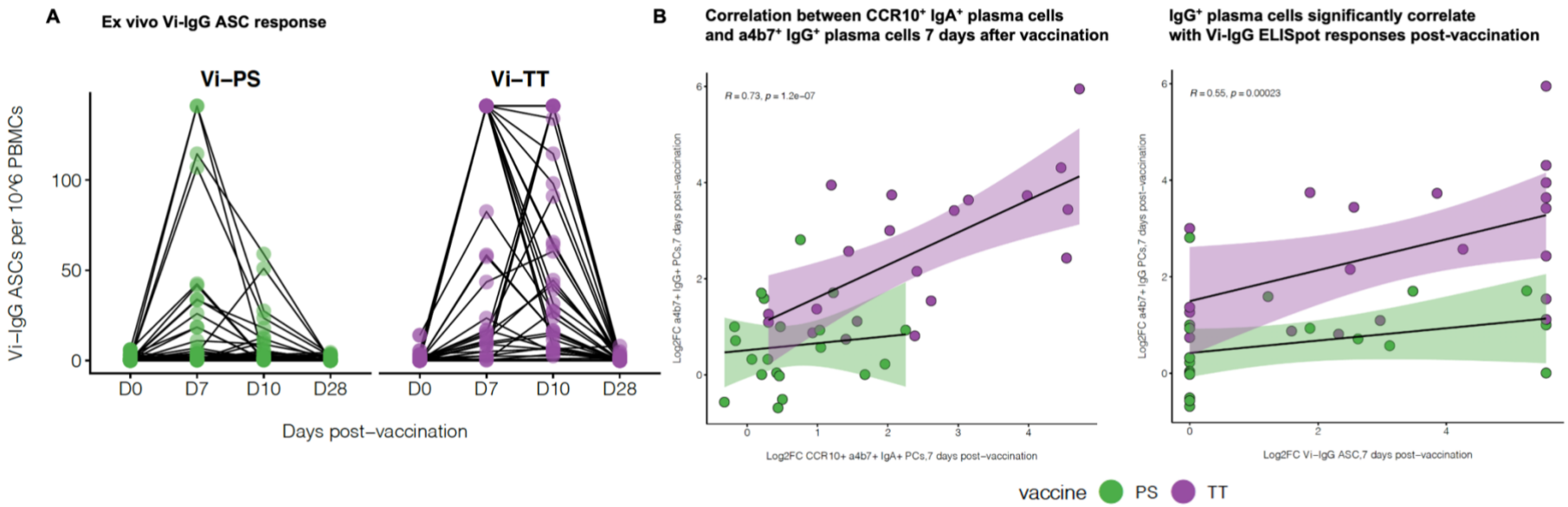


Figure 3.5. Ex vivo Vi-IgG ASC response after vaccination. Vi-TT = Vi-tetanus toxoid vaccine, Vi-PS = Vi-polysaccharide vaccine, ASC = antibody secreting cell, D0 = day of vaccination, D7 = seven days after vaccination, D10 = ten days after vaccination, D28 = 28 days after vaccination (A) Number of Vi-IgG ASCs per 10^6 PBMCs at D7 and D10 post-vaccination. (B) Spearman correlation between log2FC in IgG+ and IgA+ plasma cells. Fold changes calculated between D0 and D7. Spearman correlation between log2FC IgG+ plasma cells and Vi-IgG specific ASC response.

3.4.2 CXCR3$^+$ and CXCR3$^-$ Tfh responses are induced by Vi-TT vaccination

T-follicular helper cells (Tfh) are frequently detectable in peripheral blood following immunisation with T-dependent antigens. Circulating Tfh are characterised by expression of the canonical marker CXCR5. To evaluate cTfh subsets in detail, CD4$^+$ CXCR5$^+$ events were gated and clustered (Figure 3.6). Five CD4$^+$ CXCR5$^+$ populations were identified; cTfh could be identified by strong co-expression of PD-1 and ICOS (Figure 3.6B). In addition, Tfh had low expression of CD45RA and high levels of CCR7, indicating a central memory (CM) phenotype as has been previously described (Figure 3.6B)[195]. Other populations included T-follicular regulatory cells (Tfr) characterised by expression of CD25, PD-1 and ICOS and low CD127 as well as several CM populations with strong expression of CLA and CCR9 (Figure 3.7B).

cTfh cell responses were absent in Vi-PS recipients as expected, but readily detected in Vi-TT vaccinees, increasing significantly as a proportion of CD4$^+$ T-cells 7 days after immunisation (Figure 3.8A). No other T-cell subsets were significantly upregulated after either vaccine. A significant fold rise in T-cell subsets was detectable in the Tfh cluster only ($p = 0.002$, **) (Figure 3.8B). CXCR3 expression was generally low but detectable on a subset of Tfh, suggesting a Tfh-1 phenotype, similar to that seen after influenza vaccines[214]. Remaining Tfh were largely negative for CXCR3 and CCR6, indicating a Tfh-17 phenotype. Given the functional differences between CXCR3$^+$ and CXCR3$^-$ cTfh *in vitro,* these populations were manually gated to evaluate their kinetics separately. Both populations were similarly expanded by Vi-TT vaccination (Figure 3.8C).

3.4.3 CD56$^+$ compartment, including NK cells and DCs, is significantly perturbed by Vi-vaccination

Innate responses were detectable following both vaccinations, with similar magnitude of induction observed in both vaccine arms. Gated NK subsets (Figure 3.9A) were modestly differentially expressed and were entirely found within the CD56^{bright} compartment (Figure 3.9B). Within the CD56^{bright} NK compartment, clustering analysis identified four subsets with distinct phenotypic traits as highlighted by PCA analysis (Figure 3.10A). All populations were enriched for typical NK markers such as CD11c, NKG2A and CD161 (Figure 3.10A). Subsets

could be distinguished on the basis of differential expression of markers CD26 and CD127. All subsets had similar kinetics after vaccination (Figure 3.11) and fold change in all populations was similar between vaccine arms (Figure 3.12).

Beyond NK cells, two $CD56^{dim}$ dendritic cell populations were also observed to be differentially abundant between D0 and D7 in both vaccine arms. Two subsets of myeloid dendritic cells expressing classical DC markers (Lin^{-} $HLA^{-}DR^{+}$ $CD11c^{+}$ $CD123^{lo}$) as well as low levels of CD56 clustered separately from all other $CD56^{+}$ populations by hierarchical clustering (Figure 3.9B) highlighting a significantly divergent phenotype to other CD56-expressing cells. $CD56^{+}$ DC subsets shared common lineage markers but differed in expression of CXCR3 and PD-1 (Figure 3.10B). Frequencies of these subsets were low in baseline samples but both subsets could be easily detected by clustering and manual gating methods after immunisation (Figure 3.13A). When gated manually based on HLA-DR and CLA expression, a significant change in activation marker expression was observed between baseline and post-vaccination timepoints, suggesting a highly activated phenotype (Figure 3.13B).

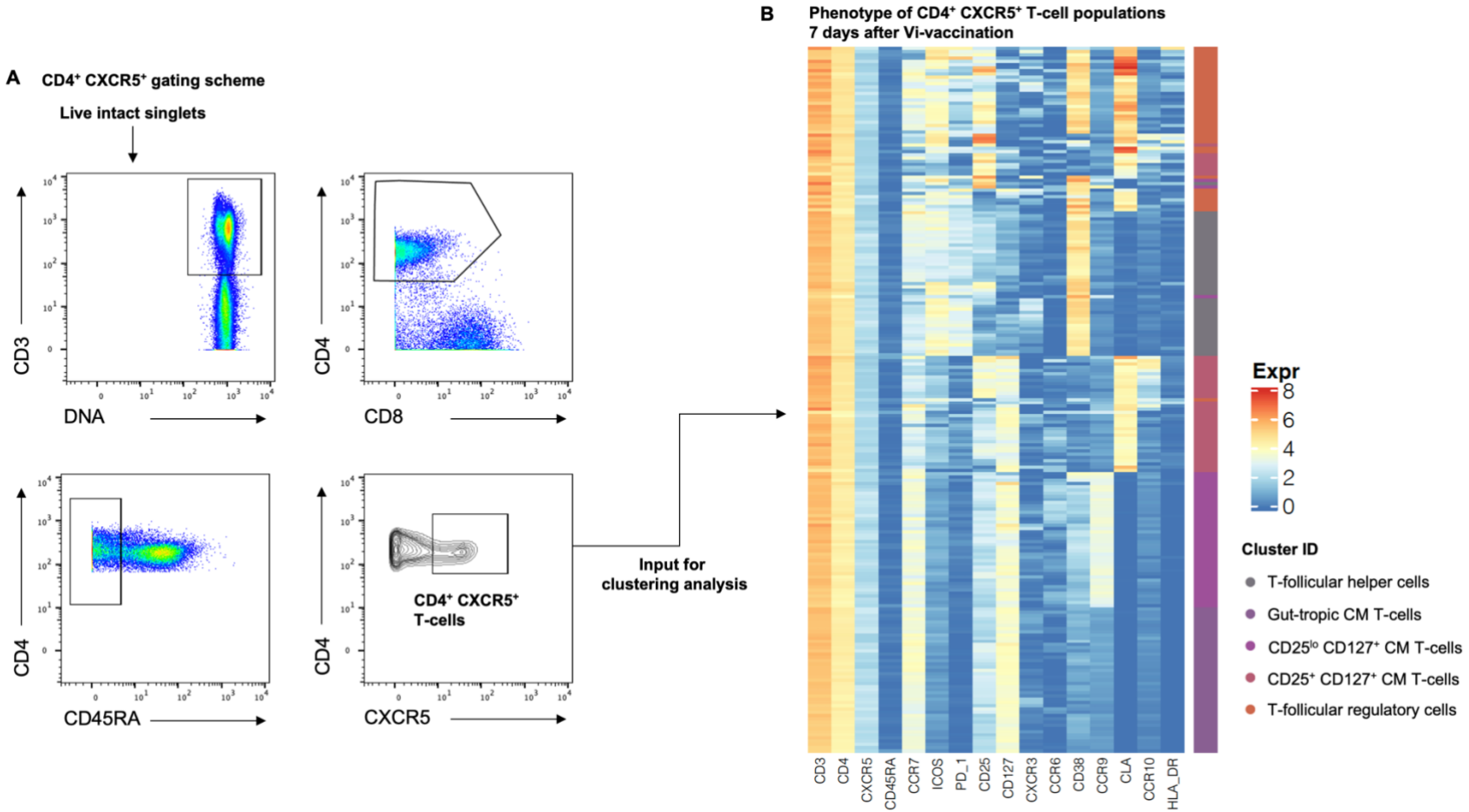


Figure 3.6. Evaluation of Tfh phenotype post-vaccination. (A) Gating scheme of CD4+ CXCR5+ T-cells prior to clustering analysis. (B) Heatmap of CD4 T-cell subset median marker expression. Five CD4⁺ CXCR5⁺ T-cell subsets were identified in peripheral blood of Vi-TT (n = 19) and Vi-PS (n = 20)-vaccinated volunteers by clustering. Each row represents one individual. Marker expression was arcsinh-transformed prior to visualisation.

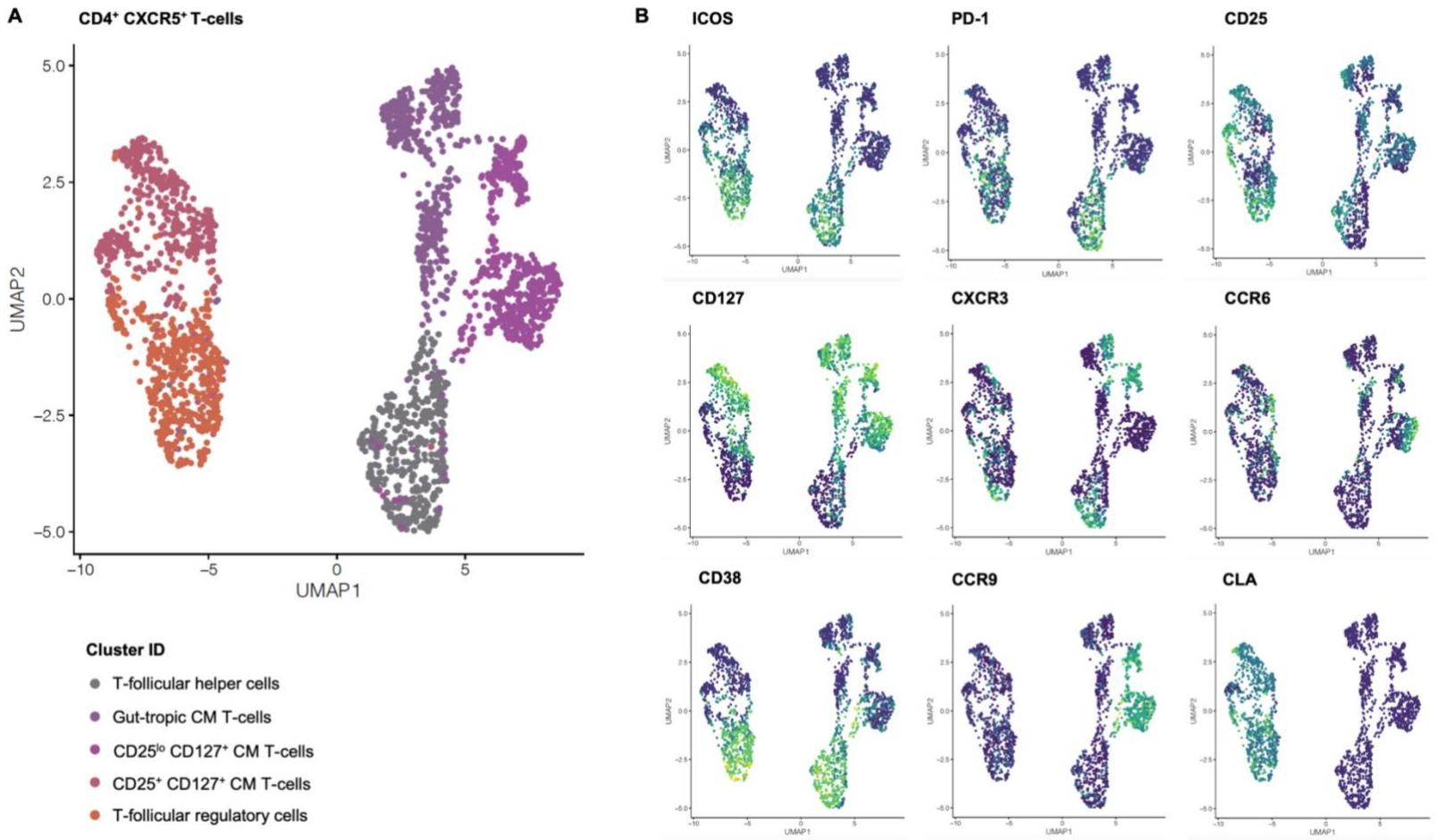


Figure 3.7. UMAP visualisation of CD4⁺ CXCR5⁺ T-cell response to vaccination. Nearest neighbours = 15, minimum distance = 0.8. (A) UMAP of CD4⁺CXCR5⁺ compartment (10,000 subsampled events visualised) coloured by cluster ID. Clustering performed by FlowSOM (self-organising maps). (B) UMAP of CD4⁺CXCR5 compartment coloured by arcsinh-transformed marker expression (cofactor = 5). Lighter colour indicates stronger expression. Markers visualised here were used in clustering.

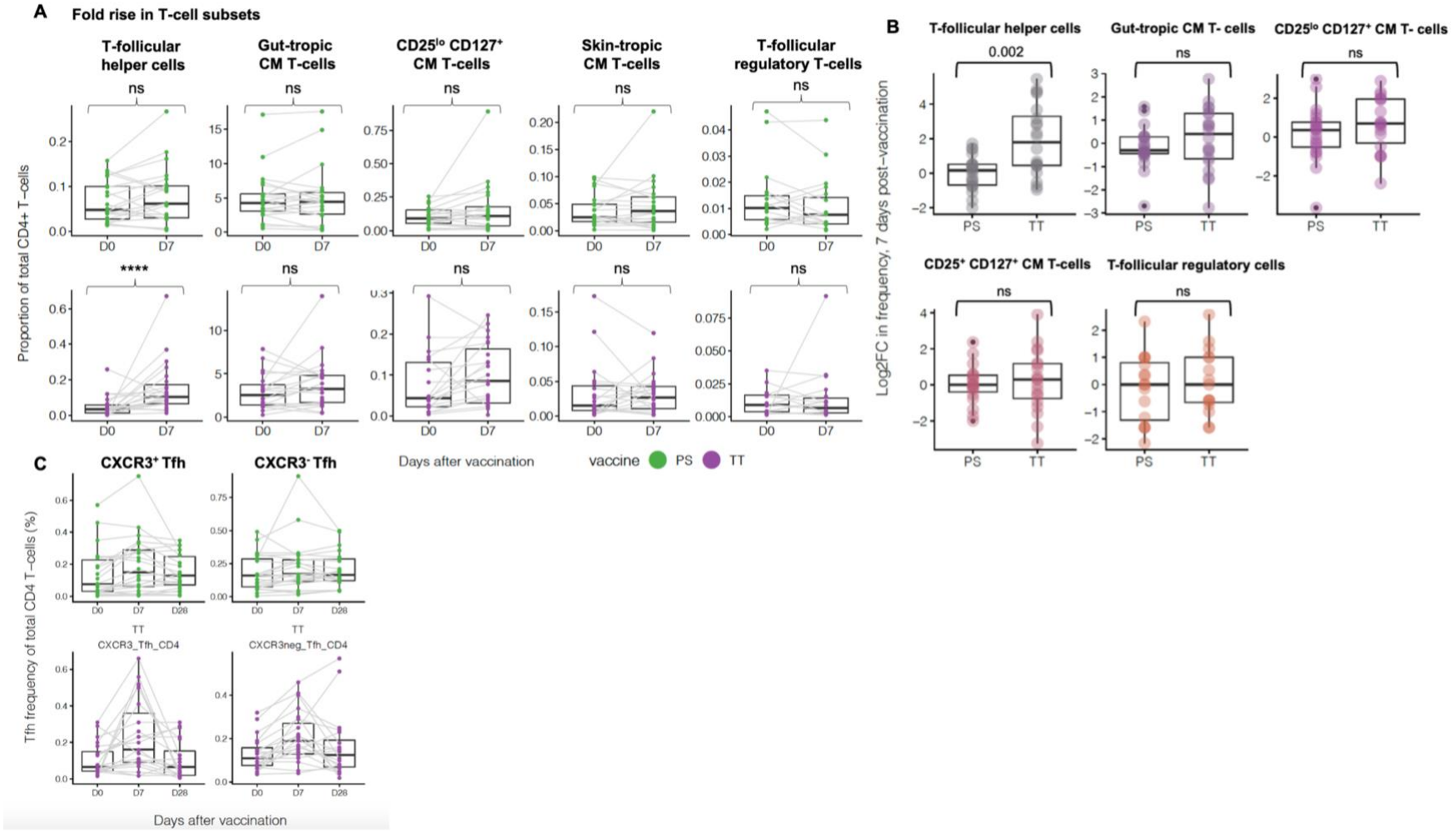


*Figure 3.8. Changes in T-cell frequency after Vi-vaccination. Vi-TT = Vi-tetanus toxoid vaccine, Vi-PS = Vi-polysaccharide vaccine, D0 = day of vaccination, D7 = seven days after vaccination (A) Change in subset frequency as a proportion of total CD4 T-cells after vaccination. Differential abundance between timepoints evaluated by negative binomial mixture models using participant ID as a covariate, adjusted for multiple testing. ns = p > 0.05, * = p < 0.05, ** = p< 0.01, *** = p <0.001, **** = p < 0.0001. Number of participants per group: Vi-TT = 19, Vi-PS = 20. (B) Log2FC in T- cell clusters 7 days after vaccination. Vaccine arms compared by Wilcox rank sum test.(C) Frequencies of CXCR3+ and CXCR3- Tfh as a proportion of total CD4 T-cells after vaccination*

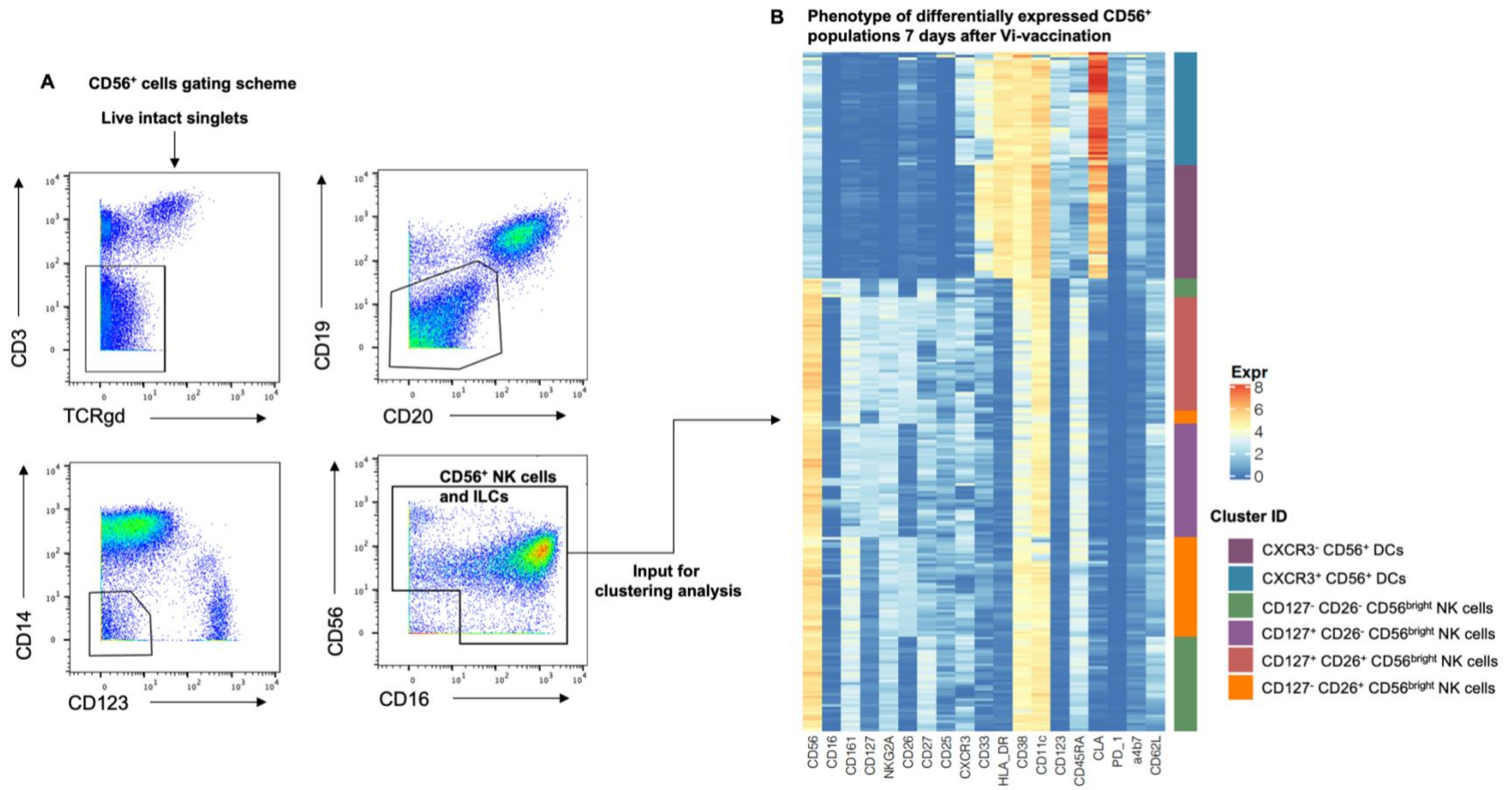


Figure 3.9. Evaluation of CD56⁺ clusters phenotype post-vaccination. (A) Gating scheme of CD56⁺ events prior to clustering analysis. (B) Heatmap of CD56⁺ clusters median marker expression. Six CD56⁺ subsets were identified in peripheral blood of Vi-TT (n = 19) and Vi-PS (n = 20)-vaccinated volunteers by clustering. Each row represents one individual. Marker expression was arcsinh-transformed prior to visualisation.

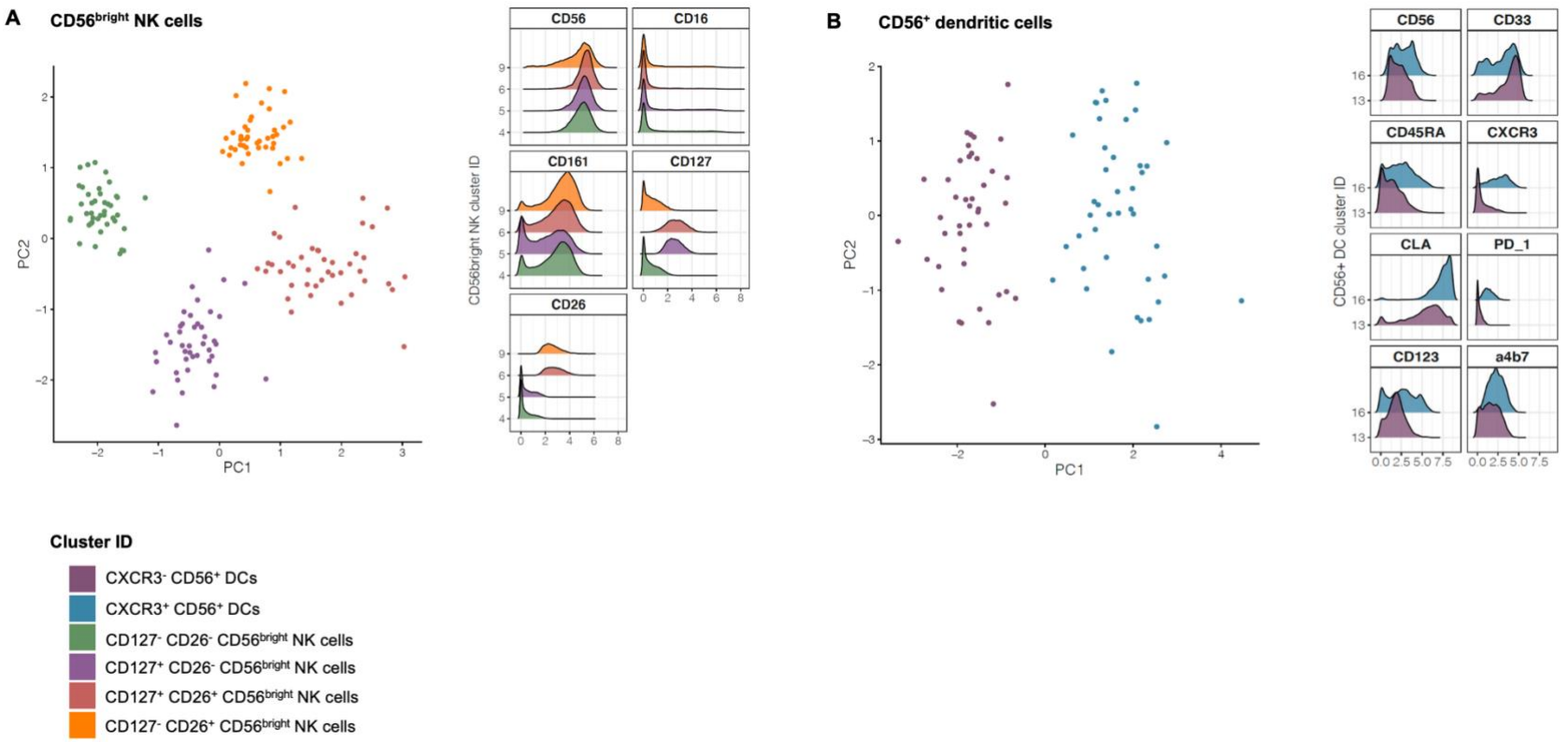


Figure 3.10. PCA plots of differentially expressed CD56^{+}clusters after Vi-vaccination. NK = natural killer. (A) PCA and density plots of CD56^{bright} NK cell subsets. (B) PCA and density plots of CD56^{+} DCs.

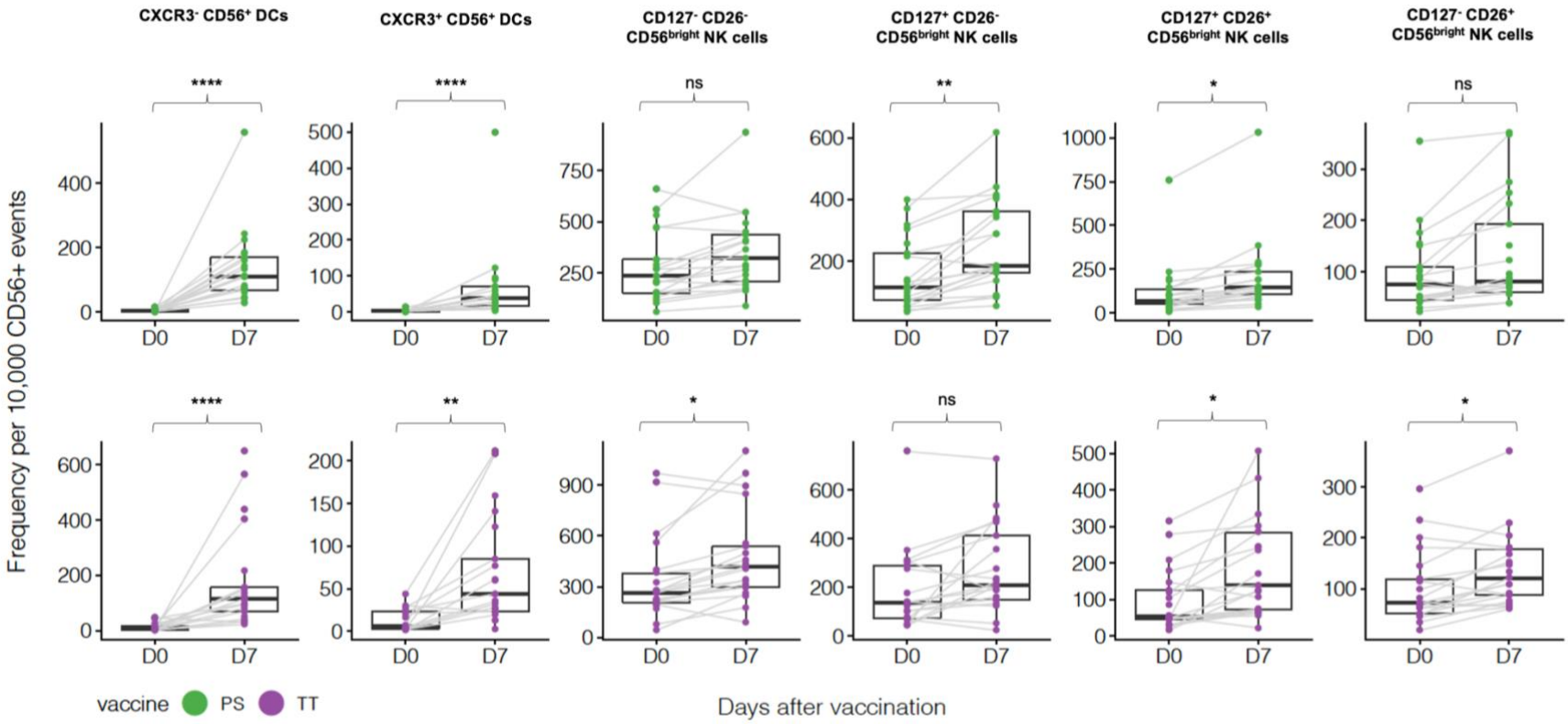


*Figure 3.11. Changes in CD56⁺ cluster frequency after Vi-vaccination. Vi-TT = Vi-tetanus toxoid vaccine, Vi-PS = Vi-polysaccharide vaccine, D0 = day of vaccination, D7 = seven days after vaccination Change in subset frequency as a proportion of total CD56⁺ events after vaccination. Differential abundance between timepoints evaluated by negative binomial mixture models using participant ID as a covariate, adjusted for multiple testing. ns = p > 0.05, * = p < 0.05, ** = p< 0.01, *** = p <0.001, **** = p < 0.0001. Number of participants per group: Vi-TT = 19, Vi-PS = 20.*

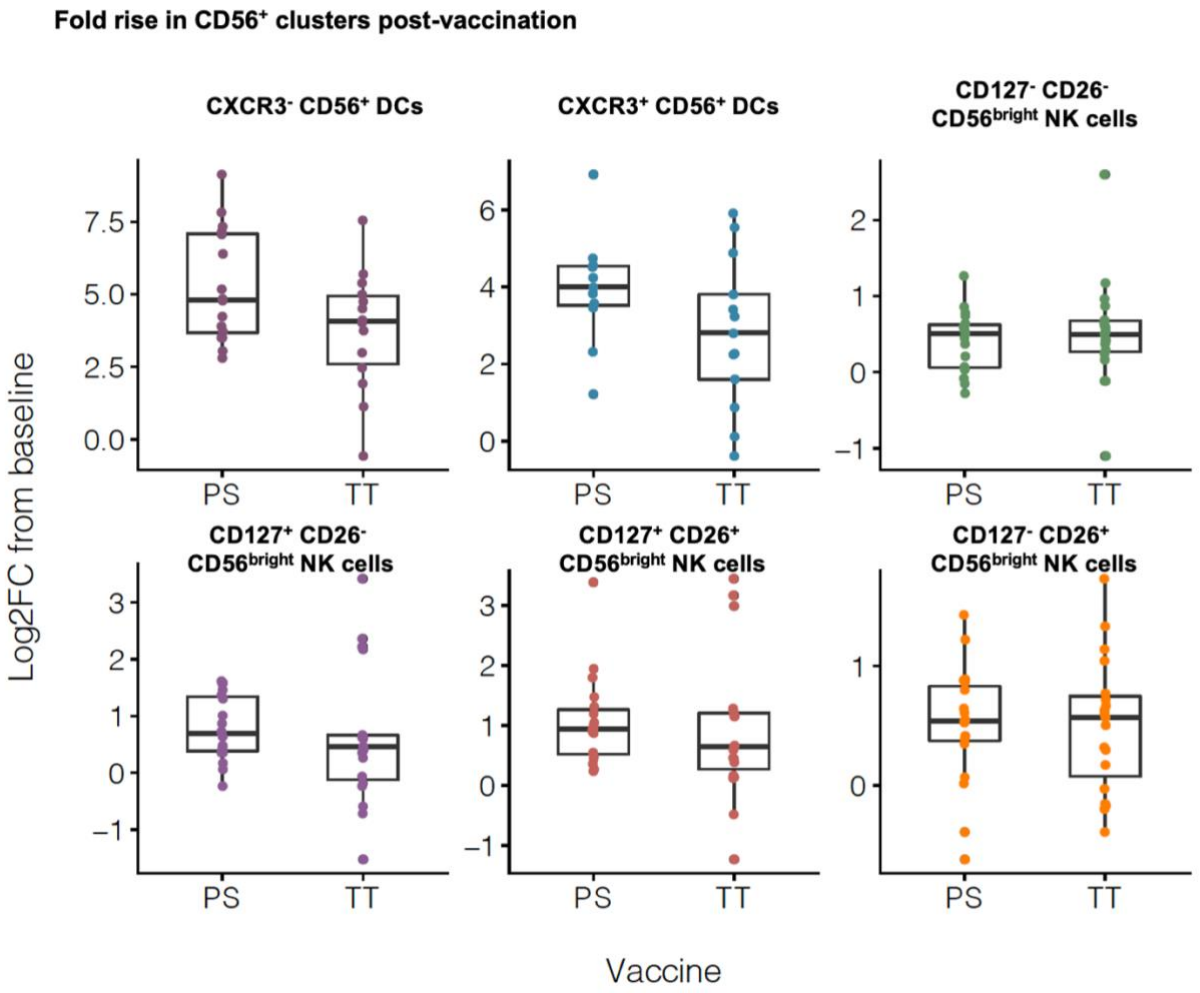


Figure 3.12. Log2FC in CD56⁺ cluster frequencies from baseline. PS = Vi-polysaccharide vaccine, TT = Vi-tetanus toxoid conjugate vaccine

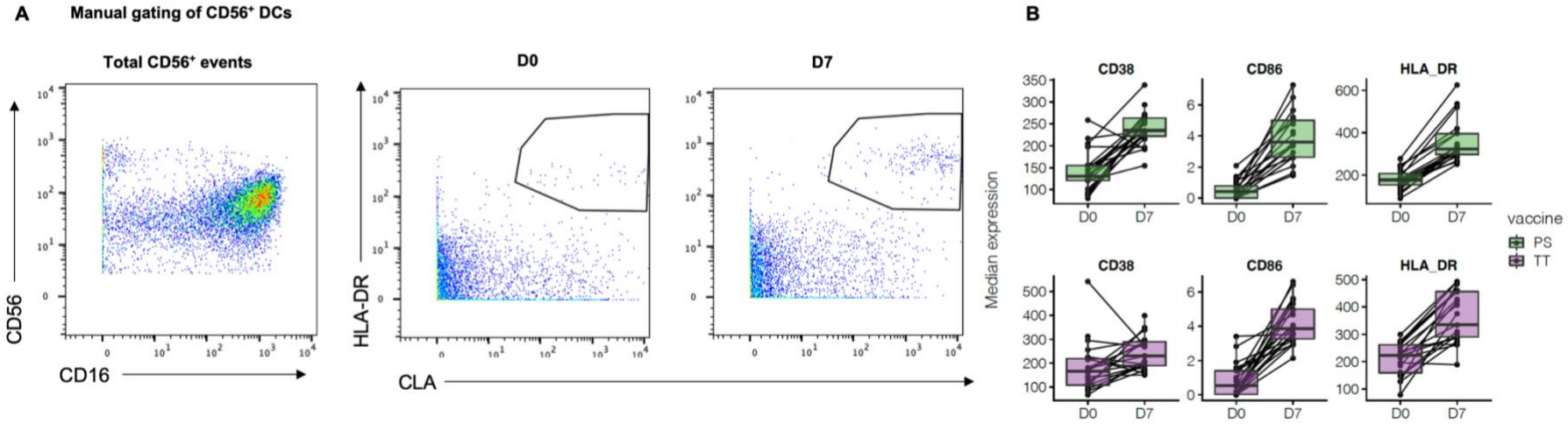


*Figure 3.13. Activation status of CD56⁺ DCs. (A) Manual gating scheme of CD56+ DCs. Representative biaxal plot of increased frequency of cells after vaccination. (B) Expression of activation markers CD38, CD86 and HLA-DR on manually gated CD56+ DCs after vaccination. ns = p > 0.05, * = p < 0.05, ** = p< 0.01, *** = p <0.001, **** = p < 0.0001.*

3.4.4 Cellular responses strongly correlate with humoral immunity in Vi-TT vaccinees

Cellular responses to vaccination were correlated with measures of humoral immunity assessed at 1 month after vaccination. Several associations were evident in Vi-TT vaccinees whilst relationships were weaker in the Vi-PS arm, possibly due to relatively lower induction of cellular immunity (Figure 3.14). $CCR10^+$ $a4b7^+$ IgA^+ plasma cells moderately correlated with Vi-IgA1 titres ($R = 0.48$, $p = 0.035$) but not Vi-IgA2 (although IgA2 titres were still induced by vaccination). In addition, the magnitude of the $CCR10^+$ $a4b7^+$ IgA^+ plasma cell response was strongly associated with fold rise in ADNP in Vi-TT recipients ($R = 0.75$, $p = 0.00051$). Interestingly, this relationship was stronger than the association with antibody titre itself. ADNP also correlated with Vi-IgG1 and Vi-IgG2 therefore several antibody isotypes may play a role in neutrophil-mediated Vi responses. In contrast, plasma cell responses in Vi-PS vaccinees did not correlate with Vi-IgA1 titre or ADNP despite both being induced by vaccination (albeit to a lesser degree than Vi-TT). Vi-IgA2 was strongly correlated with $CCR10^+$ $a4b7^+$ IgA^+ plasma cells in Vi-PS recipients ($R = 0.80$, $p = 2.4 \times 10^{-5}$), however IgA1 which is strongly induced by Vi-PS showed no association with $CCR10^+$ $a4b7^+$ IgA^+ plasma cells.

Tfh responses in Vi-TT recipients were also significantly associated with development of $CCR10^+$ $a4b7^+$ IgA plasma cells ($R = 0.53$, $p = 0.017$) but not $a4b7^+$ IgG plasma cells. Interestingly, Tfh frequency was negatively associated with induction of several $CD56^{bright}$ NK cell subsets (Figure 3.17). However, the effect of NKs on the development of antibody titres, avidity and functionality appeared minimal despite a possible negative relationship with Tfh. No significant correlations between NK responses and antibody measures could be established.

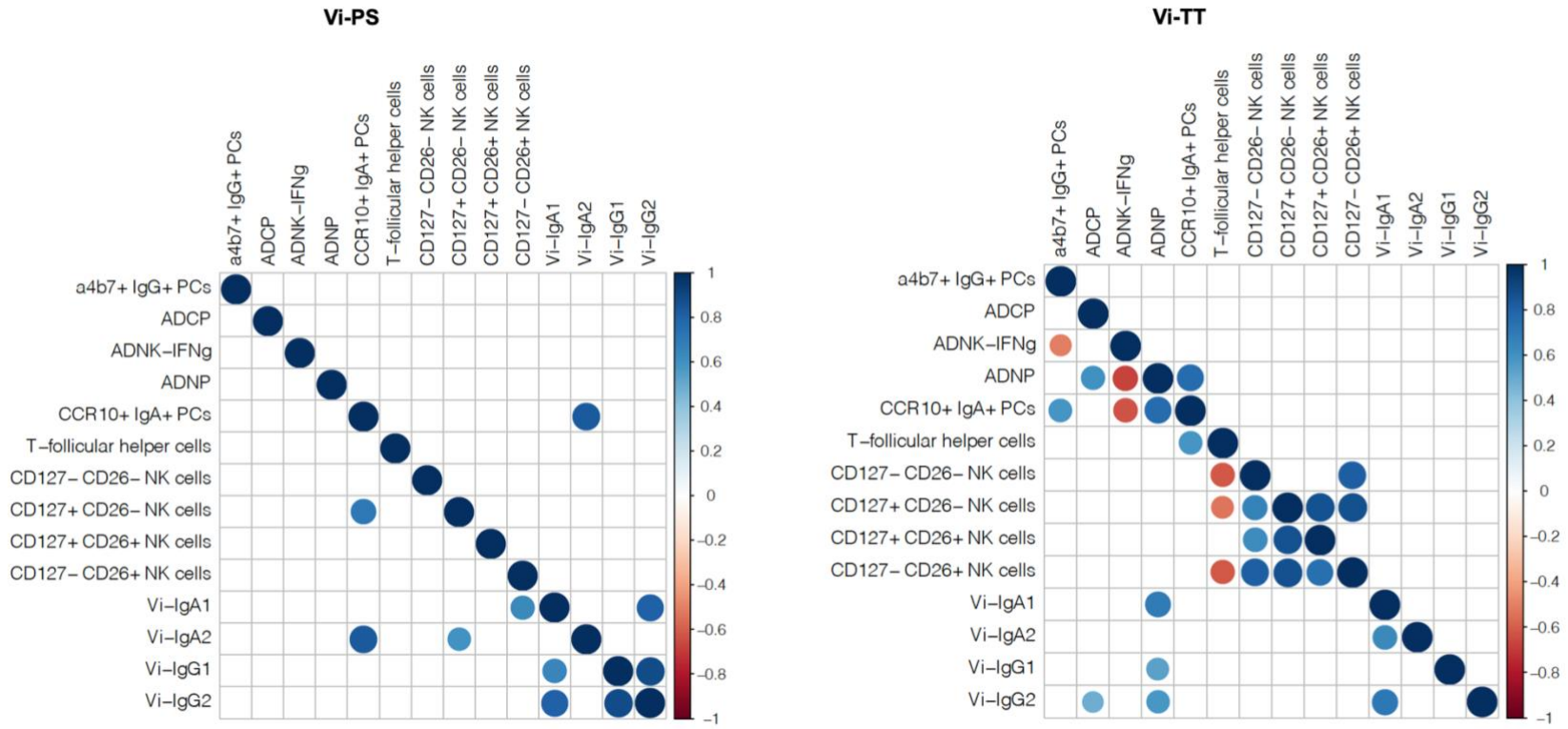


Figure 3.14. Associations between antibody functions and cellular immunity. Spearman correlation between log2FC in cell subset between D0 and D7 after vaccination and the log2FC in antibody titre or functionality one month (28 days) after vaccination. Correlation coefficients of significant correlations only are represented as circles. Strength and direction of correlation represented by colour of circle.

3.4.5 Formation of Vi-specific memory B-cells was associated with CD4 T-cell and NK responses after Vi-TT vaccination

The development of immunological memory is essential for long-term vaccine-mediated protection. Vi-specific memory B-cell responses were evaluated post-vaccination in Vi-TT and Vi-PS recipients. As expected, no evidence of memory B-cell formation was found in Vi-PS vaccinees whereas a significant increase was detected in the Vi-TT arm, 10 days after vaccination (as reported previously[136]). In the Vi-TT arm, the magnitude of the memory B-cell response to immunisation was found to be highly variable. A subset of participants (9 out of 41 individuals (22%)) had no detectable fold rise in memory B-cells post-vaccination (Figure 3.15A). This could not be explained by poor immunogenicity to vaccination in these individuals; no statistically significant association was found between ASC ELISpot responses and memory responses (Fisher's exact test, $p = 0.721$, ns). PCA analysis of cellular responses to Vi-TT immunisation identified moderate separation of high and low memory responses (Figure 3.15B). High memory responders were found to have significantly higher Tfh ($p = 0.04$, *) in contrast to low responders. Whilst elevated in high responders, fold rise in $CD56^+$ DC subsets did not meet statistical significance. Conversely, individuals with higher $CD26^+$ $CD127^+$ NK responses ($p = 0.02$, *) after immunisation and lower Tfh developed poor Vi-specific memory responses (Figure 3.16). Other NK subsets were also increased in poor memory responders although these did not reach statistical significance. Tfh and NK responses were strongly correlated, suggesting NKs may play a suppressive role in development of memory B-cells by targeting of Tfh (Figure 3.17).

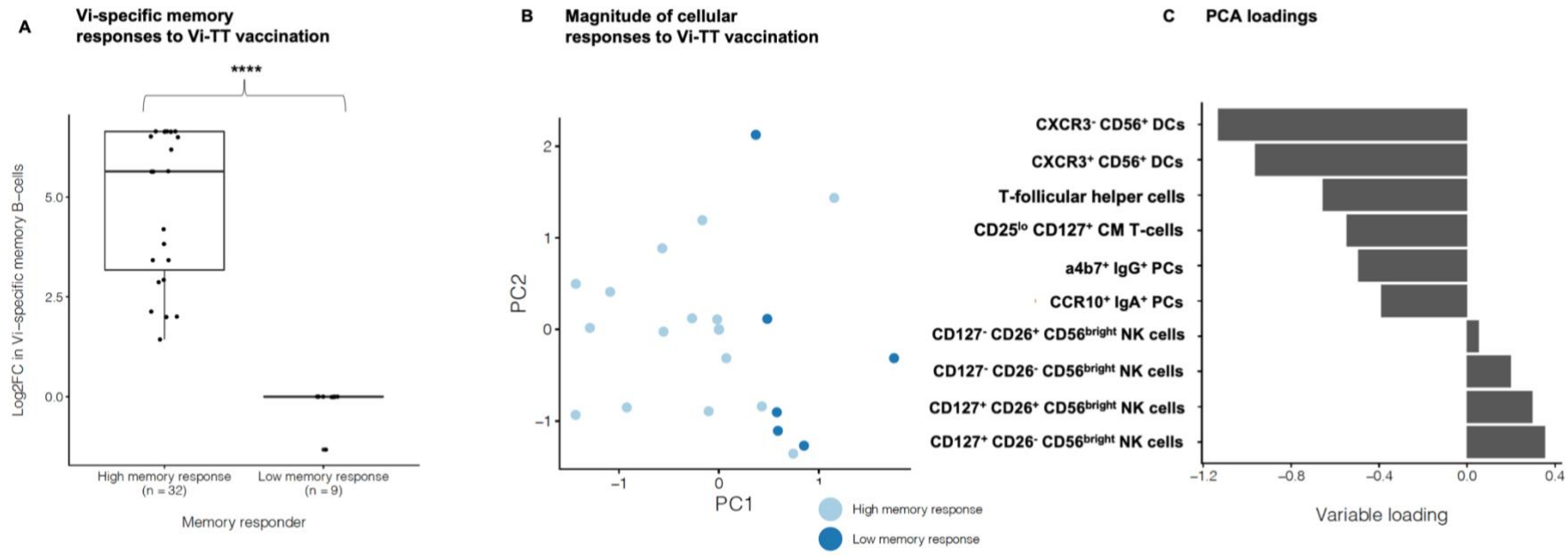


*Figure 3.15. Evaluation of high and low memory responders to Vi-TT vaccination. (A) Log2FC in Vi-specific memory B-cells 10 days after vaccination. High and low responders are compared by Wilcox rank sum test ns = p > 0.05, * = p < 0.05, ** = p< 0.01, *** = p <0.001, **** = p < 0.0001. (B) PCA analysis of differentially expressed cellular subsets after Vi-TT vaccination, coloured by memory responder status. (C) Loadings of PC1 showing strength of variable correlation with 1st principal component.*

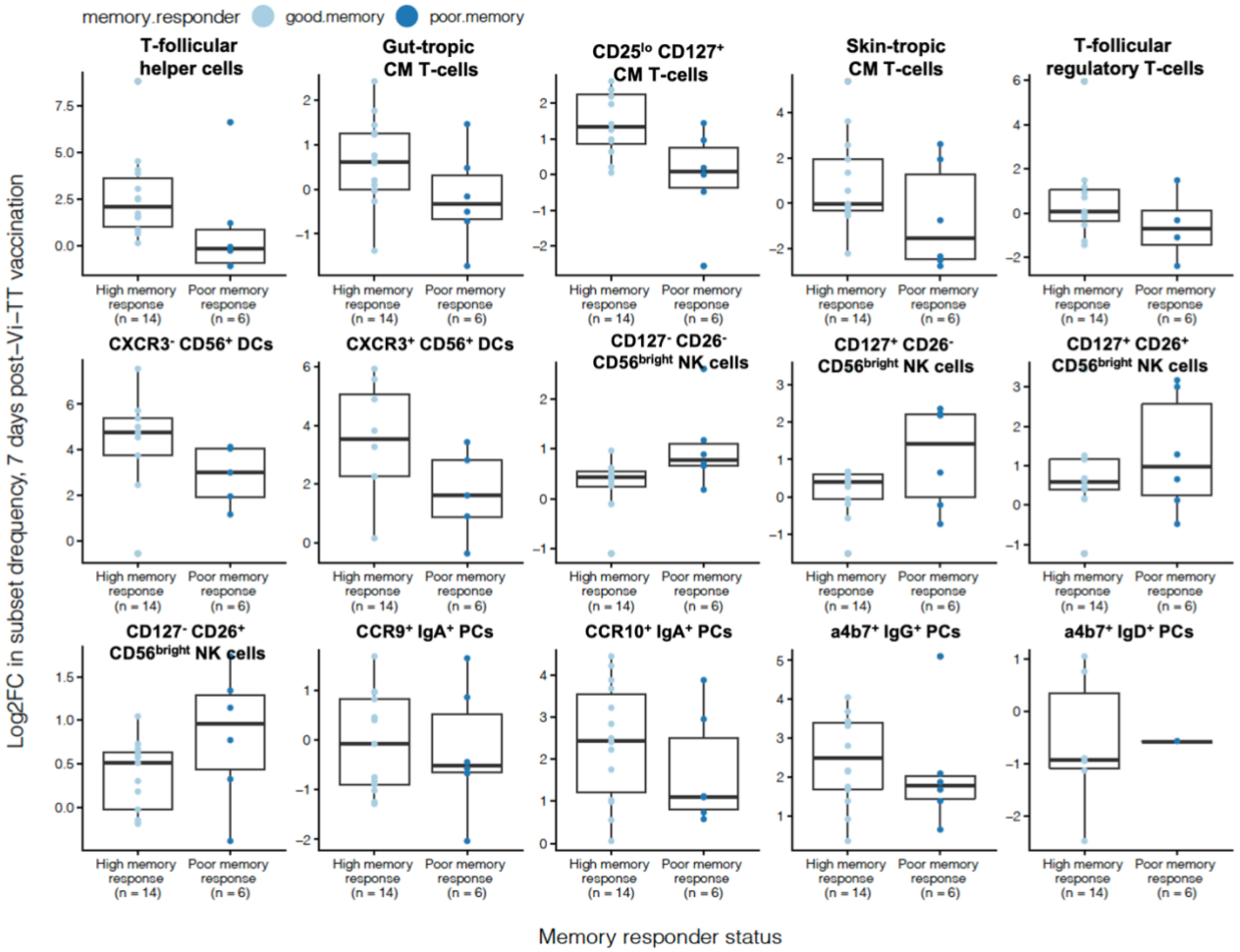


*Figure 3.16. Differences in cellular profile to Vi-TT immunisation between high and low memory responders. Log2FC in subset frequency 7 days after Vi-TT vaccination, compared between high and low memory responders. Groups are compared by Wilcox rank sum test ns = p > 0.05, * = p < 0.05, ** = p< 0.01, *** = p <0.001, **** = p < 0.0001.*

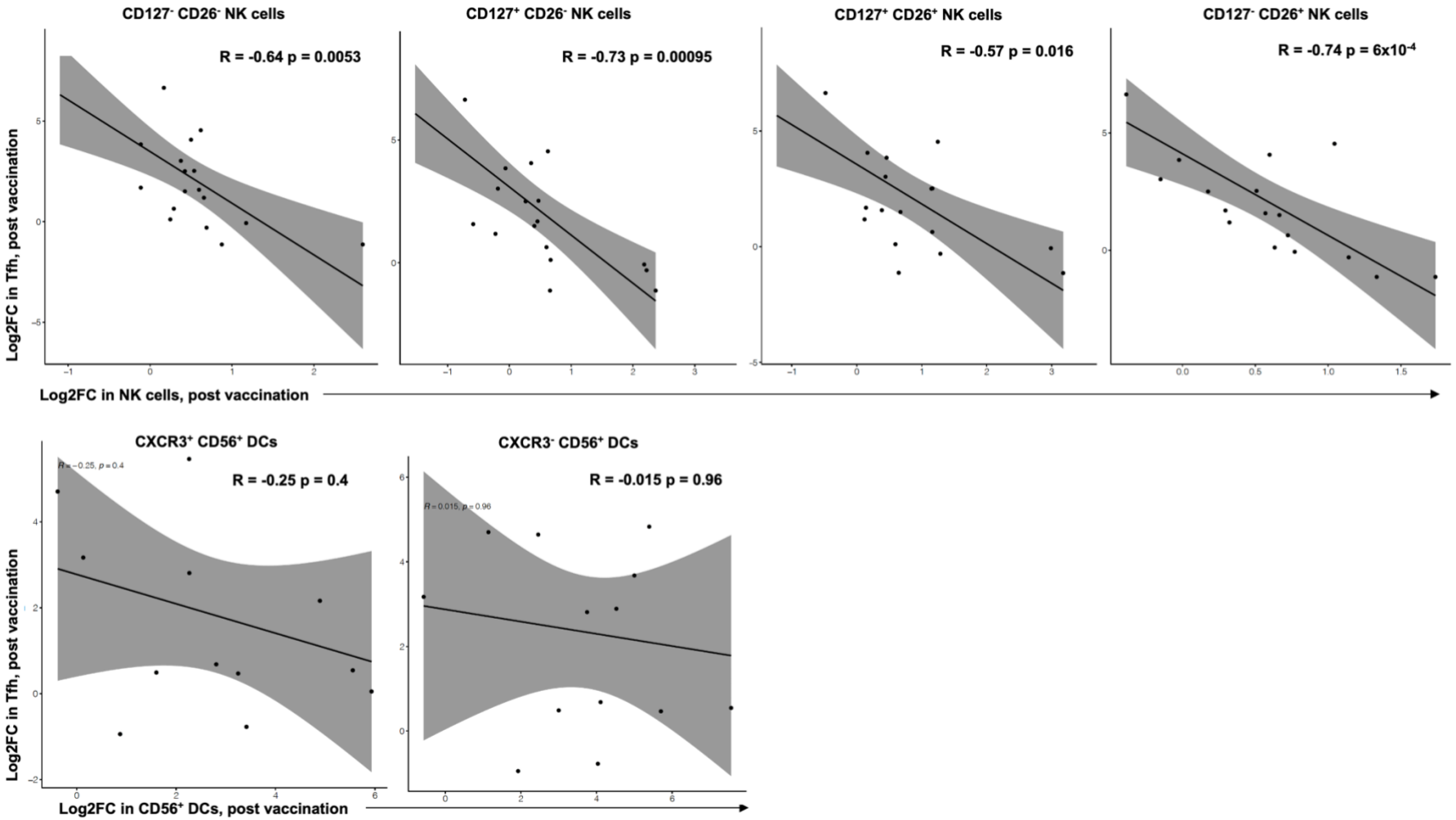


Figure 3.17. Relationship between NK cells and Tfh after Vi-TT vaccination. Vi-TT = Vi-tetanus toxoid vaccination, NK = natural killer. Spearman correlation between Log2FC in NK cell subsets, cTfh and CD56+ DCs 7 days after Vi-TT vaccination.

3.5 Discussion

This is the first study to comprehensively evaluate cellular responses to Vi-PS and Vi-TT and describe an association with protective humoral immunity. Humoral measures are widely used as correlates of protection in vaccinology, and greater understanding of how these responses develop is critical for improvement of vaccine design. This study identifies interesting associations between the primary cellular response to immunisation in peripheral blood and resultant antibody titres, functions and formation of memory B-cells.

In line with previous literature on glycoconjugate vaccines, the magnitude of the cellular response observed against Vi-TT underlies the superior immunogenicity of this vaccine when compared with plain polysaccharides. Whilst the magnitude of fold rise in both IgA- and IgG-expressing plasma cells was highly significant after vaccination in Vi-TT, the response to Vi-PS was considerably more modest (and did not meet statistical significance after correction for multiple testing). Nonetheless, a phenotypically similar plasma cell response to both immunisations was observed, with IgA responses predominating.

The parenteral administration route of Vi-vaccines has previously led to a focus on IgG responses. However, in both this analysis and previous studies examining the distribution of Vi-specific antibody subclasses post-vaccination, it has been shown that IgA (particularly IgA1) responses typically are greater[215]. IgA responses, a product of class switching, occurs against both T-cell dependent and T-cell independent antigens, suggesting this reaction can occur independently of the germinal centre. Indeed, reports in mice have shown that class switching can be largely extrafollicular with minimal involvement of GC reactions[216].

Fold rise in Vi-IgA after vaccination was positively correlated with protection in human challenge model data. Given the mucosal route of *S.* Typhi infection, the importance of IgA responses is not unexpected. The generation and persistence of Vi-specific memory IgA responses post-vaccination has not been assessed in this study although would be an important line of future enquiry.

Following Vi-PS and Vi-TT plasma cell subsets exhibited distinctive migratory marker patterns. IgA^+ plasma cells identified in peripheral blood universally expressed homing markers for mucosal sites including α4β7, CCR9 and CCR10[217]. Vaccination induced a strong increase in $CCR10^+$ $a4b7^+$ IgA^+ plasma cells in the Vi-TT group and also but to a lesser extent after Vi-PS. Expression of CCR10 on plasma cells was originally identified as a universal migratory marker of the common mucosal immune system[218]. In these reports, CCR10 expression confers responsiveness to chemokines CCL27 and CCL28. Tissue expression of these chemokines is distinct, with CCL27 being secreted by dermal epithelial cells and CCL28 being produced by several epithelial subsets in the intestinal tract (including both the colon and the small intestine)[219]. Co-expression with α4β7 increases the likelihood that these cells have a gut, rather than dermal, tropism. Integrin α4β7, recognises mucosal addressin cell adhesion molecule-1 (MAD-CAM1), an adhesion molecule expressed on high endothelial venules (HEVs) of mesenteric lymph nodes and Peyer's patches, specialised endothelium that mediates trafficking into the intestinal mucosal tissues[220]. Combined, these data imply a strong gut-tropism of plasma cells responding to both Vi-TT and Vi-PS immunisation.

The prevalence of α4β7 and CCR10 co-expression on IgA plasma cells after parenteral immunisation is slightly unusual. Expression of migratory markers is strongly associated with site of initial antigen encounter. It has been comprehensibly shown that mucosal immunisation (including oral and rectal immunisation routes[221]) induces both predominantly IgA and plasma cell responses (with some IgG) with strong α4β7 expression and minimal CD62L. In contrast, intramuscular immunisation leads to the reverse, with largely CD62L-expressing plasma cells and little α4β7[221]. Furthermore, evaluation of plasma cells isolated from mucosal sites such as the salivary gland, gastrointestinal tract, tonsil and appendix reveals that the vast majority of plasma cells are $CCR10^+$[218]. Therefore, induction of a mucosa-directed response following systemic immunisation is curious. One possibility is that systemic vaccination has reactivated a pre-existing pool of memory B-cells that has been previously primed at a mucosal surface. ASC trafficking between mucosal sites and the blood during the steady state is well-established. Mucosal plasma cells (IgA^+ $CCR10^+$ $a4b7^+$) are detectable at low frequencies in blood in the

steady state prior to immunisation[222]. Assessment of bone marrow samples also found that up to ~40% of ASCs in bone marrow express IgA, CCR10 and a4b7 suggesting that ASCs derived from mucosal responses contribute to a pool of long-lived plasma cells[222]. Clonal analysis has shown significant overlap between antibody sequences obtained from blood and intestinal IgA ASCs. In addition, intestinal and mesenteric lymph node ASCs also demonstrate sequence overlap, which further suggest recirculation of intestinal ASCs via blood[223].

The relationship between memory B-cells generated by mucosal responses and the peripheral blood has also been examined. IgD^{-} $\alpha4\beta7^{+}$ peripheral blood B-cells specific for rotavirus were identified at low frequency in healthy adults with no recent history of RV infection[224]. In addition, related IgA antibody clones were identified in populations of intestinal plasma cells and peripheral blood $CD27^{+}$ memory B-cells in patients with celiac disease[225]. The phenotype of plasma cells derived from peripheral blood memory B-cells after stimulation was not investigated therefore mucosal migratory capacity of these cells is unknown. However, these studies provide evidence for presence of mucosal antigen-specific memory B-cell responses at systemic sites.

In other examples of IgA responses to capsular antigens, authors have frequently attributed potency of the response in part to colonisation, for example of the nasopharynx in the case of pneumococcus. IgA responses to pneumococcal vaccine antigens are rare in very young children for example but dramatically increase with age[226] suggesting that mucosal colonisation accounts for a proportion of the observed responses to immunisation. Exposure to Vi by colonising organisms is assumed to be low although no extensive investigation into this has been previously conducted. *Citrobacter freundii* is a known, Vi-expressing commensal bacterium that causes invasive bacterial infections in immunocompromised individuals in hospital settings[227]. Examination of stool samples in a cohort with similar characteristics to that in the Vi vaccination study revealed that *C. freundii* carriage was reasonably common in individuals sampled (unpublished data). This analysis estimates prevalence of species from sequencing data and does not confirm expression of Vi which is known to be inducible rather than constitutive on *C. freundii* strains[228]. However, it does suggest that colonisation with Vi-

expressing *Enterobacter* species is common in UK residents and may be a possible contributor to Vi-specific immunity in colonised individuals. As a commensal rather than an invasive pathogen, it is unclear whether colonisation of this nature would be significant enough to trigger an IgA response. Quantification of faecal Vi-IgA has not assessed in this cohort but may be of interest.

In addition to a strong mucosa-directed response, IgG^+ plasma cells were also significantly increased following Vi-TT immunisation. The antigen specificity of these cells is likely to be mixed. In Vi-TT vaccinees, the majority of tetanus-specific plasma cells are likely to fall into this IgG^+ fraction and in part explain the magnitude of this response. Previous literature has shown that intramuscular vaccination with tetanus induces an IgG-dominant response with high expression of HLA-DR, CD38 and chemotactic responsiveness to CXCR3 ligands[229]. Other work has also confirmed that mucosal migratory markers such as CCR10 are rarely detected on TT-specific plasma cells[230].

This study is the first to report NK and DC responses in peripheral blood after Vi-TT and Vi-PS immunisations. $CD56^+$ dendritic cells, were found to be strongly elevated after immunisation. This population has been previously described and is functionally and phenotypically distinct from NK cells. Gene expression studies have found that $CD56^+$ DCs cluster with other subsets of myeloid dendritic cells but have some features of pDCs such as CD123 and BDCA2[231], in line with observed CD123 expression here. In keeping with a cDC phenotype, several studies have found $CD56^+$ DCs respond to TLR4 stimulation and secrete IL-12. CD56 expression on dendritic cells can be induced by several cytokines *in vitro* including IFNα[232,233], GM-CSF[232] or by IL-15[234]. Activation in this manner seems to confer cytolytic functions and enhances immunostimulatory capacity via greater antigen presentation[233]. Although numerous studies have described the effect of $CD56^+$ DCs on T-cell activation, no studies to date have investigated the effect of $CD56^+$ DCs on B-cells. The association with better memory formation may imply a role in germinal centre reactions. Whether $CD56^+$ DCs, with their enhanced antigen presenting capabilities, better engage activated, Vi-specific B-cells in the germinal centre is an unanswered question. In addition, how generalisable this

mechanism may be to other vaccinations is unclear. $CD56^+$ DCs lack systemic homing markers such as CCR7 and CD62L that are necessary for access to the lymph node and positioning within the germinal centre. Therefore, it is unclear whether these cells would be able to access activated B-cells and influence development of memory B-cells.

NK responses to vaccination were identified in the $CD56^{bright}$ compartment which comprises ~10% of NK cells in peripheral blood but make up a significantly larger proportion in tissues such as lymph nodes[235]. In this analysis, four phenotypically distinct subsets of $CD56^{bright}$ NK cells were identified on the basis of CD26 and CD127 expression. CD26, also known as dipeptidyl peptidase IV, is expressed at low levels on quiescent NK cells but is strongly upregulated in the presence of IL-2, IL-12 or IL-15[236]. Notably, CD26 deficiency has significant effects on cytotoxicity, inhibiting Fc receptor-mediated cell lysis as well as tumour cell lysis[237]. Whether this is due to impaired recognition of malignant cells or impaired release of secretory vesicles containing effector molecules has not been clearly established. Two of the four subsets in our analyses are $CD26^+$, therefore, detection of these responses could suggest that Vi-vaccinations induce Th1 cytokines such as IL-2, IL-12 and IL-15 upon immunisation that drive observed NK activation and proliferation.

The other subset defining marker is CD127, or the IL-7 receptor. Whilst CD127-expressing populations in this analysis co-express a considerable number of NK-associated markers including NKG2A and CD161, some ambiguity exists regarding their true identity. CD127 is a critical lineage marker for innate lymphoid cells (ILCs) and there is considerable heterogeneity and plasticity between subsets in terms of phenotype. Peripheral ILC1 and ILC3 subsets in humans have both been previously described to express CD56 and a number of cytokines such as IL-12 have been shown to drive conversion between NK cells and other ILC subsets. Lack of other ILC-specific lineage markers precludes further dissection of these populations to establish the relative contributions of ILCs and NK cells to vaccine responses observed here. Given some of the interesting observations between $CD56^+$ populations and development of humoral responses, further characterisation is warranted.

This study is the first to highlight a potential relationship between NK cells and generation of memory B-cells. The processes that underlie memory B-cell formation have been extensively studied but several aspects remain incompletely understood. Antigen-activated B-cells proliferate within the outer region of the B-cell follicle before migration to the B:T-cell border where germinal centres are formed. Antigen affinity is one of the critical determinants in GC B-cell fate; those with already high affinity BCRs receive the most critical signals from T-cells such as CD40 ligation and IL-21 stimulation[195]. This in turn drives the upregulation of the plasma cell transcriptional program and drives production of high affinity plasma cells. On the other hand, GC B-cells with lower antigen affinity receive limited T-cell help which activates an alternative transcriptional program promoting memory B-cell development[238].

Whilst T-cell-independent memory B-cell formation has been found to occur in some animal models[239], we find no evidence of Vi-specific memory responses in Vi-PS recipients. In addition, we observe a strong association between Tfh responses in peripheral blood and memory B-cell formation in these data. An unexpected association between $CD127^-$ $CD26^-$ $CD56^{bright}$ NK cells and failure of memory B-cell generation after Vi-TT vaccination was also noted. Although $CD127^-$ $CD26^-$ NK cells were the only significantly associated subset, other NK populations followed a similar trend. NK cells have been associated with the suppression of humoral responses in animal models of LCMV infection. NK responses in germinal centres have been shown to suppress numbers of Tfh, lower neutralising antibody titres and impair the generation of memory T-cells[240]. These effects were largely found to be perforin-dependent although effects on memory B-cells were not assessed. In humans, NK responses to vaccination have been previously reported; viral vectored immunisations such as Ad26.ZEBOV induced strong NK cell activation[201]. In addition, oral typhoid fever vaccine, Ty21a, was shown to strongly induce NK gene signatures in peripheral blood within 7 days of vaccination[241]. However, those studies did not establish a relationship with memory B-cell generation. This study provides detailed phenotypic information on the exact NK subsets that may play a role in Tfh suppression in humans. Further functional evaluation e.g. quantifying secretion of effector molecules previously shown to suppress Tfh responses and co-culture experiments would be

necessary to cement a role for NK cells in suppression of immunological memory. In addition, understanding the factors that drive NK activation after vaccination is another future line of investigation. Th1 cytokines such as IL-2, IL-15 and IL-18 are all known drivers of NK activation and proliferation. Whether Vi-vaccination triggers such responses is unclear therefore evaluation of serum cytokines at early timepoints after immunisation would provide clarity on this. Several studies have identified adaptive or "memory" NK cells that have stronger responses to stimulation with BCG antigens[242] . Whether Vi would trigger such a response is unknown. This enhanced responsiveness is epigenetically mediated by hypomethylation at key functional loci[243]. Evaluation of pre-vaccination NK cell DNA methylation profiles may be of interest in determining functional differences between individuals.

In summary, this analysis provides the first evaluation of cellular immune responses to Vi-TT and Vi-PS vaccinations and their association with protective humoral immunity. The IgA plasma cell response was significantly correlated with development of ADNP in Vi-TT vaccinees as were Vi-specific antibody titres. Tfh responses were strongly associated with the development of Vi-specific memory B-cells, with low Tfh recirculation in those who failed to mount a detectable memory response. In addition, an inverse correlation between the magnitude of Tfh and NK responses was observed. Poor memory development was associated with higher numbers of NK cells after immunisation. These findings provide insights into cellular pathways that may be responsible for generation of immunological memory and functional antibodies. Further evaluation is required to develop our understanding of these subsets in vaccine-mediated immunity.

4 PBMC signature of early infection associates with risk of developing acute typhoid fever

4.1 Introduction

Early detection and containment of bacterial infection is an essential component of protection against symptomatic disease. Cellular immunity involved in this process is multi-faceted involving a range of cell subsets. The relative contributions of innate and adaptive immunity in containment of *Salmonella* infection have been described both in humans and animals. As an intracellular pathogen, Th1 $CD4^+$ T-cell responses and specifically production of IFNγ are essential components of effective anti-bacterial immunity. Attenuated strains of *Salmonella* cause lethal, systemic bacteraemia in αβ TCR- or MHCII-deficient mice that are otherwise controlled in immunocompetent animals[106]. Other IFNγ-producing subsets including NK cells have also been shown to have an essential role in preventing lethal bacteraemia in mice with *S.* Typhimurium infection[88]. In addition, monocyte and neutrophil influx to both the intestinal tract and the spleen[91] have been shown to occur rapidly after infection, highlighting a key role of phagocytic and type II IFN-producing subsets in bacterial eradication.

Evaluating immune responses that correlate with protection prior to the development of symptoms is complex in human cases of typhoid fever. Studies of natural infection generally have limited information regarding the timing of pathogen exposure since individuals rarely know they are infected prior to symptom onset. Human challenge studies offer a unique opportunity to examine primary immune responses to infection that may associate with outcome of infection. Although cohorts are necessarily smaller, a wider range of responses can be profiled, giving the most complete picture of early immunity possible. Previously, studies of PBMC responses in human challenge models have tended to focus on individual subsets. Reports of detectable monocyte, DC and B-cell activation in peripheral blood have been made after infection however no absolute associations with protection have been made[33,244,245]. It is likely that a combination of responses is necessary for protection and therefore characterising

the breadth of the immune response to derive protective signatures would be advantageous. Signatures of cellular immunity that associate with better or worse outcomes during the early stages of infection are currently unknown.

The success of subunit vaccines targeting Vi-polysaccharides in protection against typhoid fever suggests antibodies are sufficient for prevention against symptomatic infection. A number of previous reports have suggested that cellular immunity is less pronounced in the context of immunisation although the effect of Vi-vaccination on the progression of responses to *S.* Typhi infection has never been evaluated. How anti-bacterial responses develop in the context of protective antibodies therefore requires clarification.

4.2 Chapter aims

Aim 1: to describe the cellular immune response to *S.* Typhi infection and associate with outcome of infection.

Aim 2: to evaluate the effect of vaccination on the development of cellular immunity to infection.

Aim 3: to describe host-intrinsic features such as baseline immune status and demographic characteristics that are associated with development of protective immunological responses to infection.

4.3 Methods

4.3.1 Source of samples

Samples were collected from participants challenged with *S.* Typhi at baseline, D1, D2 and D4 after infection. Details of the clinical trial, sample collection and processing are described in the Description of study samples section of the General Methods.

4.3.2 Cytokine quantification

The cytokines, CXCL1, sCD40L and CX_3CL1 were examined at baseline and 12 hours after infection. Protocols for ELISAs are provided in the Quantification of serum cytokines by enzyme linked immunosorbent assay (ELISA) section of the General Methods.

4.3.3 Antibody titre quantification and functional analysis

Quantity and functionality of Vi-specific antibodies was assessed prior to immunisation and 1-month post-vaccination. Descriptions of protocols is given in Quantification of Vi-specific antibody secreting cells (ASCs)

Number of Vi-specific ASCs were enumerated at baseline, 7 and 10 days after vaccination. Details of methods used are presented in the Detection of Vi-specific antibody-secreting cells (ASCs) post-vaccination section of the General Methods.

Quantification of Vi-specific antibody titres and Measurement of Vi-specific antibody functions in Chapter 3 Methods.

4.3.4 Differential abundance analysis

Differential expression between baseline and post-challenge timepoints was performed as described previously in the Statistical analysis section of the General Methods.

4.3.5 Partial least squares discriminant analysis (PLS-DA)

Participant diagnosis was predicted by PLS-DA using frequencies of differentially expressed PBMC clusters at the 24-hour timepoint. Model was fitted using the *MixOmics* package. All predictors were z-score standardised prior to analysis. Differentially expressed subsets with an FDR of 0.05 were included as predictors. Immune profiles were inferred by visual inspection of PCA plot and manual grouping of participants.

4.3.6 Baseline machine learning methods

Frequencies of PBMC subsets defined by manual gating were used as predictors of challenge outcome. Machine learning methods were implemented using the *caret* package. Baseline data were partitioned 75:25 with balanced distribution of outcome groups in both training and test datasets. Test set was required to have a minimum of 10 participants to ensure accurate predictions. A total of 182 machine learning algorithms performed sample classification and were individually evaluated by 10-fold cross-validation and performance on the test dataset (evaluated by confusion matrix).

4.4 Results

4.4.1 Activation of innate and adaptive subsets in PBMCs can be detected within 24 hours of oral S. Typhi infection

Perturbation within the PBMC compartment was detectable within 24 hours of infection (Figure 4.1A) (FDR = 0.01). Significantly changed populations were detected across all PBMC lineages suggesting broad activation of multiple subsets (Figure 4.1B). Some of these responses are observed universally in all participants and are discussed here.

Innate populations predominated the early response with significant changes in abundance of NK and DC subsets. $CD56^{dim}$ NK cells enriched for CD62L expression were significantly increased after challenge and remained elevated for several days after infection ($p < 0.001$) (Figure 4.2B). Cells in this population had an intermediatory phenotype with characteristics of both $CD56^{bright}$ and $CD56^{dim}$ NK cells. This included intermediate levels of inhibitory NK receptor, NKG2A and low expression of CD127 and CXCR3 (Figure 4.1B). In addition, a reciprocal reduction in another $CD56^{dim}$ population was observed in tandem with changes in the CD62L-expressing subset. These responses were significantly negatively correlated after infection ($R = -0.68$, FDR < 0.0001), suggesting bacterial infection leads to a global, compositional shift in the NK compartment after challenge (Figure 4.2C). In addition to NK cells, pDCs characterised by high expression of CXCR3 were also significantly modulated after infection ($p = 0.006$, **). A significant reduction in cell frequency was observed and persisted for several days after infection and began to recover around 4 days post-challenge (Figure 4.3B). Decline in pDCs was not associated with systemic levels of CXCR3 ligand CXCL10 suggesting reduction in frequency was not driven by CXCL10-mediated chemotaxis (Figure 4.3C).

Populations from the T-cell and B-cell lineages were also perturbed early after infection. Th17 and Tc17 cells, with well-defined roles in mucosal immunity and responses to bacterial infection[246] were modulated. Th17 cells were defined by high expression of CD4, an

effector memory (EM) phenotype (absence of CD45RA and CCR7 expression) and intermediate expression of CD161 as has been reported previously (Figure 4.4A)[247]. Additional features included strong expression of activation marker CD26 and migratory markers α4β7 and CXCR3. Manual gating of the $CD4^+$ $CD161^+$ compartment (Figure 4.4B) showed a significant increase in median expression of CXCR3 on this otherwise Th17-like population (Figure 4.4C). CXCR3 is a marker which is largely thought to be restricted to the Th1 lineage. Increased expression of CXCR3 on these cells may suggest systemic signals could be driving upregulation of CXCR3 on this population. This has been noted in previous research finding a hybrid Th1-Th17 population is often identified after infection[248].

Overall, populations from different lineages shared a number of characteristics. Upregulation of CD62L was characteristic of several of the populations identified after challenge and was enriched for expression of CXCR3. This suggests lymph node migration and responsiveness to inflammation may be critical features of early infection with *S*. Typhi. In addition, several populations expressing CD25 were identified, suggesting that IL-2 signalling may be a critical regulator of early anti-bacterial immunity.

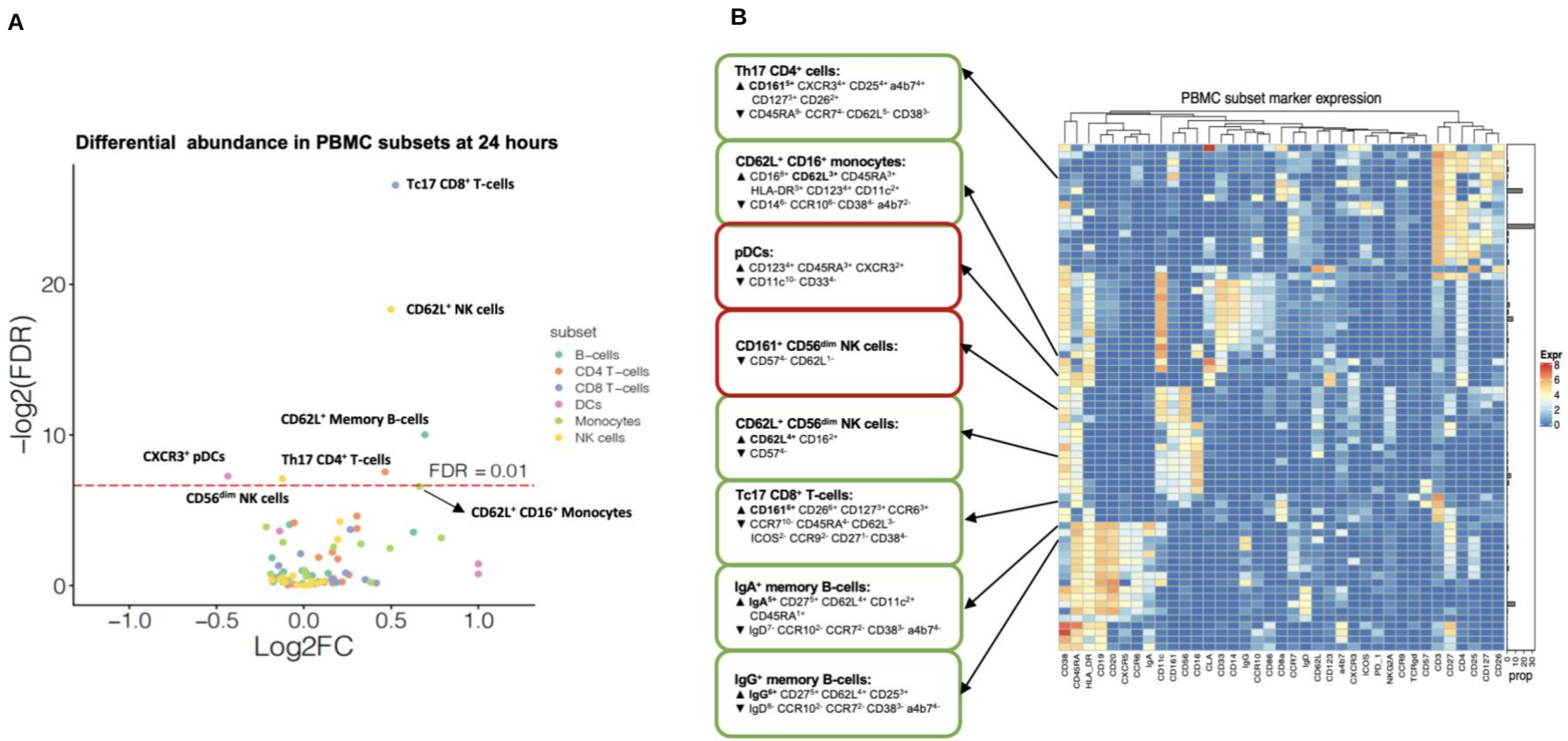


Figure 4.1. Differential abundance of PBMC subsets at 24 hours after oral infection with S. Typhi infection. (A) Volcano plot of differentially expressed subsets at 24 hours, FDR =0.01. Subsets identified by FlowSOM clustering. See General Methods for clustering markers. (B) Heatmap of all PBMC clusters identified by FlowSOM clustering. Each column represents one marker and each row represents one cluster. For visualisation, columns were clustered by hierarchical clustering. Median arcsinh-transformed marker expression visualised in heatmap. Differentially expressed clusters indicated by arrows. Enriched features of clusters (i.e. markers highly expressed by cluster in comparison to other cells within same lineage) are indicated in boxes Enrichment score calculated by MEM package.

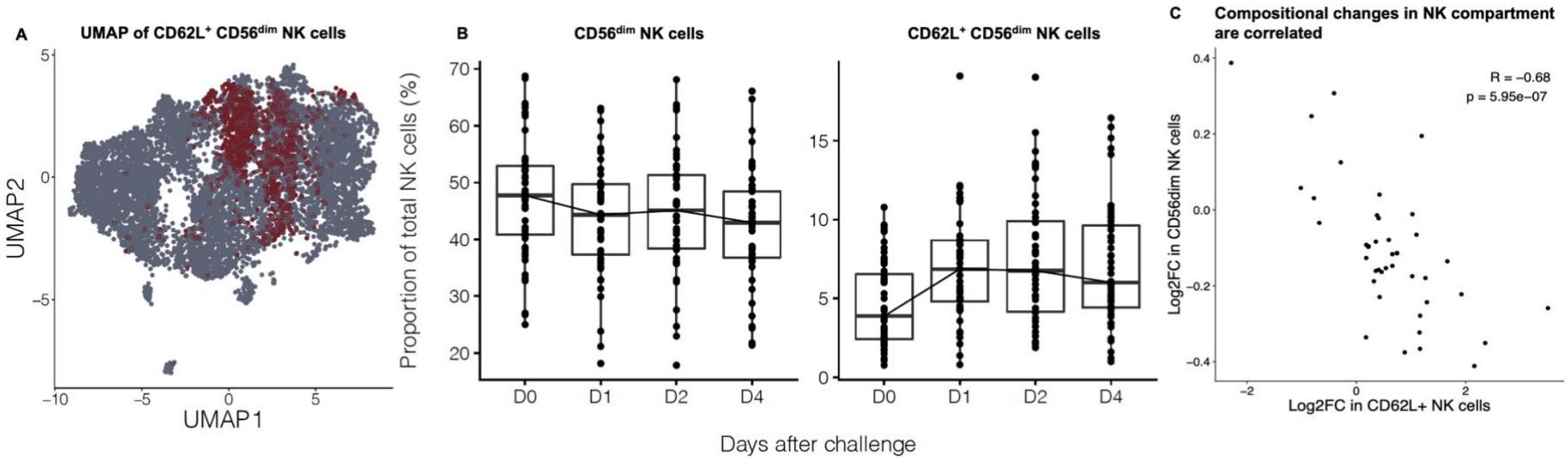


Figure 4.2. NK compartment is significantly altered by infection with S. Typhi. (A) UMAP of NK compartment (nearest neighbours = 15, minimum distance = 0.5), CD62L^{+} NK cells highlighted in maroon. (B) Significant decrease in CD56^{dim} NK cells and corresponding increase in CD62L^{+} CD56^{dim} NK cells (both diagnosed and protected participants shown). Differential abundance evaluated by negative binomial mixture models, participant ID included as a covariate. (C) Spearman correlation between log2FC in cluster frequencies.

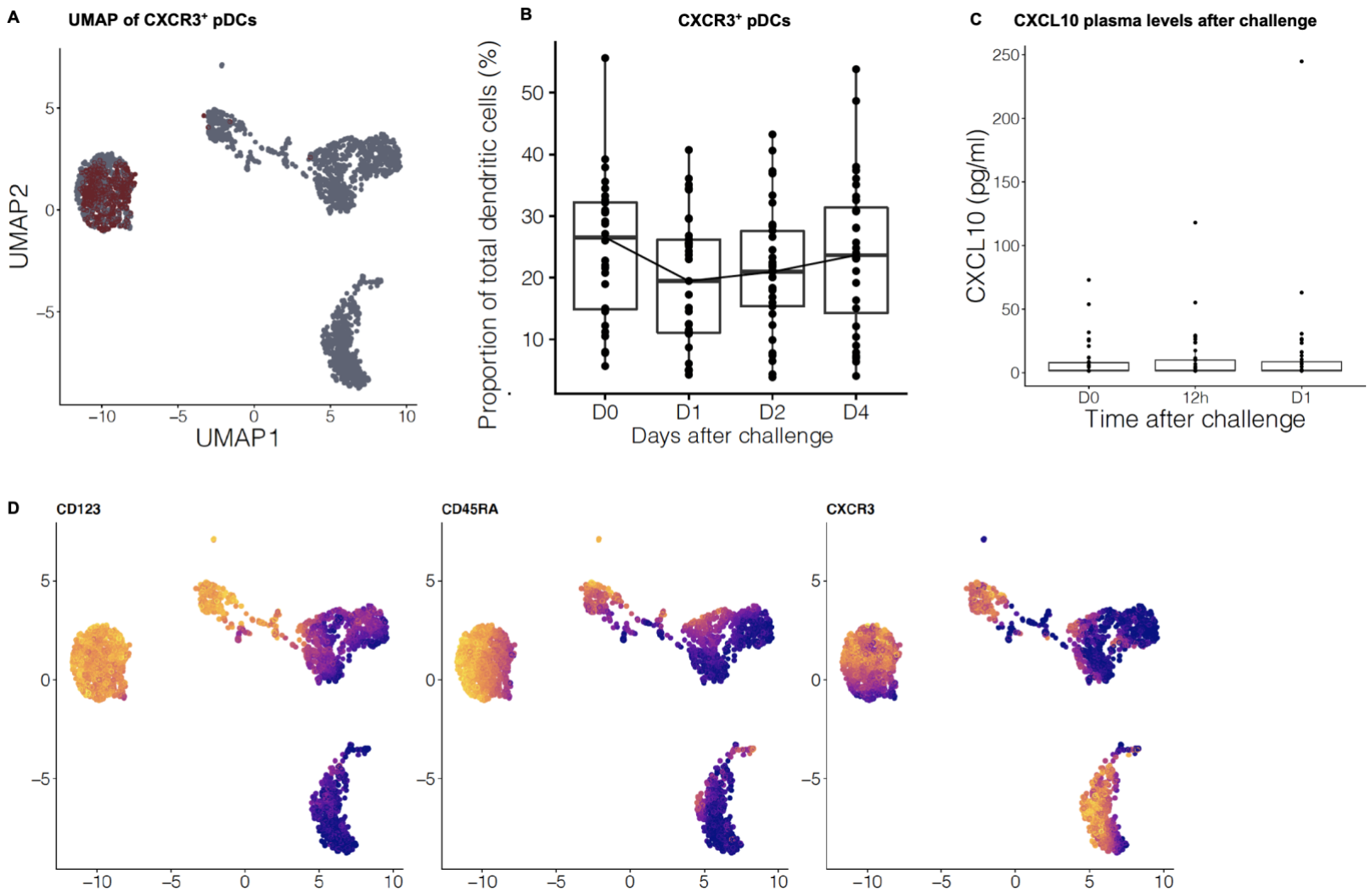


Figure 4.3. Change in frequency of pDCs after challenge. (A) UMAP of DC compartment (nearest neighbours = 15, minimum distance = 0.2), CXCR3⁺ pDC population is represented in maroon. (B) Significant decrease in CXCR3⁺ pDCs (both diagnosed and protected participants shown). Differential abundance evaluated by negative binomial mixture models, participant ID included as a covariate. (C) Changes in pDC frequency not attributable to systemic increases in CXCR3 ligand, CXCL10. (D) UMAP of CD4⁺CXCR5 compartment coloured by arcsinh-transformed marker expression (cofactor = 5). Lighter colour indicates stronger expression

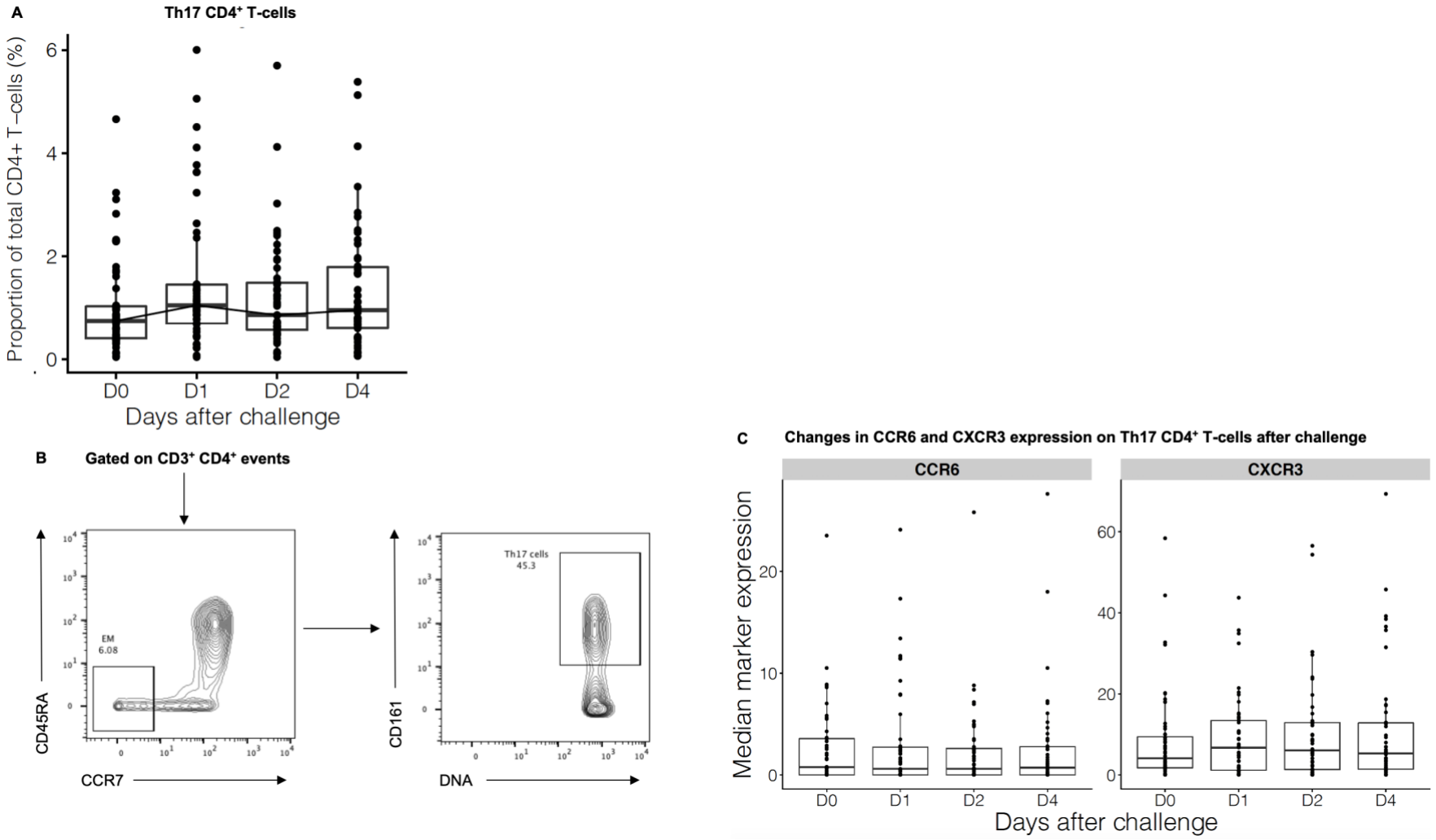


Figure 4.4. Changes in Th17 cells after challenge. (A) Frequencies of Th17 cells as a proportion of CD4⁺ T-cells at baseline and after challenge. (B) Manual gating scheme of CD4 effector memory and Th17 cells. (C) Changes in median marker expression of CCR6 and CXCR3 on CD4+ Th17 cells after challenge.

4.4.2 Outcome of infection is associated with the 24-hour response

Differentially expressed subsets at 24 hours were used to predict infection outcome. Partial least squares discriminant analysis of the 24-hour response identified 3 groups of participants with distinct immunological responses after challenge and differing likelihoods of diagnosis (Figure 4.5A). Identified profiles are referred to from here onwards as protective, intermediate and susceptible. The majority of participants (30/57, 53%) had an intermediate cellular profile in which 50% (15/30) of individuals were protected for disease and the remainder were not i.e. association between cellular profile and outcome of infection was limited. Contrastingly, almost one-fifth (12/57, 21%) of the cohort exhibited a protective cellular profile at this timepoint whilst the remainder contributed to the susceptible profile (15/57, 26%) and had the greatest likelihood of being diagnosed of any of the groups identified (12/15, 80%) (Figure 4.5C). Participant characteristics were compared between susceptibility profiles. Unexpectedly, participants with a susceptible profile were significantly younger ($p = 0.023$, *) than participants with a protective profile although median ages across all groups were similar. Groups were comparable for other demographic features reflecting the relative homogeneity of the study population.

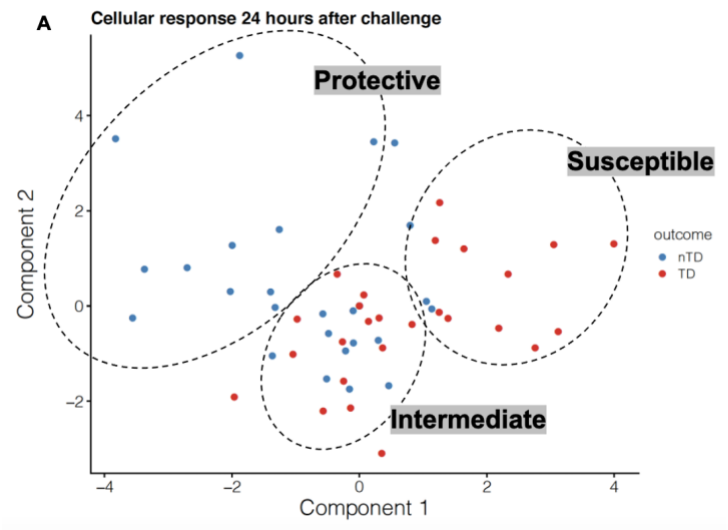
Responses driving separation of susceptibility groups were assessed (Figure 4.5B). Variables strongly correlating with protection included activated naïve B-cells and $CD16^+$ monocytes. $CD16^+$ monocytes were a unique feature of the protective profile whereas naïve B-cell activation was identifiable in both protective and intermediate groups (Figure 4.6A and C). Expansion of $CD16^+$ monocytes was evident one day after challenge with peak frequencies observed two days after infection (Figure 4.6A). $CD16^+$ monocytes had high expression of CD62L, CD38 and the IL-3 receptor, CD123 suggesting a highly activated state (Figure 4.6B).

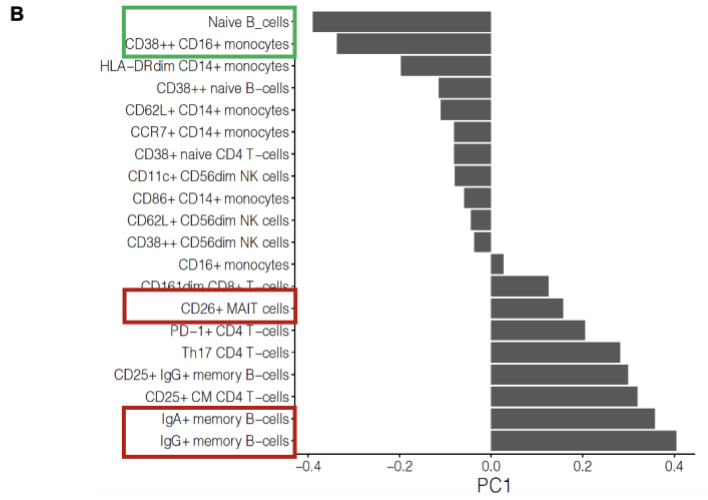
Naïve B-cells were significantly changed in the protective and susceptible groups and expressed high levels of activation markers, including HLA-DR and CD38 when compared with resting cells. Interestingly, activated naïve B-cells downregulated CCR7 and had greater levels of gut homing marker, $\alpha4\beta7$ suggesting potential for chemotaxis to the gut (Figure 4.6D).

Other profiles also exhibited unique cellular kinetics. Differential abundance of two subsets of memory B-cells with IgA and IgG surface expression respectively was greatest in susceptible individuals (Figure 4.7A). These populations were enriched for CD27 and had low expression of CXCR5 and CCR6. They were deficient in plasma cell markers such as CD38. Interestingly, IgG^+ memory subsets were enriched for CD25, a subunit of the IL-2 receptor, and had high expression of HLA-DR, pointing towards a more antigen-presenting phenotype rather than immunoglobulin secretion as has been reported previously[249]. Finally, these cells were found to have upregulated expression of CD62L, suggesting that lymph node recirculation may be a feature of susceptibility (Figure 4.7B).

Susceptible and intermediate profiles were also characterised by Tc17 activation early after infection (Figure 4.7C). Tc17 cells with a MAIT-like phenotype were also increased after infection ($p > 0.001$). As staining for invariant TCR, the hallmark identifier of MAIT cells, was not performed in this study, this population cannot be conclusively identified as MAIT cells. However, previous studies have found the majority of Tc17 cells in peripheral blood are MAIT cells and recognise MR1-expressing target cells[250]. Given the enteric nature of the infection, it is plausible that that a proportion of these cells represent MAITs. Features confirming a Tc17 lineage include high CD161 and expression of CD127 and CCR6 (Figure 4.1). Tc17 significantly correlated with decreases in pDCs suggesting a potential role for pDCs in early Tc17 activation (Figure 4.7D).

To better understand whether distinct cellular immune profiles were functionally associated with better disease control, bacterial load at disease presentation was compared between immune profiles. Susceptible individuals had significantly higher CFU of bacteria in blood compared to intermediate individuals that developed disease (Figure 4.7E). Other potential indicators of poor infection control such as CRP levels and time to diagnosis were not significantly different between immune profiles (data not shown). This implies that early responses detectable in peripheral blood associate with better control of bacteraemia in infected participants that develop symptomatic infection.





C

	Protective	Intermediate	Susceptible	*p*-value	*Significance*
No. of participants	12	30	15		
% Diagnosed (n)	8 (1)	50 (15)	80 (12)	0.001	**
Age (years)	33 (31.8 – 45.0)	26 (22.3 – 42.3)	23 (21.5 – 27.5)	0.02 (protective vs susceptible)	*
Body Mass Index	25 (24 - 27)	26 (24 - 29)	23 (22 - 28)	-	ns
Weekly alcohol units	9 (4.25 – 10.5)	4 (1.25 - 10)	5 (2.5 – 9.0)	-	ns
% Female (n)	41.7% (5)	43.3% (13)	46.7% (7)	0.963	ns
% Vaccine responders (n)	58.3 (7)	46.7 (14)	33.3 (5)	0.720	ns
% Recent travel (n)	33.3 (4)	16.7 (5)	33.3 (5)	0.345	ns

Figure 4.5. PLS-DA analysis reveals clusters of participants with differential likelihoods of diagnosis. (A) PLA-DA plot. Each dot represents one participant. Standardised cluster frequencies were used as input for analysis. Points are coloured by outcome of challenge and grouping was done by visual inspection of the plot. (B) Component 1 loadings showing strength of correlation between subset and first principal component. (C) Table of participant characteristics compared between response profiles. Continuous variables were compared by Wilcox rank sum text whereas categorical variables were assessed by Fisher's exact text. .

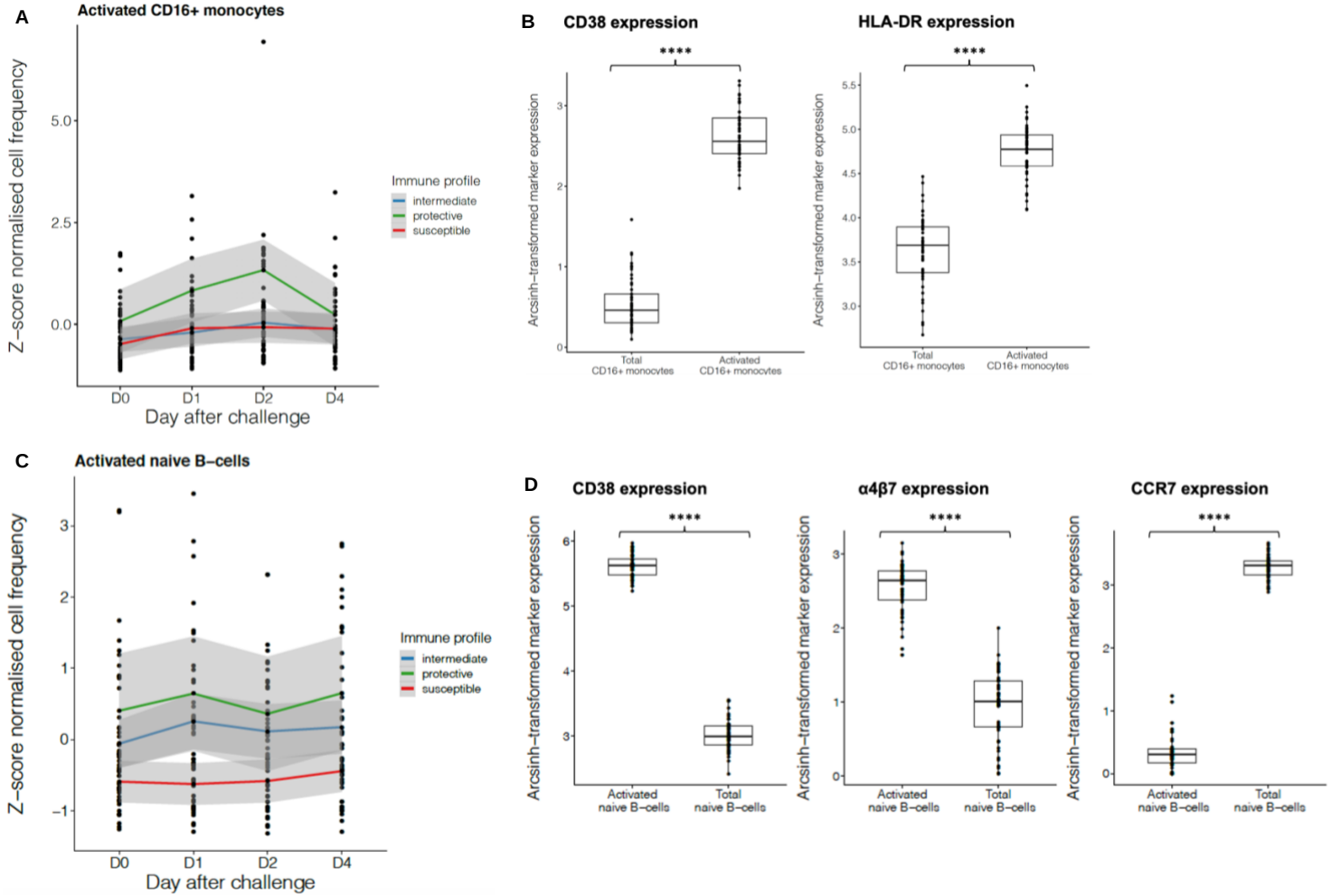


*Figure 4.6. Evaluation of cellular immunity associated with protective profile. D0 = day of challenge (one-month post-vaccination), D1 = one day after challenge, D2 = two days after challenge, D4 = four days after challenge. Significance thresholds: ns = p > 0.05, * = p < 0.05, ** = p< 0.01, *** = p <0.001, **** = p < 0.0001. (A) Kinetics of activated CD16$^+$ monocytes after infection, split by susceptibility profile (B) Differences in activation marker expression between activated and total CD16$^+$ monocytes. Groups compared by Wilcox rank sum test. (C) Kinetics of activated naïve B-cells after infection, split by susceptibility profile (D) Differences in activation marker expression between activated and total CD16$^+$ monocytes. Groups compared by Wilcox rank sum test.*

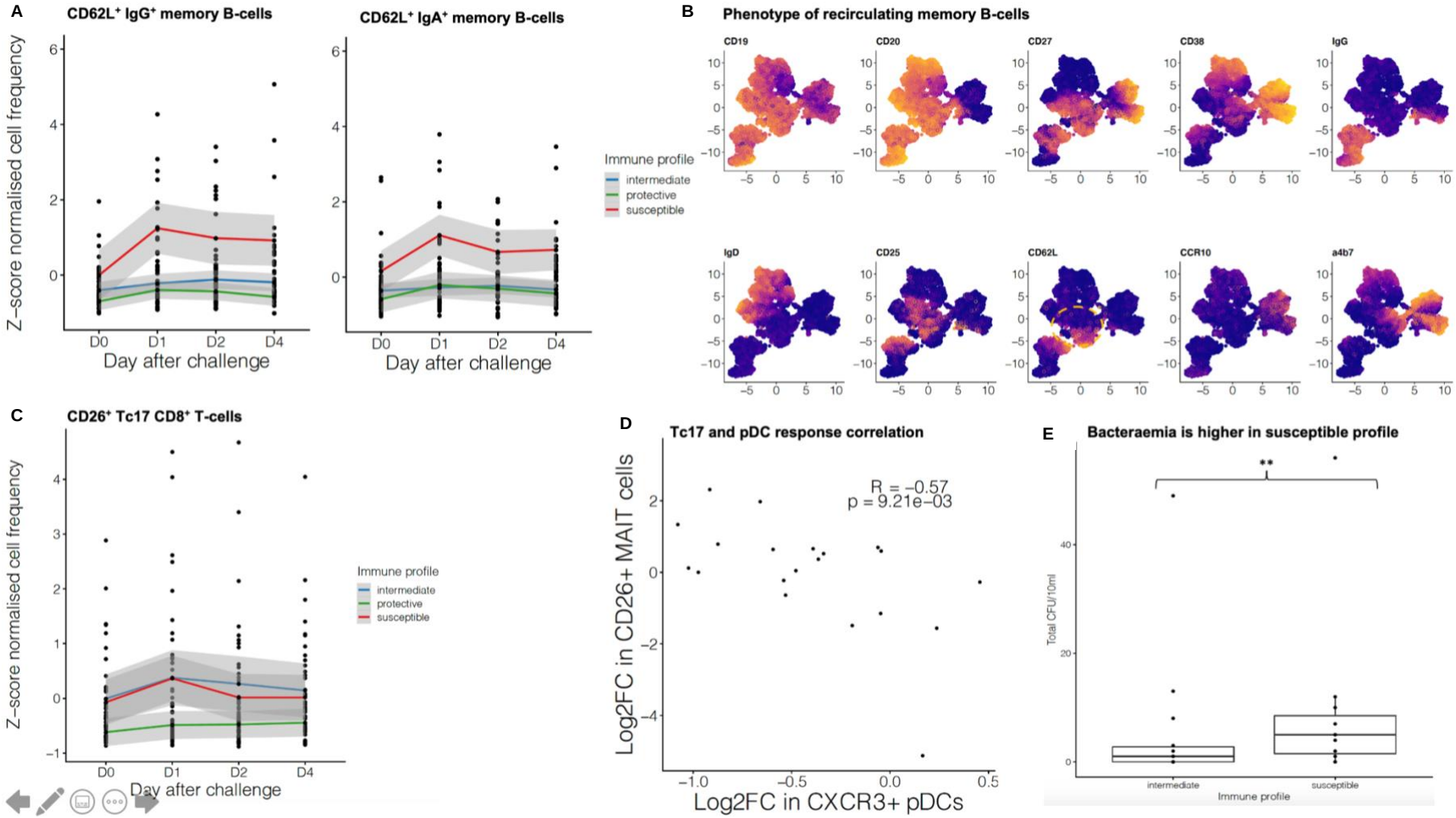


*Figure 4.7. Evaluation of cellular immunity associated with a susceptible profile. D0 = day of challenge (one-month post-vaccination), D1 = one day after challenge, D2 = two days after challenge, D4 = four days after challenge. Significance thresholds: ns = p > 0.05, * = p < 0.05, ** = p< 0.01, *** = p <0.001, **** = p < 0.0001. (A) Kinetics of CD62L⁺ memory B-cells after infection, split by susceptibility profile. (B) UMAP analysis of B-cell compartment, coloured by arcsinh-transformed marker expression (cofactor = 5). Lighter colour indicates stronger expression. (C) Kinetics of Tc17 cells after challenge, split by susceptibility profile. (D) Spearman correlation between fold rise in Tc17 cells and pDCs 1 day after challenge. (E) Comparison of bacterial burden (CFU/10mL) at diagnosis between intermediate and susceptible profiles.*

4.4.3 Vaccination status and antibody profile is modestly associated with development of cellular immunity after infection

The influence of Vi-vaccination on the development of cellular immunity to *S.* Typhi infection is unknown. The proportion of vaccinated and unvaccinated participants was compared between immune profiles (Figure 4.8A). Individuals that did not mount a detectable Vi-IgG ASC response within 10 days of immunisation (poor responders) are represented as a separate group to those that did mount a detectable ASC response (high responder). Differences in proportions did not meet statistical significance, possibly due to having too few numbers of participants (p-value = 0.132). Chi-square residuals indicate a minimal relationship between strong vaccination response and the protective immune profile (Figure 4.8B). The presence of unvaccinated individuals in all immune profiles suggests that Vi-antibodies were not an absolute requirement for the development of any responses observed but that they may modestly increase the likelihood of some responses developing rather others. It was hypothesised that if vaccination was increasing the likelihood of a particular cellular profile after infection, then antibody titre and functional features may differ between vaccinees in different immune profiles. Vi-titres were compared between immune profiles in vaccinated individuals only. Vi-IgG and IgA antibody titres were not significantly different between profiles however a significant difference between Vi-IgM titres was detected ($p > 0.001$) (Figure 4.9A). Comparison of antibody functionality revealed significant differences between immune profiles. Vi-IgG2 antibody avidity was significantly lower in susceptible individuals ($p = 0.002$, ** and $p = 0.009$, ** in comparison with protective and intermediate groups respectively) suggesting poor Vi-binding may associate with increased likelihood of diagnosis (Figure 4.9B). These individuals also had significantly greater numbers of pro-inflammatory antibodies that induce NK-mediated IFNγ release (Figure 4.9C). Notably, antibody functionality was similar between participants with protective and intermediate profiles. This indicates that, whilst low quality antibodies are significantly associated with increased risk of an unfavourable cellular profile and poor outcome, antibodies with high functionality were not sufficient for the development of a protective profile.

An association between development of susceptible immune profile and poorer quality antibodies suggests that vaccination may be modulating early signals that drive the expansion of cellular responses. To further investigate, the effect of vaccination on the early cytokine response 12 hours after infection was evaluated. CXCL1, CX_3CL1 and sCD40L were all significantly elevated within 12h of challenge (Figure 4.8C). When compared between vaccine arms and immune profiles, no significant differences were found between vaccinated and unvaccinated participants. CX_3CL1 and sCD40L were elevated in susceptible individuals when compared with other immune profiles although these differences did not reach significance (Figure 4.8C). Fold rise in cytokines was not correlated with antibody titre or antibody functional scores (data not shown).

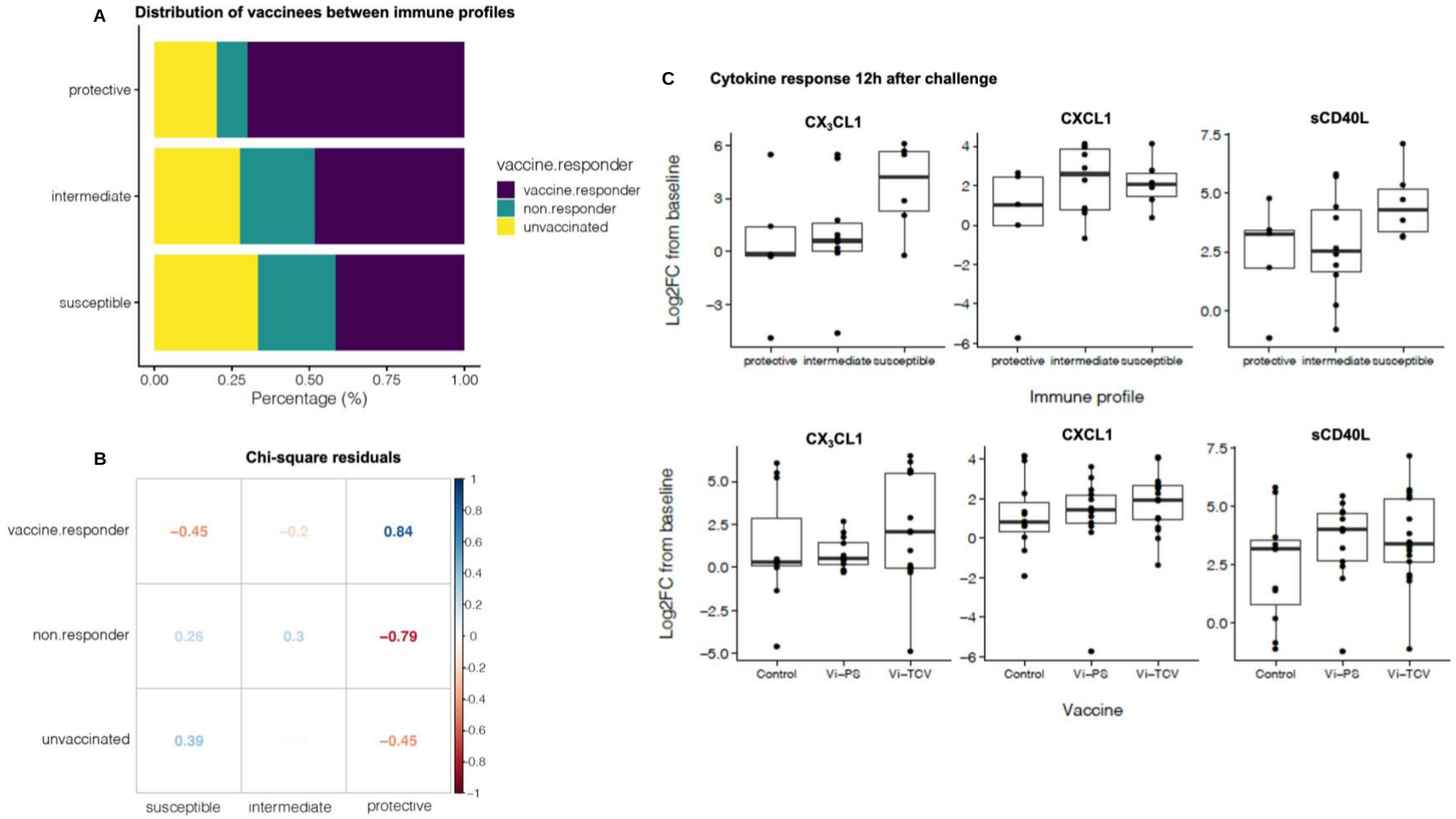


*Figure 4.8. Effect of vaccination on development of cellular immunity. (A) Bar plot showing proportions of vaccinated and unvaccinated individuals within each immune profile. Vaccinees (Vi-TT and Vi-PS) are grouped as responders or non-responders according to their Vi-IgG ELISpot response (definition discussed in the previous chapter). Significance thresholds: ns = $p > 0.05$, * = $p < 0.05$, ** = $p < 0.01$, *** = $p < 0.001$, **** = $p < 0.0001$. (B) Chi-square residuals testing association between vaccination status and immune profile. (C) Quantification of CXCL1, CX_3CL1 and sCD40L 12h after challenge, split by immune profile and vaccine arm.*

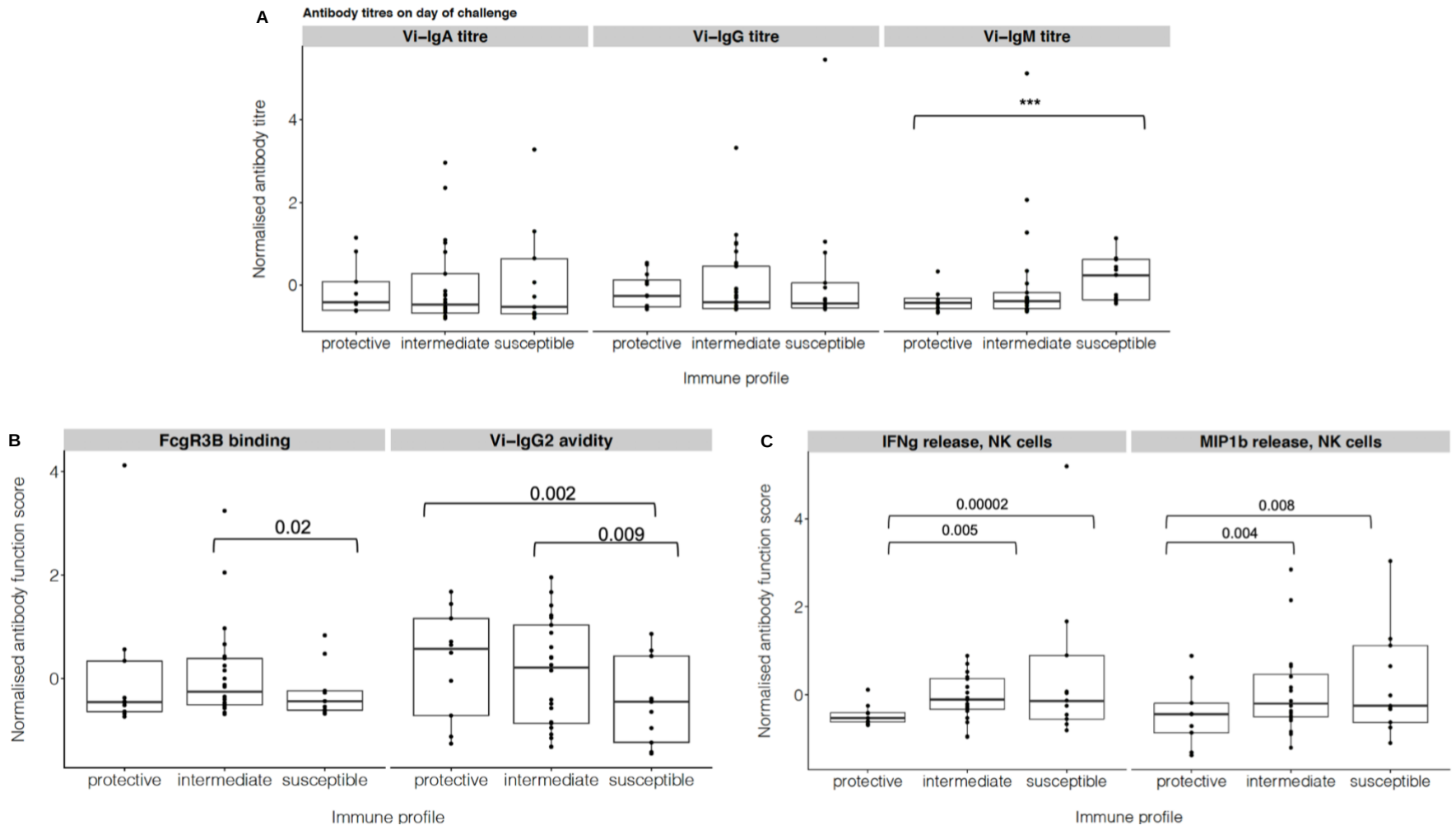


*Figure 4.9. Differences in Vi-antibody function between immune profiles. Vi-antibody functional scores were standardised and compared between immune profiles. Groups were compared by Wilcox rank sum test. Significance thresholds: ns = p > 0.05, * = p < 0.05, ** = p< 0.01, *** = p <0.001, **** = p < 0.0001.*

4.4.4 Baseline features of participant PBMC profile predict immune profile and outcome group

Given that not all individuals within a given immune profile are vaccinated, vaccination cannot be the sole factor driving differences in response to infection. Therefore, other factors were investigated to better understand host-intrinsic features and susceptibility. It was hypothesised that baseline immune status may influence the development of responses to infection and outcome of challenge. Systemic indicators of inflammation such as white blood cell count, CRP and inflammatory cytokines (TNFa, IFNg, IL-1β) were compared at baseline between immune profiles and outcome groups. No significant differences in systemic inflammatory markers were identified (Table 4.1) suggesting low systemic inflammation or activation.

Next, PBMC composition was evaluated as a predictor of challenge outcome and immune profile. Stability of PBMC profiles over time in study participants was assessed by comparing frequencies of major lineages in PBMC samples taken from pre-vaccination and pre-challenge (approximately 1 month apart). No significant differences in PBMC profiles were noted between timepoints (Figure 4.10) suggesting PBMC composition prior to challenge could be used as a stable indicator of baseline immunological status.

Machine learning methods were used to classify diagnosed and protected participant baseline samples. In total, 133 models were successfully fitted to baseline data. Model AUC ranged between 0.67 and 0.77 when applied to test data for the top 5-performing models, suggesting moderate predictive power (Figure 4.11A). No significant differences in frequency of innate subsets were identified between outcome groups, however, compositional perturbations were observed in B- and $CD4^+$ T-cell compartments (Figure 4.11C). Baseline frequency of naïve B-cells was the strongest predictor of challenge outcome with protected individuals having significantly higher numbers of naïve B-cells than diagnosed individuals. The second most predictive feature was frequencies of naïve $CD4^+$ T-cells (Figure 4.11C) which was also significantly increased in protected individuals.

Composition of the B- and T-cell compartment were compared between immune profiles (Figure 4.12). Associations between frequencies of naïve subsets and a protective profile were even more striking (Figure 4.12A). This suggests the development of early responses to infection can be predicted using baseline PBMC composition. Interestingly, higher frequencies of effector memory (EM) $CD4^+$ T-cell subsets and memory B-cell subsets (Figure 4.12) were observed in susceptible participants at baseline. Paradoxically therefore, a PBMC profile suggestive of greater antigen experience was associated with worsened outcome of infection. Parameters known to influence frequencies of naïve and effector subsets such as age were evaluated. No significant associations between participant age and baseline frequency of B-cell subsets were found suggesting observations are independent of demographic features (Figure 4.13).

*Table 4.1. Baseline inflammatory status prior to challenge. Systemic markers of inflammation were compared between susceptibility groups by Wilcox rank sum test. . Significance thresholds: ns = p > 0.05, * = p < 0.05, ** = p< 0.01, *** = p <0.001, **** = p < 0.0001.*

PARAMETER	GROUP 1	GROUP 2	GROUP 1 (N)	GROUP 2 (N)	STATISTIC	P-VALUE	SIGNIFICANCE
C-REACTIVE PROTEIN (MG/L)	intermediate	protective	30	12	216	0.963	ns
C-REACTIVE PROTEIN (MG/L)	intermediate	susceptible	30	15	200.5	0.963	ns
C-REACTIVE PROTEIN (MG/L)	protective	susceptible	12	15	67	0.963	ns
TOTAL WHITE CELLS (X10^9/L)	intermediate	protective	30	12	174.5	0.975	ns
TOTAL WHITE CELLS (X10^9/L)	intermediate	susceptible	30	15	240.5	0.975	ns
TOTAL WHITE CELLS (X10^9/L)	protective	susceptible	12	15	83	1	ns
IFNG	protective	intermediate	5	10	21	1	ns
IFNG	protective	susceptible	5	6	17	1	ns
IFNG	intermediate	susceptible	10	6	42	0.549	ns
IL1B	protective	intermediate	5	10	7	0.861	ns
IL1B	protective	susceptible	5	6	6	0.861	ns
IL1B	intermediate	susceptible	10	6	16	0.861	ns
TNFA	protective	intermediate	5	10	25	1	ns
TNFA	protective	susceptible	5	6	19	1	ns
TNFA	intermediate	susceptible	10	6	38	1	ns

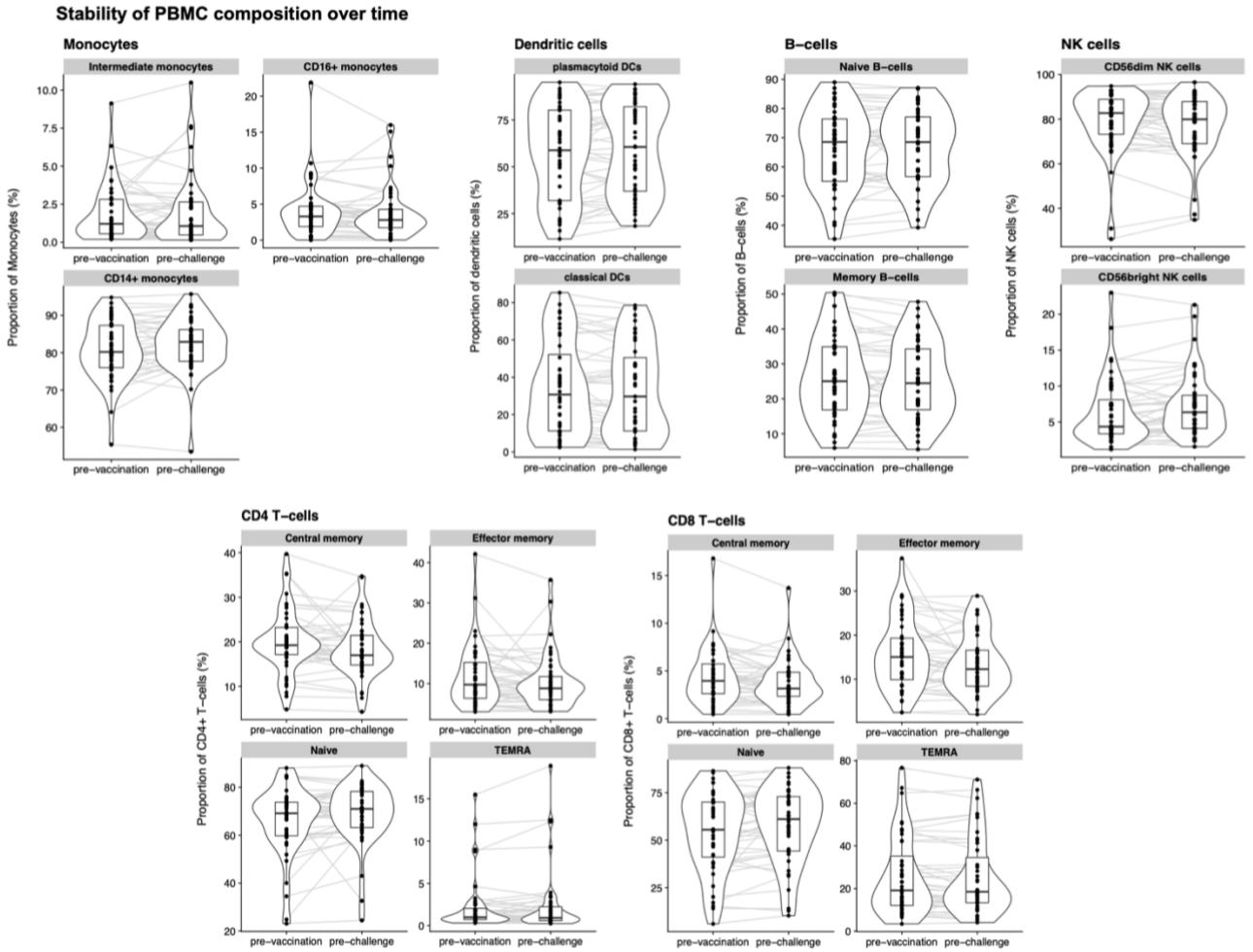


*Figure 4.10. PBMC composition stability over one month. Pre-vaccination = one month before challenge, Pre-challenge = sample collected immediately before challenge. Major cell populations were manually gated and compared between timepoints. Presented as frequency of subset lineage. Timepoints compared by Wilcox rank sum test. Significance thresholds: ns = p > 0.05, * = p < 0.05, ** = p< 0.01, *** = p <0.001, **** = p < 0.0001*

A

modelID	modelName	Accuracy	Precision	PredictAUC	Recall	Sensitivity	Specificity
17	svmRadialCost	0.7143	0.7500	0.6735	0.4286	0.6429	0.7143
18	svmRadial	0.7143	0.7143	0.6939	0.3571	0.5000	0.7143
31	snn	0.7143	0.7500	0.0000	0.4286	0.6429	0.7143
97	mlpKerasDropout	0.7857	0.8000	0.7755	0.4286	0.5714	0.7857
129	gcvEarth	0.7857	0.8000	0.7755	0.4286	0.5714	0.7857

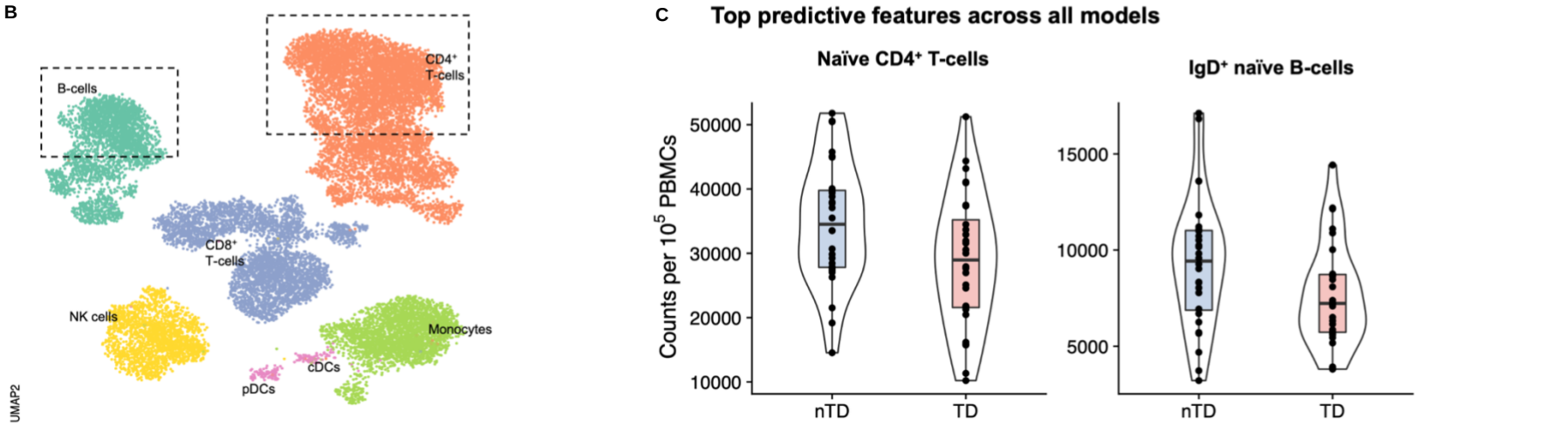


Figure 4.11. Prediction of outcome using baseline PBMC composition. Training cohort: n = 42, Test cohort: n = 15 (A) Summary table of 5 best performing machine learning models (assessed by accuracy) applied to baseline data. Manually gated subset frequencies (percentage of live cells) used as input. PredictAUC = Model area under the curve when applied to test data. (B UMAP of PBMC populations (nearest neighbours = 15, minimum distance = 0.8) coloured by cell lineage. 10,000 subsampled events presented. (C) Top predictive features identified by all 5 best performing models. Presented as frequency of live cells. nTD = not diagnosed, TD = diagnosed.

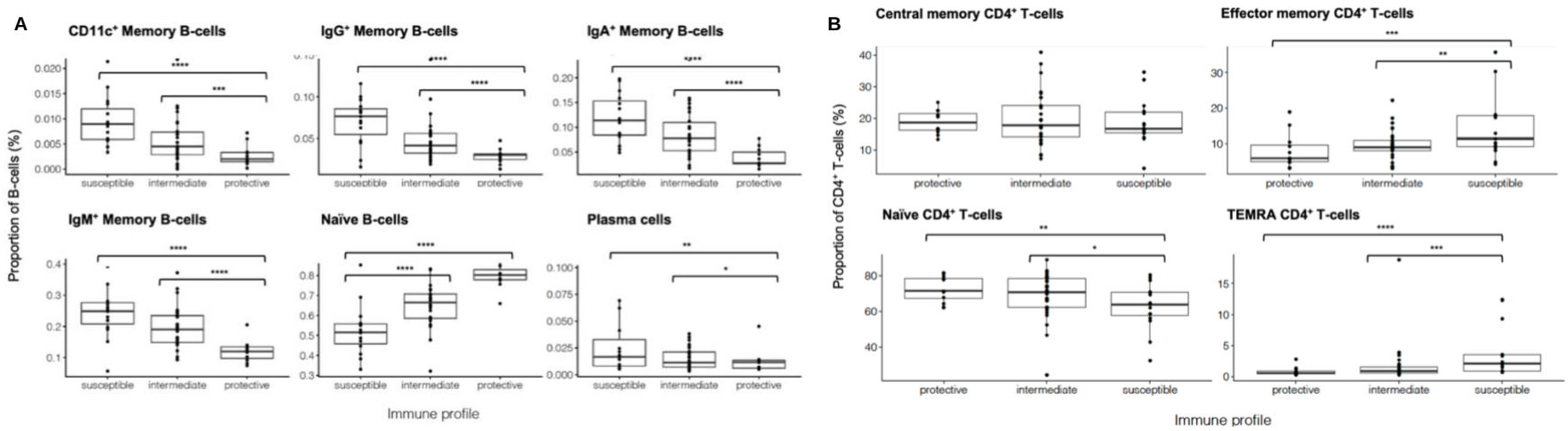


*Figure 4.12. Evaluation of association between B-cell and CD4-T-cell composition at baseline and immune profile after challenge. (A) Boxplots comparing baseline frequencies of B-cell subsets between immune profiles. (B) Boxplots comparing baseline frequencies of $CD4^+$ T-cell subsets between immune profiles. Groups compared by Wilcox rank sum test. Significance thresholds: ns = $p > 0.05$, * = $p < 0.05$, ** = $p < 0.01$, *** = $p < 0.001$, **** = $p < 0.0001$*

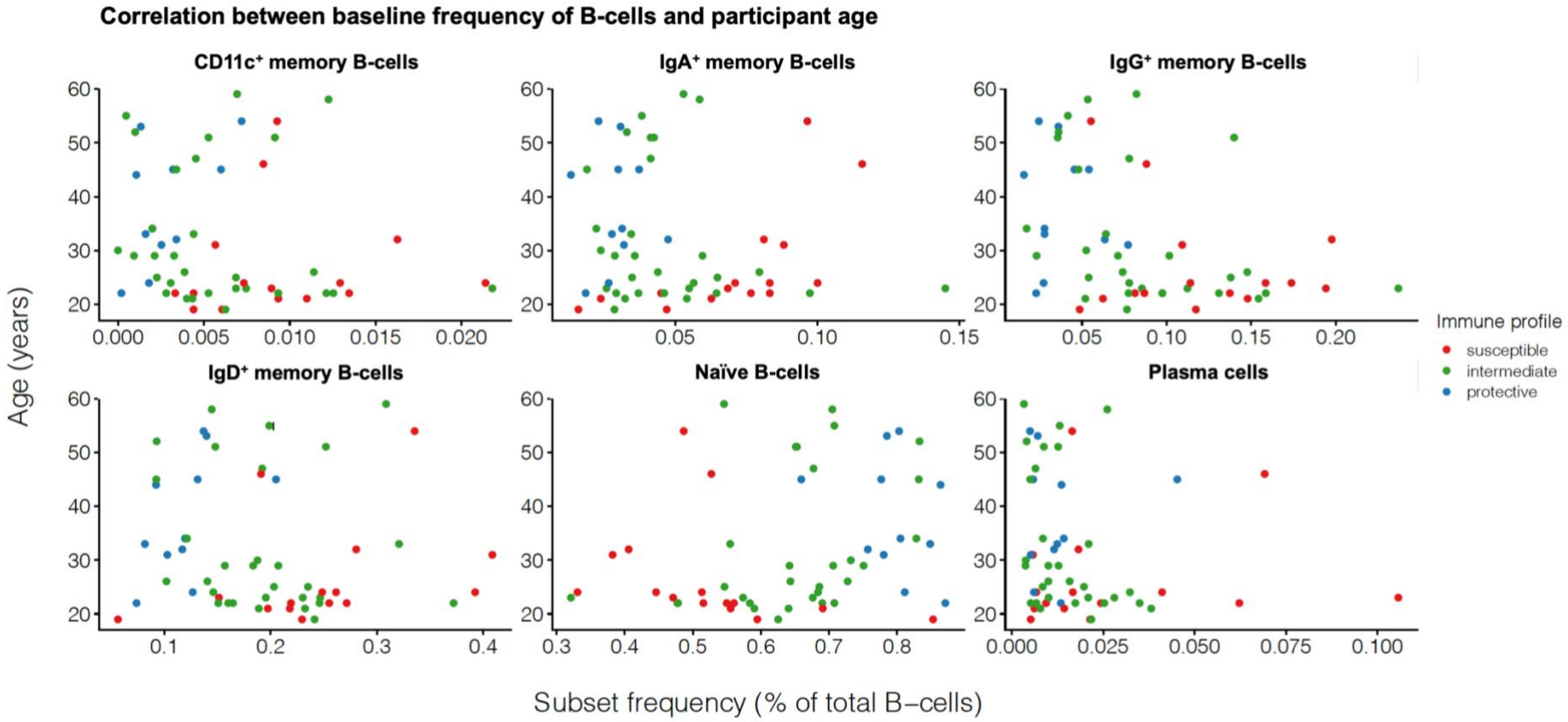


Figure 4.13. Correlation between baseline frequency of B-cell subsets and participant age. Colour indicates immune profile.

4.4.5 Detailed characterisation of NK responses to S. Typhi infection

The vast majority of participants in this analysis developed an intermediate phenotype at the 24-hour timepoint, suggesting that identified alterations in PBMC composition are insufficient to accurately stratify individuals that remain well from individuals that develop disease in this group. To further our understanding of protection in the intermediate group, a detailed phenotyping and functional assessment of NK immune responses was proposed. Investigation of the NK compartment was chosen given the strong changes observed after challenge and previous literature identifying the importance of early IFNγ production in control of *Salmonella* infection[88]. Therefore, it was hypothesised that evaluation of NK responses after challenge may confer insights into the protective signature. In this thesis, flow panel and cytotoxicity assay optimisation steps are presented. In addition, an example of NK phenotyping is shown.

The effect of cryopreservation on NK functionality was assessed (Figure 4.14). MIP1β and CD107a production were approximately halved after cryopreservation in comparison to fresh cells (24.7% to 13.1% positive cells and 20.6 to 11.5% positive cells for MIPβ and CD107a respectively) although IFNγ production was less impacted (10.8% to 9.4% positive cells). This was partially rectified by increasing assay incubation time to 5hr (MIP1β: 17% positive cells, CD107a: 17.2% positive cells). Overnight resting of cells prior to stimulation had a negative impact on production of all cytokines when stimulated with K562 cell line and IL-2 an IL-15 (IFNg: 1.02% positive cells, MIP1b: 4.3% positive cells, CD107a: 2.6% positive cells). Rested NK cells were phenotyped for lineage markers and expression of cytotoxic receptors (Figure 4.16). Overnight resting was shown to cause significant downregulation of almost all markers examined.

NK phenotyping markers are presented in Flow cytometry panel section of General Methods. Antibodies were titrated to determine optimal concentrations for use (Figure 4.17). NK phenotyping performed on one individual is presented (Figure 4.18A). Flow cytometry recapitulated NK populations observed in mass cytometry, indicating reproducibility of mass cytometry findings (Figure 4.18C). Interestingly, the NK flow panel identified a significant

proportion of additional subsets including a significant population of NKG2C^{+} CD57^{+} adaptive NK cells (Figure 4.17B). Adaptive NK cells have been well-described in literature in response to human CMV infection and their presence may be indicative of HCMV exposure. The importance of this in evaluating NK responses from *S.* Typhi-infected participants has not been confirmed.

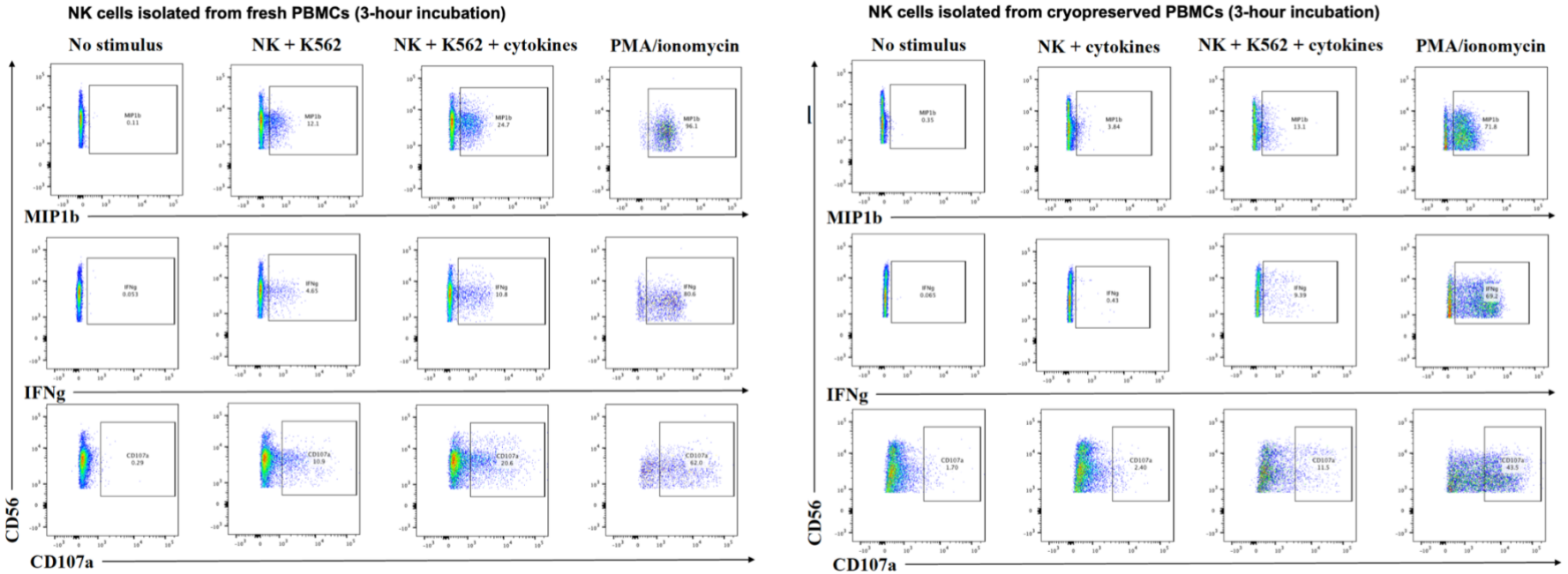


Figure 4.14. Effect of cryopreservation on NK cell cytotoxicity. NK cells were isolated from either fresh or cryopreserved PBMCs and incubated with media (no stimulus, negative control), K562 cell line (1:1 target: effector ratio), K562 cell line + IL-2 + IL-15 (see General Methods for concentrations) or PMA/ionomycin (positive control). Each condition was repeated twice (one representative example is shown here) .

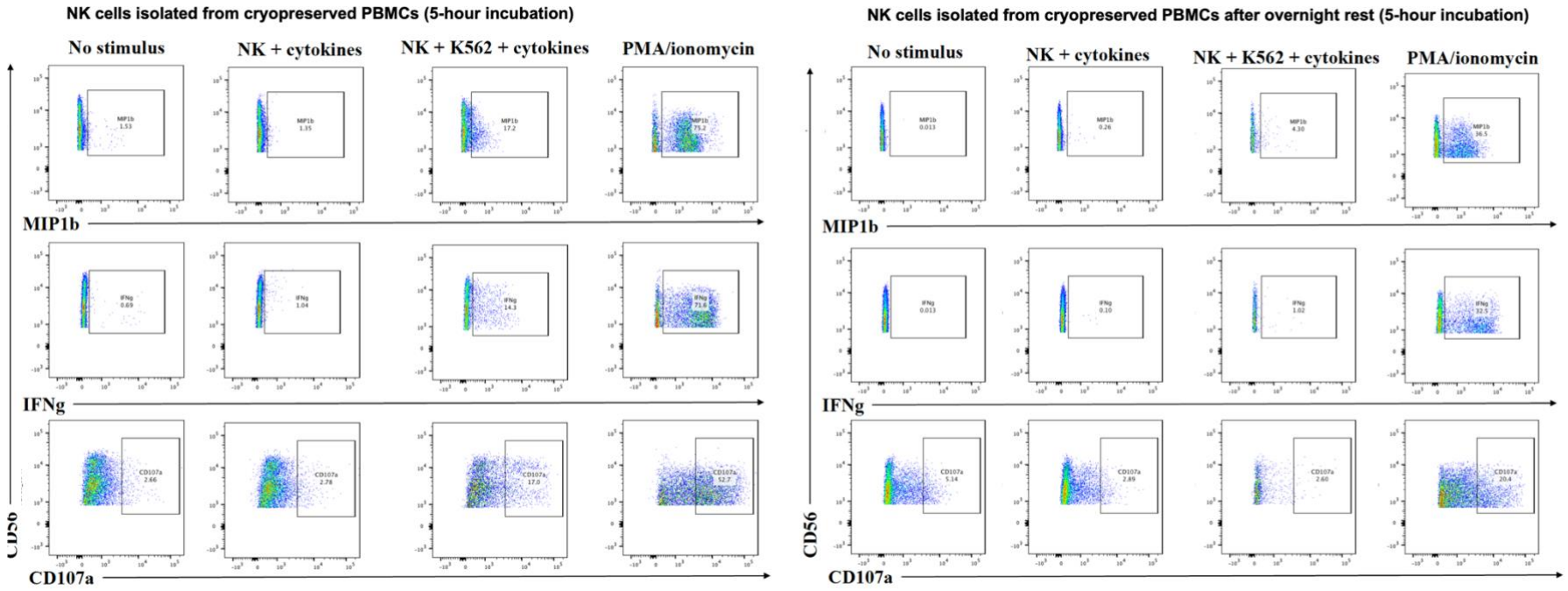


Figure 4.15. Effect of incubation time and overnight rest on NK cell cytotoxicity. NK cells were isolated from cryopreserved PBMCs and either stimulated immediately or rested overnight. Stimulation in both cases was for 5 hours. NK cells were incubated with media (no stimulus, negative control), K562 cell line (1:1 target:effector ratio), K562 cell line + IL-2 + IL-15 (see General Methods for concentrations) or PMA/ionomycin (positive control). Each condition was repeated twice (one representative example is shown here).

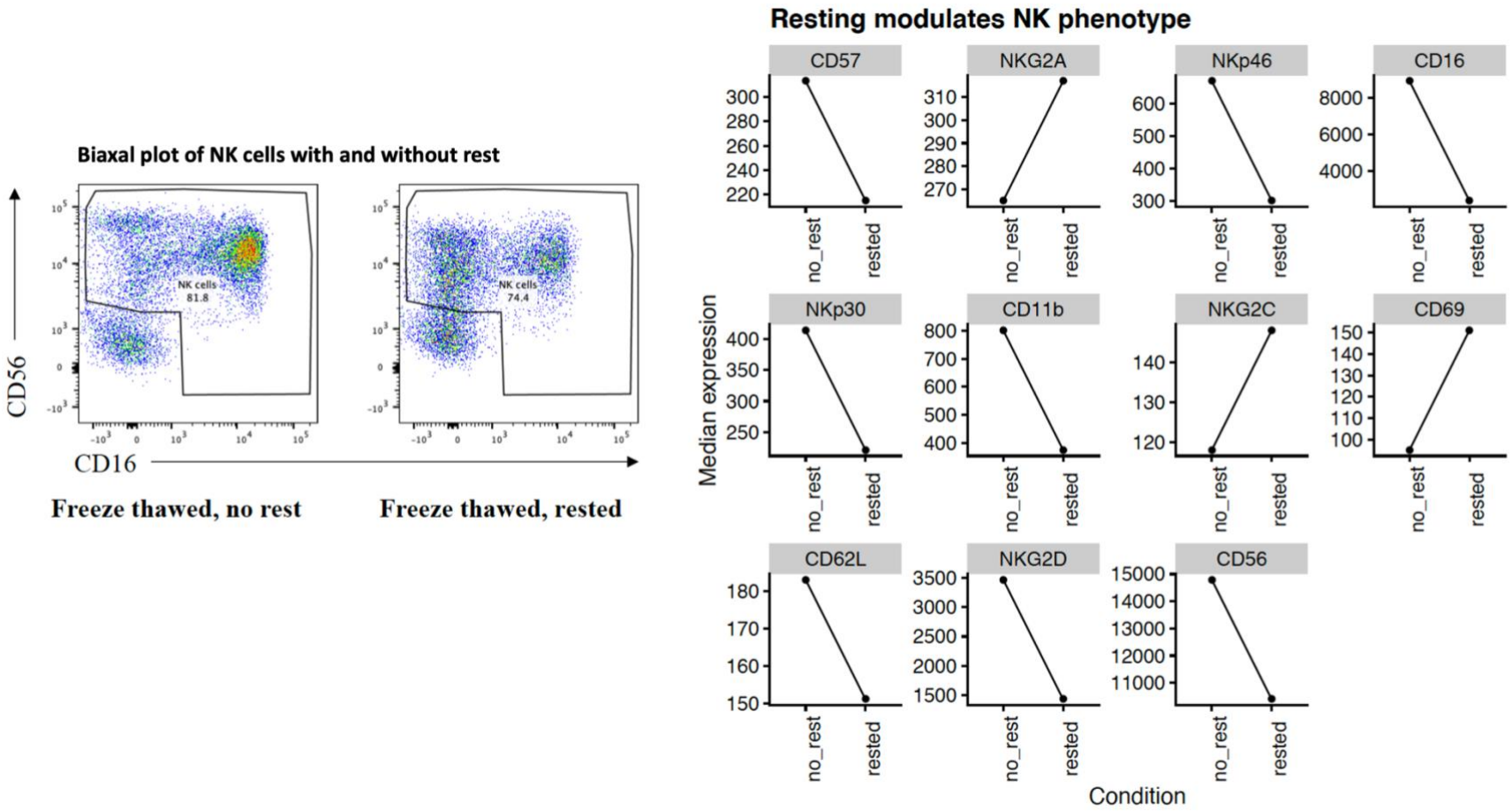


Figure 4.16. Evaluation of NK phenotype after overnight rest. Cryopreserved NK cells were stained for surface markers and median expression was compared between rested and unrested conditions (experiment conducted on one participant).

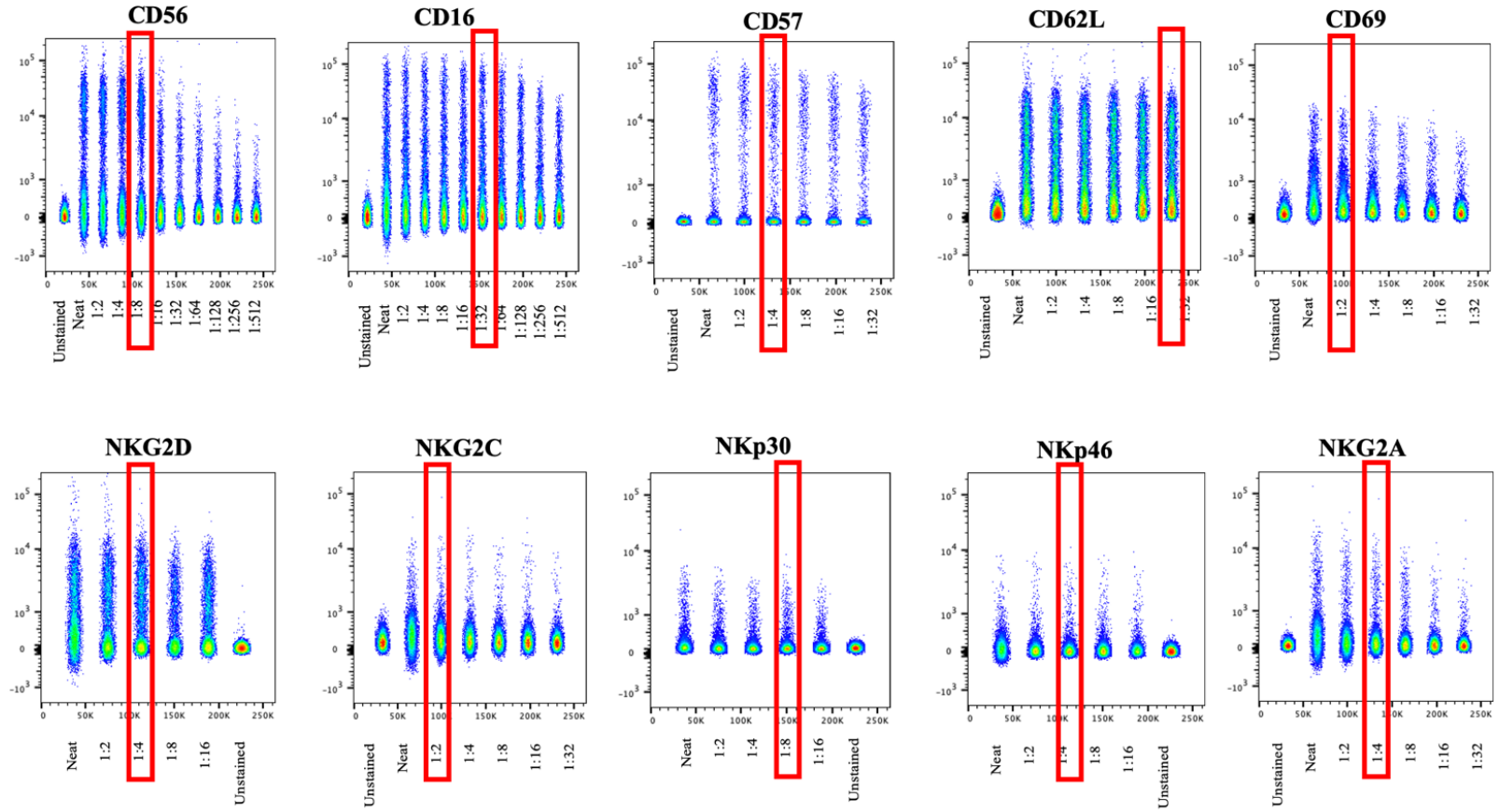


Figure 4.17. NK phenotyping antibody titrations. Antibodies were titrated on live cells. Range of dilutions tested was based on prior knowledge of marker expression. Dilutions between 1:2 and 1:512 were examined. Red boxes denote chosen dilutions for final panel.

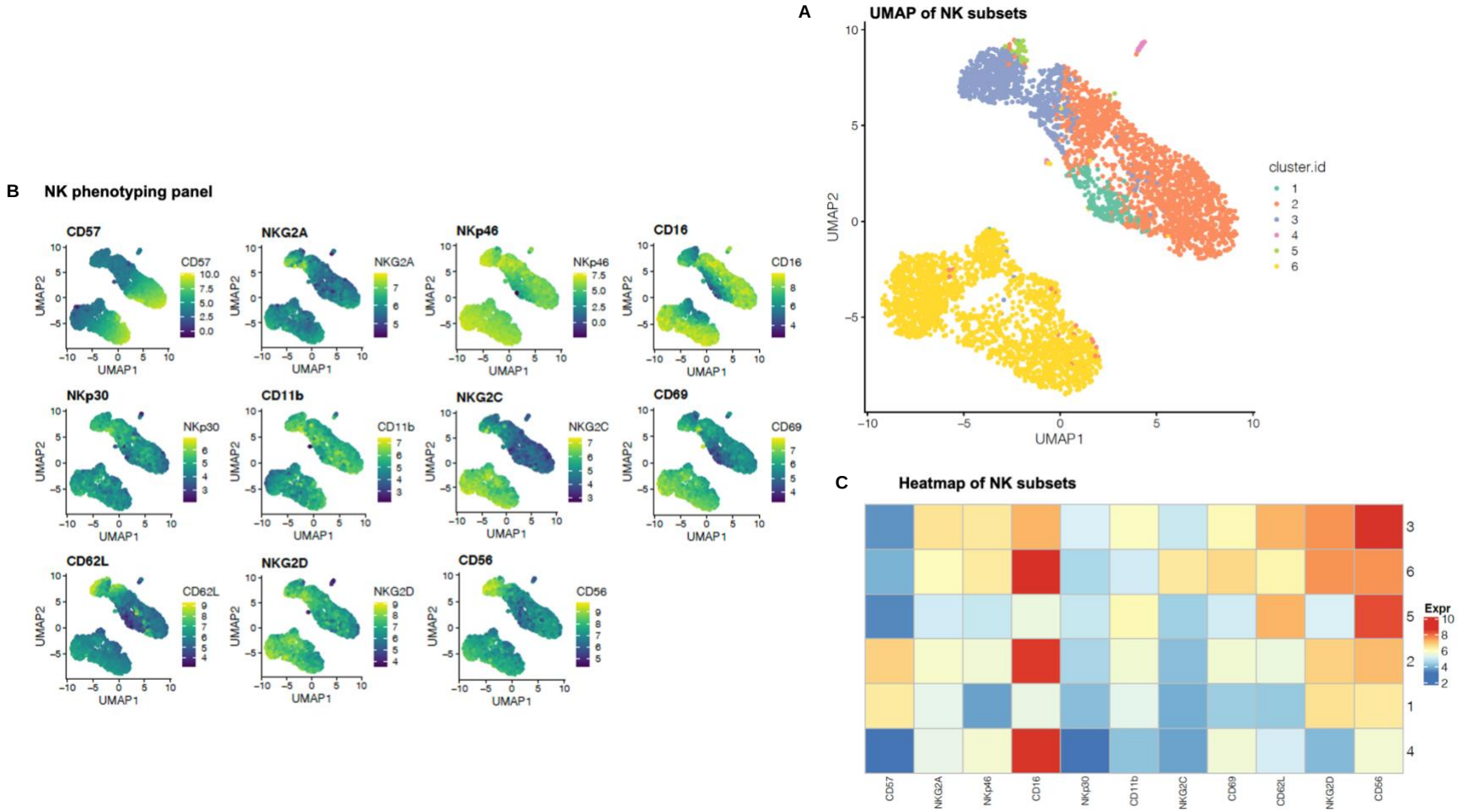


Figure 4.18. Example of NK phenotyping from one donor. (A) UMAP visualisation of NK compartment coloured by subset (identified by FlowSOM clustering). Nearest neighbours = 15, minimum distance = 0.2, 15,000 events represented. (B) UMAP visualisation of NK compartment, coloured by arcsinh-transformed marker expression (cofactor = 5). Lighter colour indicates stronger expression. (C) Heatmap of median marker expression per cluster. Each column represents a marker, each row represents an NK cluster identified by FlowSOM.

4.5 Discussion

In this analysis, it was found that participants could be stratified into outcome risk groups as early as 24 hours after infection. In approximately half of study participants, susceptibility profile following infection was sufficient to distinguish those at significantly increased risk of developing acute disease (susceptible) from those who remained well (protective). This analysis implies that PBMC responses may provide an effective biomarker of fate of infection in participants infected with *S.* Typhi. In addition, it suggests that outcome of infectious challenge may be determined very early after infection. For the remainder of the cohort, a more ambiguous phenotype with overlapping characteristics of the other two profiles was observed that poorly predicted participant prognosis (intermediate profile). Bacteraemia at disease presentation in intermediate and susceptible groups was shown to differ, suggesting differences in identified immune signatures were correlated with differing abilities to contain bacterial dissemination. Individuals with a susceptible cellular profile at 24 hours ultimately develop worsened clinical disease as defined by higher bacterial burden at diagnosis. Finally, this analysis highlights an unexpectedly strong association between baseline PBMC composition and disease susceptibility. These observations are discussed below in the context of previous literature.

A major characteristic of the protective cellular profile was the expansion of $CD16^+$ monocytes early after challenge. Whilst functional characterisation has not been performed here, a mechanistic role for $CD16^+$ monocytes in the clearance of *Salmonella* is strongly supported by the literature. $CD16^+$ monocytes perform a number of functions in immune defence including cytokine production, antibody-mediated phagocytosis, stimulating T-cell proliferation and phagocytosis[251]. Critically, $CD16^+$ monocytes are major producers of TNFα which has been shown in numerous mucosal infections to be essential for effective pathogen clearance and disease resolution. In the context of *Salmonella*, mice deficient for the TNFα receptor, p55 succumbed to infection with *S.* Typhimurium more rapidly than

immunocompetent mice[252] suggesting early TNFα production is key for successful infection control. In human studies, lower TNFα production has been previously associated with delayed resolution of clinical disease in patients presenting with typhoid fever[253]. Combined, these studies indicate the importance of TNFα in *Salmonella* clearance. This analysis identified a possible early source of cytokines that may influence the progression of disease in a more favourable clinical direction.

The role of vaccination in the development of differing immune profiles was assessed given a large proportion of individuals in the protective group are vaccinated. It was hypothesised that antibodies may influence systemic levels of cytokines that in turn drive the expansion of particular subsets. In this analysis, no associations between vaccination and cytokine responses could be elucidated. Therefore, it is not clear from this analysis whether vaccination has a modulatory effect on induction of host responses. Cytokines evaluated at 12 hours in mass cytometry participants are from a historical data set and were not generated specifically to address a hypothesis in this thesis, sample size was small and chosen cytokines were not necessarily optimal to evaluate this question. Previous literature from our laboratory has found that a far greater number of cytokine responses are altered at 12h after challenge than are analysed here[64], including Th1 and Th17 cytokines that may be highly relevant in driving responses observed here. Evaluation of a wider range of cytokines in the mass cytometry cohort may be of interest for future studies. Specifically, evaluation of cytokines known to influence monocyte expansion including IL-6 and their relationship with vaccination status are of interest. This analysis does not address the relative importance of antibodies and cellular immunity in protection. Regression analysis to examine the independent contributions of humoral and cellular immunity to protection from disease would be of interest.

In contrast to what might be expected, this analysis reinforces previously published findings from our laboratory that some pro-inflammatory host responses are in fact detrimental and associate with increased likelihood of diagnosis and worsened bacteraemia. Vaccinees in the susceptible immune profile have significantly greater numbers of antibodies that drive NK degranulation and release of IFNγ and MIP1β suggesting the NK-mediated pro-inflammatory

responses are associated with worsened bacterial control. This observation is counterintuitive and in contrast with observations made in the *S.* Typhmurium model. IFNγ is essential in anti-bacterial immunity, in particular against intracellular infections. IFNγ-deficient mice are highly susceptible to S. Typhimurium infection and Thy1-expressing NK cells (i.e. activated NK cells) were shown to provide a critical early source of IFNγ that was essential for control of bacterial replication[88]. It would be anticipated therefore that presence of antibodies mediating NK activation would be beneficial although the reverse trend is observed in here. Better understanding of NK activity is required to further our understanding of their role in immunity against *S.* Typhi. Independently of antibodies, other features of the susceptible immune profile are indicative of ongoing inflammatory responses. Individuals in this group had significantly higher recirculation of IgG^+ and IgA^+ memory B-cells expressing CD62L than any other group. Memory B-cell recall responses are a critical aspect of adaptive immunity that facilitate more rapid antibody responses upon antigen re-exposure. Unlike central memory (CM) T-cells, which constitutively express CD62L, memory B-cells lack CD62L expression in the steady state and do not traffic through peripheral lymph nodes[254], instead tending to reside in organs such as the spleen where they are optimally placed to sample antigens from peripheral blood[255]. In mice, inflammatory stimuli such as LPS have been shown to profoundly alter memory B-cell migration and increase trafficking through peripheral lymph nodes[256]. This may imply that individuals in the susceptible profile are experiencing greater inflammation within LNs during early infection which in turn is driving stronger changes in memory B-cell chemotaxis being observed in the peripheral blood.

Whether recirculation of memory B-cells actively contributes mechanistically to increased bacterial dissemination is unclear from these analyses and requires further examination. In addition, it is not clear how expression of CD62L is being modulated in these participants. In previous challenge studies, our lab has shown that IL-2 and sCD40L are significantly upregulated within 12 hours of S. Typhi infection[102] although only sCD40L levels were measured in a subset of participants profiled by mass cytometry. Whilst the association did not reach significance, participants with pronounced memory B-cell recirculation had

higher levels of sCD40L at 12 hours than any other group. Whether CD40L signalling can influence CD62L expression on memory B-cells requires clarification. Poor overlap between mass cytometry and cytokine data sets may be limiting statistical power therefore, quantification of cytokines in a larger number of people would be of great benefit in determining whether this is a true association.

Mechanistically, why greater inflammatory responses are associated with poorer prognosis is not clear from these data. The association between pro-inflammatory responses and worsened bacteraemia and clinical presentation in these participants suggests that mechanisms intended to reduce bacterial load have limited effectiveness. Confirmation of any of these speculations in humans is extremely difficult given poor accessibility of lymph nodes. However, these data somewhat paradoxically imply that early IFNγ-mediated inflammation is indicative of poorly controlled disease and has an undesirable association with outcome of infection.

Whilst $CD16^+$ monocyte expansion is associated with the greatest likelihood of remaining well, it is not an absolute requirement. In this cohort, approximately 50% of participants develop an intermediate cellular profile at 24 hours (lacking any expansion of $CD16^+$ monocytes) of which half of those do not develop clinical disease. The intermediate profile has similar functional antibodies to the protective group and some overlapping cellular features (expansion of activated, naïve B-cells, $CXCR3^+$ pDCs, NK responses, T-cell responses) yet these features were not sufficient to prevent the development of symptomatic disease. In addition, few differences between diagnosed and protected individuals of the intermediate groups could be identified in terms of PBMC responses, baseline characteristics or antibody profiles. Functional analysis of subsets responding to infection may confer additional insights and assist with participant stratification that appear otherwise phenotypically homogenous. The strength of NK perturbation after challenge was significant across all participants therefore a functional assay evaluating NK cytokine production was optimised to evaluate the role of NK cells after infection. This assay aims to reconcile seemingly

contradictory findings that antibody-mediated NK activation and IFNg production is detrimental in humans whilst essential for early pathogen containment in mice.

Beyond the peripheral blood, a number of unknown factors are likely to be contributing to protective immunity that are not being accounted for here. The focus of this analysis has been on PBMC responses. The contributions of tissue-resident populations and barrier immunity to protection are unknown in this analysis. The effects of mucus and anti-microbial peptides such as β-defensins to protection has not been investigated although recombinant β-defensins have been found to effectively reduce bacterial burden and increase survival in IP-infected mice[257]. Protection at the mucosal level is highly complex and multi-factorial, however, investigations in the *S.* Typhimurium model have highlighted some interesting responses involved in containment. Tissue-resident T-cells have been shown to provide a major source of cytokines during the early phases of invasion that are responsible for curbing bacterial growth[258]. In addition, barrier mechanisms including goblet cell closure, mucus production and mucosal antibodies are all likely to contribute to protection and have not been accounted for here. The role of gastric acid in disease progression has also (necessarily) been eliminated in these participants as a means of establishing a consistent infection rate; whether cellular immunity progresses differently in individuals without gastric acid neutralisation is unclear.

Other non-PBMC cell types, such as neutrophils and erythrocytes, are under-investigated during early infection with *S.* Typhi. As mentioned previously, neutrophils represent a key phagocytic cell population whose tissue infiltration is an essential aspect of early immunity. Given the upregulation of neutrophil chemoattractants[102] after infection, a pertinent future line of enquiry would be investigation of the granulocyte compartment after challenge. Erythrocytes have essential roles in elimination of bloodborne infections[259] although any contribution to protection from S. Typhi remains unclear.

In this analysis, a surprisingly strong association between baseline PBMC composition and responses to infection was identified. Differences in PBMC composition occurred exclusively within the B- and $CD4^+$ T-cell compartments with higher frequencies of naïve subsets in both lineages associating with better outcome. The association between frequency of

naïve subsets and protective outcome was especially striking when split by immune profile. Therefore, greater circulating levels of memory B-cell subsets and $CD4^+$ effector memory T-cells were associated with poorer outcome and development of poorly controlled infection.

Intra-individual PBMC composition was found to be highly stable during this study, whilst inter-individual PBMC composition varied significantly. The consistency of baseline frequencies across timepoints further suggests that this is a reasonably stable feature of a given individual's PBMC composition and not a transient change e.g. due to some ongoing asymptomatic infection which may be influencing responses to challenge. Homing and activation marker profiles of naïve B-cell and $CD4^+$ T-cells subsets were similar between outcome groups suggesting minimal differences in baseline activation of these compartment at baseline is associated with outcome of infection. In addition, CRP levels and inflammatory cytokines at baseline were not significantly different between immune profiles, again supporting the notion of minimal systemic activation prior to challenge which could be having an effect.

A number of factors influence PBMC composition and frequency of naïve subsets, the most significant being participant gender and age. Several reports have shown that frequency of memory populations increases with age due to acquisition of antigen experience. Whilst the age range in our study is fairly restrictive, no association between age and frequency of any B-cell subsets was identified. Equally, no association with gender was observed, despite previous studies showing that women have higher numbers of B-cells than men[260]. The influence of chronic sub-clinical infections such as CMV has been previously reported to alter PBMC composition[261]. CMV status was not an exclusion criterion for trial participation therefore rates of CMV infection in this cohort and their impact on observed associations are unknown. Other chronic infections known to influence lymphocyte count such as HIV and tuberculosis are not applicable to this cohort but may have implications outside of a clinical trial setting.

Functional or mechanistic explanations for observed associations between PBMC composition and outcome of infection are not immediately clear. The roles of B-cells in intracellular bacterial infections have been historically under-appreciated with emphasis on T-cell responses in protection taking the fore. However, B-cell deficiency in numerous, intracellular bacterial infections including *Mycobacterium* Tuberculosis[262] and *S.* Typhimurium[125] has been shown to worsen disease outcome suggesting a key role in protection. It has always been assumed that B-cell deficiency is detrimental due to attenuated antibody production during infection. However, recent papers have suggested antibody-independent roles of B-cells contribute significantly to host protection as antigen presenting cells. *Salmonella*-infected mice deficient in B-cells had fewer activated $CD4^+$ T-cells during acute infection and lower IFNγ production suggestive of poor priming[127]. The importance of B-cells as APCs in human *Salmonella* infections is not clear however further examination may be warranted in light of observations made here. Examination of differences in antigen presenting capacity between immune profiles may be of interest in future studies.

Higher frequencies of naïve subsets may correlate with greater BCR and TCR diversity and therefore increased capacity to respond to previously unseen infectious challenges. It is notable that naïve B-cell activation is a feature of early responses to disease although in protective and intermediate groups only. Conversely, whether accumulation of terminally differentiated lymphocyte subsets in susceptible participants in associated with restricted diversity is an intriguing question that could be pursued in future work.

The generalisability of baseline observations made in this study may be limited in a more diverse cohort. Challenge model participants are healthy, within a defined age range, have no chronic infections or autoimmunity. Whether baseline composition would remain a significant independent indicator of infection responses is unknown and would require further elucidation. Whether PBMC compositional shifts could prove useful in identification of individuals at high risk of poor infectious outcome may be of interest in future work. In

addition, analysis of BCR/TCR sequence diversity as well as chromatin modifications known to associate with differences in immunological age and responsiveness to infection would contribute significantly to better understanding of infectious outcomes.

5 Establishing correlates of disease severity in acute typhoid fever and their association with Vi-vaccination status

5.1 Introduction

Accurate evaluation of patient condition is central to management of therapy and identification of individuals at risk of severe clinical complications. In bacterial infection, C-reactive protein (CRP) and white blood cell count (WBC) are commonly used as prognostic indicators of patient condition and severity of illness[263]. However, no previous studies have sought to assess whether these indicators are optimally identifying patients with more symptomatic cases of disease in the context of typhoid fever. Whether better correlates of disease severity can be identified is an unanswered question.

In recent years, there has been renewed interest in the use of blood count data, and specifically blood count ratios, to stratify patients at risk of adverse outcomes. Whilst imperfect as a diagnostic of bacteraemia[264], neutrophil-to-lymphocyte ratio (NLR) has been reported to have prognostic potential in the management of hospitalised patients with bacterial infections. Sustained elevation of NLR in bacteraemic patients on therapy was indicative of poor prognosis and increased mortality[265]. NLR in this study outperformed measures such as WBC suggesting superior prognostic capability. Other blood count ratios such as monocyte-to-lymphocyte ratio (MLR) have also been investigated in the context of infectious disease outcomes, specifically as an indicator of progression from latent to active disease in management of tuberculosis patients[266]. The utility of these measures in typhoid fever has never been assessed.

Vaccinations can offer tangible health benefits to the population at large beyond direct protection of the immunised individual. An example of such benefits is the reduction in symptomatic infection and hospitalisation observed in vaccinated vs unvaccinated individuals[267] in the event that immunisation does not totally prevent the development of disease. Reductions in symptomatic disease alleviate morbidity experienced by infected individuals and burden

placed on healthcare settings, as exemplified by the current COVID-19 pandemic. An association between biomarkers of disease severity and vaccination status in typhoid fever has not been performed.

In a previous report, Vi-TT vaccination was shown to modulate presentation of typhoid fever in human challenge model participants[40] although detailed investigation of ameliorated symptoms was not performed. In addition, associations between aspects of the humoral response that are correlated with milder disease presentation have not been extensively studied.

5.2 Chapter Aims

Aim 1: to examine the association between blood count ratios and severity of typhoid fever symptom presentation in a human challenge model cohort infected with S. Typhi.

Aim 2: to examine the impact of Vi-vaccination on the correlates of disease severity and associations between different antibody subclasses and severity.

5.3 Methods

5.3.1 Source of samples

During challenge, full blood count data were taken daily as part of routine laboratory tests and general assessment in an outpatient clinic until either day of diagnosis or for a maximum of two weeks. Diagnosis was made by a sustained fever for more than 12 hours or positive aetiological identification by blood culture (see Description of study samples for full details). Following diagnosis or completion of the 2-week observation period, participants were treated either with antibiotics as described previously[40]. For some analyses, blood count data from 3 enteric fever challenge studies were combined for analysis. Included individuals were naïve at time of challenge, had no previous history of typhoid fever vaccination and received a similar challenge dose. In total, 68 individuals were included. The majority of this chapter focuses on data from participants enrolled in a Phase IIb Vi-vaccine efficacy study (see Description of study samples for details).

5.3.2 Symptom scoring and latent profile analysis

During challenge, participants completed an online diary self-assessing development of symptoms and relative severity. Participants were asked to report on the following with a grade between 0 (symptom not present) to 3 (severe): headache, feeling generally unwell, abdominal pain, constipation, cough, diarrhoea, joint pain, loss of appetite, muscle pain and nausea. Detailed descriptions of severity scoring for each symptom have been published previously[40]. In addition, participants self-reported temperatures twice daily throughout challenge.

Subpopulations of participants with differing symptom profiles at diagnosis were identified by latent profile analysis (LPA). Briefly, the probability of a participant belonging to a symptom profile was modelled using Gaussian Finite Mixture modelling fitted using the expectation-maximisation (EM) algorithm. Model-based clustering was performed using the

mClust package in R. Symptom scores taken from eDiary entries submitted on the day of diagnosis prior to initiation of antibiotics were used as input random variables. Participants with missing symptom scores were rare and excluded from analysis, no imputation was performed. Symptom scores were standardised prior to analysis. Probabilistic model selection was performed using Bayesian Information Criterion (BIC). The maximum number of profiles evaluated was 9. Model EEI with 2 profiles was chosen based on BIC. Mean standardised symptoms scores were calculated for each profile and visualised by heatmap. Demographic and immunological measurements were compared between symptom profiles, either by Wilcox Sum Rank test for non-normal, continuous variables or by Fisher's Exact test for categorical variables (calculated in R using the *stats* package).

5.4 Results

5.4.1 Blood count ratios are significantly perturbed by development of acute typhoid fever

Neutrophilia, lymphopenia and eosinopenia are classical hallmarks of systemic bacterial infection. The extent of blood count perturbation following challenge was evaluated. Neutrophils and monocytes were significantly elevated at diagnosis in comparison to individuals that remained well whereas, platelets and eosinophils were significantly reduced (Figure 5.1A). Overall, reported observations were in keeping with previous literature on typhoid fever presentation in endemic settings indicating that findings identified in challenge model participants would be applicable to cases of natural infection.

Blood count ratios were able to stratify diagnosed and protected patients more strongly than absolute counts (Figure 5.1B). Neutrophil-to-lymphocyte ratio (NLR) ($p = 3.42 \times 10^{-11}$, ****), eosinophil-to-lymphocyte ratio (ELR) ($p = 1.93 \times 10^{-11}$, ****) and monocyte-to-lymphocyte ratio (MLR) ($p = 8.73 \times 10^{-6}$, ****) were all significantly different between diagnosed participants vs participants that remained well. In diagnosed participants, age, gender or initial challenge dose were evaluated for associations with blood count ratios (Figure 5.2). No associations were observed for NLR or ELR, however MLR in male participants was found to be significantly higher than in females who develop typhoid fever ($p = 3.12 \times 10^{-8}$, ****).

As anticipated, blood count ratios offered a sensitive biomarker of disease development in cases of typhoid fever therefore further evaluation of associations with symptom profiles were conducted.

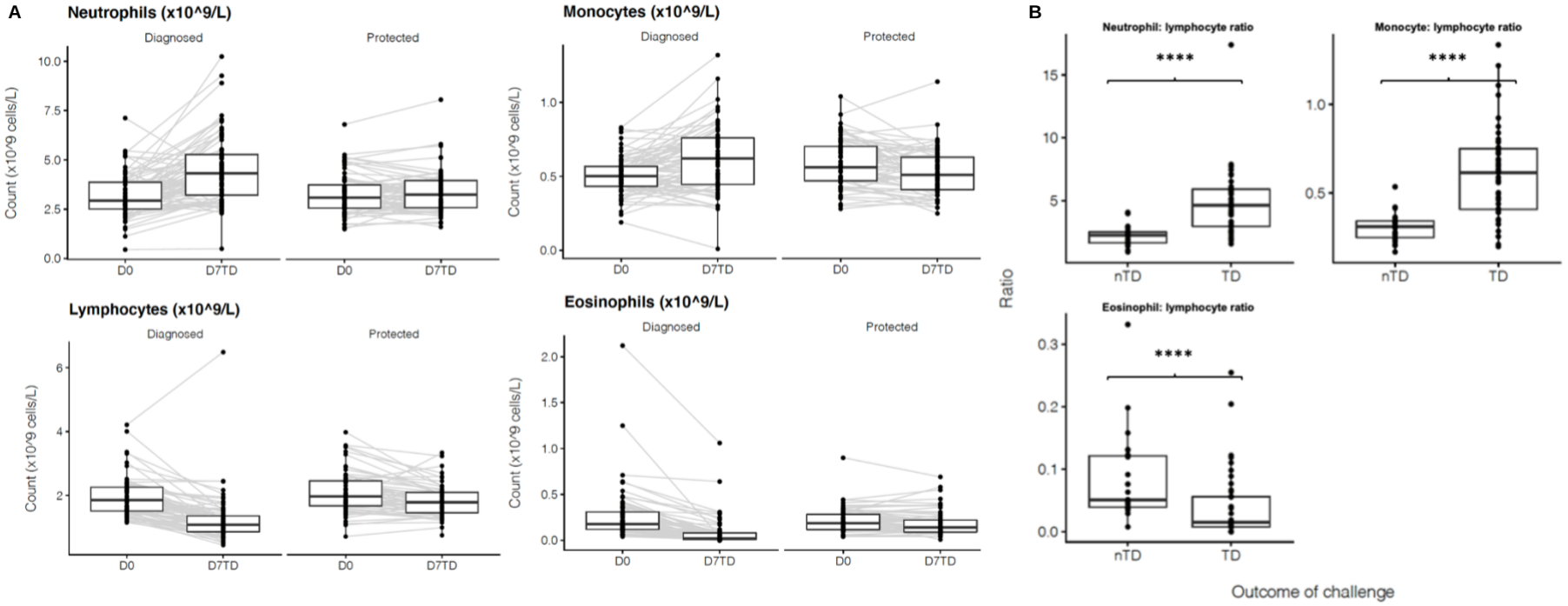


*Figure 5.1. Blood count perturbation at development of acute disease. n = 68. TD = 39 participants, nTD = 29 (A) Boxplots of neutrophil, monocyte, lymphocyte and eosinophil counts at baseline and either day of diagnosis or 7 days after infection. (B) Boxplots of neutrophil-to-lymphocyte, monocyte-to-lymphocyte and eosinophil-to-lymphocyte ratios in diagnosed and protected participants. Groups compared by Wilcox rank sum test. Significance thresholds: ns = p > 0.05, * = p < 0.05, ** = p< 0.01, *** = p <0.001, **** = p < 0.0001.*

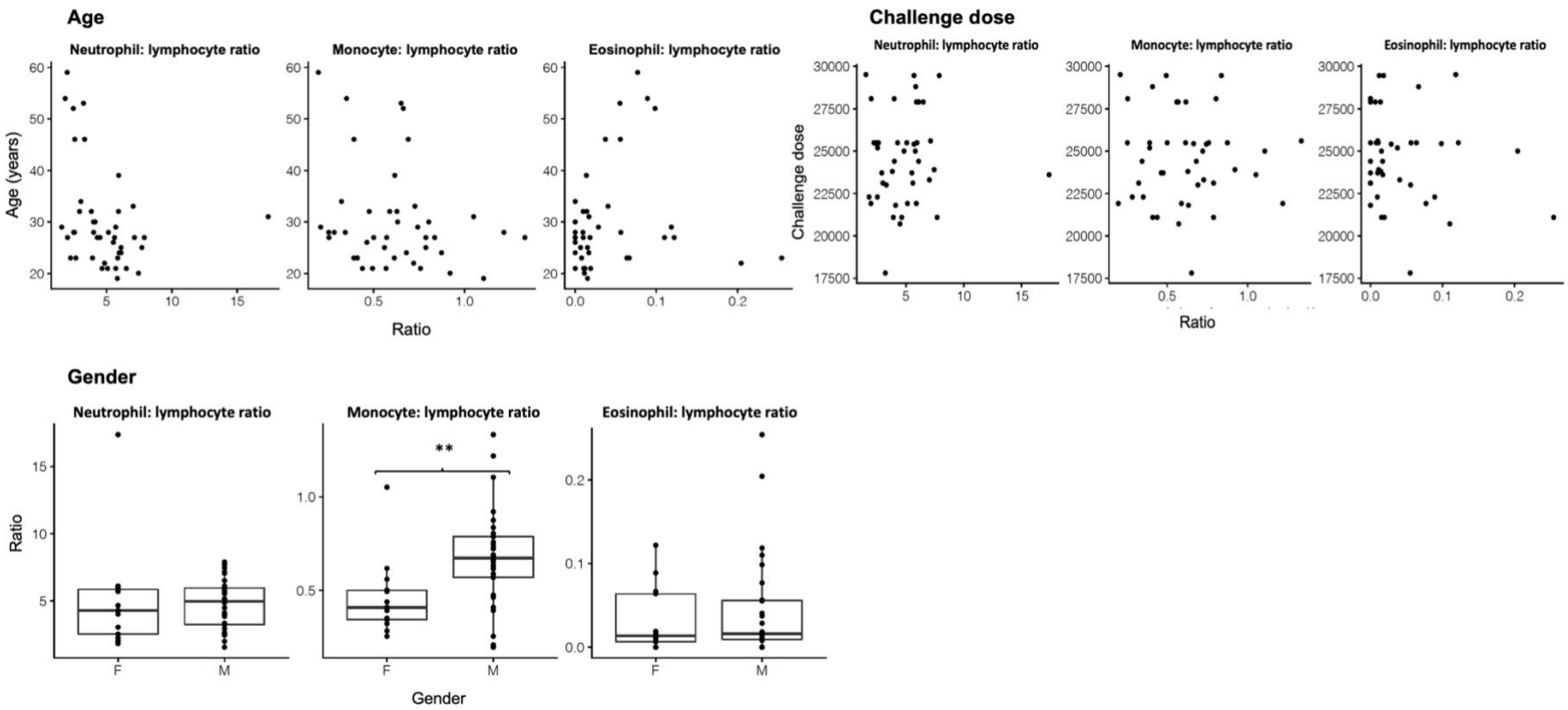


*Figure 5.2. Evaluation of potential confounding factors in blood count ratio analysis. Categorical variables were compared by Wilcox rank sum test. Significance thresholds: ns = p > 0.05, * = p < 0.05, ** = p< 0.01, *** = p <0.001, **** = p < 0.0001. Continuous variables were evaluated by Spearman correlation.*

5.4.2 Neutrophil: lymphocyte ratio (NLR) and eosinophil: lymphocyte ratio (ELR) are independent, immunological biomarkers of symptom severity in human challenge model participants with acute typhoid fever

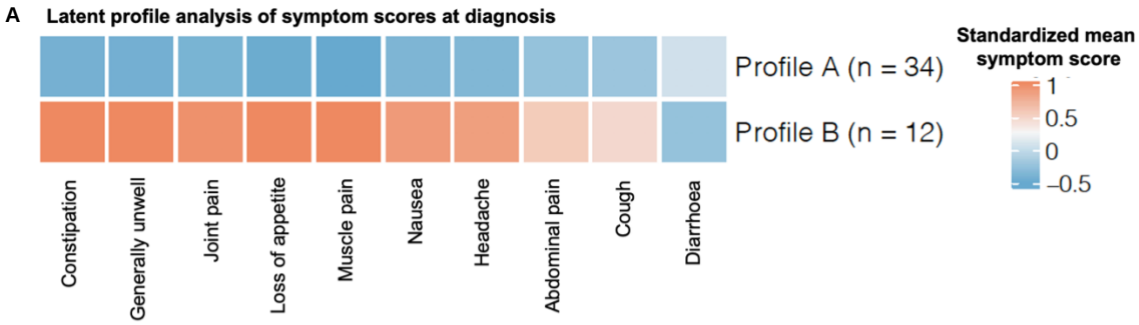
Next, associations between blood count ratios and self-reported symptom severity in participants from a vaccine efficacy trial were evaluated. Prevalence of symptoms at day of diagnosis was assessed across all participants (n = 103). Commonly reported symptoms included headache (32%, 33/103), feeling generally unwell (28%, 29/103) and loss of appetite (21%, 22/103). The symptom scoring system, with descriptions of the level of severity represented by each score, has been previously published[40]. Latent profile analysis of symptom scores recorded on the day of diagnosis identified two symptom clusters with distinctive characteristics (Figure 5.3A). Participants in profile A (n = 34) had a milder disease presentation with generally lower symptom reporting whilst Profile B (n = 12) identified a smaller subset of participants with more symptomatic disease presentation (Figure 5.3B). A subset of participants in Profile A (18%, 6/34) were completely asymptomatic (i.e. met the criteria for diagnosis by blood culture but reported no other symptoms) (Figure 5.3C). Participant demographic characteristics were similar between symptom profiles (Figure 5.3B). Participants in Profile B reported a higher average number of symptoms at diagnosis ($p = 1.02 \times 10^{-6}$, ***) and a significantly increased incidence of fever ($p = 8.97 \times 10^{-4}$, ***).

Significant associations between symptom profiles and blood count ratios were identified. ELR was strongly reduced in Profile B (higher symptom scores and greater prevalence of fever) vs Profile A (p = 0.0038, **) suggesting an association with worsened disease. A trend was also observed in NLR although this did not reach statistical significance (p = 0.0946). NLR and ELR were poorly correlated with one another suggesting these metrics may have differing associations with severity. No associations between MLR and symptom severity could be identified. Interestingly, this analysis found limited associations between CRP and

WBC participant symptom profiles. This may indicate that NLR and ELR may be better biomarkers of disease severity in enteric fever than more conventional markers.

Given their association with latent symptom profiles, NLR and ELR were examined further for associations with other indicators of symptom severity. NLR was strongly associated with additional measures of severity such as time to diagnosis and total number of symptoms (Figure 5.4). Participants diagnosed early reported a higher NLR at diagnosis. Conversely, the association between ELR and number of days until diagnosis was less strong although a clear association with number of symptoms could be found. Strikingly, evaluation of individuals' symptoms showed a trend in which self-reported symptom scores and ELR were closely mirrored (Figure 5.5). Significant differences in NLR and ELR were found between individuals with no symptoms at day of diagnosis vs participants with any reported symptoms (Figure 5.4).

A



B

Parameter	Profile A	Profile B	*p*-value	Significance
Age (years)	24.5	29.5	0.135	ns
Body Mass Index (BMI)	25	26	0.274	ns
Weekly Alcohol Intake Units	7.2	9.3	0.368	ns
Time to diagnosis (days)	8	8	0.883	ns
Number of symptoms	2	7	0.00000102	***
Neutrophil: Lymphocyte (NL) ratio	3.67	4.92	0.0946	ns
Monocyte: Lymphocyte (ML) ratio	0.55	0.62	0.427	ns
Eosinophil: Lymphocyte (EL) ratio	0.07	0.01	0.0038	**
Reported recent travel (%)	18.75	41.67	0.139	ns
UK born (%)	71.88	91.67	0.798	ns
White (%)	96.88	83.33	0.176	ns
Student (%)	53.13	58.33	0.525	ns
Fever at diagnosis (%)	12.5	66.67	0.000897	***
Female (%)	31.25	41.67	0.722	ns
Blood quant (CFU/10mL)	2	2	0.737	ns
C-reactive protein (mg/L)	14.8	17.8	0.164	ns
White blood cell count (x10^9/L)	6.48	5.71	0.274	ns

C

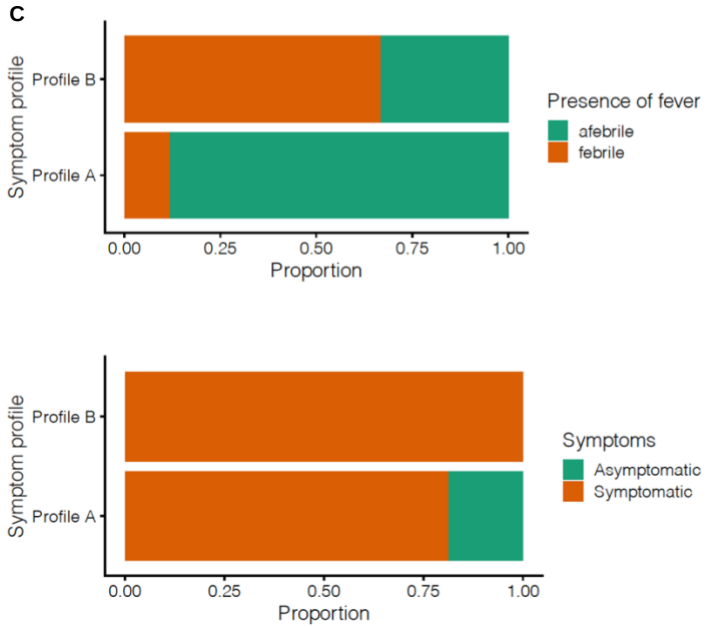


Figure 5.3. Symptom profile analysis during acute typhoid fever. (A) Heatmap of two latent profiles identified by LPA. Colour indicates median standardised scores reported by participants at diagnosis. Each row represents a symptom profile and each column represents a symptom. (B) Table of immunological and demographic parameters for each symptom profile. (C) Bar plot of proportions of febrile vs afebrile participants in each profile. (D) Bar plot of proportions of asymptomatic vs symptomatic participants in each profile.

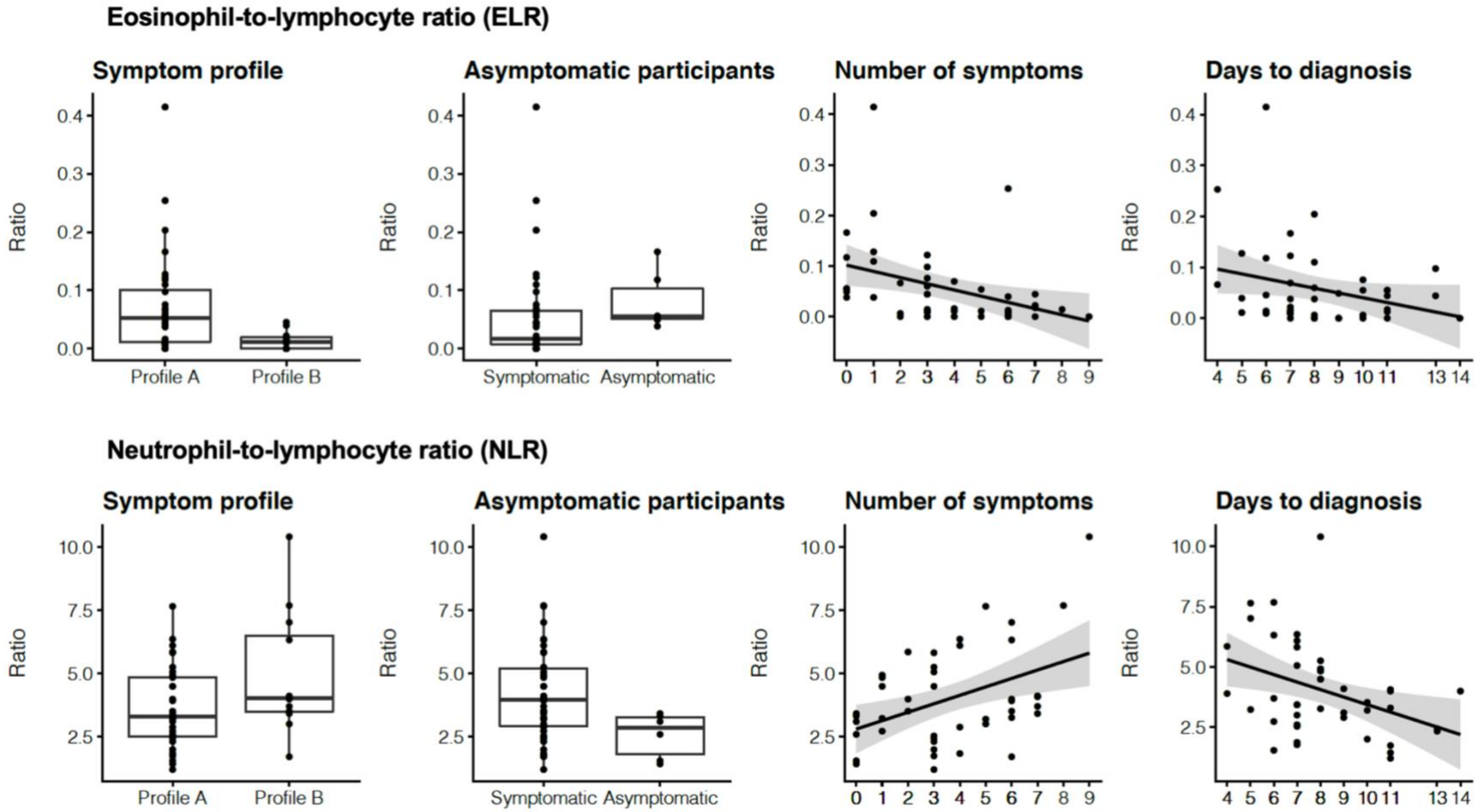


Figure 5.4. Associations between ELR, NLR and definitions of disease severity. Boxplots of NLR and ELR, compared between symptom profiles and between asymptomatic and symptomatic participants. Correlation between number of symptoms, days to diagnosis and blood count ratios.

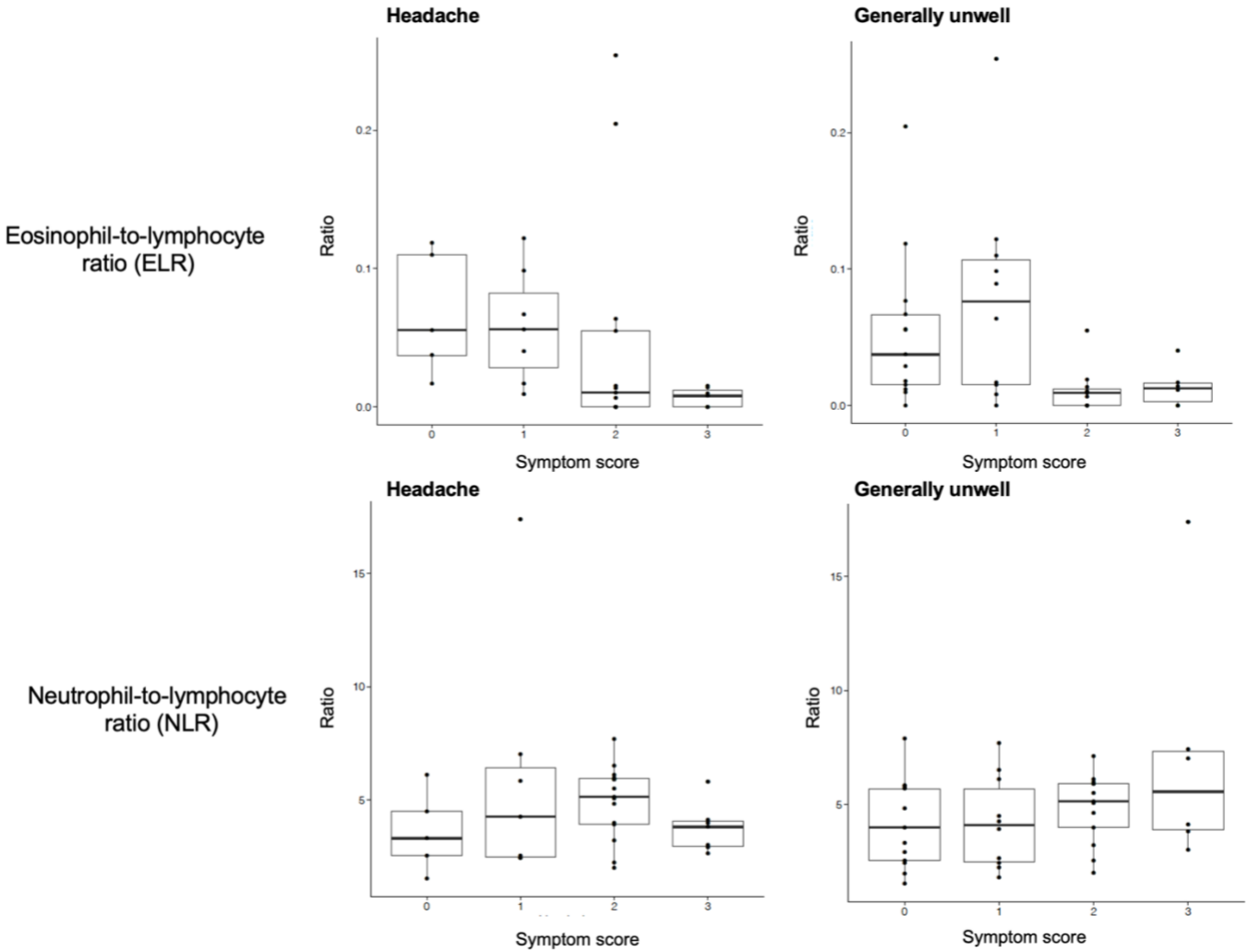


Figure 5.5. ELR is strongly associated with self-reported symptom severity. Boxplots of ELR and NLR at diagnosis, compared between severity groups for headache and feeling generally unwell (symptoms reported in the highest number of people). .

5.4.3 NLR and ELR are modulated by vaccination status and are associated with pre-challenge levels of Vi-IgG1 titres

Correlates of disease severity such as NLR and ELR may be useful in assessing the impact of interventions such as vaccination and identifying features of the serological response that are associated with milder disease. Therefore, the effect of vaccination on NLR and ELR during acute typhoid fever was evaluated. In addition, their association with symptomatic disease was also assessed.

Vi-vaccination had a significant effect on symptom reporting. Vi-TT vaccinees had significantly lower prevalence of headache, feeling unwell and cough in comparison with unvaccinated participants (Figure 5.6A). Vi-PS vaccinees also reported lower incidence of headache and cough although impact on other symptoms was not significant. Interestingly, incidence of fever was also significantly lower in Vi-TT vaccinees in comparison with unvaccinated participants ($p = 0.00886$, **). Conversely, Vi-PS was less effective at lowering fever with no significant difference between Vi-PS and unvaccinated controls ($p = 0.201$, ns). Combined, these data confirm that Vi-TT has a modulatory effect on symptom presentation during acute typhoid fever.

Comparison of NLR and ELR ratios between vaccines arms found a significant improvement in NLR at diagnosis in Vi-TT recipients ($p = 0.013$, *) and a modest improvement on ELR although this did not reach significance ($p = 0.124$, ns) (Figure 5.7A and B). In contrast, Vi-PS vaccination had no effect on NLR ($p = 0.586$, ns) or ELR ($p = 0.361$, ns) at diagnosis. To establish whether antibodies were associated with NLR in vaccinated participants were correlated with antibody titres and other serological measures in order to identify features associated with lower disease severity. A significant, inverse relationship between Vi-IgG1, Vi-IgG2 and Vi-IgG3 titres prior to challenge and NLR was found (Figure 5.8A). Vi-IgA and Vi-IgM titres were not associated with NLR. Evaluation of Vi-antibody titres in participants that develop fever found a significantly higher levels of antibodies in those that did not develop fever (Figure 5.8B).

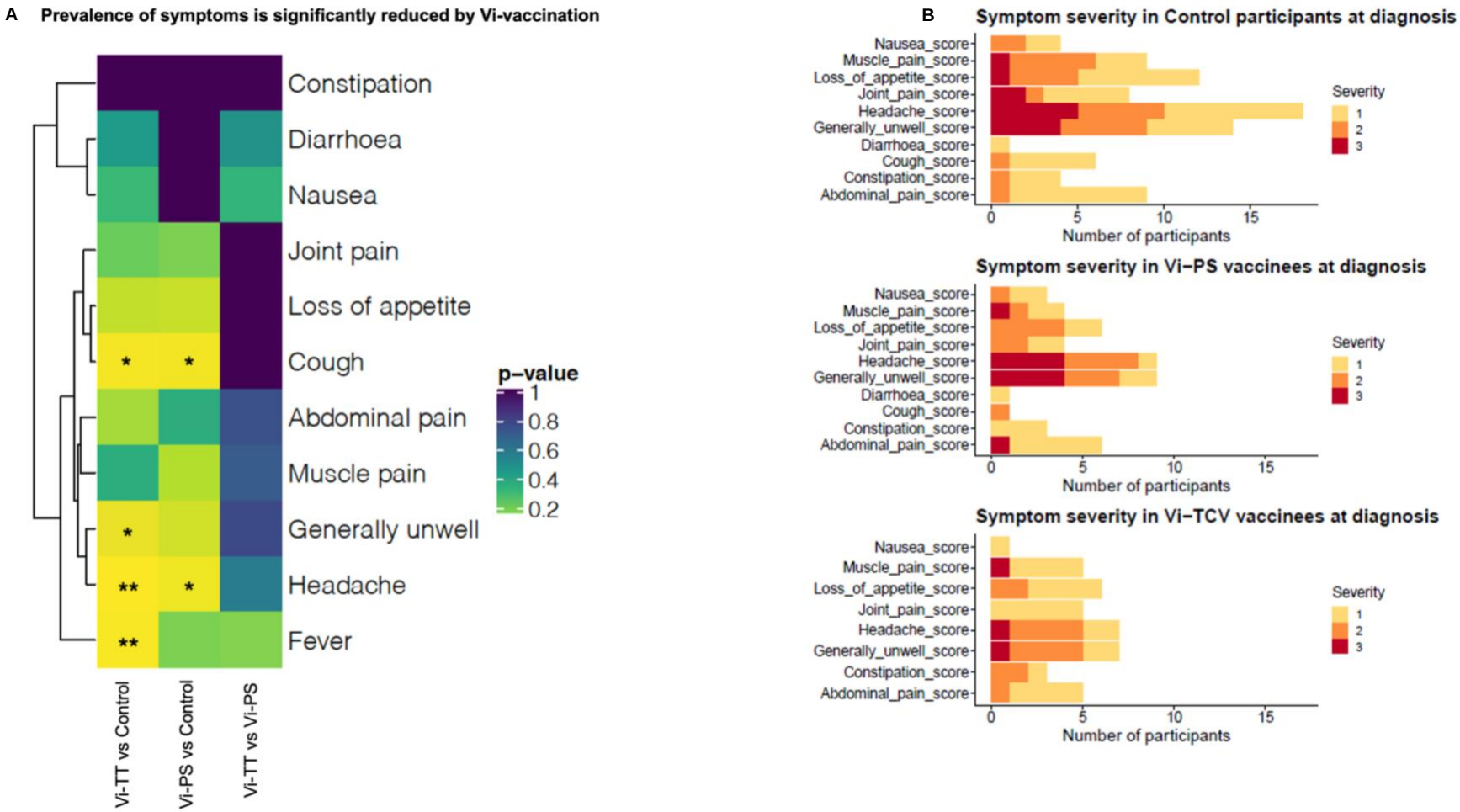
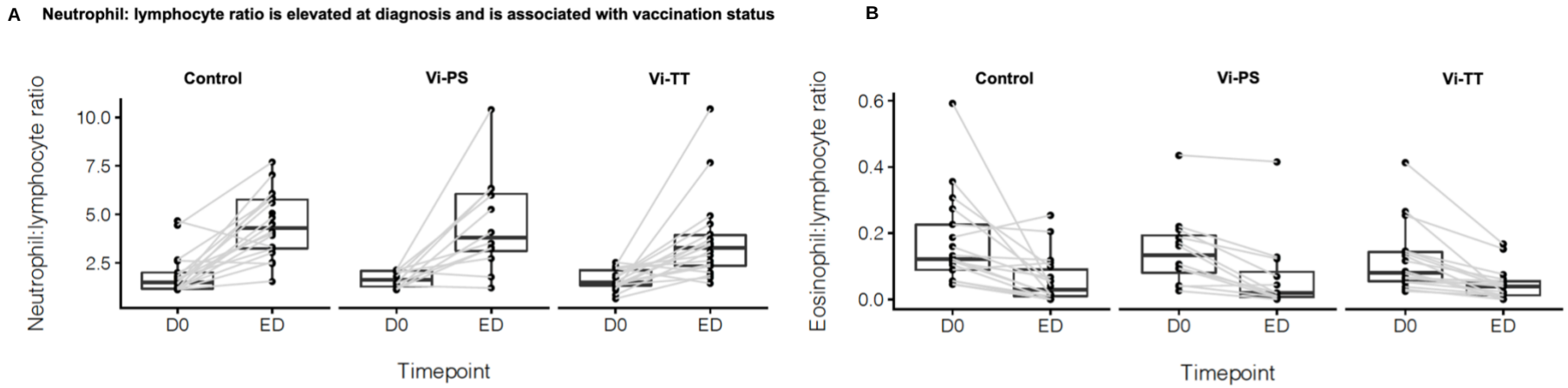


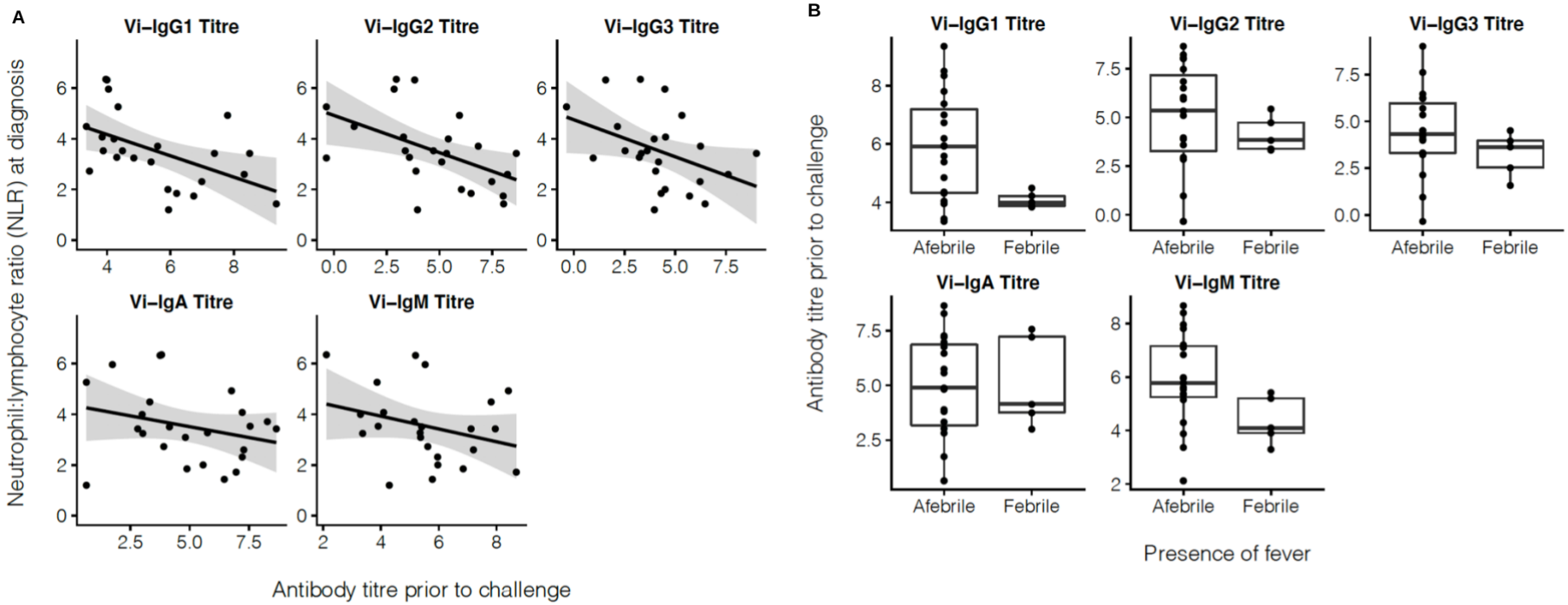
Figure 5.6. Prevalence of symptoms in Vi-vaccinated and unvaccinated participants with acute typhoid fever. (A) Heatmap of p-values generated by comparison of symptom prevalence between vaccination groups. Proportions compared by Fisher's exact test. (B) Barplot of number of participants reporting a given symptom at diagnosis. Bars coloured by proportion of participants reporting a particular severity score for that symptom.



C

Variable	Vi-TT (vs unvaccinated)	Vi-TT (vs Vi-PS vaccinees)	Vi-PS (vs unvaccinated)
Neutrophil: lymphocyte ratio	0.013 (*)	0.093 (ns)	0.586 (ns)
Eosinophil: lymphocyte ratio	0.937 (ns)	0.750 (ns)	1.000 (ns)

Figure 5.7. NLR is significantly lowered by Vi-TT vaccination. (A) Boxplots of NLR at baseline and diagnosis in each vaccine arm. (B) Boxplots of ELR at baseline and diagnosis in each vaccine arm. (C) Table of comparisons of NLR and ELR between vaccinated and unvaccinated participants. P-values and significance levels reported.



	R	*p*-value	Significance
Vi-IgG1 titre	-0.56	0.005	**
Vi-IgG2 titre	-0.57	0.003	**
Vi-IgG3 titre	-0.43	0.04	*
Vi-IgA titre	-0.22	0.29	ns
Vi-IgM titre	-0.36	0.09	ns

	n-participants (Febrile)	*n*-participants (Afebrile)	*p*-value	Significance
Vi-IgG1 titre	13	34	0.03	*
Vi-IgG2 titre	13	34	0.355	ns
Vi-IgG3 titre	13	34	0.208	ns
Vi-IgA titre	13	34	0.831	ns
Vi-IgM titre	13	34	0.04	*

Figure 5.8. NLR at diagnosis is correlated with Vi-antibody titres. (A) Spearman correlation between NLR at day of diagnosis and Vi-antibody titres at baseline prior to infection. (B) Boxplots of Vi-antibody titres at baseline, compared between participants that develop fever vs participants that remain afebrile at diagnosis.

5.5 Discussion

Correlates of disease severity are useful prognostic markers that have applications in clinical management of disease. Effective correlates have to be relatively simple to measure and clearly stratify individuals at risk of adverse outcomes or those that are responding poorly to treatment. This analysis aims to identify biomarkers of disease severity from blood count data and compare them with conventional indicators such as WBC.

In the human challenge model, blood count data accurately recapitulate key features of natural infection including development of neutrophilia, lymphopenia and eosinopenia albeit at a lower magnitude than is typically observed in endemic settings. Mean count values observed in challenge model participants are considerably lower than those reported in other literature, indicating that disease presentation is relatively subtle[268]. Monocytosis, a commonly identified phenomenon in enteric fever, is noticeably subtle here. This may be due to the sequential nature of blood count compositional changes (diagnosis is made at a relatively early stage of disease) and may arise after changes such as neutrophilia and eosinopenia. However, the model accurately represents alterations at diagnosis therefore, these findings have relevance to naturally acquired infection.

This is the first study to evaluate NLR and ELR as biomarkers of disease severity in typhoid fever. Lower ELR was strongly associated with a more symptomatic disease profile, characterised by higher numbers of symptoms and prevalence of fever. In addition, striking correlations between self-reported symptom severity and ELR were observed for almost all reported symptoms with sufficient data. The association between NLR and symptom profile did not reach significance although a clear trend was observed. Elevated NLR was significantly correlated with more rapid disease progression and higher numbers of symptoms suggesting ELR and NLR associate differently with differing definitions of severity. Importantly, NLR and ELR were better indicators of symptom severity than more traditionally used clinical indicators such as CRP and WBC. Overall, this analysis suggests that ELR and NLR should be investigated further as prognostic markers of severity in typhoid fever patients. A larger

analysis with a greater number of participants would be desirable to confirm preliminary findings reported here.

NLR has been reported in several contexts as a reliable predictor of physiological stress and critical illness and has been found to outperform white blood cell count as a biomarker of severity[269]. Despite this, clinical usage remains limited in favour of more conventional measures. NLR in the context of infectious disease has been primarily investigated as a predictor of bacteraemia with mixed success. Several meta-analyses have found that NLR can distinguish cases of bacteraemia from cases of other illness in undifferentiated patients in critical care however the discrimination is imperfect[264,269]. NLR has also been widely investigated as a predictor of bacterial infection over viral infection with moderate efficacy[270]. In this study, a strong relationship between bacteraemia and NLR could not be identified. Blood culture is routinely used in diagnosis of typhoid fever but has a notoriously poor sensitivity. Because of its stochastic nature, number of CFU in blood has been shown previously to be a relatively unreliable indicator of disease severity in cases of typhoid fever[271,272] therefore poor association between NLR and bacteraemia is not unexpected. It is possible that NLR is a more consistent indicator of bloodstream infection than blood culture alone although definitive proof of this is difficult. The association between NLR and disease progression as well as a broader clinical presentation may indicate individuals with higher NLR are experiencing a more widely disseminated infection.

ELR is less widely reported on that NLR, however this analysis identifies a strong association with symptomatic disease. Eosinopenia is a well-described feature of acute bacterial infection and has been previously shown to correlate with bacterial burden in peripheral blood although no such an association was found here. This analysis finds a highly significant connection between self-reported symptoms and ELR. For almost all symptoms assessed, a strong trend between lower ELR and higher symptom scoring was observed. Eospinophils are decreased at acute disease presentation due to sequestration at sites of inflammation. It is an

especially strong feature of typhoid fever although is seen in numerous bacterial infections. The strength of this association invites that question of whether eosinophils play a mechanistic role in the development of symptoms. Eosinophil infiltration and degranulation within inflammatory tissues has been routinely observed and has been widely reported in the context of headache and other symptoms[273].

This analysis does not explore any associations between blood count ratios and more severe complications of typhoid fever. All challenge model participants experience a relatively mild form of disease in comparison to individuals residing in endemic settings. As mentioned above, reports of neutrophilia, eosinopenia and lymphopenia are noticeably more extreme in patients presenting to hospital with typhoid fever, therefore a greater range of NLR and ELR are likely to be observed. NLR has been investigated in the context of other extreme complications including spontaneous intracranial haemorrhage whereby a sudden spike in NLR over 24 hours was observed in individuals with haemorrhage that did not survive[274]. This and other reports associating NLR with mortality suggest this may retain the capacity to be an effective metric of critical illness in typhoid fever. In addition, persistent eosinopenia has been previously shown to be an independent predictor of mortality in ICU patients with bacteraemia[265] therefore previous literature suggest both may be indicative of adverse outcomes and requires further investigation.

In this analysis, NLR and ELR were more strongly associated with symptom profiles than other measures such as CRP and WBC. Further investigation is required in order to establish the reasons for this. The absence of an association between CRP and symptom profile is unexpected as serum CRP has been previously shown to be indicative of severe complications of typhoid fever. Hospitalised patients with greater serum CRP levels are more likely to develop ileal perforations that those with lower levels[275]. This discrepancy may be as a result of timing and the relatively mild presentation of typhoid fever in the challenge model.

This analysis suggests NLR and ELR may be a better indicator of more symptomatic disease, at least in relatively mild cases of infection.

This is the first study to show NLR during acute typhoid fever is modulated by Vi-vaccination in the event of vaccine failure. In addition, this is the first report to show an association between lower NLR and asymptomatic disease presentation in vaccinated individuals. Vaccine failure in challenge models (i.e. development of disease) is considerably higher than in field studies. Several factors in the design of challenge models including the relatively high inoculum of bacteria and stomach acid neutralisation prior to ingestion contribute to this effect. The advantage of this is the capacity to investigate the modulatory effects of vaccination on disease presentation. In this study, incidence of fever was found to be lower in Vi-TT vaccinated individuals. Furthermore, a small number of Vi-TT vaccinees met criteria for diagnosis (positive blood culture) but reported no symptoms (n = 6). Despite small numbers, these findings suggest Vi-TT is modulating the presentation of disease and driving a milder clinical phenotype.

Having established NLR and ELR as biomarkers of disease severity typhoid fever, the effect of Vi-vaccination on these markers was investigated. NLR was significantly lowered by Vi-TT but not Vi-PS vaccination and correlated with Vi-IgG antibody titres. ELR, whilst improved in Vi-TT vaccinees, did not reach significance. Perturbation of NLR and ELR at diagnosis was significantly less in asymptomatic vaccinees when compared to individuals with symptoms.

Observations of milder disease presentation are in line with studies of other vaccines. Definitions of disease severity are highly varied between studies with differing symptoms examined and scoring systems employed. Studies diverge further when vaccine target pathogen, mode of action and interval between immunisation and disease are considered. Combined, these factors complicate direct comparisons between studies. However, an overall trend towards milder disease presentations in vaccinated cohorts is universally observed. Influenza

vaccinations such as A/H3N2 have modest protective efficacy, however they have been shown to be highly effective in reducing severity of symptoms. Specifically, reports have found incidence of fever is significantly reduced as well as respiratory symptoms such as cough, sneezing and sore throat[276].

This is the first study to show a correlation between vaccine-induced antibody titres and NLR during acute disease. NLR at diagnosis inversely correlates with Vi-IgG antibodies at baseline, suggesting that higher systemic titres prior to infection are strongly associated with lower physiological stress. Lower induction of Vi-IgG antibodies by Vi-PS may therefore be responsible for limited effect of Vi-PS vaccination on NLR. How antibodies are mechanistically lowering NLR is unclear. One explanation may be that antibodies are reducing bacterial load in compartments such as bone marrow or other organs. Indeed, *in vivo* assessment of *Salmonella* infection in mice showed that immmunised mice had lower disseminated infection than naive animals although this depended on specific antigen type[277]. The effect of Vi-antibodies on bacterial burden in compartments beyond peripheral blood is unknown. Another possibility is that antibodies may be critical for more rapid containment of infection in the gut after infection. This effect of vaccination may limit systemic inflammation that in turn drives increases in NLR. Assessment of chemokines known to influence neutrophil egress from bone marrow may be of interest in future investigations.

This analysis has some limitations, therefore more research is needed to resolve some of these issues. Firstly, only enteric fever caused by *S.* Typhi has been evaluated in this analysis. Whether factors such as NLR and ELR associate with disease severity in enteric fever caused by other aetiological agents is unclear. Infections caused by *S.* Paratyphi typically present with a less severe clinical phenotype. It would therefore be expected that NLR and ELR perturbation would be less extreme although confirmation would be required. As can be inferred from their evaluation in numerous conditions, these markers poorly discriminate between aetiological causes of infection. Therefore, optimal treatment still relies on positive aetiological identification.

Secondly, a number of factors are known to have confounding effects on NLR and ELR, therefore interpretation of these measures in this context requires more careful consideration[278]. Corticosteroids have a major influence on frequencies of neutrophils, eosinophils and lymphocytes in the periphery. As noted by previous reports, exogenous sources of corticosteroids therefore may inflate ratios and limit clinical utility in the context of infection. Moreover, the interpretability of these biomarkers in the context of other acute or chronic co-infections is unclear. Whether co-infections such as HIV, which may lower lymphocyte frequencies in cases of poor treatment adherence, confound their use in typhoid fever evaluation.

Thirdly, whilst NLR and ELR may serve as useful prognostic indicators in adults, the utility of these findings in a paediatric population remains unknown. Given the burden of enteric fever occurs primarily in young children, this is an important consideration. In literature, there is considerably less information on NLR and ELR in paediatric cohorts than in adults although NLR was found to have similar discriminatory potential as CRP between culture-confirmed and unconfirmed cases of bacterial infection in infants between 1 week and 90 days of age[279]. Evaluation of these measures in cases of typhoid fever in children would shed light on their utility in this population.

Finally, the duration of vaccine-mediated effects on NLR and improved disease presentation are unclear. Given that lower antibodies titres associate with higher NLR in our study, this suggests that waning of antibodies over time may lower the modulatory effects of vaccination on disease symptoms. In this study, all participants were challenged approximately 1 month after vaccination at the time of peak antibody titres. Therefore, antibody persistence is likely to be an important factor in the ameliorative effects of vaccination on disease presentation.

6 Acute phase PBMC responses classify healthy from diagnosed participants with typhoid fever.

6.1 Introduction

Many diseases initiate infection at a mucosal barrier, such as the respiratory, gastrointestinal or urogenital tracts. In many cases, the relative difficulty with accessing these sites in humans has led to the extensive use of peripheral blood to derive biological insight into host responses to infection. Characterisation of "disease signatures", usually generated from cellular, serological or molecular phenotyping studies, have several translational applications. Firstly, identification of key immunological pathways activated during infection facilitate the development of prospective therapeutics to be used in the treatment and management of a given condition. Secondly, identification of host responses that uniquely signify a particular type of infection e.g. viral vs bacterial, may reduce time to patient diagnosis by eliminating potential causes more rapidly and improving patient management. This is particularly useful in scenarios where identification of aetiological cause is difficult, either because the causative organism is not present in the bloodstream or because frequency in blood is incredibly low. In cases of typhoid fever, number of bacilli in circulation is estimated at approximately 1 CFU per mL[272]. This contributes to the stochastic nature of blood culture diagnosis with only an estimated 61% of true cases being identified by this method[10]. Therefore, additional methods to complement existing diagnostic tools would be of great interest in the context of enteric fever. Finally, understanding an association between immunological responses and clinical severity of disease is of interest. Typhoid fever has a range of clinical presentations from the relatively benign to ileal perforation and haemorrhage[280]. Whilst challenge studies cannot give insights into these more extreme presentations, a significant enough range of clinical phenotypes may be present in the model to allow examination of associations between immunological responses and severity.

A considerable number of responses during acute typhoid fever have already been described in literature. The cytokine milieu at onset of symptoms is a key driver of cellular chemotaxis and changes in PBMC composition. Of particular relevance is the CXCR3 pathway, a critical homing receptor whose expression is induced by systemic IFNγ[281]. It's ligands, CXCL9, CXCL10 and CXCL11 are unabundant in the steady state but are dramatically upregulated during inflammatory responses. Whilst the importance of the CXCR3 axis is undisputed, the breadth of responsive cellular subsets that may play a role in either disease resolution or clinical severity in cases of typhoid fever is not clear from current data. In addition, non-CXCR3 migratory axes have been less explored in the context of typhoid fever and their importance are not understood.

6.2 Chapter Aims

Aim 1: To describe the changes in PBMC composition during acute typhoid fever and the contribution of $CXCR3^+$ and $CXCR3^-$ responses.

Aim 2: To investigate the association between acute phase responses and clinical phenotype of typhoid fever presentation.

6.3 Methods

6.3.1 Source of samples

Samples were collected from participants challenged with *S.* Typhi at baseline and either 7 days after infection (D7) in individuals that remained well or day of diagnosis (TD) in individuals that developed disease. Details of the clinical trial, sample collection and processing are described in the Description of study samples section of the General Methods.

6.3.2 Mass cytometry

Sample staining and data acquisition were performed at the Human Immune Monitoring Center (HIMC). Details of the panel and protocol are given in the Phenotyping by mass cytometry section of the General Methods.

6.3.3 Cytokine measurements

TNFα, IFNγ and CXCR3 ligands were measured at baseline, D7 and day of diagnosis. Methods are described in the Quantification of serum cytokines by enzyme linked immunosorbent assay (ELISA) section of the General Methods.

6.3.4 Differential abundance analysis

Differential expression between baseline and post-challenge timepoints was performed using the *diffCyt* package as described previously in the Statistical analysis section of the General Methods.

6.3.5 Machine learning

Participant diagnosis was predicted using subsets differentially expressed from baseline as predictive variables for machine learning. Machine learning methods were implemented using the *caret* package. Models were built using both absolute frequencies of differentially expressed subsets at either D7 or day of diagnosis or log2FC in subset frequency from baseline. Data were

partitioned 75:25 with balanced distribution of outcome groups in both training and test datasets. A total of 182 machine learning algorithms performed sample classification and were individually evaluated by 10-fold cross validation.

6.4 Results

6.4.1 Global PBMC composition is perturbed by the development of clinical disease

PBMC composition was assessed at baseline and either at day of diagnosis in individuals that developed disease or 7 days after infection in individuals that remained well. PCA analysis (using gated PBMC subsets frequencies as input) revealed significant perturbation in PBMC composition from baseline in the diagnosed group, suggesting frequency of major subset lineages are significantly altered at time of acute infection (Figure 6.1A). Cytolytic and mucosal subsets included $CD56^{dim}$ NK cells and γδ T-cells were the most strongly changed with significant loss in frequencies of these cells from peripheral blood ($CD56^{dim}$ NK cells: $p = 3.62 \times 10^{-5}$, **** and γδ T-cells: $p = 1.32 \times 10^{-3}$, *** respectively). More subtle significant differences were seen in other lineages including frequencies of memory ($p = 0.0209$, *) and naïve B-cells ($p = 0.0296$, *) and CD4 T-cells. ($p = 0.0239$, *) indicating a strong adaptive response during acute infection (Figure 6.1C).

More detailed phenotypic examination was performed on all cell lineages at acute infection. Clustering and differential abundance analysis identified 15 cell populations that were significantly changed in comparison to individuals that remained well (Figure 6.2). Lymphopenia is a key feature of typhoid fever presentation; therefore, it was questioned whether reductions in some subsets resulted from bone marrow suppression or apoptosis. Down-regulated subsets were enriched for the chemokine, CXCR3, suggesting change in frequency of these populations is as a result of chemotaxis rather than other mechanisms (Figure 6.3B). Populations that were expanded at diagnosis were not significantly enriched for any particular homing receptor.

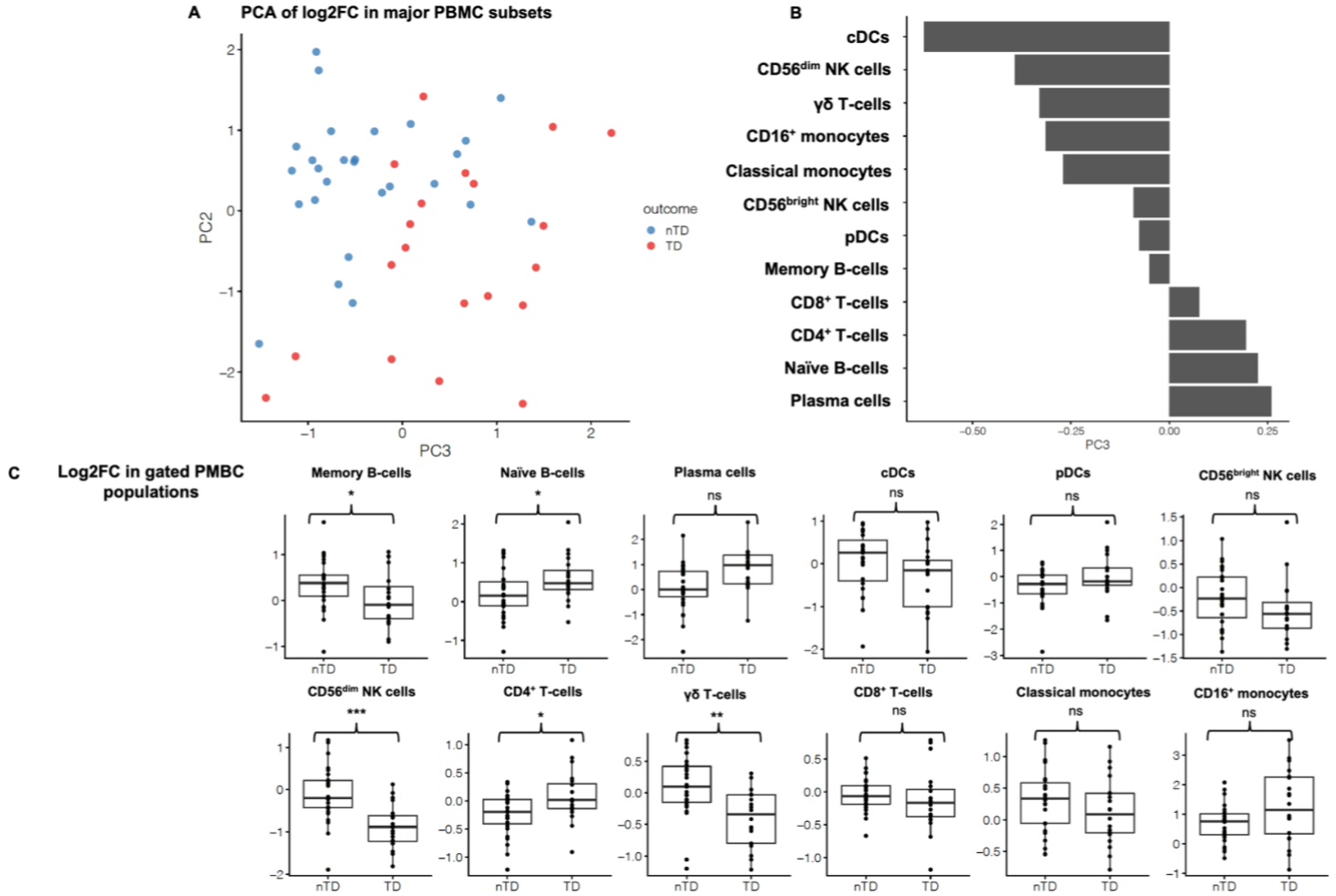


*Figure 6.1. Global perturbation of PBMCs at acute infection. TD = diagnosed, nTD = protected (A) PCA analysis of gated subset frequencies either at D7 in individuals that remained well or at diagnosis in individuals that developed acute infection. (B) PCA loadings showing variables correlated with PC3, the principal component that most significantly explained variation according to outcome. (C) Log2FC in gated subsets from baseline compared between outcome groups. Groups compared by Wilcox rank sum test. . Significance thresholds: ns = p > 0.05, * = p < 0.05, ** = p< 0.01, *** = p <0.001, **** = p < 0.0001*

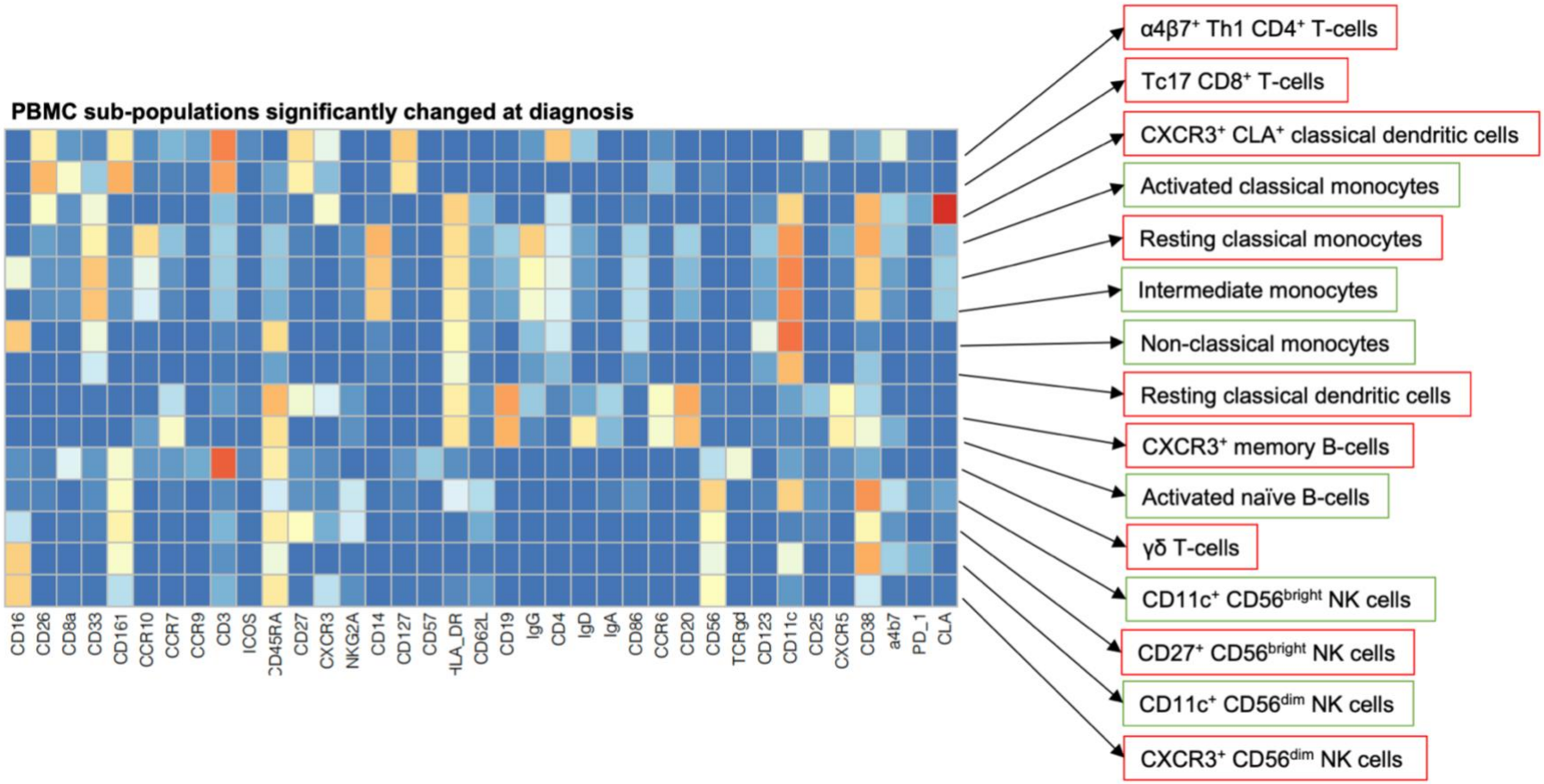


Figure 6.2. Heatmap of differentially expressed subsets at diagnosis. Colour represents median marker expression for each cluster. Each row represents a subset and each column represents a marker. Median marker expression is archsinh-transformed prior to visualisation. Cluster labels are coloured according to direction of change at diagnosis. Expanded clusters are coloured in green, contracted clusters are coloured in red.

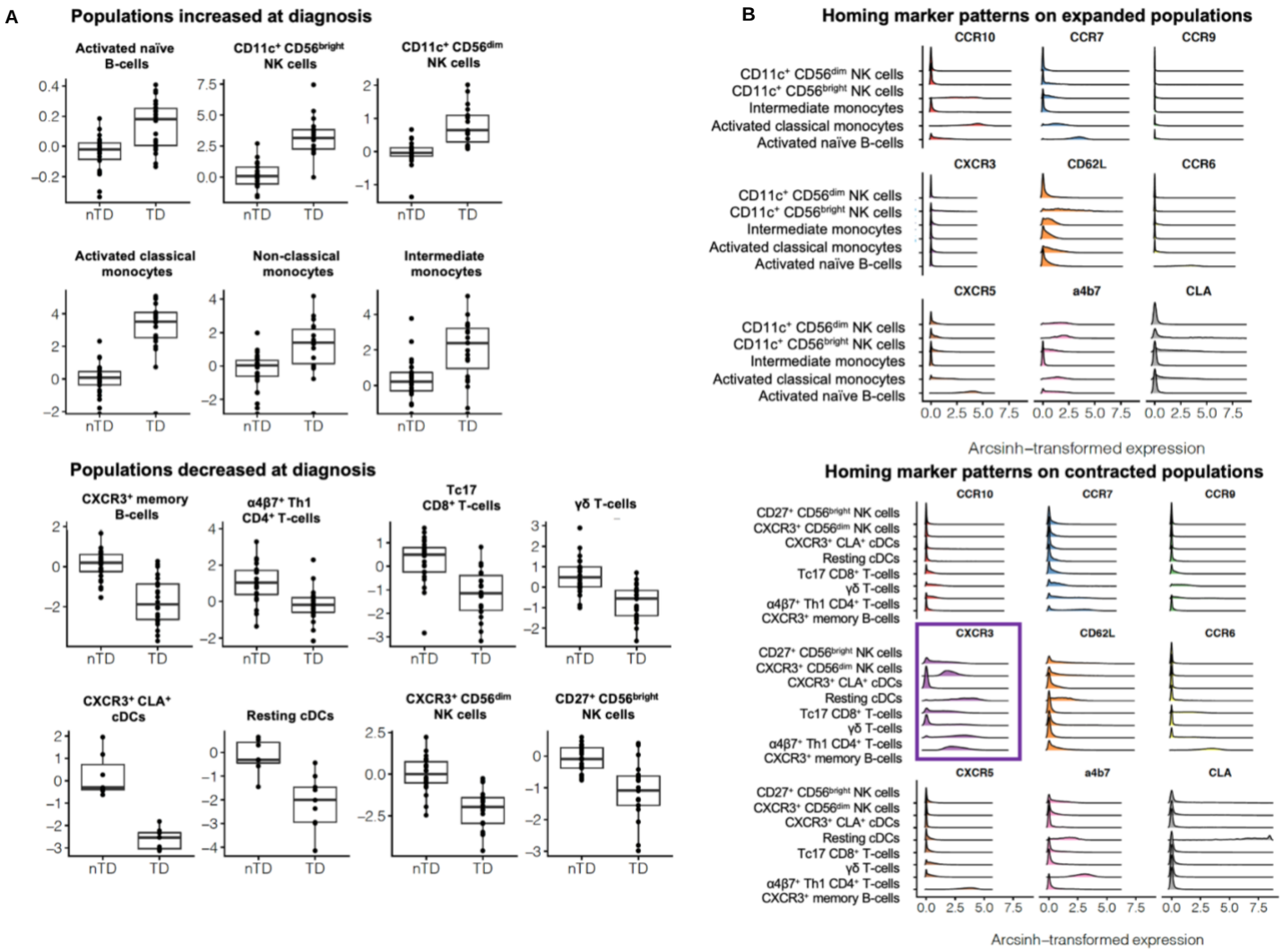


Figure 6.3. Fold change in PBMC subsets at diagnosis. (A) Boxplots of log2FC in frequency at diagnosis or 7 days after challenge are compared. Only significantly changed subsets are represented. Subsets grouped according to direction of change. (B) Density plots of subset homing marker expression, grouped according to direction of change. TD = diagnosed, nTD = protected.

6.4.2 Descriptive analysis of PBMC responses at acute infection

Clustering analysis of naïve and memory B-cells identified features of perturbed populations. A significant, albeit small increase in naïve B-cell frequency as a proportion of total B-cells was observed at diagnosis, confirming earlier gating analysis (Figure 6.6A). This subset was characterised by strong expression of IgD ($p = 5.66 \times 10\text{-}^{11}$), CCR7 ($p = 3.79 \times 10^{-9}$) and CXCR5 ($p = 5.66 \times 10^{-11}$) in contrast to total B-cells (Figure 6.6C). A second, much larger compositional shift was found in the memory compartment. Contracted $CXCR3^{+}$ memory B-cells were characterised by high CXCR3 expression in comparison to total B-cells and heterogeneous surface immunoglobulin expression, suggesting chemotaxis on memory B-cells of multiple antibody isotypes (Figure 6.6B). The effect of vaccination status on the B-cell response at diagnosis was assessed. No significant differences in either B-cell subset were observed between vaccinated and unvaccinated populations suggesting B-cell responses observed are Vi-independent responses (Figure 6.6D).

All innate compartments, including NK cells, DCs and monocytes were significantly altered by diagnosis. The relative abundance of activated classical monocytes was substantially increased from 5% (IQR = 2- 11%) of total monocytes to 52% (IQR = 33 – 67%). Expression of HLA-DR, CD38, CD45RA and CD123 was significantly increased on activated subsets in comparison to resting monocytes (Figure 6.4B). A number of unexpected features were observed on activated cells including CCR10 and IgG expression. As neither of these markers are expected to be present on monocytes, technical artefacts in these data were investigated. CCR10 and IgG expression on activated monocytes were found to strongly correlate ($R = 0.91$, $p = 2.52 \times 10^{-22}$) suggesting that antibody binding was non-specific and likely to be due to an increase in monocyte Fc receptor expression at diagnosis (Figure 6.5A). To further test this hypothesis, monocytes were isolated from PBMCs and stained with CCR10 in the presence of absence of Fc block. As anticipated, Fc block substantially reduced antibody binding, supporting assumptions that observations are not biological (Figure 6.5B). Data were sparse but

the effect of IFNγ, which has been shown previously to increase Fc receptor expression on monocytes, on non-specific staining was evaluated. A weak correlation that did not reach significance was observed (R= 0.43, p = 0.124, ns) (Figure 6.5D).

Other significant alterations included change in frequency of NK cells (Figure 6.7A). Interestingly, expanded NK cells at diagnosis expressed high levels of CD11c (Figure 6.7C). It has been previously shown that NK cells recently derived from $CD34^+$ haematopoietic progenitors cells express high levels of $CD11c$[282], suggesting this population could represent newly differentiated NK cells. In particular, $CD11c^+$ $CD56^{bright}$ NK cells were almost absent at baseline but expanded to approximately 1% of total NK cells at diagnosis (Figure 6.7B). Contracted NK subsets were phenotypically similar except for differential expression of CD27 and CXCR3. Both populations, whilst only a relatively small fraction of total NK cells, were significantly diminished at diagnosis (Figure 6.7B).

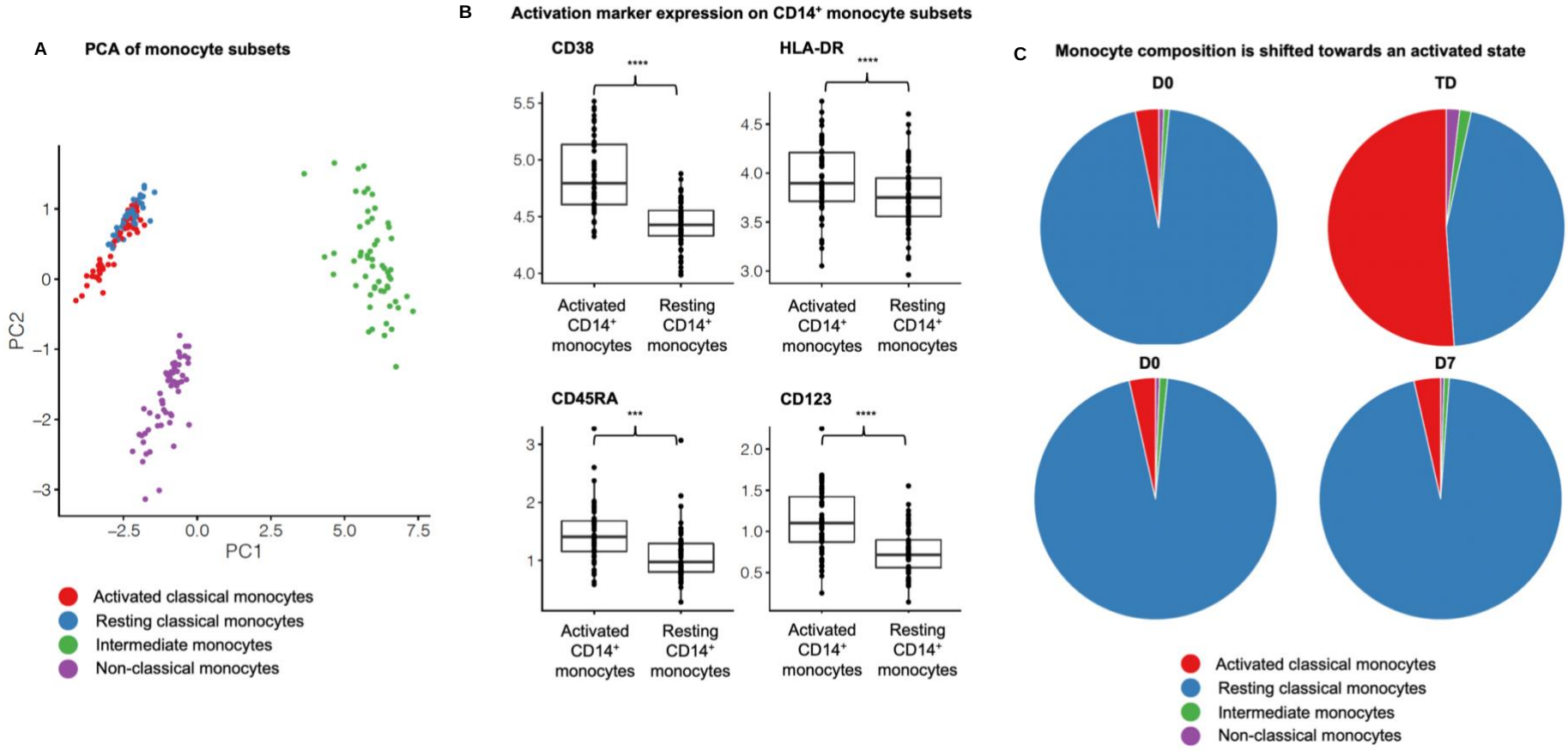


*Figure 6.4. Perturbation of the monocyte compartment at diagnosis. (A) PCA analysis of monocyte compartment, each dot represented monocyte subset from one individual. (B) Boxplots of median marker expression on activated and resting classical monocytes at diagnosis. Each dot represents median expression on each subset in one individual. Groups compared by Wilcox rank sum test. Significance thresholds: ns = p > 0.05, * = p < 0.05, ** = p< 0.01, *** = p <0.001, **** = p < 0.0001. (C) Pie chart of median compositional change in monocyte compartment in TD vs nTD groups. TD: n = 28, nTD: n = 29*

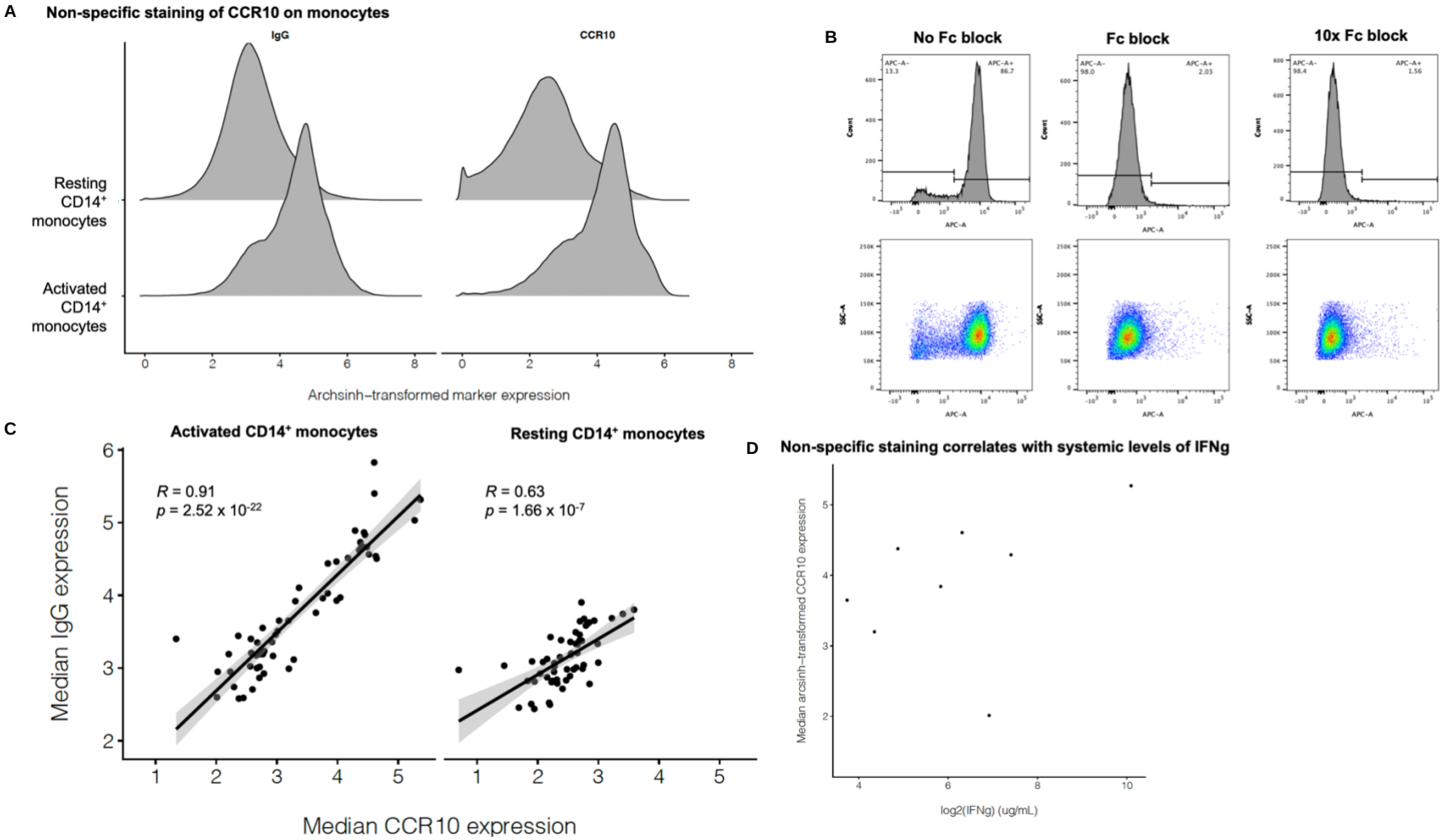


Figure 6.5. Non-specific staining of monocytes at diagnosis. (A) Density plots of IgG and CCR10 staining on activated and resting classical monocytes. (B) Effect of Fc block on CCR10 staining of monocytes.(C) Spearman correlation between IgG and CCR10 staining on activated vs resting monocytes. (D) Scatter plot of fold rise in CCR10 expression on classical monocytes vs fold rise in plasma levels of systemic IFNg.

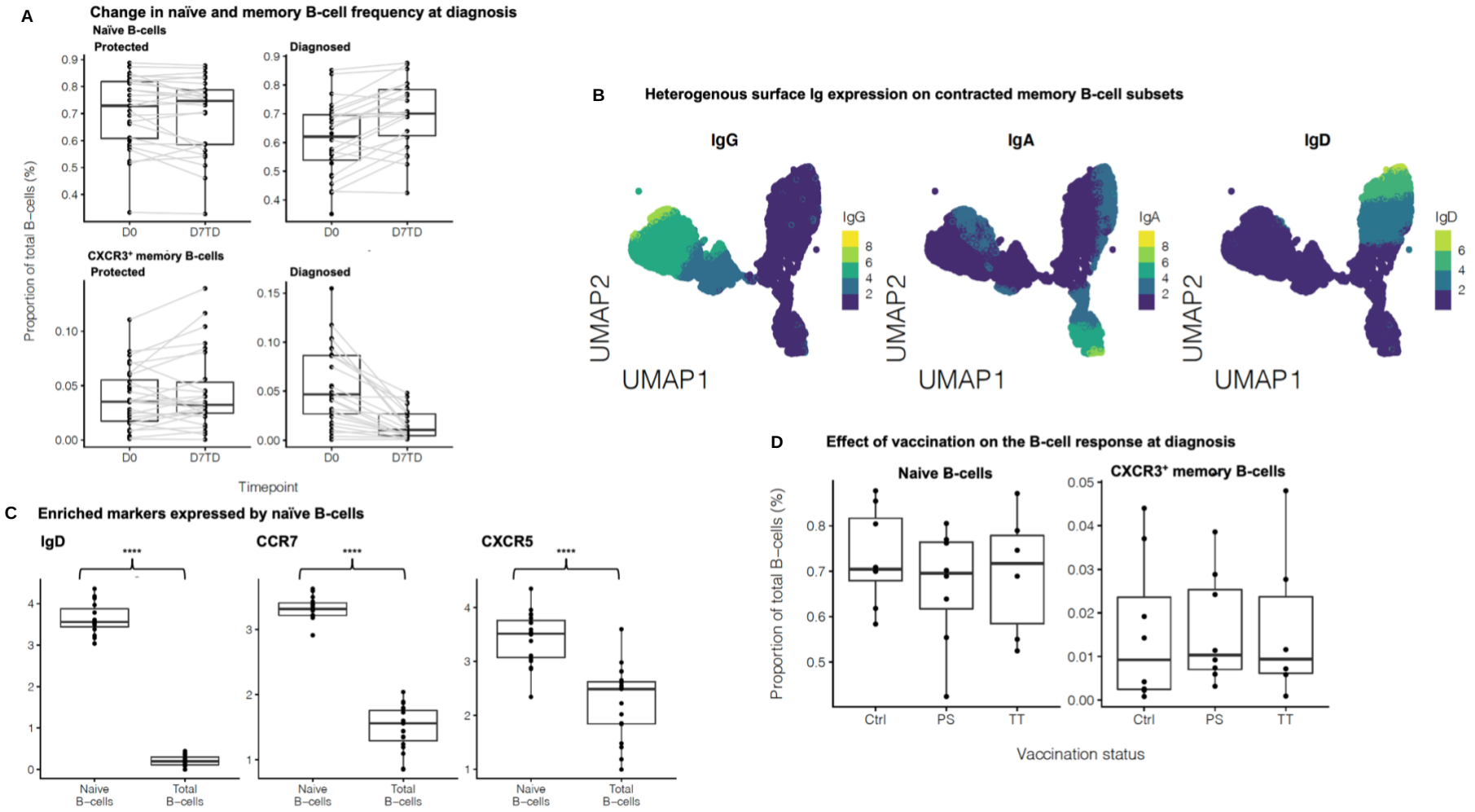


*Figure 6.6. Perturbation of the B-cell compartment at diagnosis. TD = 28 participants, nTD = 29 participants (A) Boxplots of change in B-cell subsets from baseline in diagnosed and protected individuals. (B) UMAP analysis of CXCR3⁺ B-cell compartment at diagnosis (nearest neighbours =20, minimum distance = 0.2), coloured by surface immunoglobulin expression. Lighter colour indicates higher expression. (C) Enriched markers on naïve B-cells in comparison with total B-cells. (D) Frequency of naïve and CXCR3⁺ memory B-cells at diagnosis, split by vaccine arm. Groups compared by Wilcox rank sum test. Significance thresholds: ns = p > 0.05, * = p < 0.05, ** = p< 0.01, *** = p <0.001, **** = p < 0.0001*

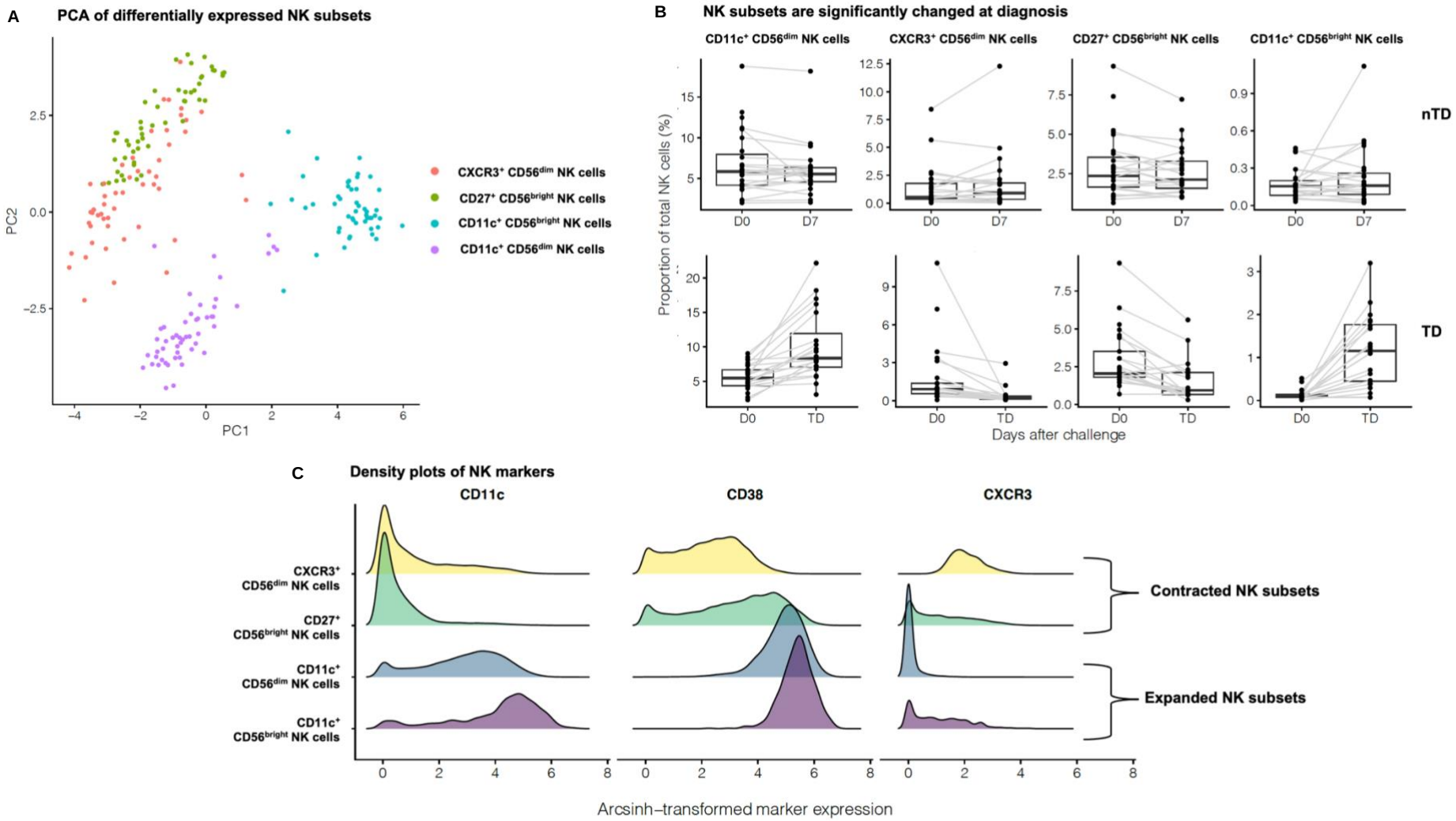


Figure 6.7. Perturbation of NK compartment at diagnosis. (A) PCA of NK subsets identified by differential abundance analysis. (B) Boxplots of NK subset kinetic, split by diagnosis.(C) Density plots

6.4.3 PBMC responses classify healthy and diagnosed samples

Features of the PBMC response that strongly distinguished healthy from diagnosed samples were assessed by machine learning. Classifier models were trained on data from either 7 days after diagnosis in individuals that remained well or day of diagnosis in individuals that developed acute disease. Models were built using either log2FC in PBMC subsets or absolute frequencies. Data from subsets previously identified as differentially expressed were included. Models built on log2FC data were highly effective at differentiating healthy from diagnosed participants (Figure 6.8). For the top 5 performing models, AUC values ranging from 0.87 to 0.92 suggesting high accuracy (Figure 6.8A). T-cell features including $\alpha4\beta7^+$ Th1 cells, $CD8^+$ Tc17 cells and γδ T-cells were highly predictive features in all models assessed (Figure 6.9). Conversely, absolute subset frequencies were less effective at distinguishing samples with AUC values ranging between 0.53 to 0.66 (Figure 6.8B).

Identified disease signature was examined in closer detail. All significantly differentially expressed T-cell subsets were strongly decreased at diagnosis and included both conventional αβ and unconventional γδ subsets (Figure 6.9B). Detailed phenotypic examination of the strongest predictive variable, γδ T-cells, showed that responding populations derived from the memory compartment, had a TEMRA phenotype and lacked CD127, the IL-7 receptor which has been previously associated with IL-17 producing-cells (Figure 6.10A). Interestingly, fold reduction in γδ T-cells was strongly correlated with rise in systemic TNFα ($R = 0.91$, $p < 0.0001$) suggesting systemic cytokines are playing a role in compositional changes (Figure 6.10B). CD4 and CD8 populations were also memory subsets with high expression of CD27 and low expression of CD45RA suggesting a central memory phenotype (Figure 6.9B). Notably, all T-cell subsets were enriched for CD161 expression when compared to total T-cells, a critical receptor found on cytolytic populations that is associated with enhanced secretion of IFNγ. This may suggest that responding subsets are primed for IFNγ production.

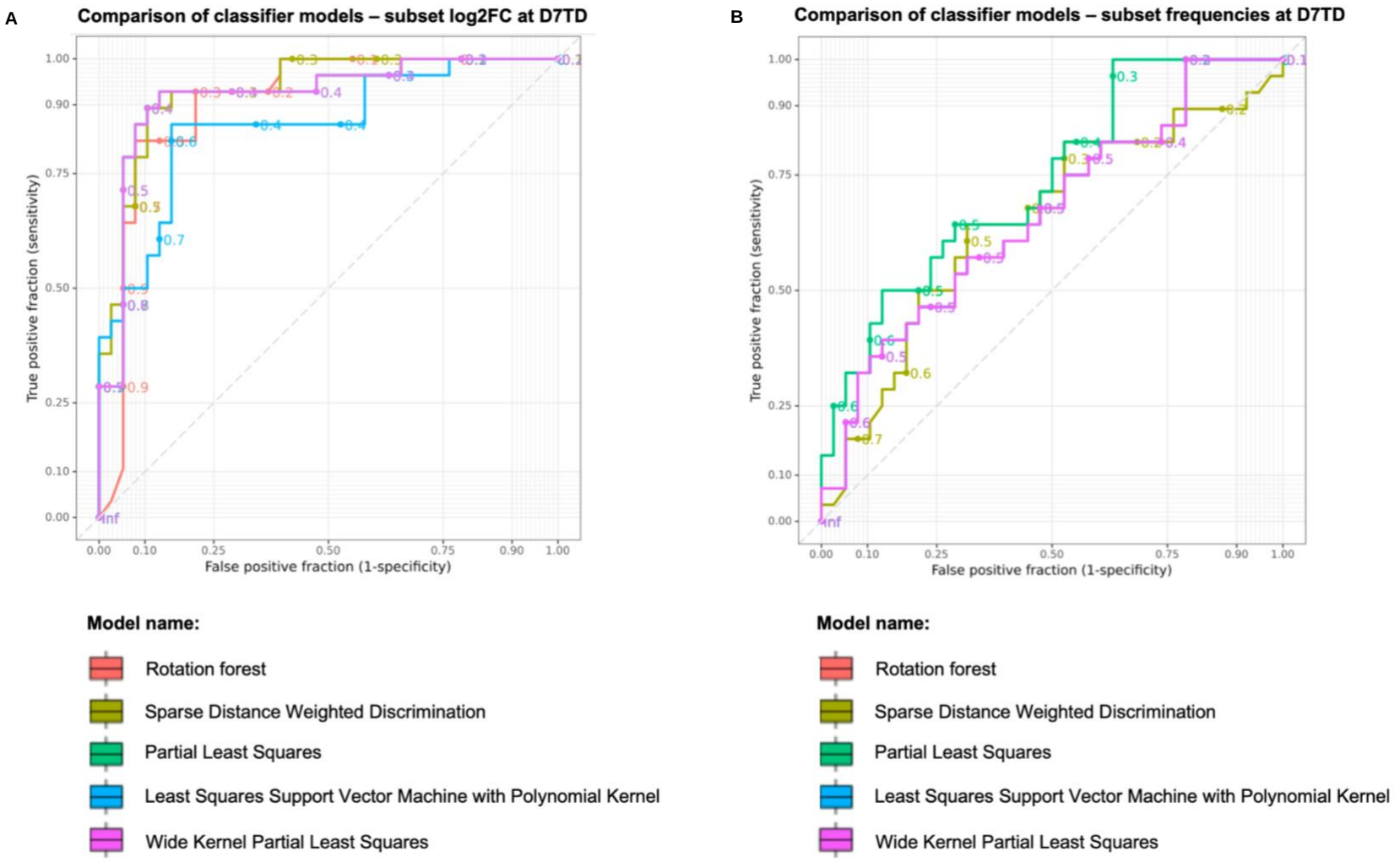


Figure 6.8. Development of a classifier model on diagnosed and healthy samples. D7TD = sample taken from either day of diagnosis (in individuals that developed acute disease) or D7 in individuals that remained well after infection. (A) ROC curves for classifier models built using log2FC in 15 differentially expressed subsets from baseline. (B) ROC curves for classifier models built using frequencies of 15 subsets at either D7 or TD.

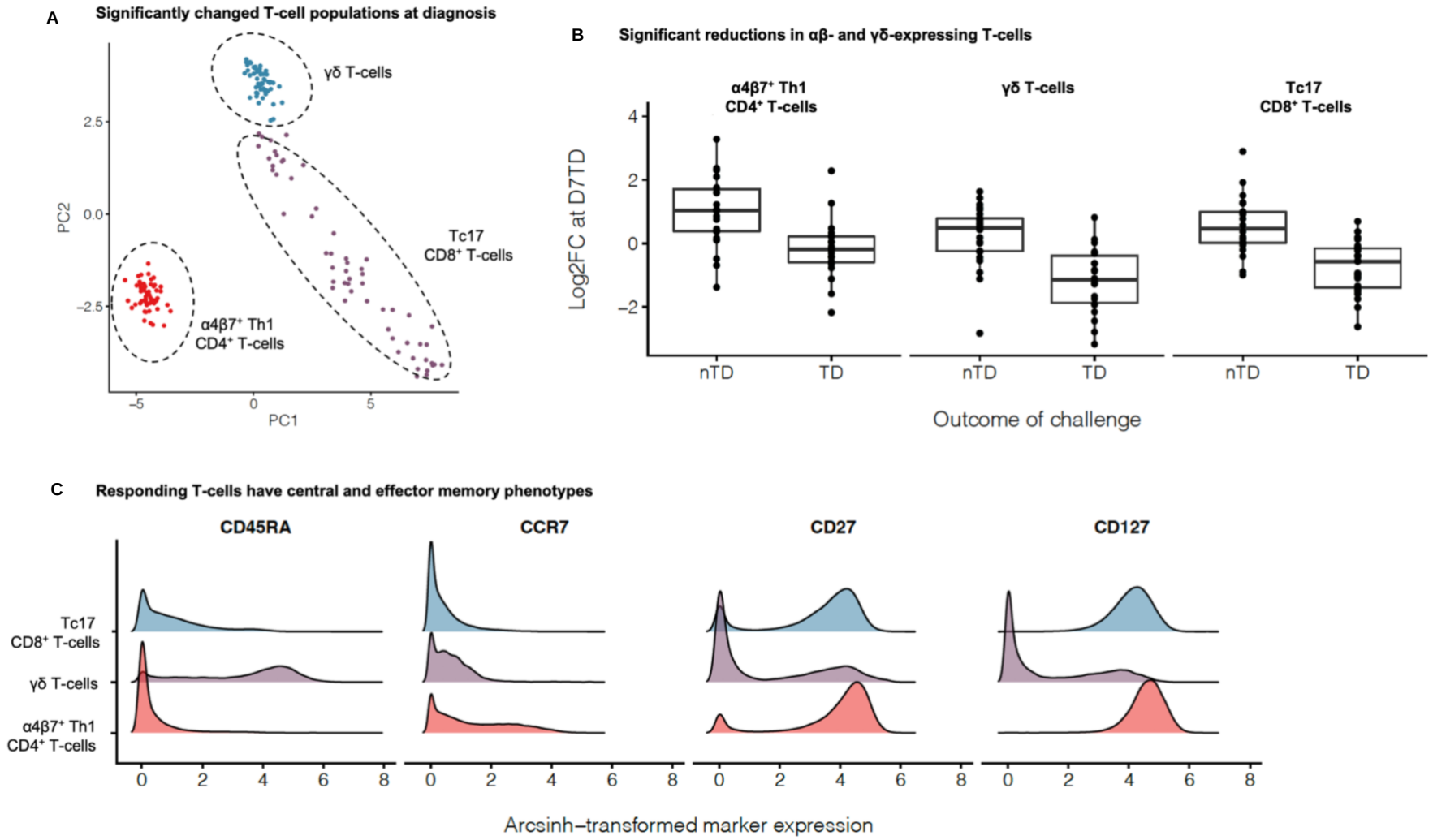


Figure 6.9. T-cell signature at diagnosis. TD = diagnosed (28 participants), nTD = protected (29 participants) (A) PCA analysis of T-cell subsets significantly changed at acute infection. (B) Log2FC in T-cell subsets from baseline (C) Density plot of CD45RA, CCR7, CD27 and CD127 on responding subsets.

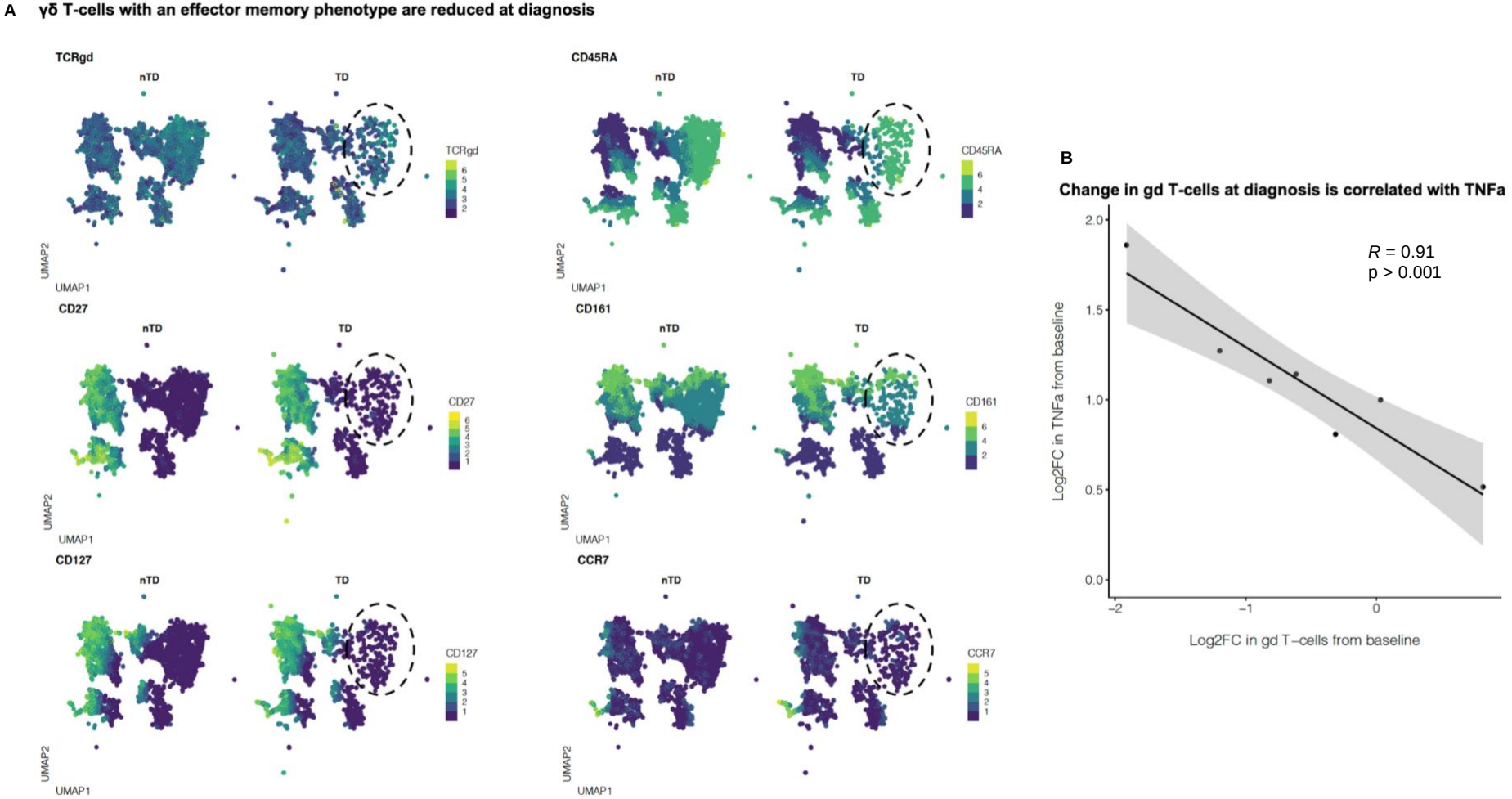


Figure 6.10. Phenotype of γδ T-cells at diagnosis. UMAP analysis of γδ T-cell compartment at D7 after infection or day of diagnosis (nearest neighbours = 17, minimum distance = 0.2). 10,000 events per condition visualised. Each UMAP coloured by marker in title, lighter colour indicates stronger expression. Circled population is the specific γδ T-cell subset that is reduced at diagnosis. (B) Spearman correlation between log2FC in γδ T-cells and systemic levels of IFNγ measured in serum.

6.4.4 Association of altered populations with clinical phenotypes

Subsets significantly altered by challenge were assessed for associations with clinical phenotypes including symptom profile, presence of fever, vaccination status and time to bacterial clearance. Univariate analysis found no significant differences between PBMC compositional changes and clinical phenotype for any of the subsets identified at diagnosis (Table 6.1). Similarly, PCA analysis of cellular responses at diagnosis did not identify any clustering of participants by clinical phenotype (Figure 6.11A).

The magnitude of cellular responses at diagnosis (i.e. fold-change in a particular subset from baseline) was correlated with time to bacterial clearance to identify potential cellular correlates of bacteraemia (Figure 6.11B). Significant associations between time to bacterial clearance and several innate populations were identified. A greater rise in activated $CD16^+$ NK cells ($R = 0.54$, $p = 0.017$) and myeloid dendritic cells ($R = 0.68$, $p = 0.042$) coupled with a decrease in resting monocytes ($R = 0.67$, $p = 0.002$) was significantly associated with greater time to bacterial clearance, suggesting that stronger innate activation may be indicative of higher bacterial burden.

*Table 6.1. Univariate statistical testing for associations between leukocyte response and clinical presentation of typhoid fever. Groups were compared by Wilcox rank sum test. Significance thresholds: ns = p > 0.05, * = p < 0.05, ** = p< 0.01, *** = p <0.001, **** = p < 0.0001.*

Subset	Group 1	Group 2	Group 1 (n)	Group 2 (n)	p-value	Significance
Activated naïve B-cells	no fever	fever	20	8	0.731	ns
CD25$^+$ memory B-cells	no fever	fever	20	8	0.447	ns
α4β7$^+$ Th1 CD4$^+$ T-cells	no fever	fever	20	8	0.438	ns
γδ T-cells	no fever	fever	20	8	0.747	ns
Tc17 CD8$^+$ T-cells	no fever	fever	20	8	0.452	ns
CXCR3$^+$ CLA$^+$ cDCs	no fever	fever	19	5	0.889	ns
Resting cDCs	no fever	fever	19	5	0.889	ns
Activated classical monocytes	no fever	fever	20	8	0.21	ns
Resting classical monocytes	no fever	fever	11	4	0.8	ns
Intermediate monocytes	no fever	fever	19	8	0.25	ns
Non-classical monocytes	no fever	fever	20	8	0.861	ns
CXCR3$^+$ CD56^{dim} NK cells	no fever	fever	18	8	0.503	ns
CD27$^+$ CD56^{bright} NK cells	no fever	fever	18	8	0.579	ns
CD11c$^+$ CD56^{bright} NK cells	no fever	fever	18	8	0.301	ns
CD11c$^+$ CD56^{dim} NK cells	no fever	fever	18	8	0.765	ns
Activated naïve B-cells	Symptom profile A	Symptom profile B	18	7	0.913	ns
CD25$^+$ memory B-cells	Symptom profile A	Symptom profile B	18	7	0.636	ns
α4β7$^+$ Th1 CD4$^+$ T-cells	Symptom profile A	Symptom profile B	18	7	0.711	ns
γδ T-cells	Symptom profile A	Symptom profile B	18	7	0.519	ns
Tc17 CD8$^+$ T-cells	Symptom profile A	Symptom profile B	18	7	0.407	ns
CXCR3$^+$ CLA$^+$ cDCs	Symptom profile A	Symptom profile B	18	4	0.222	ns
Resting cDCs	Symptom profile A	Symptom profile B	18	4	0.222	ns
Activated classical monocytes	Symptom profile A	Symptom profile B	18	7	0.596	ns

Resting classical monocytes	Symptom profile A	Symptom profile B	7	6	0.2	ns
Intermediate monocytes	Symptom profile A	Symptom profile B	18	7	0.813	ns
Non-classical monocytes	Symptom profile A	Symptom profile B	18	7	0.556	ns
CXCR3^{+} CD56^{dim} NK cells	Symptom profile A	Symptom profile B	18	7	0.256	ns
CD27^{+} CD56^{bright} NK cells	Symptom profile A	Symptom profile B	18	7	0.211	ns
CD11c^{+} CD56^{bright} NK cells	Symptom profile A	Symptom profile B	18	7	0.252	ns
CD11c^{+} CD56^{dim} NK cells	Symptom profile A	Symptom profile B	18	7	0.724	ns
Activated naïve B-cells	Symptomatic	Asymptomatic	23	3	0.909	ns
CD25^{+} memory B-cells	Symptomatic	Asymptomatic	23	3	0.273	ns
α4β7^{+} Th1 CD4^{+} T-cells	Symptomatic	Asymptomatic	23	3	0.2	ns
γδ T-cells	Symptomatic	Asymptomatic	23	3	0.182	ns
Tc17 CD8^{+} T-cells	Symptomatic	Asymptomatic	23	3	0.696	ns
CXCR3^{+} CLA^{+} cDCs	Symptomatic	Asymptomatic	20	3	0.444	ns
Resting cDCs	Symptomatic	Asymptomatic	20	3	0.444	ns
Activated classical monocytes	Symptomatic	Asymptomatic	23	3	0.316	ns
Resting classical monocytes	Symptomatic	Asymptomatic	13	1	0.4	ns
Intermediate monocytes	Symptomatic	Asymptomatic	23	3	0.222	ns
Non-classical monocytes	Symptomatic	Asymptomatic	23	3	0.315	ns
CXCR3^{+} CD56^{dim} NK cells	Symptomatic	Asymptomatic	23	3	0.222	ns
CD27^{+} CD56^{bright} NK cells	Symptomatic	Asymptomatic	23	3	0.211	ns
CD11c^{+} CD56^{bright} NK cells	Symptomatic	Asymptomatic	23	3	0.118	ns
CD11c^{+} CD56^{dim} NK cells	Symptomatic	Asymptomatic	23	3	0.842	ns
Activated naïve B-cells	Ctrl	PS	9	10	0.959	ns
Activated naïve B-cells	Ctrl	TT	9	9	0.662	ns
Activated naïve B-cells	PS	TT	10	9	0.755	ns

CD25$^+$ memory B-cells	Ctrl	PS	9	10	0.721	ns
CD25$^+$ memory B-cells	Ctrl	TT	9	9	0.491	ns
CD25$^+$ memory B-cells	PS	TT	10	9	0.95	ns
α4β7$^+$ Th1 CD4$^+$ T-cells	Ctrl	PS	9	10	0.95	ns
α4β7$^+$ Th1 CD4$^+$ T-cells	Ctrl	TT	9	9	0.345	ns
α4β7$^+$ Th1 CD4$^+$ T-cells	PS	TT	10	9	0.394	ns
γδ T-cells	Ctrl	PS	9	10	0.04	ns
γδ T-cells	Ctrl	TT	9	9	0.902	ns
γδ T-cells	PS	TT	10	9	0.054	ns
Tc17 CD8$^+$ T-cells	Ctrl	PS	9	10	0.382	ns
Tc17 CD8$^+$ T-cells	Ctrl	TT	9	9	0.779	ns
Tc17 CD8$^+$ T-cells	PS	TT	10	9	0.232	ns
CXCR3$^+$ CLA$^+$ cDCs	Ctrl	PS	8	8	0.8	ns
CXCR3$^+$ CLA$^+$ cDCs	Ctrl	TT	8	8	0.114	ns
CXCR3$^+$ CLA$^+$ cDCs	PS	TT	8	8	0.2	ns
Resting cDCs	Ctrl	PS	8	8	0.8	ns
Resting cDCs	Ctrl	TT	8	8	0.629	ns
Resting cDCs	PS	TT	8	8	0.8	ns
Activated classical monocytes	Ctrl	PS	9	10	0.731	ns
Activated classical monocytes	Ctrl	TT	9	9	0.295	ns
Activated classical monocytes	PS	TT	10	9	0.31	ns
Resting classical monocytes	Ctrl	PS	9	9	0.945	ns
Resting classical monocytes	Ctrl	TT	9	9	0.53	ns
Resting classical monocytes	PS	TT	9	9	0.247	ns
Intermediate monocytes	Ctrl	PS	9	10	0.731	ns
Intermediate monocytes	Ctrl	TT	9	9	0.133	ns
Intermediate monocytes	PS	TT	10	9	0.456	ns

Non-classical monocytes	Ctrl	PS	9	10	0.836	ns
Non-classical monocytes	Ctrl	TT	9	9	0.534	ns
Non-classical monocytes	PS	TT	10	9	0.937	ns
CXCR3^{+} CD56^{dim} NK cells	Ctrl	PS	9	8	0.412	ns
CXCR3^{+} CD56^{dim} NK cells	Ctrl	TT	9	9	0.31	ns
CXCR3^{+} CD56^{dim} NK cells	PS	TT	8	9	0.065	ns
CD27^{+} CD56^{bright} NK cells	Ctrl	PS	9	8	0.534	ns
CD27^{+} CD56^{bright} NK cells	Ctrl	TT	9	9	0.445	ns
CD27^{+} CD56^{bright} NK cells	PS	TT	8	9	0.31	ns
CD11c^{+} CD56^{bright} NK cells	Ctrl	PS	9	8	0.202	ns
CD11c^{+} CD56^{bright} NK cells	Ctrl	TT	9	9	0.202	ns
CD11c^{+} CD56^{bright} NK cells	PS	TT	8	9	1	ns
CD11c^{+} CD56^{dim} NK cells	Ctrl	PS	9	8	0.138	ns
CD11c^{+} CD56^{dim} NK cells	Ctrl	TT	9	9	0.181	ns
CD11c^{+} CD56^{dim} NK cells	PS	TT	8	9	0.699	ns

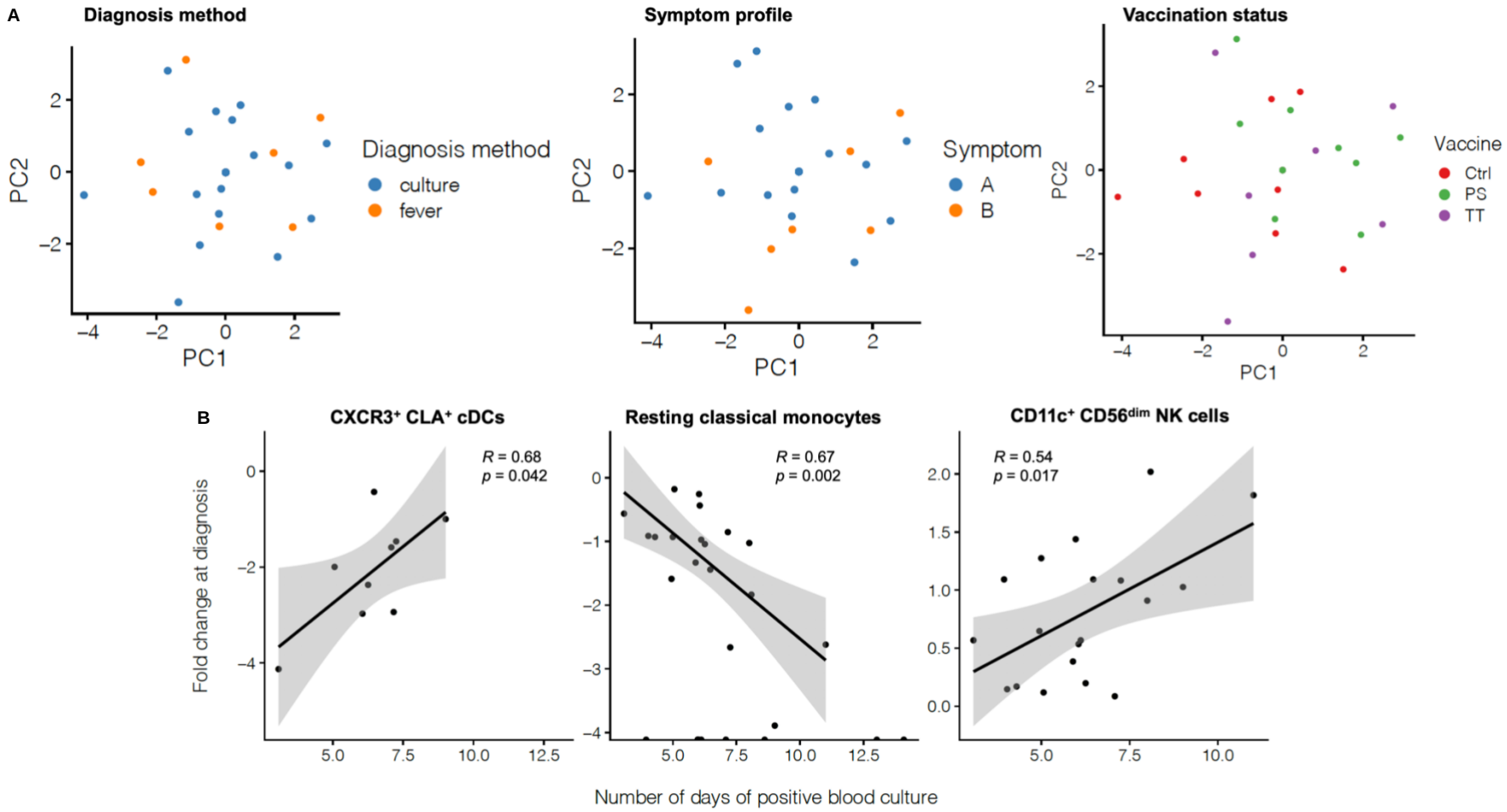


Figure 6.11. Evaluation of cellular responses at diagnosis and clinical presentation. (A) PCA analysis of cellular responses at diagnosis (log2FC data used as input), coloured by presence of fever, symptom profile (see previous chapter for definition) or vaccination status. (B) Spearman correlation between Log2FC in innate subsets at diagnosis and number of days of positive blood culture after diagnosis.

6.5 Discussion

This analysis provides a comprehensive, descriptive study of cellular immunity during acute typhoid fever. Whilst changes in some of the subsets described in this analysis are known and well-documented in animal models of *Salmonella* infection, other responses are newly reported here. In addition, this study provides a more detailed phenotypic insight into responses involved in acute infection than has previously been reported.

In this analysis, chemotaxis is a major factor in compositional change of peripheral blood at diagnosis. Many subsets that are proportionally reduced at diagnosis are $CXCR3^+$ suggesting systemic cytokines are potent drivers of compositional shift. Furthermore, CD161 expression was found across numerous contracted cytolytic subsets at diagnosis. Cross-linking of CD161 enhances IFNγ secretion from NK cells and a similar observation has been made for effector T-cells subsets suggesting that migratory subsets have enhanced cytotoxic potential[283]. Both this study and previous literature finds the CXCR3 signalling pathway to be of clear importance during acute typhoid fever. CXCR3 ligands, CXCL10 and CXCL9, but not CXCL11, are strongly upregulated at diagnosis and are known to potentiate a Th1-biased cellular response[64]. CXCL9 upregulation is largely driven by IFNγ whereas CXCL10 and CXCL11 can be modulated by both IFNγ and type I IFNs. The source of CXCR3 ligands during *Salmonella* infection has not been clearly established although F4/80-expressing iNOS-mononuclear phagocytes are thought to be major sources[284]. IFNγ stimulation of macrophages has also been found to drive CXCL10 and CXCL9 upregulation[285].

The importance of CXCR3-mediated migration in bacterial containment has been previously shown in murine of models of *Salmonella* infection. CXCR3 knockout significantly increased the rate of bacterial dissemination from the intestinal tract, which was associated with lower influx of IgA^+ plasma cells, neutrophils and $CD4^+$ T-cells[281]. In addition, containment of bacterial replication at disseminated sites such as the spleen relied on the presence of $CXCR3^+$ Th1 cells[284]. In agreement with animal models, $CXCR3^+$ $CD4^+$ T-cells are contracted in

peripheral blood at diagnosis suggesting migration to sites of inflammation. Interestingly, responding cells were observed to have a central memory phenotype ($CD45RA^{-}$ $CD27^{+}$) with high expression of CD161, suggesting at least a proportion of contracted cells are IL-17-producing Th17 cells. IL-17 production is an essential aspect of mucosal responses and plays a significant role in coordinating neutrophil recruitment to sites of inflammation[286]. Understanding the cytokine profile of contracted T-cells to confirm their exact nature would be of interest in further investigation.

Other CXCR3-expressing subsets with cytolytic activity are also notably changed during acute disease. $CXCR3^{+}$ $CD56^{dim}$ NK cells were significantly reduced at diagnosis. Effector functions of $CD56^{dim}$ NK cells include release of granzymes which are essential for eradication of infected cells during disease. NK cells have been previously found to be highly efficient at recognition and lysis of *Salmonella*-infected monocytes *in vitro* suggesting a functional role in clearance[87]. Soluble granzymes are detectable in plasma of typhoid fever patients and have been found to correlate with stage of disease[287]. *In vivo* data from a study of pregnant mice which showed lower influx of NK cells to the spleen was associated with a 1000-fold higher bacterial load[288]. In this study, phenotype of NK responses in humans during acute phase disease has been elucidated. Decreased NK cells in this study have minimal expression of CD11c. It is unclear whether this distinction applies in humans and would require further functional characterisation.

Not all contracted subsets have a clear, direct effector role in clearance of *S.* Typhi. CXCR3-expressing memory B-cell subsets comprise a small fraction of those found in circulation and are significantly decreased at diagnosis. $CD27^{+}$ memory B-cells in our study universally express CCR6 and CXCR5 in line with previous literature. CXCR3-expressing subsets reduced at diagnosis had a strongly activated profile ($CD38^{++}$) and broad surface immunoglobulin expression including IgG-, IgA- and IgD subsets. This may suggest that migration to inflamed sites is independent of antigen triggering. These observations are in line

with previous studies that have also shown B-cell frequencies can be modulated by acute presentation of typhoid fever in humans. Similar reductions in memory B-cells were observed although greater phenotypic detail is provided here[244].

A role for B-cells in resolution of typhoid fever requires further clarification. Beyond antibody production, B-cells are efficient antigen presenting cells where they have been found to be especially effective at reactivation of memory $CD4^+$ T-cells[289]. Indeed, *Salmonella*-infected mice deficient in B-cells were found to have poorer $CD4^+$ IFNγ responses and higher bacteraemia which may suggest that B-cells have an essential secondary role in propagation of $CD4^+$ T-cell responses[127]. The precise B-cell subset involved was not established in this previous report. Contraction of memory B-cells at diagnosis was poorly correlated with fold rise in IFNγ, therefore the role of B-cells in the development of Th1 responses in humans remains unclear and requires further elucidation. Notably, none of the observed B-cell responses were strongly associated with vaccination status. A single infection with S. Typhi poorly induces Vi-specific responses therefore this lack of association is not unexpected. The specificity of responding B-cells and the importance of this in responses to infection is not clear.

The relative importance of identified CXCR3-expressing subsets in anti-bacterial responses and their specific functions requires further investigation. However, this analysis confirms previously identified subsets as highly relevant to human disease and provides greater phenotypic resolution on responding populations.

CXCR3-independent migration is also evident at diagnosis. In this study, T-cell responses at diagnosis were found to sufficiently distinguish healthy and diagnosed participants with a high degree of accuracy. Classification models built on both fold change and absolute frequency data identified γδ T-cells as the most significant contributory variable. The strength of the change in frequency suggests innate-like T-cells form a significant part of responses to *S.* Typhi and may have a role in clearance of established infection. Their description as “innate-

like" T-cells is due to their rapid activation and responsiveness to non-cognate stimulation such as cytokines. Cytokine-mediated activation leads to significantly more rapid effector function than their αβ counterparts which may contribute to rapid control of disseminated infection. Contracted subsets in this study lacked homing markers therefore tissue tropism of these cells is unclear.

Data on the role of γδ T-cells during *Salmonella* infection are surprisingly limited given the importance of γδ T-cells in barrier immunity[290] however some previous studies report opposing findings to observations made here. In patients with culture-confirmed *Salmonella* infection (inclusive of typhoidal and non-typhoidal serovars), γδ T-cells were significantly increased in peripheral blood when compared with healthy controls, and this is especially pronounced in systemic vs gastrointestinal forms of disease[291]. In addition, CD161-expressing γδ T-cells (similar to the phenotype reported here) were significantly higher in *Salmonella*-infected patients than healthy controls and patients with acute bacterial enterocolitis due to other causes[292]. A range of *Salmonella* serovars were included (the majority of cases were *S.* Typhimurium, *S.* Enteriditis, *S.* Paratyphi and *S.* Typhi) although all responses appeared similar between serovars in this study. Moreover, the proportion of $CD161^+$ γδ T-cells producing IFNγ in *Salmonella*-infected patients was significantly higher than in healthy controls or disease controls. These reports suggest that γδ T-cells may have a more critical role in host responses to cases of *Salmonella* infection than in other bacterial enteric diseases.

The reason for this discrepancy between past literature and findings in this thesis are unclear. One possibility is that cellular responses reported here reflect a much early stage of the immunological response to infection than cohort studies due to the stringency of diagnostic criteria. Whether early sequestration of γδ T-cells in tissues is later followed by a subsequent expansion in peripheral blood is unknown. It has been shown previously that TNFα has a major impact on sequestration of γδ T-cells in the lymph nodes[293]. Fold change in γδ T-cells was significantly correlated with systemic levels of TNFα in our challenge model suggesting this

observation is biologically real and a critical mechanism for γδ retention in tissues during inflammation.

This and previous analyses indicate, monocytes are systemically activated in response to *Salmonella* infection and are easily identifiable during acute disease. More than 50% of classical monocytes exhibited an activated phenotype during acute infection. In this analysis, activated monocytes appeared to strongly upregulate mucosal migratory marker, CCR10, which was initially thought to suggest migration to the intestinal tract or other mucosal surfaces may be a feature of disease. Circulating classical monocytes have been previously shown to constitutively migrate to the mucosa and are essential for replenishment of intestinal macrophage populations during homeostasis[294]. In inflammatory conditions, recruited monocytes do not undergo differentiation to tolerogenic macrophages; instead, infiltrating monocytes retain their inflammatory phenotype and are major producers of iNOS, IL-1β and TNFα[294]. The chemokine pathway involved in monocyte migration to sites of inflammation is largely thought to be mediated by CCR2, therefore identification of CCR10 on monocytes was an unexpected observation. In animal studies of *S.* Typhimurium infection, the CCR2 ligands, CCL2 and CCL3, were shown to be upregulated in the PPs and MLNs of *Salmonella*-infected mice which in turn was associated with influx of inflammatory monocytes during infection[91]. In addition, CCL2 deficiency in mice is associated with greater systemic bacterial burden and mortality, suggesting that monocyte responses from an essential aspect of bacterial containment and infection resolution[295]. Previous cytokine and chemokine profiling in challenge model participants did not identify any CCR2 ligands[64]. Therefore, this may mean that chemotaxis of activated monocyte populations during typhoid fever is limited or an alternative migratory axis has greater importance in human disease.

It is likely that CCR10 expression is explained by technical issues. Artefacts due to non-specific staining were evident in the monocyte compartment at diagnosis, creating artificial signal across a number of channels. Myeloid cells have the highest surface density of Fc receptors of all

PBMC subsets, therefore non-specific staining is highly common in this population. Whilst inclusion of Fc blocking reagents to the staining mix and optimising staining incubation period can improve this issue, it is unlikely to remove all unwanted signal. This can produce potentially confounding observations, and confirmation via a separate method may be necessary. In this analysis, strong "expression" of a number of non-myeloid markers including CD20 and IgG were noted at acute disease. Non-specific staining was found to be worsened at diagnosis than at other timepoints in this study, possibly due to upregulation of Fc receptors on monocytes during acute disease. Fc receptor expression has been previously found to increase following monocyte activation, which may explain why artefacts are worse on activated vs resting monocytes. In addition, a number of pro-inflammatory cytokines including IFNγ are known in vitro to increase expression of Fc receptors[296]. A weak association between systemic IFNγ and non-specific staining was observed although data are too sparse to make a conclusion on whether Fc receptor expression has been modulated at TD by systemic cytokines. Given these factors, it is assumed from this analysis that CCR10 expression on monocytes is an artefact and has limited importance in the pathogenesis of typhoid fever.

A number of previous reports have found a more extensive cytokine milieu during acute typhoid fever than presented in challenge model participants[56]. Notable differences include absence of pyrogenic cytokines IL-1β and IL6, as well as neutrophil chemokine CXCL8. The absence of these systemic signals in Oxford participants is reflected in the milder phenotype and is an artefact of the model. Interestingly, our laboratory has also consistently reported resistin production during acute disease which has not been previously identified in field studies[64,102]. The knock-on effect of these differences on PBMC responses observed in this study is not clear. IFNγ, IFN-inducible chemokines and TNFα have the most pronounced impact on PBMC responses observed here and are potently induced under challenge model conditions. Whether additional subsets, inducible by "missing" cytokines or other systemic signals not found in challenge model participants, play roles in disease resolution is not known from these data.

This analysis found no significant associations between participant symptom profile, fever or vaccination status and the leukocyte response. This observation is disappointing. Given the convincing associations between blood count ratios and disease presentation, it was hoped that PBMC perturbation and compositional shifts may offer similar correlates of severity. In other infections, inflammatory responses, especially those driven by monocytes, are associated with the development of critical illness and complications requiring hospitalisation. Despite a clear relationship with severe illness, strong monocyte activation across all participants at diagnosis observed here could not be associated with milder presentations of disease. Absence of monocyte chemotactic factors in serum of challenge model participants at time of diagnosis may indicate that monocyte infiltration of tissues is relatively limited in these cohorts; this combined with rapid initiation of treatment prevents development of more severe pathophysiology in challenge model participants. It is plausible that NLR and ELR are more sensitive as biomarkers of disease severity and can stratify even very mild cases of typhoid fever whereas alterations in PBMCs have to be considerably more extreme before associations are detected.

The relative importance of acute phase responses in disease resolution (i.e. bacterial clearance) is difficult to elucidate in human studies as individuals initiate treatment rapidly after diagnosis. Confounding of associations between cellular responses and time to infection resolution makes mechanistic insights difficult.

It is notable that a number of previously reported observations have not been identified here. Patients with *Salmonella* bacteraemia have been previously shown to have higher levels of NKT cells in comparison to healthy controls and other cases of bloodstream infection[297]. Interestingly, percentage of NKT cells was higher in fatal infections in comparison with those that survived, suggesting this subset make be a biomarker of severe disease. iNKT responses have also been reported in animal models where they are also recruited to the lamina propria during oral *S.* Typhimurium infection and secrete IFNg in a Nod1- and Nod2-dependent

manner[298]. In our analyses, NKT cells were not significantly changed from baseline, possibly due to the relatively mild presentation of disease. Comparison of responses seen here with acute disease from naturally infected participants at different stages of disease may be of interest in future studies.

7 Final discussion

7.1 Summary of key findings

7.1.1 Primary cellular immune responses to Vi-vaccines correlate with development of serological functions and memory B-cell generation.

This is the first study to compare the primary cellular responses to Vi-TT and Vi-PS immunisation and evaluate their association with the development of protective humoral immunity and memory B-cells. Specifically, this study identifies a common plasma cell profile induced by both vaccines as well as an interesting association between NK responses and memory B-cell formation.

$CCR10^+$ IgA^+ plasma cells and $a4b7^+$ IgG^+ plasma cells are induced by Vi-vaccines which correlate with ADNP after vaccination. The differences in magnitude of the plasmas cell response between Vi-PS and Vi-TT are well described in the context of Vi-vaccines as well as other glycoconjugate immunisations[40,136]. In addition, predominance of Vi-IgA responses after vaccination have also been previously well described[215] therefore, it is expected that these results corroborate this at the cellular level. Interestingly, the IgA^+ plasma cell response following immunisation was shown to express a mucosal-directed homing profile, indicating that these cells may localise to the mucosal surface after antigen exposure. Induction of a mucosal directed response following parenteral vaccination is unusual. Individuals in this study were anticipated to be Vi-naive prior to immunisation, however, expression of CCR10 and α4β7 on responding plasma cells suggests this may not be the case. Parenteral immunisations against other enteric and respiratory infections have been shown to induce mucosal responses in recipients with previous antigen exposure. Parenteral immunisation with an inactivated polio vaccine boosted mucosal immunity in individuals with natural exposure or previous vaccination with an oral polio vaccine[299]. Boosting of mucosal immunity by parenteral polio vaccination was also found to minimise shedding, suggesting an effect of boost on indirect protection[300]. Priming status of individuals in this study was not conclusively shown with these results. Nonetheless, these findings may suggest that parenteral immunisations, in addition to systemic

responses, may enhance pre-existing mucosal immunity which could confer desirable effects on indirect protection. An effect of Vi-TT and Vi-PS immunisation on shedding has been noted in previous studies although no connection with priming or Vi-IgA responses was established[301]. However, an association between shedding and the IgA plasma cell response following Vi-TT immunisation may be of interest in future work.

This analysis is the first to show a connection between innate immunity against Vi-TT vaccination and memory B-cell formation. Circulating Tfh induced by vaccination are negatively correlated with NK responses. Low Tfh and higher NK responses are associated in turn with poor memory formation. Understanding correlates of vaccine failure are as important as correlates of protection. Whilst NK responses after vaccination have been observed previously, their role in memory B-cell formation is not well elucidated. NKT cells have been previously suggested to influence to play a role in the GC although a clear mechanistic function has not been well defined[302]. Clarification on several points is needed. Firstly, the exact identity of these cells requires elucidation as overlapping phenotypes with other subsets of innate lymphoid cells precludes identification with absolute certainty. Secondly, the action of NK subsets identified here on cTfh is not known. Whether reduced Tfh are as a result of suppressed activation, apoptosis or other effects are not clear from these analyses.

7.1.2 Distinct immunological profiles are detectable within 24 hours of infection and have differential associations with outcome of challenge.

This analysis provides the first longitudinal study of cellular immunity that develops during the course of human *S.* Typhi infection. Immunological signatures, including significant differences in baseline PBMC composition, were identified that are differentially associated with protective outcome. In addition, this is the first analysis to evaluate how early and acute immunological responses to *S.* Typhi infection develop in both Vi-vaccinated and unvaccinated participants.

Whilst an absolute association with vaccination status could not be established, we find that 75% of individuals with a protective immunological profile were vaccinated with the

majority of vaccinated participants being strong vaccine responders. Conversely, more than 50% of individuals in the susceptible group were unvaccinated or mounted poor responses to vaccination. In addition, individuals in the susceptible profile that were vaccinated had considerably higher levels of antibodies that induced previously described "undesirable" functions correlated with poor outcomes. This suggests that antibody profile and vaccination status may be associated with the development of early immunological responses after infection.

The key characteristic of the protective cellular profile was strong activation of $CD16^{+}$ monocytes. Non-classical monocytes are the primary producers of TNFα during infection. The deleterious effects of TNFα deficiency in animal models[80] and human studies[253] suggest that early induction of TNFα producing subsets may be a key aspect of protection from typhoid fever. Conversely, individuals in the susceptible profile had no evidence of monocyte expansion, had the highest peripheral bacterial burden at diagnosis, the highest levels of sCD40L and CX_3CL1 12 hours after challenge and evidence of memory B-cell recirculation for several days after infection. The association between this immune profile and poorer control of bacteraemia suggests early responses have relevance to eventual presentation of disease and should be further investigated.

Finally, this analysis identified associations between baseline PBMC composition and susceptibility to development of acute typhoid fever. Several reports have examined the influence of baseline status on progression of immune responses, although generally in the context of vaccination with highly accurate predictions of vaccine responsiveness being achieved, suggesting baseline PBMC responses confer valuable information regarding capacity to respond to infectious challenge[303] .

7.1.3 Vi-vaccination ameliorates presentation of typhoid fever

Clinical management of typhoid fever relies of metrics of severity such as CRP, white blood cell count and extent of bacteraemia. This is the first analysis to investigate whether other measures, such as blood count ratios, can better identify participants with more severe clinical

illness. Use of blood count data is advantageous in low-income settings where access to other clinical tests such as CRP are limited. It was found that NLR and ELR were distinct correlates of disease severity in human challenge model participants with typhoid fever. Higher NLR was associated with more rapid progression to disease and number of symptoms. On the other hand, lower ELR did not correlate with disease progression but strongly associated with worsened presentation of symptoms.

It has been previously shown by our laboratory that Vi-TT vaccination reduces incidence of fever, headache and feeling generally unwell in comparison with unvaccinated controls. In this follow-up analysis, it was shown that NLR, but not ELR, is significantly modulated by Vi-TT immunisation which in turn was correlated with baseline Vi-IgG antibody titres. An association between both metrics and more life-threatening complications of typhoid fever require further elucidation. Considerable work has been published previously on NLR and its association with increased risk of mortality, suggesting interventions that lower NLR may have positive impacts on adverse outcomes[264,304]. Conversely, ELR is less widely reported on therefore associations with severity in the context of typhoid fever requires further examination.

7.1.4 T-cell signature classifies healthy and diagnosed participants whilst an innate immune signature at diagnosis is predictive of bacterial clearance

This study provides a comprehensive, phenotypic overview of PBMC responses to *S.* Typhi infection at disease presentation. Acute disease was characterised by significant perturbation of all PBMC subsets. This study presents a highly discriminatory disease signature of T-cell responses that classified samples from diagnosed and protected participants with a high degree of accuracy. The most strongly predictive feature of this signature was frequency of gδ T-cells which were strongly decreased at diagnosis. Few associations with clinical phenotype could be elucidated from these data, suggesting PBMC responses are a poor biomarker of disease severity.

7.2 Limitations of the study

7.2.1 Oxford challenge model cohorts - relevance to endemic settings

The demographic of challenge study cohorts is predominantly Caucasian with only 6% of participants representing non-white backgrounds. In addition, these studies have necessarily focused on adults living in settings with access to clean drinking water and sanitation. Whilst these characteristics diverge substantially from the most likely recipients of Vi-vaccines in endemic settings, efficacy trials suggest that demographic differences have limited impact on vaccine effectiveness. The efficacy of Vi-TT in children under 16 years of age residing in Nepal was comprehensibly proven in a Phase III trial of more than 20,000 people, therefore differences in immunogenicity of Vi-TT between demographic cohorts appear minimal[155]. Efficacy of Vi-vaccines in African populations has not been formally evaluated although the impact of vaccine rollouts in several African countries will be monitored extensively for indicators of effectiveness. Furthermore, persistence of long-term immunological memory and Vi-antibody titres are also likely to be similar. In studies of other glycoconjugate vaccines, there has been limited evidence of poorer persistence of vaccine-specific antibody titres in non-Caucasian populations, therefore it is reasonable to assume that persistence of Vi-specific responses should follow a similar pattern as has been observed for other polysaccharide antigens[305,306]. This suggests other immunological mechanisms identified here are likely to remain relevant in a more diverse cohort.

Beyond demographic differences, Oxford cohorts evaluate efficacy and immune responses in a relatively small number of participants in comparison with field trials which limits statistical inference. Challenge studies are costly to run and require highly specialist knowledge both in terms of laboratory and clinical experience. In addition, the intensity of sampling during challenge and perceived risks can hinder recruitment efforts. However, the depth of information generated on all individuals in these trials is far above what would be possible in a field study. This approach gives a holistic overview of immunity against *S.* Typhi infection which can be evaluated further down the line in larger cohorts in endemic settings.

7.2.2 Representative challenge dose and strain

The challenge strain used in the Oxford model, Quailes strain, was isolated from a chronic carrier in 1958 at the University of Maryland and may differ from predominant strains in circulation today. Use of a strain with a known safety profile, that has been previously used in humans (challenge studies of the 60s and 70s) and is fully sensitive to antibiotics is both practically and ethically necessary. Whether presently circulating strains S. Typhi would induce substantially differing host responses to infection in not clear. Whilst a head-to-head comparison of virulence factors on *S.* Typhi serovars in circulation and Quailes strain has not been formally conducted, it is likely that variance in major immunodominant antigens is low. A number of these antigens, such as the Vi-epitope, are essential for virulence and pathogen fitness (as exemplified by a recent, comprehensive screening study of virulence factors in humanised mice[19]) therefore substantial variance between strains is unlikely. However, it cannot be completely ruled out that differences in some *S.* Typhi antigens may impact the development of cellular immunity after infection.

Whilst environmental reservoirs of *S.* Typhi and *S.* Paratyphi in drinking water have been characterised[307], an inoculum sufficient to cause disease is not well established. The dose given in challenge studies is suspected to be higher than inoculums encountered in endemic settings and is chosen in order to confer a consistent attack rate of ~75% in unvaccinated participants. Inclusion of bicarbonate pre-treatment in challenge studies artificially increases susceptibility and ensures consistent infection. Whether pre-treatment alters progression of infection substantially is unknown.

In this thesis, the cellular response to infection with *S.* Typhi is evaluated. *S.* Typhi is only one (albeit the most common) of the *Salmonella* serovars that contribute to cases of enteric fever globally. Whether similar signatures of immunity identified in this analysis are similar between *S.* Typhi and *S.* Paratyphi is unknown. A detailed study of cellular responses over the course of *S.* Paratyphi infection is warranted. Given the imminent rollout of Vi-TT vaccinations as part of routine immunisation programs in several endemic settings, the number of cases

attributable to *S.* Typhi will no doubt fall. A remaining challenge in enteric fever research is the successful development of an effective vaccine against paratyphoid fever. Understanding of differences between *S.* Typhi and *S.* Paratyphi infections will inform the development of more targeted and efficacious vaccines.

7.2.3 Diagnostic criteria and rapid initiation of treatment following diagnosis

The diagnostic criteria employed in this study are incredibly stringent, and Vi-TT vaccine efficacy estimates can range from 54-81% in the challenge model depending on criteria used for diagnosis[40]. The stringency is necessary from a safety standpoint however, it is likely that immunological presentation of acute disease is milder than it would be in cases presenting to hospital for example. Despite this, immune perturbation observed at diagnosis is still significant and sufficient to build an effective classifier on disease samples. Whether additional responses develop as symptomatic disease progresses, which are obscured by early antibiotic treatment in this model (and may have significance in the development of more severe clinical complications) are unclear.

Treatment of participants rapidly on development of bacteraemia and/or fever is necessary for safety reasons. However, the introduction of antibiotic usage is likely to have a confounding effect on associations between immunological responses observed at diagnosis and variables such as bacterial and fever clearance time. Therefore, associations between acute responses and disease resolution should be viewed with some caution and further investigation would be required to confirm major roles in disease clearance.

7.2.4 Contributions of tissue immunity

This examination of peripheral blood responses gives valuable insights into host immunity against typhoid fever. The contribution of tissue immunity and the mucosal barrier have not been evaluated here, however these aspects form a critical aspect of host defence.

Mucus, antimicrobial peptides and secretory IgA (sIgA) are essential components of barrier immunity in the intestinal tract that preclude pathogen adhesion to the epithelial

surface[308]. In addition, our understanding of the role of the microbiome in immune responses has advanced at a rapid pace over the last decade. It is now clearly understood that the microbiome can significantly alter immune responses to infectious diseases[309]. Evaluation of these mechanisms in human hosts and their association with protection against *S.* Typhi has not been comprehensively investigated although efforts to understand associations between diversity in the microbiota and outcome of infection are ongoing.

Cellular immunity in tissues and secondary lymphoid organs are a critical aspect of early control following bacterial invasion which have not been evaluated here. The lymphatic system is exploited by invading bacteria to initiate a systemic infection. The number of CFU identifiable within the cecal lymph nodes in orally challenged mice doubles every 6 hours[310]. indicating rapid dissemination via lymphatics. Therefore, the role of the mesenteric lymph nodes (MLNs) as a bottleneck during disease is likely to be vital in limiting systemic dissemination. Surgical removal of MLNs in mice prior to challenge leads to poorly controlled bacteraemia and increased immune-mediated tissue injury in the liver in comparison to unoperated animals[53]. Evidence from this study also supports a central role for lymph node in limiting bacterial burden in cases of human infection. Activated cellular subsets that predominate the early stages of infection against *S.* Typhi are frequently enriched for the lymph node homing marker, CD62L suggesting infection drives an upregulation in circulation through lymph nodes. Therefore, better understanding of this compartment occurring in future work is critical for better understanding of host responses correlating with bacterial containment and those correlating with dissemination. In non-lymphoid compartments, tissue-resident $CD4^+$ T-cell memory responses have been shown to be a vital aspect of protection against *Salmonella* in murine models[258].

7.3 Future directions

The purpose of this study was to identify both correlates of vaccine efficacy as well as identify key immunological pathways involved in protection from disease. A number of observations made here have implications for increasing our understanding of typhoid fever as well as our understanding of desirable responses to immunisation that support long-term protective efficacy.

7.3.1 Investigation of the mechanistic role of NK cells in memory B-cell formation after glycoconjugate vaccination

Undetectable memory B-cell responses were seen in a minority of Vi-TT vaccinees however the proportion (22%) was significant enough to warrant further investigation of mechanisms inhibiting memory B-cell formation. This line of enquiry may have relevance to other immunisations beyond glycoconjugate vaccines, especially since immunisations with alternative modes of action have been noted to activate NK cells[201]. The mechanisms driving NK activation after vaccination are unclear although cytokines are a likely mediator. In addition, the kinetics of NK responses following Vi-TT immunisation are not well-elucidated. Therefore, detailed phenotyping of NK and ILC responses after glycoconjugate vaccination as well as investigation of cytokine production would be of interest. TNFα, IL-2, IL-12, IL-15 and IL-18 are all known to drive NK proliferation and activation; profiling these responses within 24 hours of vaccination would be of interest. Several previous reports have shown that NK cells can suppress Tfh frequency and induce expression of apoptotic markers such as Annexin[199] therefore performing a similar series of experiments would have value here, both evaluating responses to glycoconjugates as well as other immunisations.

7.3.2 Mechanistic role for identified subsets in protection from acute typhoid fever

Phenotype of PBMCs has been comprehensively evaluated in this study. Whilst functional evaluations of prominent changes in peripheral blood had been planned, COVID restrictions in the laboratory CL3 suite has precluded their inclusion in this thesis. Therefore, the importance of functional differences in protection from disease has not been established. As

has been shown in a previous evaluation of humoral immunity against Vi, functional measures frequently associate better with protective status. Therefore, this line of enquiry should be continued at a later date to better understand early mechanistic correlates of protection against disease.

Given the association between monocytes and protective immunological profile, host factors that drive $CD16^{+}$ monocyte expansion are of clear interest. Single cell RNA-sequencing (scRNA-Seq) experiments conducted in collaboration with the Weissman Institute have shown a strong type I IFN gene signature in the monocyte compartment at 12 hours after infection (unpublished data), suggesting this signalling pathway may play a role in early monocyte activation. Whilst numbers were small and the specific monocyte subset was not elucidated, protected individuals tended to have higher upregulation of interferon-regulated genes (ISGs) further supporting a role for this pathway in driving protective responses.

7.3.3 Contribution of mucosal immunity to protection

This analysis reveals heterogeneity of early host responses to *S.* Typhi infection that are detectable in peripheral blood. Improving our understanding of the intermediate profile is of interest. Approximately 50% of participants in this group develop acute typhoid fever yet they have a similar systemic cellular and antibody profiles to other individuals in this group that remain well. This may indicate that immune mechanisms at non-systemic sites are critical for effective protection from disease.

Access to the mucosal surface in humans is often difficult and a relatively invasive procedure. Therefore, evaluation of antibodies, antimicrobial peptides and cytokines in stool is often used as a proxy in studies of human mucosal immunity. Evaluation of secretory antibodies via this approach is particularly common given the astonishingly high rate of sIgA release into the intestinal lumen (several grams per day). The effectiveness of immune exclusion (i.e. agglutination of invading bacterial species within the intestinal lumen) in protection against *S.* Typhi is likely to be shaped by an individual's infection history and the cross-reactivity of luminal IgA. Therefore, evaluation of sIgA responses in challenge participants at baseline may

confer an understanding of how baseline immune status at the mucosa may differentiate participants that develop acute disease and remain well in otherwise indistinguishable groups.

7.3.4 Evaluation of baseline PBMC differences

Due to the striking differences in B-cell composition prior to challenge with accumulation of antigen-experienced subsets correlating poorly with outcome, it is hypothesised that lower BCR diversity is a risk factor in typhoid fever infection. Increasing clonality is typically studied as a feature of advancing age and is one of the major factors contributing to poorer responses to infection and immunisation in the elderly[311]. In this analysis, a lower frequency of naïve B-cells was independent of participant age suggesting that this phenomenon remains relevant to responses to infection even in younger people without comorbidities. Given a strong association with early response profile to infection with *S.* Typhi and risk of acute disease, further investigation of the baseline BCR repertoire is warranted. Clonal bottlenecks could be evaluated by BCR sequencing. Comparison of B-cell clonotypes between susceptibility profiles would assist with understanding whether specific B-cell clones are conserved between individuals and associated with greater likelihood of protection. Identified BCR signatures would require validation in an independent cohort. This work would assist with furthering our understanding of B-cell characteristics that may influence early responses to infection which may differ from those that predominate during acute disease. A similar approach could also be taken for CD4 T-cells which had a similar albeit less strong relationship with early responses to infection. Bulk TCR sequencing of participant baseline samples has already been performed with clonal analysis being completed at present.

7.3.5 Comparison of blood signatures with other diseases

In this analysis, a signature of *S.* Typhi infection was identified that strongly delineated samples taken at disease presentation from those from individuals that remained well. A disease signature based entirely on T-cell responses was found to be most discriminatory with

frequency of γδ T-cells consistently being identified as the strongest predictive feature. A translational application of this work would be to evaluate its discriminatory power against other febrile illnesses. A comparison with the primary cause of paratyphoid fever, *S.* Paratyphi A, may be especially useful to increase our understanding of differences in clinical presentation between *Salmonella* serovars. As a human restricted pathogen with no widely accepted animal model, immunity against *S.* Paratyphi A is less well-explored in comparison to *S.* Typhi therefore this type of study would be extremely welcome.

A secondary comparison with viral causes of febrile illness that co-circulate in the region would also be of interest. In enteric fever research, a multitude of studies using single cell technologies have performed similar comparisons to describe blood signatures that may have utility as diagnostics. These have predominantly focused on serum-derived parameters (antibodies, metabolites) or RNA rather than cellular signatures, presumably due to significantly higher costs of cellular evaluation[312]. Previous studies have tended to focus on single datasets (i.e. transcriptomics, metabolomics, serology); whilst distinctive features were identified in all datasets, each standalone study did not have the sufficient power to act as a suitable diagnostic. Mass cytometry is poorly suited to use in diagnostics; the cost, machinery and technical expertise required are all prohibitive obstacles. Whilst costs of running mass cytometry are likely to fall over time as has been the case with other single cell technologies, other factors will continue to preclude its implementation in settings beyond research. However, identification of unique features of host responses to *S.* Typhi infection may inform future efforts in diagnostics therefore comparative studies remain of interest.

Another follow up objective for this work would be integration of mass cytometry data with other parameters measured in the same participants. The challenge model offers a unique opportunity in enteric fever research to integrate multiple "omic" datasets. Integration efforts have a number of objectives: identification of clinical disease subtypes, biomarker prediction and conferring biological insight. No strong associations between clinical phenotype and acute disease response were noted in analysis of PBMCs therefore scope for disease subtyping may be limited. However, there is strong rationale for conducting dataset integration to further

biological insight and develop a holistic understanding of host responses to S. Typhi infection. Given the wealth of data that has been generated in the challenge model, dataset integration is an attractive future endeavour although challenges regarding overlap of sufficient numbers of participants and timepoints between datasets exist. Handling of the longitudinal nature of data also presents a significant challenge.

7.3.6 Development of a composite prognostic marker for typhoid fever management

NLR and ELR have potential as prognostic indicators in case management of typhoid fever, however their associations with severe clinical complications such as intestinal perforation and mortality have not been previously assessed. Complications of typhoid fever in hospitalised patients are relatively commonplace (over 26%), even in the context of treatment[280] therefore accurate assessment of patient condition is essential. The observation that NLR is lowered by Vi-TT vaccination is being verified in data from a phase III efficacy trial conducted in Nepal. Clarification if an association between NLR, vaccination and additional complications of typhoid fever will be a valuable addition to this work.

Furthermore, the importance of severity biomarkers in young children and teenagers is of interest as these populations suffer the greatest burden of disease. Data taken from field trials will include younger age groups allowing for evaluation of biomarkers in this cohort.

7.3.7 Role of granulocyte compartment in infection

Whilst antibody-mediated functions of neutrophils have been evaluated and found to contribute significantly to protective outcome[136], the effect of infection on neutrophil phenotype and composition has not been evaluated in previous challenge studies. In addition, changes in frequencies of other granulocytes such as basophils and eosinophils during early disease have been poorly characterised despite upregulation of chemokines at the 12-hour response that would be expected to initiate chemotaxis.

Logistical issues have impeded previous efforts to examine granulocyte responses in human challenge models. Granulocytes are highly sensitive to cryopreservation meaning long-term storage of these cells is not possible. A range of cryopreserving agents, including dimethyl sulfoxide and glycerol, have been evaluated for this purpose with highly inconsistent results achieved. The lack of success in this area has significantly limited capacity of researchers to further investigate the effect of infection on granulocyte composition and its association with outcome.

A possible solution to these restrictions would be collection and fixation of whole blood samples. Although functional evaluations are precluded by this approach, this offers an opportunity to assess phenotypic changes in the granulocyte compartment, as has been done in this thesis for PBMCs, over the course of infection. More recent challenge studies have collected whole blood samples for this purpose and will seek to perform an evaluation of this nature in future work.

7.4 Contribution to the field and final conclusions

The goal of this thesis was to further knowledge of host responses during infection and vaccination that associate with protection against typhoid fever. A particularly important aspect of this analysis is the immunological insight into the early stages of infection that are often missed in endemic settings. This analysis also seeks to clarify how immunity develops in the context of interventions such as vaccination. It is hoped that these observations provide a foundation for hypothesis generation which can be investigated in subsequent research.

Findings from this thesis contribute directly to the field of enteric fever research and support wider efforts in understanding of disease. Current international priorities include the development of effective diagnostics, combatting antimicrobial resistance, generating evidence of Vi-TT effectiveness and development of interventions and vaccines against paratyphoid fever. This work aligns with several of these goals by providing insight into the development of immunological memory against Vi-TT, as well as defining a PBMC signature of infection which may have some utility in diagnostics. In addition, the work provides an excellent comparator for future investigations of immunity against serovars causing paratyphoid fever. These comparisons may assist with development of more universal interventions against typhoidal *Salmonella*.

Although this study offers some interesting contributions to the field, much of the immune response to *S.* Typhi infection remains to be clarified. As highlighted above, a number of avenues of exploration – granulocytic responses, sIgA and other baseline factors – remain to be examined. These highlighted examples represent the "low hanging fruit" for which samples have already been collected and techniques for evaluation are already available within the University of Oxford.

This dataset and others like it may also be of interest to the wider scientific community particularly to the field of computational immunology and bioinformatics. As high-dimensional data become increasingly commonplace and a holistic approach to immunology pervades, the demand for dataset integration tools is likely to increase. Model systems such as the challenge

model, with a multitude of datasets available, provide an excellent platform for the development of such tools. Additionally, as application of machine learning techniques becomes more prevalent in immunology publications, better strategies will be required to contend with issues concerning overfitting and reproducibility, an especially frequent problem in immunology where datasets are typically small. Whilst use of simpler models and mindfulness of outliers, as has been done here, assist with reducing these issues, progress in this area is needed to gain maximal insights from immunological data.

In conclusion, challenge models and the data they generate serve to accelerate our understanding of typhoidal *Salmonella* infections. Almost all research in the field of infectious disease seeks to understand the following three questions: how does the immune system function during disease, how do these responses differ between protected and diagnosed individuals and how are these responses modulated in the context of clinical interventions such as vaccination. This work takes several steps to improving our understanding of these three objectives in the context of typhoid fever.

8 Bibliography

1. Marchello, C. S., Hong, C. Y. & Crump, J. A. Global typhoid fever incidence: A systematic review and meta-analysis. *Clin. Infect. Dis.* **68**, S105–S116 (2019).
2. Stanaway, J. D. *et al.* The global burden of typhoid and paratyphoid fevers: a systematic analysis for the Global Burden of Disease Study 2017. *Lancet Infect. Dis.* **19**, 369–381 (2019).
3. Kaljee, L. M. *et al.* Social and Economic Burden Associated with Typhoid Fever in Kathmandu and Surrounding Areas: A Qualitative Study. *J. Infect. Dis.* **218**, S243–S249 (2018).
4. John A. Crump & Stephen P. Luby, and E. D. M. The global burden of typhoid fever. Bull World Health Organ. *Bull. World Health Organ.* **82**, 346–353 (2004).
5. Buckle, G. C., Walker, C. L. F. & Black, R. E. Typhoid fever and paratyphoid fever: Systematic review to estimate global morbidity and mortality for 2010. *J. Glob. Health* **2**, 1–9 (2012).
6. Mogasale, V. *et al.* Burden of typhoid fever in low-income and middle-income countries: A systematic, literature-based update with risk-factor adjustment. *Lancet Glob. Heal.* **2**, e570–e580 (2014).
7. Kim, J. H., Mogasale, V., Im, J., Ramani, E. & Marks, F. Updated estimates of typhoid fever burden in sub-Saharan Africa. *Lancet Glob. Heal.* **5**, e969 (2017).
8. Warren, J. L., Crawford, F. W. & Weinberger, D. M. The burden of typhoid fever in low- and middle-income countries : A meta-regression approach. 1–21 (2017) doi:10.1371/journal.pntd.0005376.
9. Holloway, K. A., Kotwani, A., Batmanabane, G., Puri, M. & Tisocki, K. Antibiotic use in South East Asia and policies to promote appropriate use: reports from country situational analyses. *BMJ* **358**, j2291 (2017).
10. Mogasale, V., Ramani, E., Mogasale, V. V. & Park, J. Y. What proportion of Salmonella

Typhi cases are detected by blood culture? A systematic literature review. *Ann. Clin. Microbiol. Antimicrob.* **15**, 1–8 (2016).

11. Thakur, K. T. *et al.* Lumbar puncture refusal in Sub-Saharan Africa: A call for further understanding and intervention. *Neurol. Glob. Perspect.* **84**, 47–61 (2015).
12. Crump, J. A. Progress in Typhoid Fever Epidemiology. *Clin. Infect. Dis.* **68**, S4–S9 (2019).
13. EDSALL, G. *et al.* Studies on infection and immunity in experimental typhoid fever. I. Typhoid fever in chimpanzees orally infected with Salmonella typhosa. *J. Exp. Med.* **112**, 143–166 (1960).
14. Blackwell, J. M. *et al.* SLC11A1 (formerly NRAMP1) and disease resistance. *Cell. Microbiol.* **3**, 773–784 (2001).
15. Canonne-Hergaux, F., Gruenheid, S., Govoni, G. & Gros, P. The Nramp1 protein and its role in resistance to infection and macrophage function. *Proc. Assoc. Am. Physicians* **111**, 283–289 (1999).
16. Tsolis, R. M., Xavier, M. N., Santos, R. L. & Bäumler, A. J. How to become a top model: Impact of animal experimentation on human Salmonella disease research. *Infect. Immun.* **79**, 1806–1814 (2011).
17. Mathur, R. *et al.* A mouse model of salmonella typhi infection. *Cell* **151**, 590–602 (2012).
18. Song, J. *et al.* Absence of TLR11 in Mice Does Not Confer Susceptibility to Salmonella Typhi. *Cell* **164**, 827–828 (2016).
19. Karlinsey, J. E. *et al.* Genome-wide Analysis of Salmonella enterica serovar Typhi in Humanized Mice Reveals Key Virulence Features. *Cell Host Microbe* **26**, 426-434.e6 (2019).
20. Proetzel, G., Editors, M. V. W. & Walker, J. M. *Mouse Models for Drug Discovery. Methods and Protocols. Second Edition*. *Anticancer research* vol. 36 (2016).
21. Libby, S. J. *et al.* Humanized nonobese diabetic-scid IL2rγnull mice are susceptible to lethal Salmonella Typhi infection. *Proc. Natl. Acad. Sci. U. S. A.* **107**, 15589–15594

(2010).

22. Cuturi, M. C. & Walker, J. M. *Suppression and Regulation of Immune Responses IN Series Editor*. vol. II.

23. Wahl, A. & Victor Garcia, J. The use of BLT humanized mice to investigate the immune reconstitution of the gastrointestinal tract. *J. Immunol. Methods* **410**, 28–33 (2014).

24. Sato, T. *et al.* Single Lgr5 stem cells build crypt-villus structures in vitro without a mesenchymal niche. *Nature* **459**, 262–265 (2009).

25. Yin, Y. & Zhou, D. Organoid and enteroid modeling of Salmonella Infection. *Front. Cell. Infect. Microbiol.* **8**, (2018).

26. de Lau, W. *et al.* Peyer's Patch M Cells Derived from Lgr5+ Stem Cells Require SpiB and Are Induced by RankL in Cultured 'Miniguts'. *Mol. Cell. Biol.* **32**, 3639–3647 (2012).

27. Zhang, Y. G., Wu, S., Xia, Y. & Sun, J. Salmonella-infected crypt-derived intestinal organoid culture system for host–bacterial interactions. *Physiol. Rep.* **2**, 1–11 (2014).

28. Lock, J. Y., Carlson, T. L. & Carrier, R. L. Mucus models to evaluate the diffusion of drugs and particles. *Adv. Drug Deliv. Rev.* **124**, 34–49 (2018).

29. Waddington, C. S. *et al.* Advancing the management and control of typhoid fever: A review of the historical role of human challenge studies. *J. Infect.* **68**, 405–418 (2014).

30. Hornick, R. B. *et al.* Typhoid Fever: Pathogenesis and Immunologic Control. *N. Engl. J. Med.* **283**, 739–746 (1970).

31. Sprinz, H., Gangarosa, E. J., Williams, M., Hornick, R. B. & Woodward, T. E. Histopathology of the upper small intestines in typhoid fever. Biopsy study of experimental disease in man. *Am. J. Dig. Dis.* **11**, 615–624 (1966).

32. Glynn, J. R., Hornick, R. B., Levine, M. M. & Bradley, D. J. Infecting dose and severity of typhoid: Analysis of volunteer data and examination of the influence of the definition of illness used. *Epidemiol. Infect.* **115**, 23–30 (1995).

33. Salerno-Goncalves, R. *et al.* Challenge of humans with wild-type Salmonella enterica serovar typhi elicits changes in the activation and homing characteristics of mucosal-

associated invariant T cells. *Front. Immunol.* **8**, 1–13 (2017).

34. Fresnay, S. *et al.* Importance of Salmonella typhi-responsive CD8+ T cell immunity in a human typhoid fever challenge model. *Front. Immunol.* **8**, (2017).

35. Fresnay, S. *et al.* Salmonella Typhi-specific multifunctional CD8+ T cells play a dominant role in protection from typhoid fever in humans. *J. Transl. Med.* **14**, 1–14 (2016).

36. Toapanta, F. R. *et al.* Oral wild-type Salmonella Typhi challenge induces activation of circulating monocytes and dendritic cells in individuals who develop typhoid disease. *PLoS Negl. Trop. Dis.* **9**, 1–18 (2015).

37. McArthur, M. A. *et al.* Activation of Salmonella Typhi-Specific Regulatory T Cells in Typhoid Disease in a Wild-Type S. Typhi Challenge Model. *PLoS Pathog.* **11**, 1–18 (2015).

38. Rapaka, R. R. *et al.* Human Salmonella Typhi exposure generates differential multifunctional cross-reactive T-cell memory responses against Salmonella Paratyphi and invasive nontyphoidal Salmonella. *Clin. Transl. Immunol.* **9**, 1–19 (2020).

39. Napolitani, G. *et al.* Clonal analysis of Salmonella-specific effector T cells reveals serovar-specific and cross-reactive T cell responses. *Nat. Immunol.* **19**, 742–754 (2018).

40. Jin, C. *et al.* Efficacy and immunogenicity of a Vi-tetanus toxoid conjugate vaccine in the prevention of typhoid fever using a controlled human infection model of Salmonella Typhi: a randomised controlled, phase 2b trial. *Lancet* **390**, 2472–2480 (2017).

41. Darton, T. C. *et al.* Using a Human Challenge Model of Infection to Measure Vaccine Efficacy: A Randomised, Controlled Trial Comparing the Typhoid Vaccines M01ZH09 with Placebo and Ty21a. *PLoS Negl. Trop. Dis.* **10**, 1–27 (2016).

42. Coburn, B., Grassl, G. A. & Finlay, B. B. Salmonella, the host and disease: a brief review. *Immunol. Cell Biol.* **85**, 112–118 (2007).

43. Holt, K. E. *et al.* Pseudogene accumulation in the evolutionary histories of Salmonella enterica serovars Paratyphi A and Typhi. *BMC Genomics* **10**, 36 (2009).

44. McClelland, M. *et al.* Comparison of genome degradation in Paratyphi A and Typhi,

human-restricted serovars of Salmonella enterica that cause typhoid. *Nat. Genet.* **36**, 1268–1274 (2004).

45. Liu, S. L., Ezaki, T., Miura, H., Matsui, K. & Yabuuchi, E. Intact motility as a Salmonella typhi invasion-related factor. *Infect. Immun.* **56**, 1967–1973 (1988).

46. Dufresne, K., Saulnier-Bellemare, J. & Daigle, F. Functional Analysis of the Chaperone-Usher Fimbrial Gene Clusters of Salmonella enterica serovar Typhi. *Front. Cell. Infect. Microbiol.* **8**, 26 (2018).

47. Jones, B. D., Ghori, N. & Falkow, S. Salmonella typhimurium initiates murine infection by penetrating and destroying the specialized epithelial M cells of the Peyer's patches. *J. Exp. Med.* **180**, 15–23 (1994).

48. Nickerson, K. P. *et al.* Salmonella Typhi Colonization Provokes Extensive Transcriptional Changes Aimed at Evading Host Mucosal Immune Defense During Early Infection of Human Intestinal Tissue. *EBioMedicine* **31**, 92–109 (2018).

49. Zhou, D., Mooseker, M. S. & Galán, J. E. An invasion-associated Salmonella protein modulates the actin-bundling activity of plastin. *Proc. Natl. Acad. Sci. U. S. A.* **96**, 10176–10181 (1999).

50. Patel, J. C. & Galán, J. E. Manipulation of the host actin cytoskeleton by Salmonella--all in the name of entry. *Curr. Opin. Microbiol.* **8**, 10–15 (2005).

51. Schreiber, F. *et al.* The Hd, Hj, and Hz66 flagella variants of Salmonella enterica serovar Typhi modify host responses and cellular interactions. *Sci. Rep.* **5**, 7947 (2015).

52. Tartera, C. & Metcalf, E. S. Osmolarity and growth phase overlap in regulation of Salmonella typhi adherence to and invasion of human intestinal cells. *Infect. Immun.* **61**, 3084–3089 (1993).

53. Voedisch, S. *et al.* Mesenteric lymph nodes confine dendritic cell-mediated dissemination of Salmonella enterica serovar typhimurium and limit systemic disease in mice. *Infect. Immun.* **77**, 3170–3180 (2009).

54. Vazquez-Torres, A. *et al.* Extraintestinal dissemination CD18-expressing phagocytes. *Nature* **401**, 623–626 (1999).

55. Jack, R. S. *et al.* Lipopolysaccharide-binding protein is required to combat a murine gram-negative bacterial infection. *Nature* **389**, 742–745 (1997).

56. Keuter, M. *et al.* Patterns of proinflammatory cytokines and inhibitors during typhoid fever. *J. Infect. Dis.* **169**, 1306–1311 (1994).

57. Butler, T., Ho, M., Acharya, G., Tiwari, M. & Gallati, H. Interleukin-6, gamma interferon, and tumor necrosis factor receptors in typhoid fever related to outcome of antimicrobial therapy. *Antimicrob. Agents Chemother.* **37**, 2418–2421 (1993).

58. Takeuchi, A. Electron microscope studies of experimental Salmonella infection. I. Penetration into the intestinal epithelium by Salmonella typhimurium. *Am. J. Pathol.* **50**, 109–136 (1967).

59. Beuzón, C. R. *et al.* Salmonella maintains the integrity of its intracellular vacuole through the action of SifA. *EMBO J.* **19**, 3235–3249 (2000).

60. McGourty, K. *et al.* Salmonella inhibits retrograde trafficking of mannose-6-phosphate receptors and lysosome function. *Science* **338**, 963–967 (2012).

61. Crawford, R. W. *et al.* Gallstones play a significant role in Salmonella spp. gallbladder colonization and carriage. *Proc. Natl. Acad. Sci. U. S. A.* **107**, 4353–4358 (2010).

62. González, J. F., Alberts, H., Lee, J., Doolittle, L. & Gunn, J. S. Biofilm Formation Protects Salmonella from the Antibiotic Ciprofloxacin In Vitro and In Vivo in the Mouse Model of chronic Carriage. *Sci. Rep.* **8**, 222 (2018).

63. Song, J. *et al.* A mouse model for the human pathogen Salmonella typhi. *Cell Host Microbe* **8**, 369–376 (2010).

64. Gibani, M. M. *et al.* Investigation of the role of typhoid toxin in acute typhoid fever in a human challenge model. *Nat. Med.* **25**, 1082–1088 (2019).

65. Leclerc, J.-M., Dozois, C. M. & Daigle, F. Salmonella enterica serovar Typhi siderophore production is elevated and Fur inactivation causes cell filamentation and attenuation in macrophages. *FEMS Microbiol. Lett.* **364**, (2017).

66. Sousa Gerós, A., Simmons, A., Drakesmith, H., Aulicino, A. & Frost, J. N. The battle for iron in enteric infections. *Immunology* **161**, 186–199 (2020).

67. Zhao, L. *et al.* Vi-Suppressed wild strain Salmonella typhi cultured in high osmolarity is hyperinvasive toward epithelial cells and destructive of Peyer's patches. *Microbiol. Immunol.* **45**, 149–158 (2001).

68. Winter, S. E. *et al.* A rapid change in virulence gene expression during the transition from the intestinal lumen into tissue promotes systemic dissemination of Salmonella. *PLoS Pathog.* **6**, e1001060 (2010).

69. Keestra-Gounder, A. M., Tsolis, R. M. & Bäumler, A. J. Now you see me, now you don't: the interaction of Salmonella with innate immune receptors. *Nat. Rev. Microbiol.* **13**, 206–216 (2015).

70. Wangdi, T. *et al.* The Vi capsular polysaccharide enables Salmonella enterica serovar typhi to evade microbe-guided neutrophil chemotaxis. *PLoS Pathog.* **10**, e1004306 (2014).

71. Hirose, K. *et al.* Survival of Vi-capsulated and Vi-deleted Salmonella typhi strains in cultured macrophage expressing different levels of CD14 antigen. *FEMS Microbiol. Lett.* **147**, 259–265 (1997).

72. Looney, R. J. & Steigbigel, R. T. Role of the Vi antigen of Salmonella typhi in resistance to host defense in vitro. *J. Lab. Clin. Med.* **108**, 506–516 (1986).

73. Wilson, R. P. *et al.* The Vi capsular polysaccharide prevents complement receptor 3-mediated clearance of Salmonella enterica serotype Typhi. *Infect. Immun.* **79**, 830–837 (2011).

74. Baker, S. *et al.* Detection of Vi-negative Salmonella enterica serovar typhi in the peripheral blood of patients with typhoid fever in the Faisalabad region of Pakistan. *J. Clin. Microbiol.* **43**, 4418–4425 (2005).

75. Liaquat, S. *et al.* Virulotyping of Salmonella enterica serovar Typhi isolates from Pakistan: Absence of complete SPI-10 in Vi negative isolates. *PLoS Negl. Trop. Dis.* **12**, e0006839 (2018).

76. Wain, J. *et al.* Vi antigen expression in Salmonella enterica serovar Typhi clinical isolates from Pakistan. *J. Clin. Microbiol.* **43**, 1158–1165 (2005).

77. Saha, M. R., Ramamurthy, T., Dutta, P. & Mitra, U. Emergence of Salmonella typhi Vi antigen-negative strains in an epidemic of multidrug-resistant typhoid fever cases in Calcutta, India. *The National medical journal of India* vol. 13 164 (2000).

78. Hone, D. M. *et al.* A galE via (Vi antigen-negative) mutant of Salmonella typhi Ty2 retains virulence in humans. *Infect. Immun.* **56**, 1326–1333 (1988).

79. Hiyoshi, H. *et al.* Mechanisms to Evade the Phagocyte Respiratory Burst Arose by Convergent Evolution in Typhoidal Salmonella Serovars. *Cell Rep.* **22**, 1787–1797 (2018).

80. Nauciel, C. & Espinasse-Maes, F. Role of gamma interferon and tumor necrosis factor alpha in resistance to Salmonella typhimurium infection. *Infect. Immun.* **60**, 450–454 (1991).

81. Nauciel, C. Role of CD4+ T cells and T-independent mechanisms in acquired resistance to Salmonella typhimurium infection. *J. Immunol.* **145**, 1265–1269 (1990).

82. Caligiuri, M. A. Human natural killer cells. *Blood* **112**, 461–469 (2008).

83. Garcia-Peñarrubia, P., Koster, F. T., Kelley, R. O., McDowell, T. D. & Bankhurst, A. D. Antibacterial activity of human natural killer cells. *J. Exp. Med.* **169**, 99–113 (1989).

84. Puente, J. *et al.* Effect of Salmonella typhi wild type and O-antigen mutants on human natural killer cell activity. *Int. J. Immunopharmacol.* **22**, 355–364 (2000).

85. Lindemann, R. A. Bacterial activation of human natural killer cells: role of cell surface lipopolysaccharide. *Infect. Immun.* **56**, 1301–1308 (1988).

86. Miranda, D. *et al.* Lysis of salmonella typhi intracellularly infected U937 cells by human natural killer cells: effect of protein kinase inhibitors. *Am. J. Ther.* **10**, 32–39 (2003).

87. Blanco, L. *et al.* Effect of Salmonella-infected human monocytes on natural killer cell cytotoxicity. In vitro studies. *Int. Immunopharmacol.* **1**, 1285–1293 (2001).

88. Kupz, A. *et al.* Contribution of Thy1+ NK cells to protective IFN-γ production during Salmonella typhimurium infections. *Proc. Natl. Acad. Sci. U. S. A.* **110**, 2252–2257 (2013).

89. Lapaque, N., Walzer, T., Méresse, S., Vivier, E. & Trowsdale, J. Interactions between

Human NK Cells and Macrophages in Response to Salmonella Infection . *J. Immunol.* **182**, 4339–4348 (2009).

90. Müller, A. A. *et al.* An NK Cell Perforin Response Elicited via IL-18 Controls Mucosal Inflammation Kinetics during Salmonella Gut Infection. *PLoS Pathog.* **12**, e1005723 (2016).

91. Rydström, A. & Wick, M. J. Monocyte Recruitment, Activation, and Function in the Gut-Associated Lymphoid Tissue during Oral Salmonella Infection . *J. Immunol.* **178**, 5789–5801 (2007).

92. Wong, K. L. *et al.* The three human monocyte subsets: implications for health and disease. *Immunol. Res.* **53**, 41–57 (2012).

93. Lund, H., Boysen, P., Åkesson, C. P., Lewandowska-Sabat, A. M. & Storset, A. K. Transient Migration of Large Numbers of CD14(++) CD16(+) Monocytes to the Draining Lymph Node after Onset of Inflammation. *Front. Immunol.* **7**, 322 (2016).

94. Watson, K. G. & Holden, D. W. Dynamics of growth and dissemination of Salmonella in vivo. *Cell. Microbiol.* **12**, 1389–1397 (2010).

95. Worley, M. J., Nieman, G. S., Geddes, K. & Heffron, F. Salmonella typhimurium disseminates within its host by manipulating the motility of infected cells. *Proc. Natl. Acad. Sci. U. S. A.* **103**, 17915–17920 (2006).

96. Vazquez-Torres, A. & Fang, F. C. Cellular routes of invasion by enteropathogens. *Curr. Opin. Microbiol.* **3**, 54–59 (2000).

97. Jakubzick, C. *et al.* Minimal differentiation of classical monocytes as they survey steady-state tissues and transport antigen to lymph nodes. *Immunity* **39**, 599–610 (2013).

98. Darton, T. C. *et al.* Blood culture-PCR to optimise typhoid fever diagnosis after controlled human infection identifies frequent asymptomatic cases and evidence of primary bacteraemia. *J. Infect.* **74**, 358–366 (2017).

99. De Jong, H. K. *et al.* Expression and function of S100A8/A9 (calprotectin) in human typhoid fever and the murine Salmonella model. *PLoS Negl. Trop. Dis.* **9**, e0003663

(2015).

100. Kankwatira, A. M., Mwafulirwa, G. A. K. & Gordon, M. A. Non-typhoidal salmonella bacteraemia--an under-recognized feature of AIDS in African adults. *Trop. Doct.* **34**, 198–200 (2004).

101. Abuaita, B. H. *et al.* Comparative transcriptional profiling of the early host response to infection by typhoidal and non-typhoidal Salmonella serovars in human intestinal organoids. *bioRxiv* (2020).

102. Blohmke, C. J. *et al.* Interferon-driven alterations of the host's amino acid metabolism in the pathogenesis of typhoid fever. *J. Exp. Med.* **213**, 1061–1077 (2016).

103. Raffatellu, M. *et al.* The Vi capsular antigen of Salmonella enterica serotype Typhi reduces Toll-like receptor-dependent interleukin-8 expression in the intestinal mucosa. *Infect. Immun.* **73**, 3367–3374 (2005).

104. Ravindran, R., Foley, J., Stoklasek, T., Glimcher, L. H. & McSorley, S. J. Expression of T-bet by CD4 T cells is essential for resistance to Salmonella infection. *J. Immunol.* **175**, 4603–4610 (2005).

105. Mittrücker, H.-W., Köhler, A. & Kaufmann, S. H. E. Characterization of the murine T-lymphocyte response to Salmonella enterica serovar Typhimurium infection. *Infect. Immun.* **70**, 199–203 (2002).

106. Hess, J., Ladel, C., Miko, D. & Kaufmann, S. H. Salmonella typhimurium aroA- infection in gene-targeted immunodeficient mice: major role of CD4+ TCR-alpha beta cells and IFN-gamma in bacterial clearance independent of intracellular location. *J. Immunol.* **156**, 3321–3326 (1996).

107. Dunstan, S. J. *et al.* Variation at HLA-DRB1 is associated with resistance to enteric fever. *Nature genetics* vol. 46 1333–1336 (2014).

108. Salazar-Gonzalez, R. M. *et al.* CCR6-mediated dendritic cell activation of pathogen-specific T cells in Peyer's patches. *Immunity* **24**, 623–632 (2006).

109. de Jong, R. *et al.* Severe mycobacterial and Salmonella infections in interleukin-12 receptor-deficient patients. *Science* **280**, 1435–1438 (1998).

110. Mizuno, Y. *et al.* Th1 and Th1-inducing cytokines in Salmonella infection. *Clin. Exp. Immunol.* **131**, 111–117 (2003).

111. Tobar, J. A. *et al.* Virulent Salmonella enterica serovar typhimurium evades adaptive immunity by preventing dendritic cells from activating T cells. *Infect. Immun.* **74**, 6438–6448 (2006).

112. Alaniz, R. C., Cummings, L. A., Bergman, M. A., Rassoulian-Barrett, S. L. & Cookson, B. T. Salmonella typhimurium coordinately regulates FliC location and reduces dendritic cell activation and antigen presentation to CD4+ T cells. *J. Immunol.* **177**, 3983–3993 (2006).

113. Tobar, J. A., González, P. A. & Kalergis, A. M. Salmonella Escape from Antigen Presentation Can Be Overcome by Targeting Bacteria to Fcγ Receptors on Dendritic Cells . *J. Immunol.* **173**, 4058–4065 (2004).

114. Srinivasan, A., Foley, J., Ravindran, R. & McSorley, S. J. Low-dose Salmonella infection evades activation of flagellin-specific CD4 T cells. *J. Immunol.* **173**, 4091–4099 (2004).

115. Labuda, J. C. *et al.* Unexpected Role of CD8 T Cells in Accelerated Clearance of Salmonella enterica Serovar Typhimurium from H-2 Congenic mice. *Infect. Immun.* **87**, (2019).

116. van der Velden, A. W. M., Copass, M. K. & Starnbach, M. N. Salmonella inhibit T cell proliferation by a direct, contact-dependent immunosuppressive effect. *Proc. Natl. Acad. Sci. U. S. A.* **102**, 17769–17774 (2005).

117. Luu, R. A. *et al.* Delayed expansion and contraction of CD8+ T cell response during infection with virulent Salmonella typhimurium. *J. Immunol.* **177**, 1516–1525 (2006).

118. Albaghdadi, H., Robinson, N., Finlay, B., Krishnan, L. & Sad, S. Selectively reduced intracellular proliferation of Salmonella enterica serovar typhimurium within APCs limits antigen presentation and development of a rapid CD8 T cell response. *J. Immunol.* **183**, 3778–3787 (2009).

119. López-Medina, M., Carrillo-Martín, I., Leyva-Rangel, J., Alpuche-Aranda, C. & Ortiz-

Navarrete, V. Salmonella impairs CD8 T cell response through PD-1: PD-L axis. *Immunobiology* **220**, 1369–1380 (2015).

120. McArthur, M. A. & Sztein, M. B. Heterogeneity of multifunctional IL-17A producing S. Typhi-specific CD8+ T cells in volunteers following Ty21a typhoid immunization. *PLoS One* **7**, e38408 (2012).

121. Fresnay, S. *et al.* Importance of Salmonella Typhi-Responsive CD8+ T Cell Immunity in a Human Typhoid Fever Challenge Model. *Front. Immunol.* **8**, 208 (2017).

122. Mastroeni, P., Villarreal-Ramos, B. & Hormaeche, C. E. Adoptive transfer of immunity to oral challenge with virulent salmonellae in innately susceptible BALB/c mice requires both immune serum and T cells. *Infect. Immun.* **61**, 3981–3984 (1993).

123. Mittrücker, H. W., Raupach, B., Köhler, A. & Kaufmann, S. H. Cutting edge: role of B lymphocytes in protective immunity against Salmonella typhimurium infection. *J. Immunol.* **164**, 1648–1652 (2000).

124. Cunningham, A. F. *et al.* Salmonella induces a switched antibody response without germinal centers that impedes the extracellular spread of infection. *J. Immunol.* **178**, 6200–6207 (2007).

125. Mastroeni, P., Simmons, C., Fowler, R., Hormaeche, C. E. & Dougan, G. Igh-6(-/-) (B-cell-deficient) mice fail to mount solid acquired resistance to oral challenge with virulent Salmonella enterica serovar typhimurium and show impaired Th1 T-cell responses to Salmonella antigens. *Infect. Immun.* **68**, 46–53 (2000).

126. Ugrinovic, S., Ménager, N., Goh, N. & Mastroeni, P. Characterization and development of T-Cell immune responses in B-cell-deficient (Igh-6(-/-)) mice with Salmonella enterica serovar Typhimurium infection. *Infect. Immun.* **71**, 6808–6819 (2003).

127. Nanton, M. R., Way, S. S., Shlomchik, M. J. & McSorley, S. J. Cutting Edge: B Cells Are Essential for Protective Immunity against Salmonella Independent of Antibody Secretion . *J. Immunol.* **189**, 5503–5507 (2012).

128. Darton, T. C. *et al.* Identification of Novel Serodiagnostic Signatures of Typhoid Fever Using a Salmonella Proteome Array. *Front. Microbiol.* **8**, 1794 (2017).

129. Liang, L. *et al.* Immune profiling with a Salmonella Typhi antigen microarray identifies new diagnostic biomarkers of human typhoid. *Sci. Rep.* **3**, 1043 (2013).

130. Gilman, R. H. *et al.* Evaluation of a UDP-glucose-4-epimeraseless mutant of Salmonella typhi as a liver oral vaccine. *J. Infect. Dis.* **136**, 717–723 (1977).

131. Gibani, M. M. *et al.* Homologous and heterologous re-challenge with salmonella typhi and salmonella paratyphi a in a randomised controlled human infection model. *PLoS Negl. Trop. Dis.* **14**, 1–25 (2020).

132. Watson, C. H. *et al.* A cross-sectional seroepidemiological survey of typhoid fever in Fiji. *PLoS Negl. Trop. Dis.* **11**, e0005786 (2017).

133. House, D. *et al.* Antibodies to the Vi capsule of Salmonella Typhi in the serum of typhoid patients and healthy control subjects from a typhoid endemic region. *J. Infect. Dev. Ctries.* **2**, 308–312 (2008).

134. Nolan, C. M. *et al.* Vi serology in the detection of typhoid carriers. *Lancet (London, England)* **1**, 583–585 (1981).

135. Charles, R. C. *et al.* Identification of immunogenic Salmonella enterica serotype Typhi antigens expressed in chronic biliary carriers of S. Typhi in Kathmandu, Nepal. *PLoS Negl. Trop. Dis.* **7**, e2335 (2013).

136. Jin, C. *et al.* Vi-specific serological correlates of protection for typhoid fever. *J. Exp. Med.* **218**, (2020).

137. Pabst, O. & Slack, E. IgA and the intestinal microbiota: the importance of being specific. *Mucosal Immunol.* 1–10 (2019) doi:10.1038/s41385-019-0227-4.

138. Kirchhelle, C., Pollard, A. J. & Vanderslott, S. Typhoid-From Past to Future. *Clin. Infect. Dis.* **69**, S375–S376 (2019).

139. Vanderslott, S., Phillips, M. T., Pitzer, V. E. & Kirchhelle, C. Water and Filth: Reevaluating the First Era of Sanitary Typhoid Intervention (1840-1940). *Clin. Infect. Dis.* **69**, S377–S384 (2019).

140. Chapman, J. The contribution of infrastructure investment to Britain's urban mortality decline, 1861–1900. *Econ. Hist. Rev.* **72**, 233–259 (2019).

141. Ravenel, M. P. THE CROYDON EPIDEMIC OF TYPHOID FEVER. *Am. J. Public Health* **28**, 644–646 (1938).

142. Berendes, D. *et al.* The influence of household- and community-level sanitation and fecal sludge management on urban fecal contamination in households and drains and enteric infection in children. *Am. J. Trop. Med. Hyg.* **96**, 1404–1414 (2017).

143. Berendes, D. M. *et al.* Associations between open drain flooding and pediatric enteric infections in the MAL-ED cohort in a low-income, urban neighborhood in Vellore, India. *BMC Public Health* **19**, 1–11 (2019).

144. National Institute of Population Research and Training (NIPORT). Bangladesh demographic and health survey 2017-18. *USAID* 1–511 (2020).

145. International Institute for Population Sciences (IIPS) and ICF. National Family Health Survey (Nfhs-4) 2015-16. 1–671 (2015).

146. National Institute of Population Studies (NIPS) & ICF. *Pakistan Demographic and Health Survey Demographic and Health Survey*. (2019).

147. Levine, M. M., Ferreccio, C., Black, R. E. & Germanier, R. Large-scale field trial of Ty21a live oral typhoid vaccine in enteric-coated capsule formulation. *Lancet (London, England)* **1**, 1049–1052 (1987).

148. Levine, M. M. *et al.* Duration of efficacy of Ty21a, attenuated Salmonella typhi live oral vaccine. *Vaccine* **17 Suppl 2**, S22-7 (1999).

149. Simanjuntak, C. H. *et al.* Oral immunisation against typhoid fever in Indonesia with Ty21a vaccine. *Lancet (London, England)* **338**, 1055–1059 (1991).

150. Klugman, K. P. *et al.* Protective activity of Vi capsular polysaccharide vaccine against typhoid fever. *Lancet (London, England)* **2**, 1165–1169 (1987).

151. Klugman, K. P., Koornhof, H. J., Robbins, J. B. & Le Cam, N. N. Immunogenicity, efficacy and serological correlate of protection of Salmonella typhi Vi capsular polysaccharide vaccine three years after immunization. *Vaccine* **14**, 435–438 (1996).

152. Sur, D. *et al.* A cluster-randomized effectiveness trial of Vi typhoid vaccine in India. *N. Engl. J. Med.* **361**, 335–344 (2009).

153. Acharya, I. L. *et al.* Prevention of typhoid fever in Nepal with the Vi capsular polysaccharide of Salmonella typhi. A preliminary report. *N. Engl. J. Med.* **317**, 1101–1104 (1987).

154. Mai, N. L. *et al.* Persistent efficacy of Vi conjugate vaccine against typhoid fever in young children. *The New England journal of medicine* vol. 349 1390–1391 (2003).

155. Shakya, M. *et al.* Phase 3 Efficacy Analysis of a Typhoid Conjugate Vaccine Trial in Nepal. *N. Engl. J. Med.* **381**, 2209–2218 (2019).

156. Bhutta, Z. A. *et al.* Immunogenicity and safety of the Vi-CRM197 conjugate vaccine against typhoid fever in adults, children, and infants in south and southeast Asia: results from two randomised, observer-blind, age de-escalation, phase 2 trials. *Lancet. Infect. Dis.* **14**, 119–129 (2014).

157. Lyon, C. E. *et al.* In a randomized, double-blinded, placebo-controlled trial, the single oral dose typhoid vaccine, M01ZH09, is safe and immunogenic at doses up to 1.7 x 10(10) colony-forming units. *Vaccine* **28**, 3602–3608 (2010).

158. Capeding, M. R. *et al.* Safety and immunogenicity of Vi-DT conjugate vaccine among 6-23-month-old children: Phase II, randomized, dose-scheduling, observer-blind Study. *EClinicalMedicine* **27**, 100540 (2020).

159. Hohmann, E. L., Oletta, C. A., Killeen, K. P. & Miller, S. I. phoP/phoQ-deleted Salmonella typhi (Ty800) is a safe and immunogenic single-dose typhoid fever vaccine in volunteers. *J. Infect. Dis.* **173**, 1408–1414 (1996).

160. Hone, D. M. *et al.* Evaluation in volunteers of a candidate live oral attenuated Salmonella typhi vector vaccine. *J. Clin. Invest.* **90**, 412–420 (1992).

161. Tacket, C. O. *et al.* Clinical acceptability and immunogenicity of CVD 908 Salmonella typhi vaccine strain. *Vaccine* **10**, 443–446 (1992).

162. Tacket, C. O. & Levine, M. M. CVD 908, CVD 908-htrA, and CVD 909 live oral typhoid vaccines: a logical progression. *Clin. Infect. Dis. an Off. Publ. Infect. Dis. Soc. Am.* **45 Suppl 1**, S20-3 (2007).

163. Raj, K. V. A. WHO Pre-qualifies BE's typhoid conjugate vaccine. *Biological E Limited*

1 https://www.biologicale.com/news.html (2020).

164. Duff, N. New research from Pakistan finds children are protected from typhoid with new vaccine. *Sabin Institute* https://www.coalitionagainsttyphoid.org/new-research-from-pakistan-finds-children-are-protected-from-typhoid-with-new-vaccine/ (2020).

165. Soble, A., Patel, Z., Sosler, S., Hampton, L. & Johnson, H. Gavi support for typhoid conjugate vaccines: Moving from global investments to country introduction. *Clin. Infect. Dis.* **71**, S160–S164 (2020).

166. Yousafzai, M. T. *et al.* Ceftriaxone-resistant Salmonella Typhi Outbreak in Hyderabad City of Sindh, Pakistan: High Time for the Introduction of Typhoid Conjugate Vaccine. *Clin. Infect. Dis.* **68**, S16–S21 (2019).

167. Pitzer, V. E. *et al.* Predicting the Impact of Vaccination on the Transmission Dynamics of Typhoid in South Asia: A Mathematical Modeling Study. *PLoS Negl. Trop. Dis.* **8**, 40 (2014).

168. Bilcke, J. *et al.* Cost-effectiveness of routine and campaign use of typhoid Vi-conjugate vaccine in Gavi-eligible countries: a modelling study. *Lancet Infect. Dis.* **19**, 728–739 (2019).

169. Wangdi, K. *et al.* Diversity of infectious aetiologies of acute undifferentiated febrile illnesses in south and Southeast Asia: A systematic review. *BMC Infect. Dis.* **19**, 1–17 (2019).

170. Shrestha, P. *et al.* Non-malarial febrile illness: A systematic review of published aetiological studies and case reports from Southern Asia and South-eastern Asia, 1980-2015. *BMC Med.* **18**, 1–14 (2020).

171. Maze, M. J. *et al.* The epidemiology of febrile illness in sub-Saharan Africa: implications for diagnosis and management. *Clin. Microbiol. Infect.* **24**, 808–814 (2018).

172. World Health Organization. *Global antimicrobial resistance surveillance system (GLASS) report. Geneva: World Health Organisation* (2018).

173. Dagan, R. & Klugman, K. P. Impact of conjugate pneumococcal vaccines on antibiotic resistance. *Lancet Infect. Dis.* **8**, 785–795 (2008).

174. Tomczyk, S. *et al.* Prevention of Antibiotic-Nonsusceptible Invasive Pneumococcal Disease with the 13-Valent Pneumococcal Conjugate Vaccine. *Clin. Infect. Dis.* **62**, 1119–1125 (2016).

175. Azmatullah, A., Qamar, F. N., Thaver, D., Zaidi, A. K. M. & Bhutta, Z. A. Systematic review of the global epidemiology, clinical and laboratory profile of enteric fever. *J. Glob. Health* **5**, (2015).

176. Debellut, F. *et al.* Forecasting demand for the typhoid conjugate vaccine in low- and middle-income countries. *Clin. Infect. Dis.* **68**, S154–S160 (2019).

177. World Health Organization. At least 80 million children under one at risk of diseases such as diphtheria, measles and polio as COVID-19 disrupts routine vaccination efforts, warn Gavi, WHO and UNICEF. https://www.who.int/news/item/22-05-2020-at-least-80-million-children-under-one-at-risk-of-diseases-such-as-diphtheria-measles-and-polio-as-covid-19-disrupts-routine-vaccination-efforts-warn-gavi-who-and-unicef (2020).

178. Abbas, K. *et al.* Routine childhood immunisation during the COVID-19 pandemic in Africa: a benefit–risk analysis of health benefits versus excess risk of SARS-CoV-2 infection. *Lancet Glob. Heal.* **8**, e1264–e1272 (2020).

179. Pollard, A. J. & Bijker, E. M. A guide to vaccinology: from basic principles to new developments. *Nat. Rev. Immunol.* **21**, (2020).

180. Pollard, A. J., Perrett, K. P. & Beverley, P. C. Maintaining protection against invasive bacteria with protein- polysaccharide conjugate vaccines. *Nat. Rev. Immunol.* **9**, 213–220 (2009).

181. Li, X. *et al.* Estimating the health impact of vaccination against ten pathogens in 98 low-income and middle-income countries from 2000 to 2030: a modelling study. *Lancet* **397**, 398–408 (2021).

182. Klein Klouwenberg, P. & Bont, L. Neonatal and infantile immune responses to encapsulated bacteria and conjugate vaccines. *Clin. Dev. Immunol.* **2008**, (2008).

183. Guinamard, R., Okigaki, M., Schlessinger, J. & Ravetch, J. V. Absence of marginal zone B cells in Pyk-2-deficient mice defines their role in the humoral response. *Nat.*

Immunol. **1**, 31–36 (2000).

184. Martin, F., Oliver, A. M. & Kearney, J. F. Marginal zone and B1 B cells unite in the early response against T-independent blood-borne particulate antigens. *Immunity* **14**, 617–629 (2001).

185. Dammers, P. M., Visser, A., Popa, E. R., Nieuwenhuis, P. & Kroese, F. G. Most marginal zone B cells in rat express germline encoded Ig VH genes and are ligand selected. *J. Immunol.* **165**, 6156–6169 (2000).

186. Tierens, A., Delabie, J., Michiels, L., Vandenberghe, P. & De Wolf-Peeters, C. Marginal-zone B cells in the human lymph node and spleen show somatic hypermutations and display clonal expansion. *Blood* **93**, 226–234 (1999).

187. Weller, S. *et al.* Human blood IgM 'memory' B cells are circulating splenic marginal zone B cells harboring a prediversified immunoglobulin repertoire. *Blood* **104**, 3647–3654 (2004).

188. Buzelé, R., Barbier, L., Sauvanet, A. & Fantin, B. Medical complications following splenectomy. *J. Visc. Surg.* **153**, 277–286 (2016).

189. Okada, T. *et al.* Antigen-engaged B cells undergo chemotaxis toward the T zone and form motile conjugates with helper T cells. *PLoS Biol.* **3**, e150 (2005).

190. Auner, H. W., Beham-Schmid, C., Dillon, N. & Sabbattini, P. The life span of short-lived plasma cells is partly determined by a block on activation of apoptotic caspases acting in combination with endoplasmic reticulum stress. *Blood* **116**, 3445–3455 (2010).

191. MacLennan, I. C. M. *et al.* Extrafollicular antibody responses. *Immunol. Rev.* **194**, 8–18 (2003).

192. Paus, D. *et al.* Antigen recognition strength regulates the choice between extrafollicular plasma cell and germinal center B cell differentiation. *J. Exp. Med.* **203**, 1081–1091 (2006).

193. Taylor, J. J., Pape, K. A. & Jenkins, M. K. A germinal center-independent pathway generates unswitched memory B cells early in the primary response. *J. Exp. Med.* **209**, 597–606 (2012).

194. Phipps, J. P. & Haas, K. M. An Adjuvant That Increases Protective Antibody Responses to Polysaccharide Antigens and Enables Recall Responses. *J. Infect. Dis.* **219**, 323–334 (2019).

195. Crotty, S. T Follicular Helper Cell Biology: A Decade of Discovery and Diseases. *Immunity* **50**, 1132–1148 (2019).

196. Crotty, S. T Follicular Helper Cell Differentiation, Function, and Roles in Disease. *Immunity* vol. 41 529–542 (2014).

197. Morita, R. *et al.* Human Blood CXCR5+CD4+ T Cells Are Counterparts of T Follicular Cells and Contain Specific Subsets that Differentially Support Antibody Secretion. *Immunity* **34**, 108–121 (2011).

198. Koutsakos, M. *et al.* Circulating TFH cells, serological memory, and tissue compartmentalization shape human influenza-specific B cell immunity. *Sci. Transl. Med.* **10**, eaan8405 (2018).

199. Rydyznski, C. E. *et al.* Affinity Maturation Is Impaired by Natural Killer Cell Suppression of Germinal Centers. *Cell Rep.* **24**, 3367–3373 (2018).

200. Rydyznski, C. E. & Waggoner, S. N. Boosting vaccine efficacy the natural (killer) way. *Trends Immunol.* **36**, 536–546 (2015).

201. Wagstaffe, H. R. *et al.* Ebola virus glycoprotein stimulates IL-18 dependent natural killer cell responses. *J. Clin. Invest.* (2020) doi:10.1172/jci132438.

202. Klugman, K. P., Koornhof, H. J., Robbins, J. B. & Le Cam, N. N. Immunogenicity, efficacy and serological correlate of protection of Salmonella typhi Vi capsular polysaccharide vaccine three years after immunization. *Vaccine* **14**, 435–438 (1996).

203. Shousun, S., Klugman, K. P. & Hunt, S. Re-examination of immune response and estimation of anti-Vi IgG protective threshold against typhoid fever-based on the efficacy trial of Vi conjugate in young children. *Vaccine* **32**, 2359–2363 (2014).

204. Voysey, M. & Pollard, A. J. Seroefficacy of VI polysaccharide–tetanus toxoid typhoid conjugate vaccine (typbar TCV). *Clin. Infect. Dis.* **67**, 18–24 (2018).

205. Jang, M. S., Sahastrabuddhe, S., Yun, C. H., Han, S. H. & Yang, J. S. Serum

bactericidal assay for the evaluation of typhoid vaccine using a semi-automated colony-counting method. *Microb. Pathog.* **97**, 19–26 (2016).

206. Borrow, R., Balmer, P. & Miller, E. Meningococcal surrogates of protection - Serum bactericidal antibody activity. *Vaccine* **23**, 2222–2227 (2005).

207. Juel, H. B. *et al.* Salmonella Typhi bactericidal antibodies reduce disease severity but do not protect against typhoid fever in a controlled human infection model. *Front. Immunol.* **8**, 1–11 (2018).

208. Tobar, J. A., González, P. A. & Kalergis, A. M. Salmonella Escape from Antigen Presentation Can Be Overcome by Targeting Bacteria to Fcγ Receptors on Dendritic Cells . *J. Immunol.* **173**, 4058–4065 (2004).

209. Lindow, J. C., Fimlaid, K. A., Bunn, J. Y. & Kirkpatrick, B. D. Antibodies in action: Role of human opsonins in killing Salmonella enterica serovar Typhi. *Infect. Immun.* **79**, 3188–3194 (2011).

210. Waddington, C. S. *et al.* An outpatient, ambulant-design, controlled human infection model using escalating doses of salmonella typhi challenge delivered in sodium bicarbonate solution. *Clin. Infect. Dis.* **58**, 1230–1240 (2014).

211. Schuyler, R. P. *et al.* Minimizing Batch Effects in Mass Cytometry Data. *Front. Immunol.* **10**, 2367 (2019).

212. Diggins, K. E., Greenplate, A. R., Leelatian, N., Wogsland, C. E. & Irish, J. M. Characterizing cell subsets using marker enrichment modeling. *Nat. Methods* **14**, 275–278 (2017).

213. Levine, J. H. *et al.* Data-Driven Phenotypic Dissection of AML Reveals Progenitor-like Cells that Correlate with Prognosis. *Cell* **162**, 184–197 (2015).

214. Bentebibel, S. E. *et al.* Induction of ICOS+CXCR3+CXCR5+ T H cells correlates with antibody responses to influenza vaccination. *Sci. Transl. Med.* **5**, 176ra32 (2013).

215. Dahora, L. C. *et al.* IgA and IgG1 Specific to Vi Polysaccharide of Salmonella Typhi Correlate With Protection Status in a Typhoid Fever Controlled Human Infection Model. *Front. Immunol.* **10**, (2019).

216. Roco, J. A. *et al.* Class-Switch Recombination Occurs Infrequently in Germinal Centers. *Immunity* **51**, 337-350.e7 (2019).

217. Mora, J. R. & von Andrian, U. H. Differentiation and homing of IgA-secreting cells. *Mucosal Immunology* vol. 1 96–109 (2008).

218. Kunkel, E. J. *et al.* CCR10 expression is a common feature of circulating and mucosal epithelial tissue IgA Ab-secreting cells. *J. Clin. Invest.* **111**, 1001–1010 (2003).

219. Mohan, T., Deng, L. & Wang, B.-Z. CCL28 chemokine: An anchoring point bridging innate and adaptive immunity. *Int. Immunopharmacol.* **51**, 165–170 (2017).

220. Gorfu, G., Rivera-Nieves, J. & Ley, K. Role of β7 Integrins in Intestinal Lymphocyte Homing and Retention. *Curr. Mol. Med.* **9**, 836–850 (2009).

221. Quiding-Järbrink, M. *et al.* Differential expression of tissue-specific adhesion molecules on human circulating antibody-forming cells after systemic, enteric, and nasal immunizations. A molecular basis for the compartmentalization of effector B cell responses. *J. Clin. Invest.* **99**, 1281–1286 (1997).

222. Mei, H. E. *et al.* Blood-borne human plasma cells in steady state are derived from mucosal immune responses. *Blood* **113**, 2461–2469 (2009).

223. Tabibian-Keissar, H. *et al.* B-cell clonal diversification and gut-lymph node trafficking in ulcerative colitis revealed using lineage tree analysis. *Eur. J. Immunol.* **38**, 2600–2609 (2008).

224. Weitkamp, J.-H. *et al.* VH1-46 is the dominant immunoglobulin heavy chain gene segment in rotavirus-specific memory B cells expressing the intestinal homing receptor alpha4beta7. *J. Immunol.* **174**, 3454–3460 (2005).

225. Snir, O. *et al.* Analysis of Celiac Disease Autoreactive Gut Plasma Cells and Their Corresponding Memory Compartment in Peripheral Blood Using High-Throughput Sequencing. *J. Immunol.* **194**, 5703–5712 (2015).

226. Nieminen, T., Käyhty, H., Leroy, O. & Eskola, J. Pneumococcal conjugate vaccination in toddlers: mucosal antibody response measured as circulating antibody-secreting cells and as salivary antibodies. *Pediatr. Infect. Dis. J.* **18**, 764–772 (1999).

227. Whalen, J. G., Mully, T. W. & English, J. C. 3rd. Spontaneous Citrobacter freundii infection in an immunocompetent patient. *Archives of dermatology* vol. 143 124–125 (2007).

228. Snellings, N. J., Johnson, E. M., Kopecko, D. J., Collins, H. H. & Baron, L. S. Genetic regulation of variable Vi antigen expression in a strain of Citrobacter freundii. *J. Bacteriol.* **145**, 1010–1017 (1981).

229. Odendahl, M. *et al.* Generation of migratory antigen-specific plasma blasts and mobilization of resident plasma cells in a secondary immune response. *Blood* **105**, 1614–1621 (2005).

230. Mei, H. E. *et al.* Plasmablasts With a Mucosal Phenotype Contribute to Plasmacytosis in Systemic Lupus Erythematosus. *Arthritis Rheumatol. (Hoboken, N.J.)* **69**, 2018–2028 (2017).

231. Yu, H. *et al.* Human BDCA2+CD123+CD56+ dendritic cells (DCs) related to blastic plasmacytoid dendritic cell neoplasm represent a unique myeloid DC subset. *Protein Cell* **6**, 297–306 (2015).

232. Gruenbacher, G. *et al.* CD56+ human blood dendritic cells effectively promote TH1-type gammadelta T-cell responses. *Blood* **114**, 4422–4431 (2009).

233. Papewalis, C. *et al.* IFN-alpha skews monocytes into CD56+-expressing dendritic cells with potent functional activities in vitro and in vivo. *J. Immunol.* **180**, 1462–1470 (2008).

234. Anguille, S. *et al.* Interleukin-15-induced CD56(+) myeloid dendritic cells combine potent tumor antigen presentation with direct tumoricidal potential. *PLoS One* **7**, e51851 (2012).

235. Dogra, P. *et al.* Tissue Determinants of Human NK Cell Development, Function, and Residence. *Cell* **180**, 749-763.e13 (2020).

236. Bühling, F. *et al.* Expression and functional role of dipeptidyl peptidase IV (CD26) on human natural killer cells. *Nat. Immun.* **13**, 270–279 (1994).

237. Klemann, C., Wagner, L., Stephan, M. & von Hörsten, S. Cut to the chase: a review of

CD26/dipeptidyl peptidase-4's (DPP4) entanglement in the immune system. *Clin. Exp. Immunol.* **185**, 1–21 (2016).

238. Suan, D. *et al.* CCR6 Defines Memory B Cell Precursors in Mouse and Human Germinal Centers, Revealing Light-Zone Location and Predominant Low Antigen Affinity. *Immunity* **47**, 1142-1153.e4 (2017).

239. Obukhanych, T. V & Nussenzweig, M. C. T-independent type II immune responses generate memory B cells. *J. Exp. Med.* **203**, 305–310 (2006).

240. Cook, K. D., Kline, H. C. & Whitmire, J. K. NK cells inhibit humoral immunity by reducing the abundance of CD4+ T follicular helper cells during a chronic virus infection. *J. Leukoc. Biol.* **98**, 153–162 (2015).

241. Blohmke, C. J. *et al.* Induction of Cell Cycle and NK Cell Responses by Live-Attenuated Oral Vaccines against Typhoid Fever. *Front. Immunol.* **8**, 1276 (2017).

242. O'Sullivan, T. E., Sun, J. C. & Lanier, L. L. Natural Killer Cell Memory. *Immunity* **43**, 634–645 (2015).

243. Wiencke, J. K. *et al.* The DNA methylation profile of activated human natural killer cells. *Epigenetics* **11**, 363–380 (2016).

244. Toapanta, F. R. *et al.* Oral Challenge with Wild-Type Salmonella Typhi Induces Distinct Changes in B Cell Subsets in Individuals Who Develop Typhoid Disease. *PLoS Negl. Trop. Dis.* **10**, e0004766 (2016).

245. Toapanta, F. R. *et al.* Gut-homing conventional plasmablasts and CD27- plasmablasts elicited after a short time of exposure to an oral live-attenuated Shigella vaccine candidate in humans. *Front. Immunol.* **5**, (2014).

246. Guglani, L. & Khader, S. A. Th17 cytokines in mucosal immunity and inflammation. *Curr. Opin. HIV AIDS* **5**, 120–127 (2010).

247. Maggi, L. *et al.* CD161 is a marker of all human IL-17-producing T-cell subsets and is induced by RORC. *Eur. J. Immunol.* **40**, 2174–2181 (2010).

248. Nikitina, I. Y. *et al.* Th1, Th17, and Th1Th17 Lymphocytes during Tuberculosis: Th1 Lymphocytes Predominate and Appear as Low-Differentiated CXCR3(+)CCR6(+)

Cells in the Blood and Highly Differentiated CXCR3(+/-)CCR6(-) Cells in the Lungs. *J. Immunol.* **200**, 2090–2103 (2018).

249. Brisslert, M. *et al.* Phenotypic and functional characterization of human CD25+ B cells. *Immunology* **117**, 548–557 (2006).

250. Fergusson, J. R., Fleming, V. M. & Klenerman, P. CD161-expressing human T cells. *Front. Immunol.* **2**, 1–7 (2011).

251. Narasimhan, P. B., Marcovecchio, P., Hamers, A. A. J. & Hedrick, C. C. Nonclassical Monocytes in Health and Disease. *Annu. Rev. Immunol.* **37**, 439–456 (2019).

252. Auffray, C. *et al.* Monitoring of blood vessels and tissues by a population of monocytes with patrolling behavior. *Science* **317**, 666–670 (2007).

253. House, D. *et al.* Cytokine release by lipopolysaccharide-stimulated whole blood from patients with typhoid fever. *J. Infect. Dis.* **186**, 240–245 (2002).

254. Woodland, D. L. & Kohlmeier, J. E. Migration, maintenance and recall of memory T cells in peripheral tissues. *Nat. Rev. Immunol.* **9**, 153–161 (2009).

255. Palm, A. K. E. & Henry, C. Remembrance of Things Past: Long-Term B Cell Memory After Infection and Vaccination. *Front. Immunol.* **10**, 1787 (2019).

256. Shenoy, G. N. *et al.* Recruitment of memory B cells to lymph nodes remote from the site of immunization requires an inflammatory stimulus. *J. Immunol.* **189**, 521–528 (2012).

257. Maiti, S. *et al.* Effective control of Salmonella infections by employing combinations of recombinant antimicrobial human β-defensins hBD-1 and hBD-2. *Antimicrob. Agents Chemother.* **58**, 6896–6903 (2014).

258. Benoun, J. M. *et al.* Optimal protection against Salmonella infection requires noncirculating memory. *Proc. Natl. Acad. Sci. U. S. A.* **115**, 10416–10421 (2018).

259. Minasyan, H. Mechanisms and pathways for the clearance of bacteria from blood circulation in health and disease. *Pathophysiol. Off. J. Int. Soc. Pathophysiol.* **23**, 61–66 (2016).

260. Abdullah, M. *et al.* Gender effect on in vitro lymphocyte subset levels of healthy individuals. *Cell. Immunol.* **272**, 214–219 (2012).

261. Derhovanessian, E., Larbi, A. & Pawelec, G. Biomarkers of human immunosenescence: impact of Cytomegalovirus infection. *Curr. Opin. Immunol.* **21**, 440–445 (2009).

262. Achkar, J. M., Chan, J. & Casadevall, A. Role of B cells and antibodies in acquired immunity against Mycobacterium tuberculosis. *Cold Spring Harb. Perspect. Med.* **5**, a018432 (2014).

263. Simon, L., Gauvin, F., Amre, D. K., Saint-Louis, P. & Lacroix, J. Serum procalcitonin and C-reactive protein levels as markers of bacterial infection: a systematic review and meta-analysis. *Clin. Infect. Dis. an Off. Publ. Infect. Dis. Soc. Am.* **39**, 206–217 (2004).

264. Jiang, J. *et al.* The neutrophil-lymphocyte count ratio as a diagnostic marker for bacteraemia: A systematic review and meta-analysis. *Am. J. Emerg. Med.* **37**, 1482–1489 (2019).

265. Terradas, R. *et al.* Eosinophil count and neutrophil-lymphocyte count ratio as prognostic markers in patients with bacteremia: a retrospective cohort study. *PLoS One* **7**, e42860 (2012).

266. Naranbhai, V. *et al.* Ratio of monocytes to lymphocytes in peripheral blood identifies adults at risk of incident tuberculosis among HIV-infected adults initiating antiretroviral therapy. *J. Infect. Dis.* **209**, 500–509 (2014).

267. Amit, S., Regev-Yochay, G., Afek, A., Kreiss, Y. & Leshem, E. Early rate reductions of SARS-CoV-2 infection and COVID-19 in BNT162b2 vaccine recipients. *Lancet (London, England)* vol. 397 875–877 (2021).

268. Abdool Gaffar, M. S., Seedat, Y. K., Coovadia, Y. M. & Khan, Q. The white cell count in typhoid fever. *Trop. Geogr. Med.* **44**, 23–27 (1992).

269. de Jager, C. P. C. *et al.* Lymphocytopenia and neutrophil-lymphocyte count ratio predict bacteremia better than conventional infection markers in an emergency care unit. *Crit. Care* **14**, R192 (2010).

270. Naess, A., Nilssen, S. S., Mo, R., Eide, G. E. & Sjursen, H. Role of neutrophil to lymphocyte and monocyte to lymphocyte ratios in the diagnosis of bacterial infection in patients with fever. *Infection* **45**, 299–307 (2017).

271. Wain, J. *et al.* Quantitation of bacteria in bone marrow from patients with typhoid fever: relationship between counts and clinical features. *J. Clin. Microbiol.* **39**, 1571–1576 (2001).

272. Wain, J. *et al.* Quantitation of bacteria in blood of typhoid fever patients and relationship between counts and clinical features, transmissibility, and antibiotic resistance. *J. Clin. Microbiol.* **36**, 1683–1687 (1998).

273. O'Connell, E. M. & Nutman, T. B. Eosinophilia in Infectious Diseases. *Immunol. Allergy Clin. North Am.* **35**, 493–522 (2015).

274. Zhang, R. *et al.* Neutrophil-to-lymphocyte ratio predicts hemorrhagic transformation in ischemic stroke: A meta-analysis. *Brain Behav.* **9**, e01382 (2019).

275. Olubuyide, I. O., Brown, N. M., Higginson, J. & Whicher, J. T. The value of C-reactive protein in the diagnosis of intestinal perforation in typhoid fever. *Ann. Clin. Biochem.* **26 (Pt 3)**, 246–248 (1989).

276. Deiss, R. G. *et al.* Vaccine-associated reduction in symptom severity among patients with influenza A/H3N2 disease. *Vaccine* **33**, 7160–7167 (2015).

277. Coward, C. *et al.* The effects of vaccination and immunity on bacterial infection dynamics in vivo. *PLoS Pathog.* **10**, e1004359 (2014).

278. Karakonstantis, S., Kalemaki, D., Tzagkarakis, E. & Lydakis, C. Pitfalls in studies of eosinopenia and neutrophil-to-lymphocyte count ratio. *Infect. Dis. (London, England)* **50**, 163–174 (2018).

279. Hamiel, U. *et al.* Diagnostic markers of acute infections in infants aged 1 week to 3 months: a retrospective cohort study. *BMJ Open* **8**, e018092 (2018).

280. Marchello, C. S., Birkhold, M. & Crump, J. A. Complications and mortality of typhoid fever: A global systematic review and meta-analysis. *J. Infect.* **81**, 902–910 (2020).

281. Chami, B. *et al.* CXCR3 plays a critical role for host protection against Salmonellosis. *Sci. Rep.* **7**, 10181 (2017).

282. Ramírez-Ramírez, D. *et al.* Early Differentiation of Human CD11c(+)NK Cells with γδ T Cell Activation Properties Is Promoted by Dialyzable Leukocyte Extracts. *J.*

Immunol. Res. **2016**, 4097642 (2016).

283. Pozo, D. *et al.* CD161 (human NKR-P1A) signaling in NK cells involves the activation of acid sphingomyelinase. *J. Immunol.* **176**, 2397–2406 (2006).

284. Goldberg, M. F. *et al.* Salmonella Persist in Activated Macrophages in T Cell-Sparse Granulomas but Are Contained by Surrounding CXCR3 Ligand-Positioned Th1 Cells. *Immunity* **49**, 1090-1102.e7 (2018).

285. Valledor, A. F. *et al.* Selective roles of MAPKs during the macrophage response to IFN-gamma. *J. Immunol.* **180**, 4523–4529 (2008).

286. Song, X., He, X., Li, X. & Qian, Y. The roles and functional mechanisms of interleukin-17 family cytokines in mucosal immunity. *Cell. Mol. Immunol.* **13**, 418–431 (2016).

287. de Jong, H. K. *et al.* Expression of intra- and extracellular granzymes in patients with typhoid fever. *PLoS Negl. Trop. Dis.* **11**, e0005823 (2017).

288. Pejcic-Karapetrovic, B. *et al.* Pregnancy impairs the innate immune resistance to Salmonella typhimurium leading to rapid fatal infection. *J. Immunol.* **179**, 6088–6096 (2007).

289. Iijima, N. *et al.* Dendritic cells and B cells maximize mucosal Th1 memory response to herpes simplex virus. *J. Exp. Med.* **205**, 3041–3052 (2008).

290. Ribot, J. C., Lopes, N. & Silva-Santos, B. γδ T cells in tissue physiology and surveillance. *Nat. Rev. Immunol.* **21**, 221–232 (2021).

291. Hara, T. *et al.* Predominant activation and expansion of V gamma 9-bearing gamma delta T cells in vivo as well as in vitro in Salmonella infection. *J. Clin. Invest.* **90**, 204–210 (1992).

292. Hoshina, T., Kusuhara, K., Saito, M., Mizuno, Y. & Hara, T. NKRP1A+ γδ and αβ T cells are preferentially induced in patients with Salmonella infection. *Hum. Immunol.* **73**, 623–628 (2012).

293. Young, A. J., Seabrook, T. J., Marston, W. L., Dudler, L. & Hay, J. B. A role for lymphatic endothelium in the sequestration of recirculating gamma delta T cells in TNF-alpha-stimulated lymph nodes. *Eur. J. Immunol.* **30**, 327–334 (2000).

294. Bain, C. C. & Schridde, A. Origin, Differentiation, and Function of Intestinal Macrophages. *Front. Immunol.* **9**, 2733 (2018).

295. Depaolo, R. W., Lathan, R., Rollins, B. J. & Karpus, W. J. The chemokine CCL2 is required for control of murine gastric Salmonella enterica infection. *Infect. Immun.* **73**, 6514–6522 (2005).

296. Fairchild, K. D., Hudson, R. G., Douglas, S. D., McKenzie, S. E. & Polin, R. A. Effect of gamma interferon on expression of Fc gamma receptors in monocytes of newborn infants and adults. *Clin. Diagn. Lab. Immunol.* **3**, 464–469 (1996).

297. Jason, J. *et al.* Natural T, gammadelta, and NK cells in mycobacterial, Salmonella, and human immunodeficiency virus infections. *J. Infect. Dis.* **182**, 474–481 (2000).

298. Selvanantham, T. *et al.* Nod1 and Nod2 enhance TLR-mediated invariant NKT cell activation during bacterial infection. *J. Immunol.* **191**, 5646–5654 (2013).

299. Parker, E. P., Molodecky, N. A., Pons-Salort, M., O'Reilly, K. M. & Grassly, N. C. Impact of inactivated poliovirus vaccine on mucosal immunity: implications for the polio eradication endgame. *Expert Rev. Vaccines* **14**, 1113–1123 (2015).

300. Connor, R. I. *et al.* Mucosal immunity to poliovirus. *Mucosal Immunol.* (2021) doi:10.1038/s41385-021-00428-0.

301. Gibani, M. M. *et al.* The impact of vaccination and prior exposure on stool shedding of salmonella typhi and salmonella paratyphi in 6 controlled human infection studies. *Clin. Infect. Dis.* **68**, 1265–1273 (2019).

302. Lang, M. L. How do natural killer T cells help B cells? *Expert Rev. Vaccines* **8**, 1109–1121 (2009).

303. Tsang, J. S. *et al.* Global analyses of human immune variation reveal baseline predictors of postvaccination responses. *Cell* **157**, 499–513 (2014).

304. Cai, J. *et al.* The Neutrophil-to-Lymphocyte Ratio Determines Clinical Efficacy of Corticosteroid Therapy in Patients with COVID-19. *Cell Metab.* **33**, 258-269.e3 (2021).

305. Guthridge, S., McIntyre, P., Isaacs, D., Hanlon, M. & Patel, M. Differing serologic responses to an haemophilus influenzae type b polysaccharide-neisseria meningitidis

outer membrane protein conjugate (PRP-OMPC) vaccine in australian aboriginal and caucasian infants - implications for disease epidemiology. *Vaccine* **18**, 2584–2591 (2000).

306. Greenberg, D. P. *et al.* Immunogenicity of Haemophilus influenzae type b tetanus toxoid conjugate vaccine in young infants. The Kaiser-UCLA Vaccine Study Group. *J. Infect. Dis.* **170**, 76–81 (1994).

307. Karkey, A. *et al.* The Ecological Dynamics of Fecal Contamination and Salmonella Typhi and Salmonella Paratyphi A in Municipal Kathmandu Drinking Water. *PLoS Negl. Trop. Dis.* **10**, e0004346 (2016).

308. Pabst, O. & Slack, E. IgA and the intestinal microbiota: the importance of being specific. *Mucosal Immunology* vol. 13 12–21 (2020).

309. Libertucci, J. & Young, V. B. The role of the microbiota in infectious diseases. *Nat. Microbiol.* **4**, 35–45 (2019).

310. Kaiser, P., Slack, E., Grant, A. J., Hardt, W.-D. & Regoes, R. R. Lymph node colonization dynamics after oral Salmonella Typhimurium infection in mice. *PLoS Pathog.* **9**, e1003532 (2013).

311. Crooke, S. N., Ovsyannikova, I. G., Poland, G. A. & Kennedy, R. B. Immunosenescence and human vaccine immune responses. *Immun. Ageing* **16**, 25 (2019).

312. Baker, S., Blohmke, C. J., Maes, M., Johnston, P. I. & Darton, T. C. The Current Status of Enteric Fever Diagnostics and Implications for Disease Control. *Clin. Infect. Dis. an Off. Publ. Infect. Dis. Soc. Am.* **71**, S64–S70 (2020).